Genotoxic responses at low doses for chemicals requiring metabolic activation using different human cell lines.

Shah, Ume-Kulsoom

Genotoxic Responses At Low Doses For Chemicals Requiring Metabolic Activation Using Different Human Cell Lines

Ume-Kulsoom Shah

A thesis submitted for the partial fulfilment of the requirement for the degree of Doctor Of Philosophy

DNA Damage and Cancer Research Group
Institute of Life Sciences
College of Medicine
Swansea University

DECLARATION

The work has not previously been accepted in substance for any degree and is not being concurrently submitted in candidature for any degree.

Signed.

Date....11-12-14.....

STATEMENT 1

This thesis is the result of my own investigation, except where otherwise stated. Where correction services have been used, the extent and nature of the correction is clearly marked in a footnote (s).

Other sources are acknowledged by footnotes giving explicit references. A bibliography is appended.

Signed

Date...11-12-14.....

STATEMENT 2

I hereby give consent for my thesis, if accepted, to be available for photocopying and for inter-library loan, and for the title and summary to be made available to outside organisations.

Signed.

Date....11-12-14.....

ACKNOWLEDGEMENTS

I would like to express my special thanks to my supervisor Professor Gareth Jenkins for his constant encouragement, guidance and enthusiasm to complete this work. I particularly appreciate his support during difficult times and in providing valuable feedback and constructive comments throughout this study. I am also very grateful to have Dr Shareen Doak, as my second supervisor for her guidance, motivation and valuable advice during my research. I express my thanks to Anna for providing advice and support on my day to day work and in reviewing draft version of thesis. I would also like to thank Dr George Johnson for his constructive comments and help with statistical analysis of the data. My special thanks to Dr Paul Fowler and Dr Andrew Scott (Unilever) for their positive feedback and support.

Special thanks to my colleagues particularly Bella, Adam, Ben, James, Katija, Kate, Bushra, Abdullah, Jatin, Ellie, Neenu, Jane and Hasan for their friendship, valuable suggestions, support and encouragement throughout this study.

I would like to thank everyone in our research group for their cooperation, encouragement and providing a friendly environment. However, Margaret and Sally deserve special thanks for their technical advice and help.

I would like to acknowledge support of my family friends and members for their encouragement and support throughout my studies. I would like to thank my husband and children for their continuous love, encouragement, and patiently listening to my moaning. I appreciate love and patience of my son and daughter during busy periods when I was unable to give them quality time. I am also grateful for Abba jee and Amma jee to remember me always in their prayers.
My parents deserve special appreciation as provided their support and prayed for my success throughout their lives, unfortunately both of them passed away during the course of this study thus I dedicate my work to them.

I would also like to express my gratitude to Unilever for their financial support for this study.

SUMMARY

Pro-carcinogens e.g. B[a]P and PhIP require metabolic activation to exert genotoxicity. Both B[a]P and PhIP are known to cause different types of cancers, however, very little is known about the dose response of these two chemicals at low concentrations. This study was conducted to determine the effect of low doses of B[a]P and PhIP and their exposure time on cell lines with varying levels of metabolic activity.

Micronucleus and HPRT assays were conducted to determine the effect of low doses of B[a]P on micronuclei induction and mutation frequency following 4 or 24 h exposure. MCL-5 and HepG2 cell lines showed higher induction of micronuclei irrespective of B[a]P dose and exposure time. Micronuclei induction was least in AHH-1 while TK-6 cells showed no micronuclei induction. HPRT assay also showed higher mutation frequency in MCL-5 as compared to AHH-1 at both time exposures. Analysis of mutation spectra of MCL-5 and AHH-1 HPRT mutants revealed that the type of mutations observed in B[a]P treated cells were different to those observed in untreated control B[a]P-induced mutations were predominantly G→T transversions. Real time PCR assays revealed higher induction of CYP1A1 and CY1A2 enzymes in response to B[a]P in MCL-5 and HepG2 cell lines.

Studies on PhIP showed significantly higher cytotoxicity, genotoxicity and mutation frequency in the MCL-5 and HepG2 cell lines than AHH-1 cells. Micronucleus assays (24h) revealed 1.56 and 1.9-.fold increase in micronuclei induction in MCL-5 and HepG2, respectively as compared to control. A similar trend was observed in 4h PhIP exposure study, where MCL-5 and HepG2 had 1.83 and 1.92-.fold increase respectively. These findings are in line with the metabolic potential of the cell lines. Real-time PCR assays showed that over all, expression of CYP1A1 and CY1A2 was higher in HepG2 than MCL-5 following PhIP exposure for 24h. PhIP was observed to induce a significantly higher mutation frequency in MCL-5 cell lines than untreated control. Mutation type also varied among PhIP treated and untreated control of MCL-5. PhIP treated MCL-5 cells showed predominantly G→T transversions.

These studies showed that cells with higher metabolic activity are relatively more capable of activating B[a]P and PhIP and therefore show higher genotoxicity in response to dose and exposure of these pro-carcinogens. Considering the results of this study, potential risk of B[a]P and PhIP induced cancers has been discussed.

ABBREVIATIONS

<	Less than
>	More than
%	Percentage
n	Number of mutants
p	Probability
h	Hours
A	Adenine
ANOVA	One way analysis of variance
B[a]P	Benzo-a-pyrene
BPDE	Benzo-a-pyrene diol epoxide
C	Cytosine
COM	Committee on Mutatgenicity
cDNA	Complementary DNA
C	Carbon
°C	Centigrade
dd	Dideoxy nucleotide
DNA	Deoxyribonucleic acid
DMSO	Dimethyl Sulphoxide
EDTA	Ethylamine Diamine Tetraacetic acid
H	Hydrogen
HT	Hypoxanthine Thymine
HPRT	Hypoxanthine guanine phosphoribosyl transferase
hsp	Heat shock protein
dH_2O	Distilled water
IARC	International Agency for Research Council
L	Litre
M	Molar
mA	Milliamps
min	minutes
MF	Mutation frequency
Mg	Milligram
ml	Millilitre
µl	Microlitre
µM	Micromole
mM	Millimole
mRNA	Messenger RNA
NADPH	Nicotinamide Adenine Dinucleotide Phosphate Hydrogenase
N	Nitrogen
OECD	Organization for Economic Cooperation and Development
PBS	Phosphate Buffered Saline
PE	Platting efficiency
PhIP	2-Amino-1-methyl-6-phenylimidazo[4,5-b]pyridine
ppb	Parts per billion
RNA	Ribonucleic acid
Rpm	Revolutions per minutes

ROS	Reactive Oxygen Species
RT-PCR	Reverse Transcription-Polymerase Chain Reaction
SDS	Sodium Dodecyl Sulphate
T	Thymine
TTC	Threshold for Toxicological Concern
6TG	6 Thioguanine
6TGMP	6-thioguanine monophosphate

CONTENTS

Chapter 1

General Introduction

The genotoxicity of an agent represents its ability to cause genetic alterations in the target cell/tissue/organ. These genotoxic agents include chemical compounds, air pollutants, nanoparticles and radiation from different sources. Studies to date have shown that several factors including type of agent, dose, frequency of exposure and interaction with the host, etc. influence the ability of an agent to initiate genetic alterations (Millar and Ramos, 2001). The majority of genetic alterations starts with DNA damage in the form of DNA adduct formation leading to alterations in nucleotide sequence such as point mutations, and/or changes in the chromosome number or structure. These alterations if not repaired by the cell could become permanent and trigger carcinogenic processes in the target organ. The DNA sequence within the genes and their arrangement in the chromosomes are highly conserved and any change in sequence or structure may have harmful consequences on the organism. If such mutations occur in germ cells, they tend to cause heritable effects in the offspring which sometime result in the evaluation of a species, but if mutations occur in tumour suppressor genes or proto-oncogenes of somatic cells then they may lead to unregulated cell division and cancer (Loeb and Loeb, 2000). Therefore, genotoxicology deals with the assessment of a chemical's (or agent's) ability to induce such DNA damage in the absence of cell death, because DNA damage is the underlying cause of mutations that promote carcinogenesis as well as other diseases (Loeb and Loeb, 2000)

Genotoxins induce mutations through DNA damage by various mechanisms. Firstly, a genotoxin may form a direct interaction with DNA to produce a lesion and cause mutation e.g. mitomycin C and 4-nitroquinoline-1-oxide interact directly with the DNA helix. Such chemicals are sufficiently electrophilic in nature and have been reported to cause genotoxicity by direct damage to DNA by forming DNA adducts (Lu, 1991). These adduct are capable of covalently binding with the nucleophilic centres of DNA and also with cellular proteins. In some instances these DNA adducts are efficiently repaired, however DNA repair processes are not error-free and some adducts may be missed (or mis-repaired) by the repair machinery. The replication of the unrepaired adducts results in the formation of fixed mutations which appear as mutated cells (Miller and Miller, 1971). DNA damage can also arise via indirect mechanisms, such as when the agents interact with cellular components (other than DNA) and

this leads to indirect DNA damage e.g chemicals promoting reactive oxygen species (ROS) induction which can damage DNA (Wiseman and Halliwell, 1996). Another indirect source of genotoxins is where DNA damage is induced through metabolic activation of the compound into a more toxic form. For example, metabolic activation of polycyclic aromatic hydrocarbons (PAH's) and heterocyclic aromatic amines (HAA's) produce metabolic products which can covalently interact with DNA and form DNA adducts (Dipple, 1984; Hecht, 1999). Such agents are also known as pro-carcinogens; once exposed to eukaryotic cells, cellular mechanisms break down these agents into by-products that are sometimes able to bind with DNA to initiate carcinogenic processes (Guengerich, 2000; IARC, 2010).

1.1 Mutations results from DNA damage

Mutations can be caused by exogenous (environmental) and endogenous (errors in the cellular systems of the cell) factors. The physical or chemical substances that induce mutations in DNA are defined as mutagens and the mechanism is called mutagenesis. Exogenous sources of DNA damage include exposure to UV radiation from sun which causes cross-linking between adjacent pyrimidinse (Cytosine and Thymine) bases in the DNA strand (Ravanat *et al*, 2001). Another environmental source of mutation is ionizing radiation (X-rays) that produces free radicals within the cells that lead to the formation of ROS and results in DNA strand breaks or apurinic/apyrimidinic sites. Certain chemicals like alkylating agents and aromatic amines are also exogenous sources and cause small alterations in DNA. Alkylating agents like ethylmethanesulfonate (EMS) alter the base's structure which results in specific DNA mispairing. Some chemicals act as a base analogue and are incorporated into the DNA in place of normal bases, and cause mispairing of DNA, for example, 5-bromouracil is an analogue of thymine and 2-amino-purine is an analogue of adenine (Griffiths *et al*, 2000). Mispaired DNA bases form fixed mutations when the DNA strand is replicated and an incorrect base is incorporated opposite the DNA lesion. In addition to these environmental factors, chemicals in foods also cause DNA damage and produce alterations (Ames *et al*, 1995; Marnett and Plastaras, 2001).

DNA damage can also result from endogenous sources including DNA replication errors, spontaneous lesions and transposable genetic elements. The major endogenous processes that lead to significant DNA damage are:

- Oxidation of bases, like 8-oxo-7,8-dihydroguanine (8-oxoG) induced by reactive oxygen species that lead to DNA strand breaks (Shibutani *et al*, 1991). These ROS are

induced in cells during normal physiological processes such as respiration and enzymatic reactions.

- Methylation, such as formation of 7-methylguanine or O^6-Methylguanine (Ames *et al,* 1991). This methyl group comes endogenously as a result of enzymatic reaction of O^6-methylguanine-DNA methyltransferases
- Hydrolysis of bases such as depurinations, depyrimidations and deamination (cytosine to uracil). It has been estimated that each cell undergoes 10,000 depurination per day (Lindahl and Nyberg, 1972).
- Bulky adduct formation e.g. benzo[a]pyrene diol epoxide –dG adduct. These DNA adducts are formed due to the cellular CYP450 enzymatic reactions

It appears that irrespective to the source of DNA damage, the mechanism by which these agents can cause mutation generally involves the incorporation of a base change into the DNA, where they have the propensity to mispair (Griffiths *et al*, 2000) and cause DNA mutation. If these lesions occurred at high frequency then there is a possibility of missing/escaping DNA repair mechanisms and the production of fixed mutations during replication by DNA polymerases (Loeb and Cheng, 1990).

1.2 Type of mutations

Mutations can appear at different genetic levels and they can range from small changes arising from a single nucleotide change to large chromosomal changes. Gene mutations are well documented because such mutations may initiate the cancer events (Knudson, 1971; Loeb and Loeb, 2000).

1.2.1 Gene mutations

Gene mutations appear as a result of changes in the small stretches of nucleotides in DNA. These mutations manifest themselves in the malfunctioning of genes and appear as following:

Point mutations

Point mutations usually occur when only one base substitution alters. Point mutations include transitions and transversions. A purine base is replaced by another purine (adenine or guanine) in transitions, and in transversions, a purine is replaced by a pyrimidine (thymine and cytosine) or *vice versa* (Pecorino, 2006). Such mutations may be silent (no change in amino acid sequence or cell phenotype), missense (abnormal protein function due to change in amino acid) and nonsense (change in triplet codon to a stop codon leading to a non-

functional protein). The reading frame of DNA is read in a triplicate code; therefore if a base sequence is altered due to either an insertion or deletion, the code will be changed completely. This is termed a frameshift mutation. Sometimes at the third position of codon is referred to as the wobble position. At this position Uracil (U) and Cytosine (C) may be read by a Guanine (G) in the anticodon. Similarly Adenine (A) and Guanine may be read by Uracil. In tRNA there is one modified nucleotide is Inosine (I). If tRNA contains I in the anticodon at the wobble position, this tRNA may read codons having A, U and C in the third position. This could be a potential source of translation error, if the mismatch were to cause the wrong amino acid to be incorporated into the protein.

Deletions

Deletions can be single base deletion or more. But the deletion of DNA can manifest when exons are skipped during mRNA maturation which results in the loss of information for protein translation.

Insertions

An insertion mutation is caused by an insertion of one or more nucleotide into the DNA sequence. This type of mutation occurs due to polymerase slippage in repeated sequences during DNA replication.

1.2.2 Chromosomal Mutations

Mutations can also affect large segments of DNA (>1kb) and can encompass sizeable segments of chromosomes and even whole chromosomes.

Change in chromosome number

In this type of mutation, also called aneuploidy, gain or loss of a chromosome(s) takes place. The mechanism of aneuploidy in the cell is often due to the failure of the chromosomes to separate equally into the daughter cells. It appears as a result of abnormal disjunction during meiosis in gametocytes and during mitosis in somatic cells. Indirect genotoxins (aneugens) such as carbendazim, colchicine, nocodazole and mebendazole modify the spindle of the dividing cells leading to improper chromosome segregation in the daughter cells. Such imbalance of the genetic information is the reason for many reproduction failures (Boue and Lazer, 1975), cancer (Boveri, 1914) and other hereditary genetic defects (Korenberg, 1994).

Change in chromosome structure

This mutation appears due to addition or deletion or re-arrangement of a fragment(s) of a chromosome, also known as clastogenicity. The following are the most noticeable chromosomal structural mutations (Figure 1.1).

1. Deletion or insertion

   The loss of a chromosomal segment is called deletion. Chromosome deletions often occur due to double strand breaks separating a fragment from the end of a chromosome, which is not incorporated into the daughter nuclei. These are often seen as micronuclei in the cytoplasm.

2. Duplication

   The presence of two copies of a chromosomal region is called duplication. They occur by misreplication, amplifying the DNA sequence contained within.

3. Inversion

   A segment of chromosome is reversed in orientation and rejoins the chromosome.

4. Translocation

   A segment of chromosome is exchanged for another part of a different chromosome. This occurs in two stages; firstly double strand breaks lead to deletion events and the fragments are then wrongly joined to another chromosome.

The location of the mutation within a gene will determine the resulting consequence. If the mutation arises within the promoter region, this may result in the change of expression of that gene, causing either an over expression or under expression of that particular gene product. On the other hand, a mutation within the coding region of the gene may result in the protein product of the gene having altered structure and function (Pecorino, 2006).

1.2.3 Mutations and cancer

In normal cells mutations are occurring at a rate of 10^{-10} mutations per nucleotide per cell per generation (Jackson and Loeb, 2001) and it has been estimated that between four and seven mutations in key genes are necessary to produce most human cancers (Sarasin 2003). There is a correlation between mutation rate and cancer, as mutations are essential for cancer evolution. Cancer is a genetic disease with cells containing multiple mutations, indicating that tumour progression is driven by mutagenesis (Sarasin, 2003; Loeb and Loeb, 2000). As an early event of carcinogenesis, mutations occur in genes which maintain genetic stability in normal cell leading to a generation of pre-cancerous cells with genetic instability resulting in a cascade of mutations some of which enable cancer cells to bypass the host regulatory

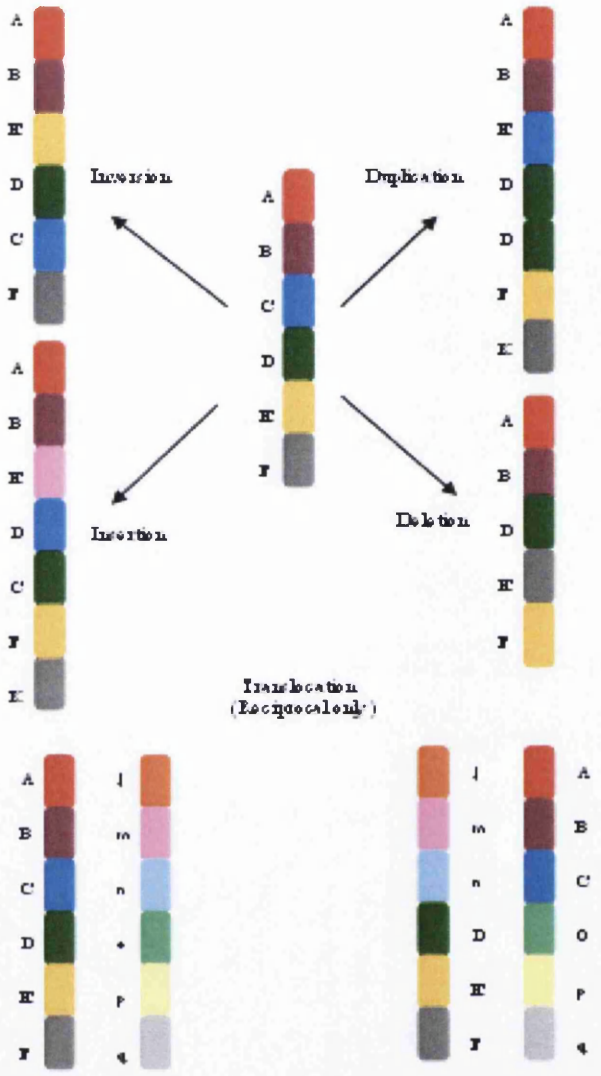

Figure 1.1 Modification of chromosome structure by insertion, deletion, duplication, inversion and translocation. Modified figure from www.tutorhelpdesk.co.uk.

processes that control cell progression, gene adaptation and apoptosis (Loeb and Loeb, 2000). Normal mutation rates followed by selective advantage of mutated clones are enough to produce the numerous mutations found in human cancers (Sarasin, 2003; Loeb *et al*, 2003). A number of exogenous sources introduce mutations into DNA at a much higher level than spontaneous and therefore, it is important to detect substances which pose a risk to the human population. Genetic toxicology is the field that aims to test chemicals for their genotoxic, mutagenic and carcinogenic potential (Loeb and Loeb, 2000).

1.3 Genetic toxicology and hazard identification

Human populations are surrounded by a vast array of genotoxic agents and therefore it is important to determine genotoxic potential of the compounds with which we come across as

part of our daily life, in order to ensure safe exposure. Knowledge and awareness of genotoxic potential is not only useful to categorize and regulate these agents but also helps to devise strategies on safe use and/or protection against these agents (Doak *et al*, 2007).

Genotoxicity of a chemical is determined by *in vitro* (mammalian) and *in vivo* (animal models) tests. Initially, genotoxicity was only associated with external agents, however, later studies showed that endogenous processes and viruses could also lead to carcinogenicity (Peyton, 1911). The first step in determining risk to humans is to identify the hazardous compound; therefore, The International Agency for Research on Cancer (IARC, 2010) has developed several groups to categorize carcinogens:

Group1: Carcinogenic to humans

Group 2A: Probably carcinogenic to humans

Group 2B: Possibly carcinogenic to humans

Group 3: Not classifiable as to its carcinogenicity to humans

Group 4: Probably not carcinogenic to humans

Genotoxicology assays provide vital information on the effect of a genotoxin on the target, the dose dependant responses, possible mode of action and potential damage to DNA. Mode of action appears to play an important role in determining risk of any genotoxin, therefore, it is important to undertake specific genotoxic assays to gain a better understanding of the effects of genotoxins.

1.4 Regulatory genotoxicity testing

In vivo and *in vitro* genotoxicity tests are designed to detect compounds which induce genetic damage directly or indirectly by various mechanisms. Many countries have developed guidelines for testing the genotoxicity of new chemicals to ensure the standardisation of assay methodology. No single test alone can predict the entire spectrum of inducible mutations, because of the variety of genetic events that can occur (Cimino, 2006). There is a general consensus that genotoxicity testing should consist of two stages i.e. stage 1 involving basic *in vitro* tests and stage 2 involving *in vivo* genotoxicity testing on compounds observed to be positive in stage 1 testing (COM, 2000). In 2011, the Committee on Mutagenicity (COM) also recommended to consider stage 0 that involves preliminary considerations on the physio-chemical properties of the test agent.

Stage 1 assays are based on *in vitro* testing such as:

- a bacterial gene mutation assay (Ames test) which uses strains of *Salmonella typhimurium* and *Escherichia coli* that require specific amino acid supplements to

detect point mutations. Initially these tests were conducted on agar plates, however, further developments of the procedures led to development of a more robust system known as the fluctuation method. The fluctuation method uses liquid culture medium in a 96 well plate format and mutation frequency is counted by scoring the number of wells that turn yellow from purple. Several commercial kits are available which use this test and thus offer a high throughput screening procedure. These kits are also available with rat liver S9 fraction supplements to mimic mammalian metabolic conditions. There are different genotoxic end points that are required to be assessed, therefore, it is recommended to use more than one test to detect genotoxic potential of any agent. Bacterial gene mutation assays are therefore combined with:

- *In vitro* micronucleus assay to assess chromosome damage. This method is the most popular for genotoxicity testing because it has an ability to measure both chromosome number changes and chromosome breakage, is simple to score, accurate, and widely used in different cell types.

These assays help to determine the hazard of a test agent with respect to DNA damage, gene mutations, chromosome damage and aneuploidy (COM, 2011). In the case of a negative result at stage 1, stage 2 testing is normally not required, however, if the test agent is believed to have a prolonged human exposure then stage 2 testing may be considered.

A positive result in stage 1 would lead to further investigation using *in vivo* testing. Stage 2 test involves a variety of assays and a testing strategy is decided on a case to case basis. The rodent chromosome aberration assays to investigate aneuploidy and clastogenicity and the rodent transgenic gene mutation assay and/or comet assay for DNA damage induction are most commonly used in stage 2 (COM., 2011).

1.5 Dose-response relationships

Genotoxic potential of any chemical is assessed by dose dependant responses whereby the effect of different doses is used to assess its ability to cause genotoxicity. Results of dose dependant studies are then used to plot dose-dependent curves. The shape of the curve reflects the dose related potency of the chemical. Regulatory bodies use the shape of the dose dependant curve in determining recommendations for the chemical. The different shapes of dose-response curves are shown in Figure 1.2.

Linear, supralinear and sublinear responses are shown for DNA adducts that may lead to mutations involved in initiation of cancer (Swenberg *et al*, 1995).

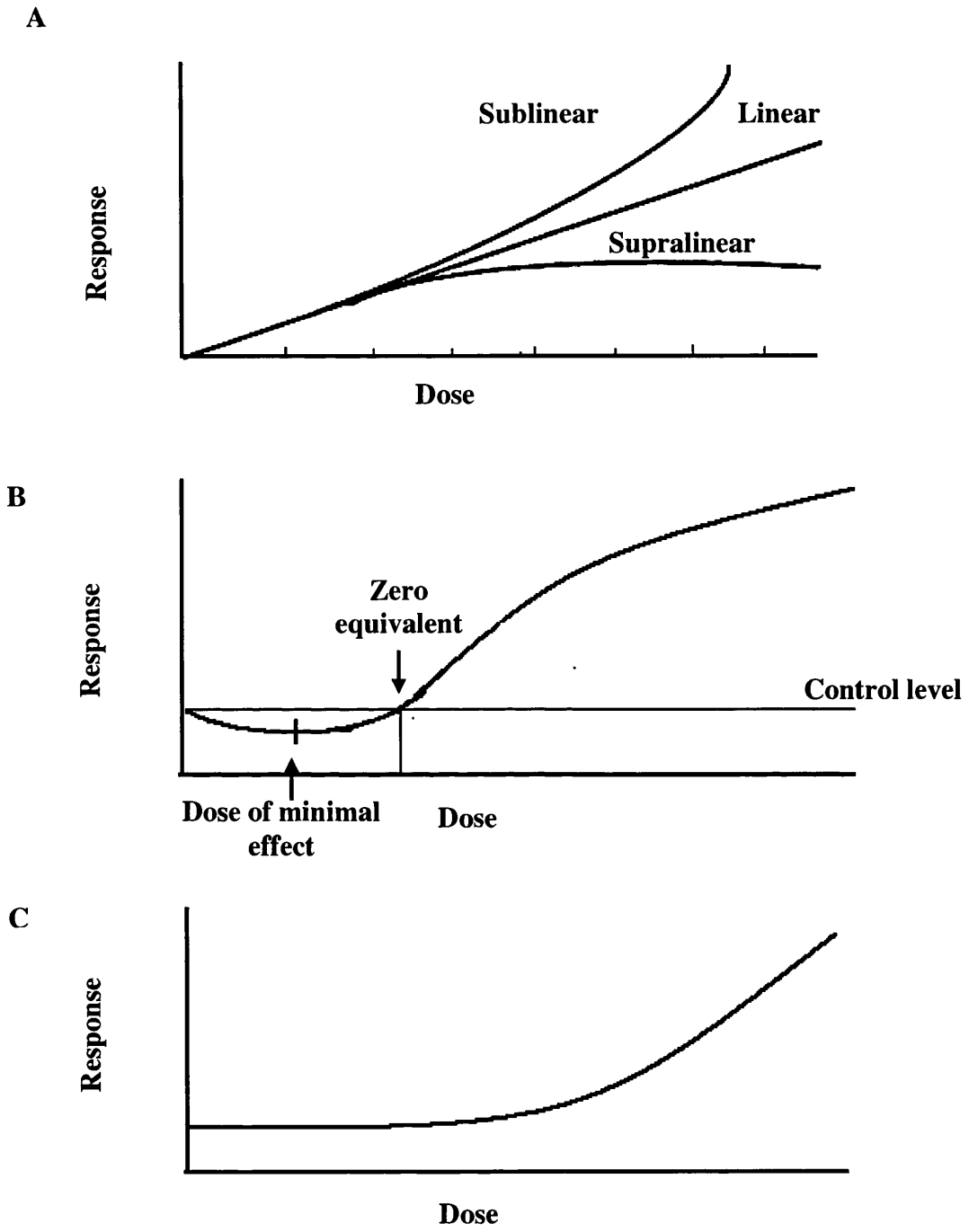

Figure 1.2 Theoretical dose-response curves. A- Sublinear when detoxification or DNA repair is saturated, Linear when there is no safe exposure and Supralinear when metabolic activation is saturated. B- J-shapes curved then there is hormesis and C- Threshold dose response. Modified from Lutz, 1998 and Swenberg *et al*, 1995.

1.5.1 Supralinear and sublinear

Generally supralinear and sublinear mutations are distinguished at higher doses whereas linearity appears at low doses of chemical. Supralinear dose-response can appear when saturation of metabolic enzymes are reached. Pro-carcinogens that require metabolic activation to convert into DNA reactive electrophiles, are capable of covalently binding with DNA and form adducts. Supralinear dose-response was observed in rat lungs where higher

concentrations were less effective and causing O^6-methylguanine (O^6MeG) adducts (Swenberg *et al*, 1995). These effects could be attributed to cell death due to toxicity at higher doses thus removing damaged cells from population (Supralinearity). Sublinearity could involve an increased adduct fixation through increased cell division in response to cytotoxic doses of genotoxin (Lutz, 1990).

1.5.2 Linear dose-response

The linear dose-response was described after the discovery of x-ray induced mutations in Drosophila by Hermann J. Muller in 1927 (Calabrese, 2009). The hypothesis of a linear dose-response relationship without a threshold at low doses was proposed on the basis of single-hit model of action (Crebelli, 2000) based on historical work with ionising radiation (UNSCEAR, United Nations Scientific Committee on the Effects of Atomic Radiation, 1958). Recently this model was extended to chemical mutagens, based on the theory that the interaction of a single molecule of a mutagen with DNA is sufficient to cause a mutation that can potentially trigger a carcinogenic process (Knudson, 1971). It is now known that not all DNA damage cause mutations (Swenberg *et al*, 2008), but there are some cases where mutagenicity is proportional to DNA damage due to poor adduct repair or increased mispairing potential during DNA replication, such as for aflatoxin B1 or benzo[a]pyrene (Crebelli, 2000).

According to the regulatory bodies, the linear model is a default prediction of low dose adverse effects in response to genotoxic carcinogens meaning that there is no safe level of DNA damage, there is no safe level of exposure. It was also assumed that the direct acting genotoxins (including clastogens) have a linear relationship between exposure to genotoxin, DNA damage and induction of mutation (Henderson *et al*, 2000). Linear models could be applied to all the chemicals but not for aneugens and non-genotoxic carcinogens, due to their mode of action that affects cell division and/or loss or gain of whole chromosomes (Calabrese, 2009).

1.5.3 J-shaped dose response

Many toxicological studies have observed a biphasic dose-response where there are decreases in the response (measured as genetic damage) to levels below the negative control at low doses followed by a substantial increase in measured damage at high doses. This biphasic response is called a J-shape or U-shape dose-response and the concept is called hormesis. In some cases hormesis (also referred to as an inverted U shaped dose-response) arises as a consequence of low doses of a chemical causing stimulation (e.g. of repair) and high doses

causing inhibition of cellular processes such as growth and reproduction or cell proliferation (Calabrese and Baldwin, 2001). In toxicology, hormesis is illustrated by a J-shaped curve, reflecting that low doses give a lower response compared to the negative control and high doses reflect the occurrence of endpoints in the form of cancer incidence. It was observed that when fore-stomach and kidneys of the male F344 rat were exposed to caffeic acid it produced a J-shaped dose-response due to the cell proliferation that induced tumour formation (Lutz *et al*, 1997).

It has been postulated that all synthetic and naturally occurring chemicals are toxic at high doses and at low doses all chemicals have a hormetic effect (Rozman, 2005), making linear risk assessment models obsolete. So far 1600 toxicological dose-response relationships are in agreement with the hormesis hypothesis (Calabrese and Baldwin, 2001). Hormesis was interpreted as an adaptive response characterized by biphasic dose responses. Induction of DNA repair is an adaptive response to DNA damage. The hormetic dose-response represents the effects of a repair process that slightly overshoots the original homeostatic set point to result in a low-dose stimulatory response (Calaberase, 2009). For example, *Escherichia coli* bacteria treated with low level of alkylating agent N-methyl-N-nitro-N-nitrosoguanidine (MNNG), induced mutations for 20min and then become resistant due to the induction of the repair of O^6-methylguanine (Cairns, 1980). Similar DNA repair capability was observed when the liver of rats was exposed to nitrosamines (Lutz, 1982).

1.5.4 Threshold dose-response

In genetic toxicology, dose and frequency of exposure to a genotoxic agent plays an important role in determining the level of DNA damage. Therefore, even at lower doses for many chemicals there is a risk of genetic damage and response can be linear or non-thresholded (Kirsch-Volders *et al*, 2000). However, many studies have reported a non-linear dose dependant response for most genotoxic agents, which have non-DNA targets, e.g. nocodazole, colchicine, carbendazim (Elhajouji *et al*, 2011). These studies showed no or little effect below a certain dose and thus supporting the theory of a threshold existence. These studies concluded that depending upon the chemical involved no observable effect is seen below a certain dose and this dose or concentration was termed as a No Observable Effect Level (NOEL). As the concentration of chemical increases from a NOEL, a statistically significant genotoxic effect is observed and thus these doses were referred to as Low Observable Effect Level (LOEL) e.g. a study examining low dose genotoxicity of MMS and EMS in the human cell line AHH-1 reported NOEL concentrations of 0.85 and 1.40μg/ml for MMS and EMS,

respectively ($p<0.05$) above which, increases in chromosomal damage were observed in the form of micronuclei formation (Doak *et al*, 2007).

Considering the variability in cell types and protective mechanisms within cells, it is understandable to expect some degree of variation in NOEL and LOEL values; therefore, for *in vivo* data in order to obtain safe exposure levels, regulators use a variation factor of 100 to establish NOEL and LOEL for each compound. The critical dose (often the NOEL) is divided by 100 to obtain a safe exposure level. This 100 value takes into account and represents 10 times variability within species and another 10 times factors is applied to counter any variation among humans (WHO, 1987).

The threshold model was used in 1920/1930s in establishing radiation health standards. In 1928 the International Committee on Radiation Protection (ICRP) recommended a tolerance dose 1/100 of a 600r of erythema dose in 30 days for occupational radiation exposure. Similarly the second radiation standard report was published in 1934 by The National Council on Radiation Protection and Measurement (NCRPM), stating that a safe whole body exposure is 0.1r/day for hard x-rays (Calabrese, 2009).

The concept of thresholds in genotoxicity has been discussed extensively and it has been accepted for aneugens, topoisomerase, and polymerase inhibitors on the basis of experimental data and mechanistic reasons (Elhajouji *et al*, 2011). Recent studies with alkylating agents such as MMS and EMS support the existence of threshold dose-response for clastogens (Doak *et al*, 2007). There are many biological mechanisms which are induced at low doses such as redundant targets, detoxification and error-free DNA repair which are involved in establishing the threshold dose response (Jenkins *et al*, 2005). However, the acceptance of threshold is based on a case-by-case basis together with strong experimental evidence, along with understanding of the mechanisms involved in the mutagen-target interactions (Elhajouji *et al*, 2011).

1.5.4.1 Definitions of Threshold

A threshold dose is a dose of chemical below which it does not induce any effect after exposure although it has a potential to induce it (Kirsch-Volders *et al*, 2000). In toxicology, biological or practical threshold is an actual dose below which there was no dose- response. This type of threshold is characterised by the inflection point which is the point where the change in the gradient is at its maximum (Johnson *et al*, 2009). For the better understanding of threshold dose response it is important to calculate the NOEL and LOEL. According to the European Centre for Ecotoxicology and Toxicology of Chemicals (ECETOC) definition, an

absolute threshold is "a concentration below which a cell would not 'notice' the presence of the chemical. In other words, the chemical is present but does not interact with the cellular target". This is almost impossible to measure. The 'pragmatic' threshold is a concentration below which any effect is considered biologically unimportant (Lovell, 2000) (Figure 1.3) and often leads to no increase in adverse event (DNA damage) above the background level.

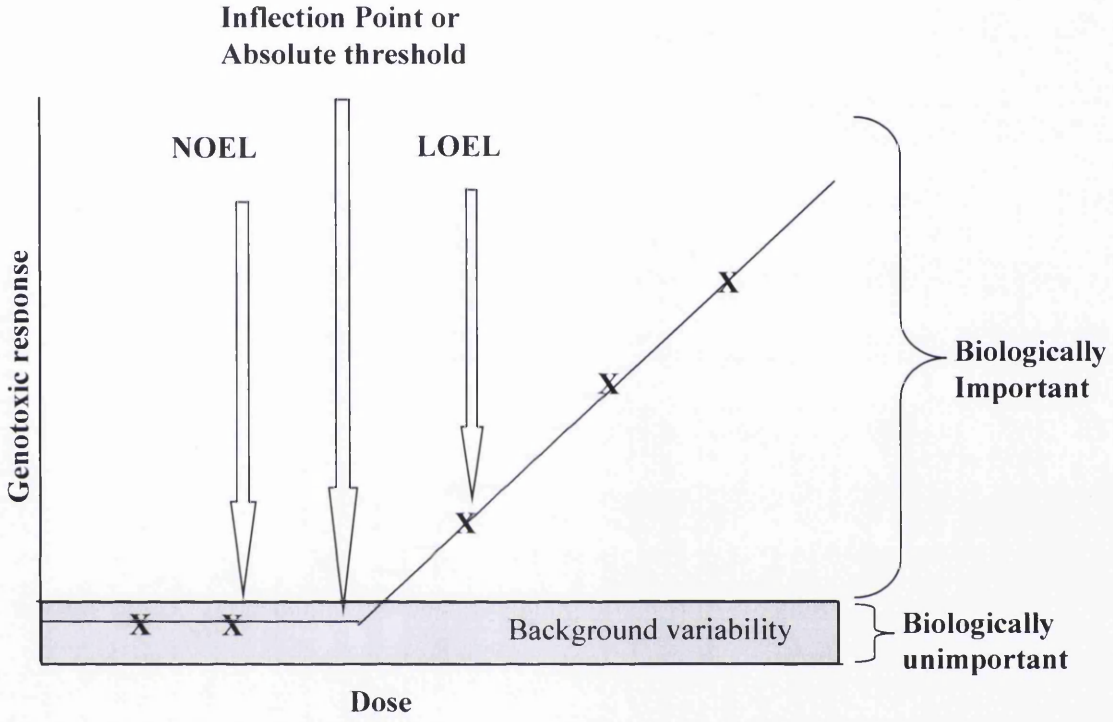

Figure 1.3 The dose-response curve showing the absolute threshold. Modified from Johnson *et al*, (2009) and Lovell, (2000).

The threshold values can be estimated by using statistical approaches, based upon the identification of no observed (adverse) effect levels (NOAEL) or lowest observed (adverse) effect levels (LOAELS) (Lovell, 2000). A NOAEL is the highest dose that does not cause an adverse effect, whereas the LOAEL is the lowest dose that causes the adverse effects (COT-IGHRC, 2007)

According to Lutz (1998) a true threshold dose is a point in the dose response curve where a slope 0 changes into a slope >0. It is difficult to find a true threshold for a substance which has variable background rate. However a practical threshold dose can be set from the linear part of the dose-response curve hidden within the background variability (Lutz, 1998) (Figure 1.3-Shaded area represent the background variability). The background value is always variable for every biological mechanism (Kirsch-Volders *et al*, 2009). The NOELs and LOELs are heavily dependent upon dose spacing, more doses, and more accurate responses.

Nowadays, a threshold level is commonly used to determine or establish a safe limit of a chemical for human use. In toxicology in general, thresholds are accepted but the linear argument has dominated. This threshold limit is derived from dose dependant responses, mathematical and statistical models so as to cover any variability. Typically a threshold level is a value between NOEL and LOEL (Kirsch-Volders *et al*, 2009) and can be confirmed by mathematical modelling and statistics (Jenkins *et al*, 2005). In another assumption, a threshold corresponds to the inflection point between the first statistically significant and the last non-statistically significant concentrations, and can be estimated by using mathematical modelling (Lynch *et al*, 2003). Toxicity testing recommendations such as recent COM guidelines (2011) state however that the justification of the threshold utilising statistical modelling is not enough and the biological mechanisms involved in establishing the threshold also need to be assessed (Lynch *et al*, 2003).

1.5.4.2 Mechanisms of threshold

There are significant differences in the mechanisms involved in thresholds for non-DNA damaging agents and DNA-damaging agents (Jenkins *et al*, 2005). The interpretation of the threshold results for all types of end points are dependent on (1) the number and identity of the targets (2) the mode of interaction between the target and agent and (3) the quantification of the end point and its sensitivity (Kirsch-Volders *et al*, 2000).

Kirsch-Volders *et al* (2000) further described the relationship between the mutagen, the target and the endpoint and proposed the following models depending upon the mode of action of mutagen and interaction with the target. These models included;

- Single hit, single target: whereby a single change in one base can lead to mutation. This model represents no threshold levels as any concentration of mutagen is able to bring about mutations in the absence of repair mechanisms. In this model, mutations are defined as a DNA lesions leading to alterations in a gene or chromosome.
- Single hit, multiple targets and multiple hit, single target: represents a variety of scenarios where a single hit on multiple targets or multiple hits on a single target produces a dose dependant response exhibiting theoretical threshold levels (Kirsch-Volders *et al*, 2000). This model involves multiple events to bring alterations in α and β tubulins, topoisomerase, K+ and Ca+ channels and spindle nuclear membrane.

Since these models require multiple interactions and events, several protective mechanisms such as detoxification of the genotoxic agents, exclusion from the cell or nucleus, conjugation, DNA repair of the induced damage, apoptosis or necrosis can influence threshold

levels (Jenkins *et al*, 2005). Another mechanism involved in producing the threshold is DNA redundancy in which some DNA mutations are in redundant parts of the genome (inter-genic regions or introns) and do not alter protein function. Also noted with redundant non-DNA targets, e.g. the effect in spindle fibres, where many need to be damaged to disrupt chromosome segregation (Jenkins *et al*, 2005).

1.5.4.3 Endpoints and their sensitivity

The threshold dose can be used for various genetic endpoints such as DNA adducts and DNA and chromosome damage (Kirsch-Volders *et al*, 2003). If the endpoint involves a different target, three different levels can be considered at the cellular level namely:

Proximal: the point is close but still different from the target, for example gene mutations, chromosomal structural mutations;

Intermediate: the endpoint is separated by some steps from the target, for example analysis of repair and metabolic pathways; and

Distal: the end point is the result of the complex alterations of cellular activities, after the initial interaction of compound with the target, such as apoptosis, necrosis and cell survival (Kirsch-Volders *et al*, 2003). The main endpoints for the analysis of threshold dose response are DNA adducts formation, gene mutation and chromosomal aberration.

A genotoxic threshold indicates that chemical will not produce any mutation below a critical exposure level and therefore, reduces the risk for the induction of cancer.

1.6 Genotoxic threshold for carcinogens

Carcinogenic compounds that lack the ability to induce DNA damage directly or indirectly (Cohen, 2004) and have multiple cellular targets in humans and animals are known as non-genotoxic. It is now generally accepted by the scientific community and regulators that NOELs exist for chemicals that are non-genotoxic carcinogens, such as hormones and tumour promoters (Madle *et al*, 2000). Non-genotoxic carcinogens are considered to have a "real threshold" (reviewed by Kirsch-Volders *et al*, 2000).

1.6.1 Genotoxic threshold for non-DNA reactive genotoxins

The carcinogenic effect of non-DNA reactive chemicals may include an increase in cell proliferation or modification of multiple cellular targets, lipid peroxidation, protein adduct, inhibition of repair enzymes, proteins controlling cell cycle, apoptosis related genes, defense proteins against oxidative damage, metabolizing enzymes and tubulins of the mitotic or

meiotic spindle. Capen (1998) identified that thyroid-stimulating hormone (TSH) increased the mitogenic effect in rat follicular cells that appeared in the form of increased cell numbers (IARC WG, 1999) or because of toxicity and regeneration in rodents i.e. sodium saccharin (Cohen *et al*, 2004), melamine, chloroform, d-limonene (Cohen and Arnold, 2011). Other non-DNA reactive genotoxins include spindle poisons such as nocodazole (Elhajoujii *et al*, 1995) which induces tumour in humans. All of these agents have dose response relationships between exposure and tumour formation in animals (Cohen and Arnold, 2010). According to previous regulations of non-DNA reactive genotoxins, these compounds do not have a threshold mode of action. It was proved with more research that there are exceptions to this and that needs justification (Madle *et al*, 2000). Currently there are few examples of non-DNA reactive compounds having a threshold mode of action e.g. spindle poisons such as carbendazim, colchicine, nocodazole and mebendazole (Elhajoujii *et al*, 1995; Kirsch-Volders *et al*, 2003). Mechanistically relevant thresholds for non-DNA reactive chemicals have only been shown *in vitro* (reviewed by Kirsch-Volders *et al*, 2003) and these include aneugens, (Elhajouji *et al*, 1995), spindle inhibitors (Elhajouji *et al*, 1997) and topoisomerase II inhibitors (Lynch *et al*, 2003). A "statistical" or "apparent" threshold has been attributed to these types of chemicals (reviewed by Bolt *et al*, 2004) because they are connected with rapid degradation and other mechanisms that reduce the target exposure (reviewed by Kirsch-Volders *et al*, 2000).

1.6.2 Genotoxic threshold for DNA reactive genotoxins

DNA acting genotoxins are believed to cause DNA damage by "one hit" theory therefore the concept of a threshold for direct acting agents (e.g ionizing radiation and alkylating agents) has generally not been accepted by regulatory authorities (Kirsch-Volders *et al*, 2000), however, new evidence is changing that attitude. For such agents, a linear non-threshold (LNT) model is usually applied whereby DNA damage at any level is considered unsafe (Henderson *et al*, 2000). On the other hand, most researchers believe that a threshold may exist as cells may also tolerate low levels of damage. This exposure to low levels could arise exogenously (from diet e.g. heterocyclic amine) or endogenously (oxidative stress).

The ability of organisms to tolerate low levels of chemicals has highlighted the need to assess each chemical for the existence of a threshold on an agent-by-agent basis (Jenkins *et al*, 2005). Due to uncertainty of certain chemical carcinogens, a LNT extrapolation is assumed as a precaution. Based on discussions by Streffer *et al,* (2004), Bolt and Degen (2004) proposed

a flow scheme to aid in the risk assessment of the four basic types/groups of chemical carcinogens (Figure 1.4). The four groups include:-

A: Genotoxic carcinogens, that are non-thresholded and therefore a LNT model is applied for low-dose assessment. The ALARA principle ("as low as reasonably achievable"), technical feasibility and socio-political considerations all contribute to the regulation of these chemicals. An example of a chemical that fits this group is Aflatoxin B_1 (European Commission, 2006; Streffer *et al*, 2004).

B: Genotoxic carcinogens, where we can not adequately support the existence of a threshold. A LNT extrapolation is applied based on the precautionary principle which aims to protect humans in the absence of full scientific knowledge. Acrylamide is an example of a borderline case (Committee on toxicity, 2002; Streffer *et al*, 2004).

C: Genotoxic carcinogens which have been shown to have an apparent threshold with the supporting mechanistic data. The NOEL is used to decide health-based exposure limits. Formaldehyde shows an apparent threshold (Streffer *et al*, 2004).

D: Non-genotoxic carcinogens and non-DNA reactive carcinogens show a real threshold. A NOEL can be used to decide health-based exposure limits. An example of a non-DNA reactive genotoxin is nocodazole (Elhajouji *et al*, 1997).

Determination of threshold mechanism varies among non-DNA reactive and DNA reactive chemicals. Multiple targets are involved in non-DNA reactive chemicals, for example Elhajouji *et al*, (1997) reported that colchicine can only induce non-disjunction when concentrations are high enough to damage sufficient molecules to disrupt spindle formation. In case of direct acting agents, DNA repair mechanisms and single hit theory are considered to be significant in determining threshold. Hengstler *et al* (2003) reported that even a single hit of aflatoxin may be able to form a bulky adduct. Direct acting alkylating agents are believed to have a non-linear dose response and thus one hit theory does not apply and there is a safe exposure level and *in vitro* studies by Doak *et al* (2007) and Seager *et al* (2012) support this concept.

1.7 Existence of threshold in Indirect-acting genotoxins (pro-carcinogens)

The indirect-acting genotoxins require metabolic activation and therefore, they are called pro-carcinogens. The pro-carcinogens themselves are not usually carcinogenic, but their metabolism results in by-products that are active carcinogens which interact directly with DNA to exert their carcinogenicity. For example, aflatoxin B1 is hepatically metabolized to

an epoxide intermediate that interacts with DNA causing liver cancer (Smela *et al*, 2001). Similarly in cigarette smoke there are many pro-carcinogens such as PAH's that turn into active carcinogens in lung cells. Since a pro-carcinogen's ability to cause carcinogenetic effects is dependent on cellular mechanisms, therefore, dose dependant responses are believed to be much more complex than those observed in direct acting carcinogenic agents.

As compared to direct acting agents, little is known about the threshold of pro-carcinogenic agents and further studies are required to understand the dose dependant response of chemicals that require metabolic activation to cause carcinogenic effects.

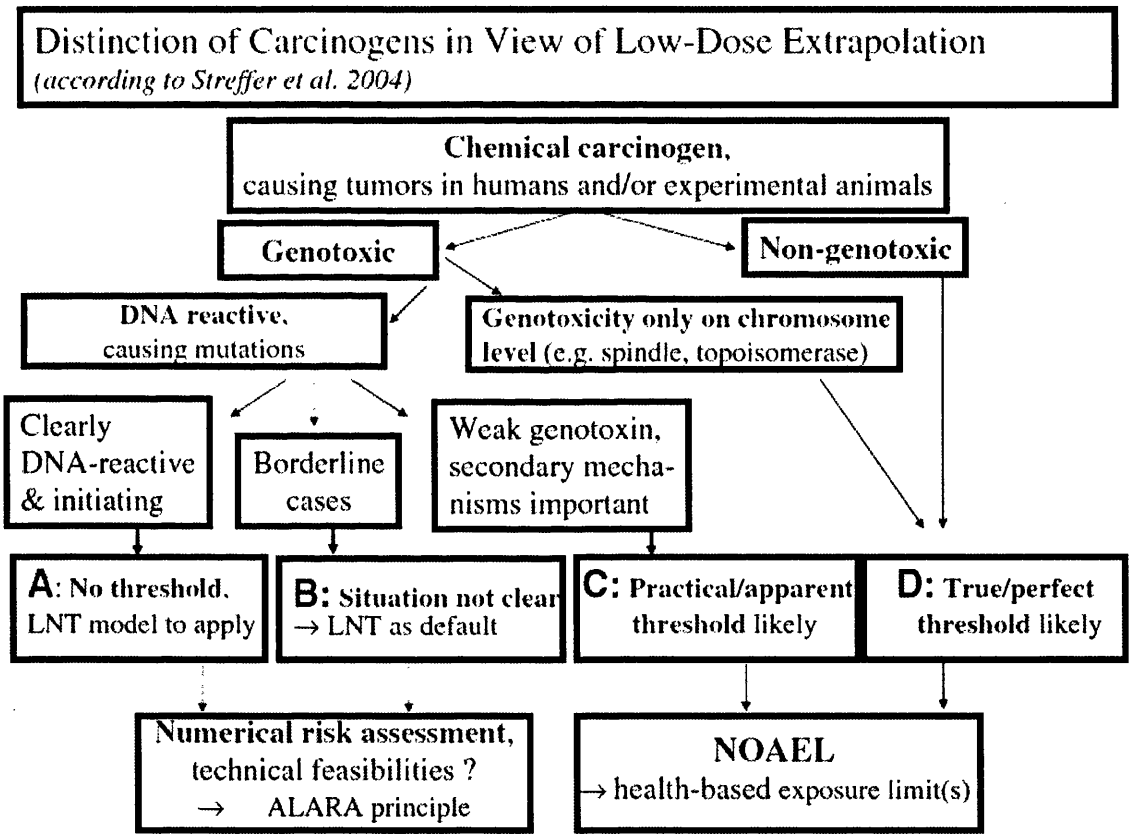

Figure 1.4 Adaption of a flow scheme proposed by Bolt and Degen (2004) according to discussions by Streffer *et al* (2004) for risk assessment and standard setting for chemical carcinogens.

1.7.1 Metabolic activation of pro- carcinogens

The concept of metabolic activation originated in 1960s when Miller and Miller (1966) suggested that 'carcinogens could either be electrophiles as such or are metabolically activated to electrophiles which covalently bind to cellular macromolecules.' Later on DeBaun and team discovered that the aromatic amide, 2-acetylaminofluorene (2-AAF), was metabolically activated to a reactive electrophile, *N*-hydroxy-2-acetylaminofluorene which

reacts with DNA, forming DNA adducts and ultimately leads to mutations in rodents, due to the presence of cofactor 3′-phosphoadenosine-5′-phosphosulphate (PAPS), required by sulfutransferases (SULTs) (DeBaun *et al*, 1968).

A variety of metabolic processes have been identified in the activation of many classes of carcinogens, primarily involving cytochrome P450 enzymes (Guengerich, 2000). Other enzyme systems were also identified that participate in the metabolism of various carcinogens. All of the enzymatic pathways involved in the metabolisms have different kinetics and saturation levels (Guengerich, 2000).

Some metabolic processes lead to the activation to reactive electrophiles but some may lead to inactivation of the chemicals by increasing aqueous solubility that is excreted through urine or faeces. Therefore exposure to any chemical initiates competing metabolic pathways for activation versus inactivation due to the differences in levels of each of the enzyme processes in human individuals, variability in induction and environmental influences on induction or inhibition of enzymes (Boddy and Ratain, 1997).

1.7.2 Cytochrome P 450 enzymes and carcinogenesis

Cytochrome P450 enzymes are primarily found in liver cells but are also located in cells throughout the body. Within cells, cytochrome P450 enzymes are located in a structure involved in protein processing and transport (endoplasmic reticulum) and the energy-producing centres of cells (mitochondria). The enzymes found in mitochondria are generally involved in the synthesis and metabolism of internal substances, such as steroid, hormones, cholesterol and other fatty acids. The enzymes in the endoplasmic reticulum usually metabolize external substances, primarily medications and environmental pollutants (Nebert and Russell, 2002). These enzymes produced from the cytochrome P450 genes are involved in the formation (synthesis) and breakdown (metabolism) of various molecules and chemicals within cells. (Nebert and Russell, 2002; Guengerich, 2008)). There are approximately 60 CYP genes in humans.

Each cytochrome P450 gene is named with CYP, indicating that it is part of the cytochrome P450 gene family. The gene is also given a number associated with a specific group within the gene family, a letter representing the gene's subfamily, and a number assigned to the specific gene within the subfamily. For example, the cytochrome P450 gene that is in group 1, subfamily A, gene 1 is written as *CYP1A1(*Nelson *et al*, 2004). All cytochrome P450 are part of a superfamily and divided into families, sub-families and individual P450s according to the identity of their amino acid sequences. The major CYP's; 1A1 and 1A2 enzymes are involved

in the metabolism of polycyclic aromatic hydrocarbons and heterocyclic amines, nitrosamines, azo-dyes and alkylating agents (Gonzalez and Gelboin, 1994).

When carcinogens enter into a body, they undergo several metabolic pathways. It is metabolized by the Phase I enzymes that include microsomal CYP families and epoxide hydrolases. The metabolites are further modified by the Phase II enzymes includeing UDP-glucuronosyltransferase (UGTs), sulfutransferases, glutathione S-transferases and N-acetyltransferases. These metabolic pathways result in inactivation or detoxification. In this pathway, after carcinogenic exposure, the cell metabolize the carcinogen and converts it into an activated form or discharges it through a specific transport system or converts the metabolites into more active or toxic intermediates that may form DNA–adducts and result in mutations which may lead to cell death or cancer when DNA repair mechanisms fail to fix the damage (Gonzalez and Gelboin, 1994) (Figure 1.5).

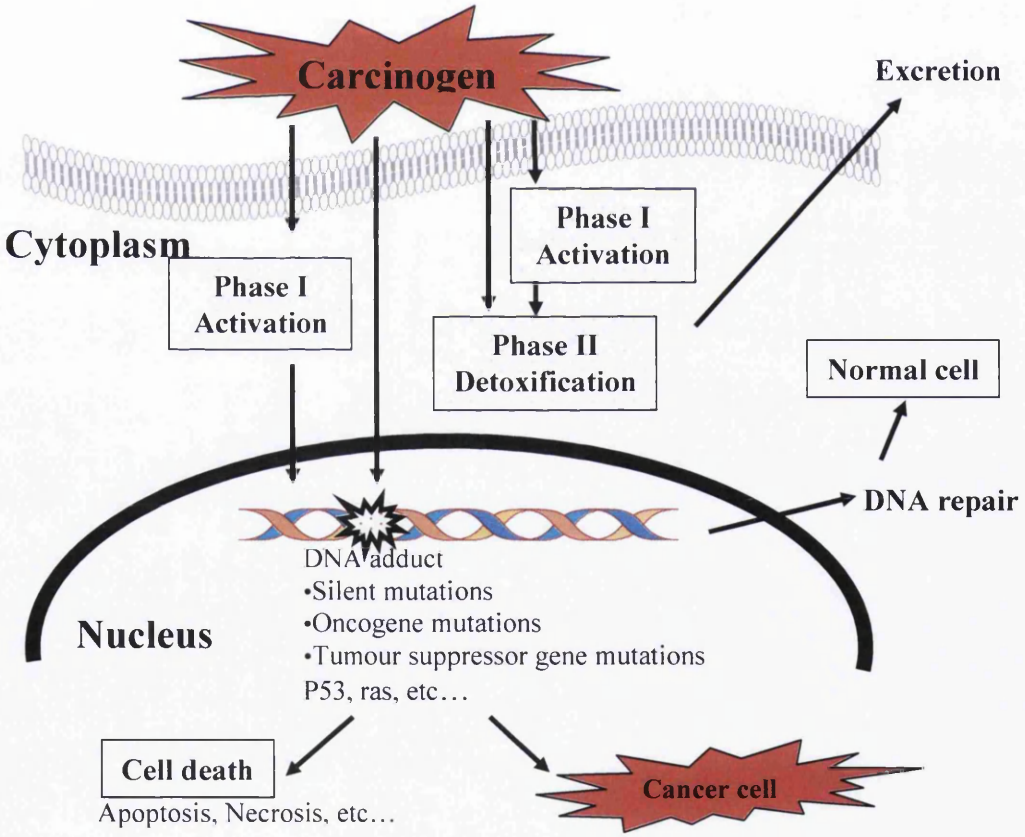

Figure 1.5 Activation and detoxification pathway of carcinogens. Figure modified from Oyama *et al*, (2004).

1.7.3 CYP450 and genetic polymorphism

The frequency of variants at a gene locus when occurring greater than 1% of the same population is termed a genetic polymorphism (Vineis and Porta, 1996). Various

epidemiological studies have proved the correlation between genetic polymorphisms in xenobiotic-metabolizing enzymes and cancer susceptibility in humans. Individuals have different and unique combinations of polymorphic forms of xenobiotic-metabolizing enzymes such as some people have defective enzymes that activate polycyclic aromatic hydrocarbons (PAHs) but normal enzymes for detoxification. In contrast, other people have normal enzymes to activate PAHs and defective enzymes to detoxify them. The genetic polymorphism in the CYP enzymes may be due to a single nucleotide polymorphism (SNP) and one SNP locus occurs per 1,000 nucleotides approximately in an individual to give those different appearances and characters (Buetow *et al*, 1999; William, 2001; Ingelman-Sunberg, 2001). High-throughput technology like DNA microarrays has identified SNPs in CYP genes which give differences in the transcriptional and translational efficiencies, the enzyme properties and their activities For example polymorphisms of CYP 1A1 and GST are associated with the risk of lung cancer in smokers who have high CYP1A1 and low GST activity (Bartsch *et al*, 2000). SNPs in the genes encoding Phase I and Phase II enzymes differ among racial groups and individuals because of the difference in induction of enzyme expression by the increased exposure to carcinogens (Nagata and Yamazoe, 2002).

The activity of P450 depends upon the components constituting the electron transport system in microsomal membranes e.g. NADPH-cytochrome *P*450 reductase, cytochrome b_5 and NADPH-cytochrome b_5 reductase. The NADPH-cytochrome P450 reductase mediates an electron transfer from NADPH to P450, essential for catalytic function of P450. The level of these factors controls the activity of the expressed P450 whereas, the level of the reductase activity varies among cell lines, it is generally low compared to the levels in the liver (Glatt *et al*, 1990).

Microsomal epoxide hydrolase (mEH) plays an important role in the activation and detoxification of many xenobiotic compounds. It catalyzes the conversion of epoxide into glycols. For example some polycyclic aromatic hydrocarbons (PAH) like BaP are activated by P450-dependent epoxidation and then epoxide is hydrated by mEH. It was found by Glatt *et al*, (1990) that the mEH activity varied among cell lines.

Some other enzymes like N-acetyltransferases, detoxify the reactive intermediates produced by the metabolic activation of chemicals. These enzymes catalyzed the conjugation reactions, such as acetylation, sulfunation, glucuronidation and glutathione conjugation.

The aryl hydrocarbon receptor (AHR) binds a wide variety of xenobiotic compounds and acts as a mediator of the induction of certain xenobiotic drug metabolizing enzymes, is responsible for the toxicity of halogenated aromatic hydrocarbons such as 2,3,7,8-tetrachloro-dibenzo-*p*-

dioxin (TCDD) or PAHs (Hankinson, 1995; Gasiewicz and Collins, 2008) and is also an important component of normal development (Nguyen and Bradfield, 2008). The AHR is a basic helix-loop-helix cytosolic protein which forms a complex with two heat shock protein 90 (HSP90) molecules and XAP2 (X associated protein 2). The regulation of CYP1A1, 1A2 and 1B1 via the AHR signalling pathway has been reported extensively activation (Nguyen and Bradford, 2008).

1.7.4 Metabolism of carcinogens in normal human cells

To understand the role of metabolic activation of chemicals in inducing cancers, primary cultures of normal human epithelial tissues and liver cells have been extensively used for the chemical to induce mutations as it is not possible to induce cancer in a primary culture. The advantages of human tissue and cells used to study the carcinogen metabolism are:

1. They provide the activating system in cell mediated mutagenesis assays;
2. It is easy to measure the unscheduled DNA synthesis in cells and tissues treated with the carcinogen; and
3. Can measure the metabolites and their ultimate carcinogenic form by measuring their binding to cellular macromolecules, especially DNA.

At the biological active dose the binding of the carcinogenic metabolite to DNA represents an important measure for the amount of active metabolites available within the tissues.

A considerable number of chemicals including those originating from industrial processes and occupational exposure require metabolic activation to cause carcinogenicity. There are three major classes of chemicals requiring metabolic activation:

- Polycyclic aromatic hydrocarbons (PAH): such as Benzo[a]pyrene (B[a]P). These hydrocarbons are found everywhere such as automobile exhaust, cigarette smoke and cause lung cancer;
- Heterocyclic amines, *N*-nitrosamines: ingestion or inhalation of certain compounds such as 4-(methylnotrosoamine)-1-(3-pyridyl)-1-butanone (NNK), from the environment or from nitrosation of exogenous amino precursors in the body are associated with an increased risk of oesophageal cancer due to the *in situ* formed nitrosamines (Bartsch *et al*, 1983); and
- Aromatic amines, through occupational exposure or cigarette smoke are considered to be the major factor of human bladder cancer.

Other than tissues and cells, extracellular systems (from human tissues) were also used to determine the activity of enzymes involved in the metabolism of carcinogens and as activation

systems in mammalian and bacterial mutation assays. In standard *in vitro* genotoxicity testing, the induced rat liver S9 fraction has been adopted as an external activating system, to generate electrophilic metabolites that react with macromolecules like DNA and proteins (Ames *et al*, 1973; Paolini, 1997). The induced rat liver S9 fraction is known as a 'metabolite factory' in the Ames test and other *in vitro* genotoxicity tests, especially Aroclor 1254-induced rat S9 fraction to identify different types of compounds as mutagens.

This enzyme system provides a reliable, robust and readily available bio-activation system in rodents at a time when human-derived systems were rare and unavailable. It was believed that rodent systems can standardized more easily than an exogenous human derived system originating from human tissue samples which are known to have significant biological variation.

In later studies, the rat liver S9 fraction was not used as a metabolic activation system in *in vitro* genotoxicity testing due to the fact that the rat and human CYP1A enzyme and other CYP enzymes are different in structure and function from each other and have their own substrate specificity and pathways involved in drug metabolism (Guengerch, 1997) (Figure 1.6). For example in rat liver S9 mix, the expression levels of CYP1A and 2B enzymes are elevated after 5,6-benzoflavone induction, but other enzymes show less or decreased expression (Guengerich *et al*, 1982). This system favours the CYP-mediated metabolism (Phase I) whereas Phase II enzymes, are not active in the reduced form of the nicotinamide adenine dinucleotide phosphate (NADPH)-supplemented S9 system (S9 mix) because other cofactors and additives e.g., uridine diphosphate glucuronic acid, glutathione, acetyl-coenzyme A, etc. would be needed (Ku *et al*, 2007; Obach and Dobo, 2008).

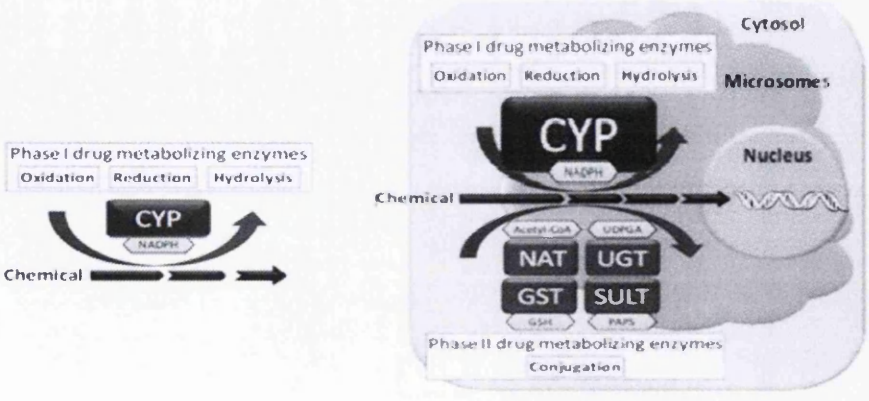

Rat liver S9 mix **Human hepatocyte**

Figure 1.6 Comparison of rat liver S9 mix and human hepatocytes. Image modified from Hashizome and Oda, 2012.

In some cases the detection of genotoxic potential is dependent on metabolites that are formed in target cells by endogenous enzymes; therefore a standard *in vitro* system does not represent the optimum testing system. Application of active metabolite extracellularly showed negative results due to low penetration into the cell and access to DNA or interaction of these metabolites with components of S9 or cell membrane. For example electrophilic metabolites of a chemical bind to serum or S9 proteins, forming protein adduct, and reduces the rate of binding to DNA to form DNA adducts.

Therefore, the rat *in vitro* system was replaced with a human system to identify the metabolites hazardous for humans.

1.8 Establishment of genetically engineered cell lines

Many cell lines have been established for metabolic studies in toxicological testing. Most of them possess no or very little levels of P450 activities. To overcome this problem two metabolic activation systems have been used. One is an externally added cell-mediated system, in which target cells are co-cultivated with primary cultured hepatocytes. The other is a S9 mix prepared from the rat liver homogenates and added to the culture medium to activate the test compound by the enzymes present in the S9 mix. The S9 mix method has been used most widely but has its own limitations such as it decreases the viability of cultured cells due to its toxicity and secondly the test compounds are metabolized in the culture medium but not inside the cells therefore short lived metabolites with high chemical reactivity bind to the surface of the cells and only few metabolites are able to penetrate through the cell membranes and react with target macromolecules to exert toxicity.

Variation within human populations for enzyme induction after drug intake and the genetic polymorphism of certain enzymes, make it impossible to use human liver S9 mix to predict the risks for test compounds. Therefore genetically engineered mammalian cell lines, stably expressing P450 enzymes were established by Doehmer *et al*, (1998). The advantages of such cell lines were

1 The presence of metabolic activation system of the test compound which is responsible for the consequences of cytotoxicity or mutagenicity occur within the cell.

2 These cells were highly sensitive to short-lived active metabolites which directly react with targeted macromolecules in the same cells.

3 The cells carrying human P450 which are useful to ascertain the roles of human P450s in the activation of mutagens.

1.8.1. Cells with stably expressed P450

The transfection method is used to establish the cells which stably express P450. The expression vectors containing cDNA or *P*450 genes are introduced to recipient cells simultaneously with vectors containing a drug resistance gene.

Many cell lines have been established that stably express *P*450 including AHH-1, MCL-5, Chinese hamster cell lines (V79, CHO and CHL), SV40-transformed skin fibroblasts, XPA (xeroderma pigmentosum group A), HeLa, HepG2, MCF-7 (mammary tumur), BEAS-2B (bronchial epithelial cells) and KH293 (kidney) (Sawada and Kamataki, 1989).

Detailed information will be given in study design for AHH-1, MCL-5, TK6 and HepG2 cell lines used in this thesis.

Study design

Carcinogenic chemicals belonging to polycyclic aromatic hydrocarbon (e.g, B[a]P) and heterocyclic aromatic amines (e.g, 2-amino-1-methyl-6-phenylimidazo[4,5-b]pyridine (PhIP)) are strongly correlated with the aetiology of human cancer. The current study examines the genotoxic and mutagenic responses of these chemicals at lower concentrations (μM) There is no information regarding B[a]P and PhIP at concentrations that are relevant to human exposure, which is important for the risk-assessment of such carcinogens. Human cells selected on the basis of their different metabolic competencies and were exposed to chemicals individually. The genotoxicity and mutagenicity were assessed using cytokinesis-blocked micronucleus assay (CBMN) and hypoxanthine-guanine phosphoribosyltransferase (HPRT) assay respectively. The detailed information about chemicals, cell lines and techniques are as followed.

1.9 Polycyclic aromatic hydrocarbons

Polycyclic aromatic hydrocarbons (PAHs) are major contaminants of the environment and some have mutagenic and carcinogenic properties. PAHs are present in coal tar, motor vehicle engine exhausts, wood fires, volcanic activity, refuse burning, oil contamination by disposal or spills, cooking food and they can be formed in the incomplete combustions of organic matter, and thus are present everywhere in the environment (ATSDR, 1995; Phillips, 1999, Lah, 2011). Therefore, human exposure is often unavoidable. In industrial processes, such as fossil-fuel processing, aluminium production, steel and iron factories, wood impregnation and road paving, exposure to PAHs is increased (Baird *et al*, 2005). A long term exposure to PAH and inhalation through smoking has been linked to increased risk of lung cancer (Belpomme *et al*, 2007). Cigarette smoke condensate is highly enriched in PAH and its uptake is greater in smokers as compared to non-smokers (Hecht, 2006). These compounds have been described as a 'smoking gun' and are considered major carcinogenic agents in cigarette smoke (Smith *et al*, 2000; Tretyakova *et al*, 2002). According to Roemer *et a*l (2004) each cigarette contains approximately 3-50ng of PAH carcinogens.

PAHs are a large group of highly lipophilic organic compounds containing two or more benzene rings fused to each other or to other hydrocarbon rings and are soluble in organic solvents (Figure 1.7). PAHs occur in complex mixtures which consist of hundreds of compounds. They have high melting and boiling points, and very low aqueous solubility. They are light sensitive, heat resistant, corrosion resistant and having characteristic UV absorbance spectra. PAHs usually exist as colourless, white or pale yellow solids.

Approximately 500 PAHs have been identified in the atmosphere (WHO, 1987) and 50 have been identified at hazardous waste sites in the USA (ATSDR, 1995). They are mostly used as intermediates in pharmaceuticals, agricultural products, photographic products, thermosetting plastics, lubricating materials, dyes and pigments, diluents for wood preservatives, pesticides etc.

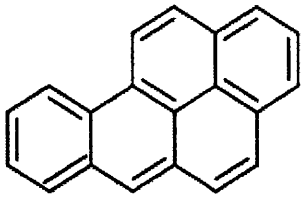

Benzo[a]pyrene

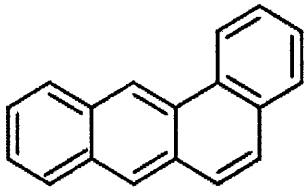

Benz[a]anthracene

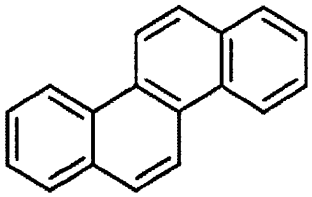

Chrysene

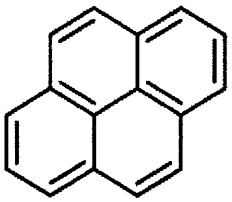

Pyrene

Figure 1.7 Some common polycyclic aromatic hydrocarbons and their structures present in the environment and food. Chemical structures drawn using freeware at www.emolecule.com.

PAHs can be divided into ''Bay Region'' and ''K-region'' compounds on the basis of their structure and activity. Pullmans (1955) described that the interaction between a K-region and some cellular constituents was responsible for initiating the carcinogenic process. Later on, Jerina and Daly (1976) suggested that the 'bay region' (Figure 1.8) was another structural feature that was required for carcinogenic activity and that the strength of the carcinogenic PAH is correlated with the formation of carbonium ion within the bay region of molecule. For example, the biological activity of B[a]P is dependent on the metabolic formation of the reactive diol epoxide (Boyland, 1950) which initiates the carcinogenic process by binding covalently to specific targets in DNA (Dipple, 1985).

As previously mentioned, epidemiological studies have shown a correlation between cigarette smoking, level of PAH exposure and the formation of DNA adducts in human tissues (Poirier *et al*, 2000). Carcinogenic effects of a PAH rely on the balance between host cell ability to activate PAH into a carcinogenic intermediate or being able to remove it from the cell. These processes vary among different chemicals and are dependent on chemical structure, solubility

and distribution within host tissue or cells as well as availability and/or activity of cellular mechanisms to transform a PAH to a carcinogenic agent (Millar and Ramos, 2001).

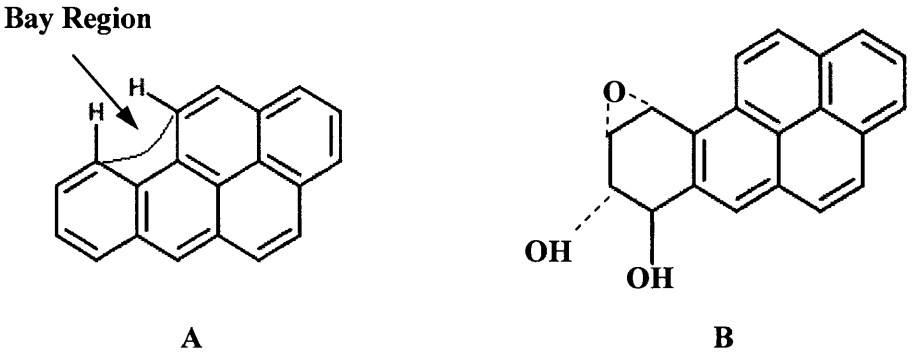

Figure 1.8 Bay region reactive site on benzo[a]pyrene (A) and carcinogenic metabolite Benzo[a]pyrene-dihydrodiol -9,10-epoxide (B). Modified chemical structures from Dipple (1985) and drawn using freeware at www.emolecule.com.

If a genotoxic metabolite is produced and forms DNA adducts, and if DNA repair mechanisms fail to repair the DNA, it could lead to permanent mutations (Boysen and Hecht, 2003). Moreover if these mutations occur in tumour suppressing regions such as the *TP53* gene, then it could lead to tumour formation (Hainaut and Pfeifer, 2001, Vähäkangas, 2003).

Metabolic activation of PAH

Humans are exposed to PAHs through inhalation, ingestion and dermal contact. Their lipophilic nature enables them to penetrate through lipid rich cellular membranes (Yu, 2005). They are metabolized mainly in the liver, kidneys and lungs and are converted either into water-soluble compounds and excreted in the form of bile, urine and breast milk or are converted into carcinogenic forms and exert local carcinogenicity.

Metabolic activation of carcinogens like PAH, involve different enzymatic pathways that either end in the detoxification and then formation of non-reactive metabolites or results in the production of intermediate compounds that bind to DNA to initiate a carcinogenic process (Figure 1.9).

There are three main pathways for PAHs activation; formation of PAH radical cation involving cytochrome P450 peroxidase, formation of PAH-o-quinones by dihydrodiol dehydrogenase-catalyzed oxidation and creation of dihydrodiol epoxide by cytochrome P450 enzymes (Guengerich, 2000). PAH exposure induces expression of Phase I enzymes such as cytochrome P450s (CYPs), epoxide hydrolase (EH), peroxidase, catechol-O-methyltransferase, peroxidases and aldo-keto reductase that oxidizes PAH-transdihydrodiols to redox-active o-quinones which increase reactive oxygen species (ROS) and oxidative

damage to DNA by producing 8-oxo-dGuo mutagenic lesions (Quinn *et al*, 2008). Phase II metabolism is basically a detoxification phase and the enzymes involved are glutathione transferases (GST), uridine diphosphate-glucuronosyl transferases (UGT), epoxide hydrolases (EH) and sulfotransferases (SULTs) (Baird *et al*, 2005; Shimada, 2006). Metabolites from SULTs and UGTs are polar conjugates and excreted from the body (Bansal *et al*, 1981). GSTs are also involved in conjugation of PAH and important for quenching and detoxifying ROS and their derivatives (Bonner *et al*, 2005).

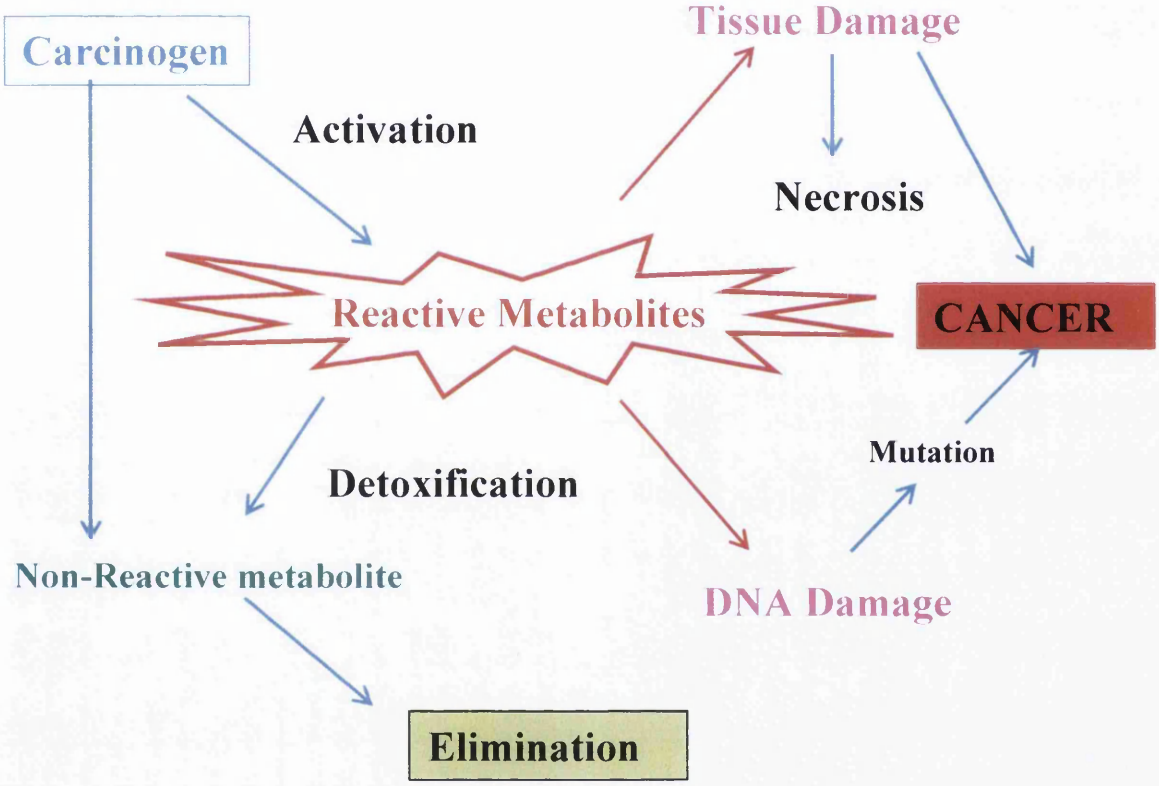

Figure 1.9 The general overall fate of a polycyclic aromatic hydrocarbon (PAH) within the cell. Modified from web.sls.hw.ac.uk

Cytochrome P450, particularly CYP1A1, 1A2, 1B1 and 3A4 play an important role to attach an epoxide group to a PAH that could lead to its conversion into a dihydrodiol by epoxide hydrolase. This metabolite may be further metabolized by CYPs to form a diol epoxide (DE), which is essential to initiate pathways for DNA adduct formation and cancer initiation (Guengerich, 2000; Shimada and Fuiji-Kuriyama, 2004).

Similarly, a metabolic process was reported by Zhong *et al*, (2011), whereby a change in a PAH's surface properties can alter the ability of the PAH to cause mutation. i.e. highly lipophilic PAH such as B[a]P diffuse slowly into tissues (IARC, 2010). Such lipophilic molecules can bio-accumulate and are thought to be involved in the production of reactive

electrophilic products that are capable of binding to DNA and producing DNA adducts (Irigaray and Belpomme, 2010). If cellular mechanisms failed to repair DNA damage, it could then lead to permanent mutations and cancer (Boysen and Hecht, 2003).

In vivo AhR develops immunological and reproductive functions and adaptive responses to light and xenobiotics (Muñoz and Albores, 2011). Nebert *et al* (2000) described the role of the AhR in PAH metabolism. They reported that PAHs act as ligands for AhR to induce CYPs which in turn increase metabolism of PAHs. This pathway involves binding of a PAH to AhR-interacting protein to form a complex with other proteins (Figure 1.10). Translocation to the nucleus and subsequent heterodimerisation of this complex with the AhR nuclear translocator (ARNT) leads to binding with DNA via xenobiotic-responsive elements (XRE; 5′-TNGCGTG-3′) situated in the promoter region of CYP1A and CYP1B and other genes involved in the PAH metabolism (Shimada *et al*, 2002). Hence, PAH's can increase the CYP expression and activity through the AhR receptor binding ability. The role of AhR in the carcinogenic process may be positive or negative, depending on the level and length of exposure, cellular context and other conditions within the tissue (Gasiewicz, 2008).

Different factors including human heterogeneity in AhR inducing genes are believed to influence PAH- related carcinogenesis (ATSDR, 1990). Polymorphisms of Phase I and II enzymes affect the metabolizing rate and adduct formation. Similarly, DNA repair variability can be associated with the DNA damage within populations and species (Binkova *et al*, 2007).

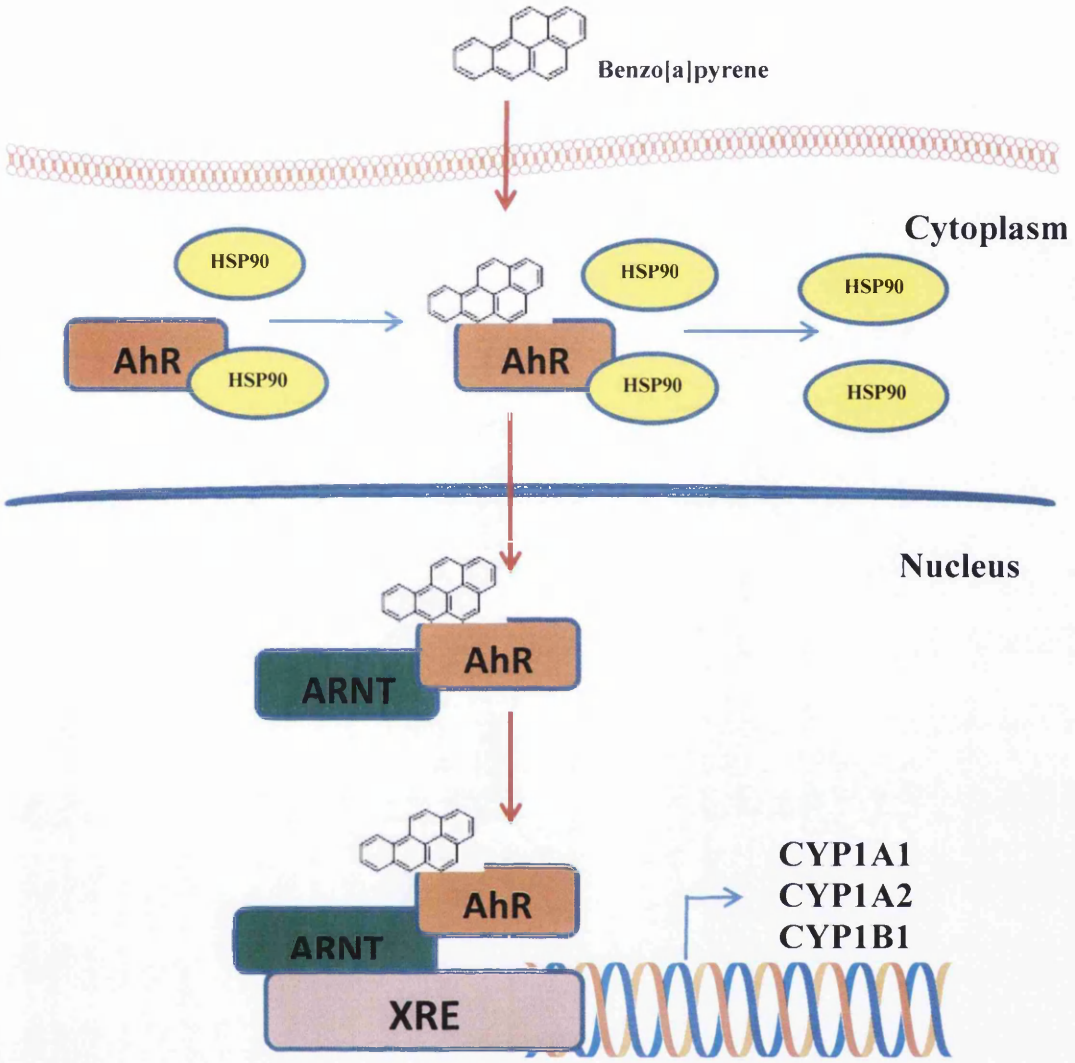

Figure 1.10 Aryl hydrocarbon receptor (AhR) activation pathway involves, binding of Polycyclic Aromatic Hydrocarbon (PAH) like Benzo[a]pyrene to AhR, which changes to AhR- PAH complex in the presence of other proteins such as heat shock protein (hsp90). Upon its translocation to nucleus, AhR-PAH binds with AhR nuclear translocator (ARNT) which then activates transcription of genes involved in CYP1A1, CYP1A2, and CYP1B1 expression. Modified from Muñoz and Albores (2011).

1.9.1 Benzo[a]pyrene

Among PAHs, B[a]P is one of the most extensively studied pro-carcinogens. It is a large flat molecule, having five aromatic benzene-like rings fused together in a honey comb-like structure (Figure 1.11). Its crystals are yellowish and needle-like with a faint odour (ATSDR, 1995). It has a melting point at 178°C, with a very low vapour pressure ($7.3x10^{-7}$ Pa at 25°C) and low water solubility ($3.8\mu gL^{-1}$ at 25°C) (WHO, 1998). It can pass easily through the cell membranes and travel quickly into cells.

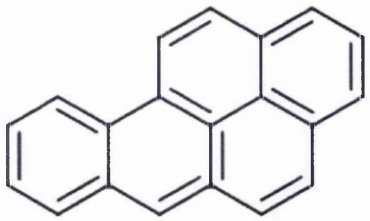

Figure 1.11 Molecular structure of benzo[a]pyrene. Chemical structure drawn using freeware at www.emolecule.com

B[a]P is an environmental pollutant generated through the burning of fossils fuels or wood, vehicle exhaust emission, heat and power generation, industrial processes or oil contamination and is commonly found as a mixture with other PAHs like in, cigarette smoke, charcoal-cooked food and industrial waste by-products (ATSDR, 1995; TEACH, 2007). Human environmental exposure to B[a]P mainly occurs through cigarette smoking, the ingestion of contaminated food and water (ATSDR, 1995), with significant concentrations found in Western diet such as fried and grilled meats (Table 3.1). Both environmental and dietary factors are associated with an increased risk of different organ cancers (Botteri *et al*, 2008), autoimmune (Neal *et al*, 2008) and inflammatory diseases (Klareskog *et al*, 2007).

Table 1.1 Concentrations of benzo[a]pyrene in food and environment. Modified from Uno and Makishima (2009).

Items	B[a]P concentrations
Tobacco smoke	20-40ng/cigarette
Diesel exhaust	<5ng/m^3
Sesame oils	0.36ng/g
Peanuts	0.44ng/g
Fried chicken	5.3-5.6ng/g
Potato chips	<4.1ng/g
Grilled beef	58.8-66.3ng/g
Grilled lamb	42.0-45.6ng/g
Smoked diet beef	5.5ng/g
Smoked cheeses	0.2-2.4ng/g

The daily intake of B[a]P in the average human diet has been estimated to range from 120-2800ng/day (Hattemer-Frey and Travis, 1991). B[a]P has been detected in concentrations ranging from 20 to 40ng per cigarette in mainstream cigarette smoke, 40 to 79ng per cigarette in side-stream smoke, and 96 to 292ng per cigar in mainstream cigar smoke. Concentration of

B[a]P in full flavoured cigarettes has also been reported to be about 9 -10ng per cigarette (Hoffmann and Hoffmann, 1997), which is equivalent to an intake of about 200ng/day for a pack-a-day cigarette smoker (Scherer *et al*, 2000).

Metabolism of B[a]P

B[a]P is transported across the membrane by lipoproteins (Hanson-Painton *et al*, 1981). The protein carriers present in the cytoplasm are actively involved in transferring the B[a]P to the microsomes but are also capable of accepting the oxidized B[a]P from the microsomes. Therefore, it is possible that such active transport processes can be saturated at high doses. B[a]P presence activates the AhR, which binds with AhR nuclear translocator (ARNT) and induces the expression of genes involved in B[a]P metabolism (Figure 1.10).

Toxic metabolites of B[a]P

Metabolic activation of B[a]P produces multiple products which can lead to cytotoxicity, cause DNA and protein damage and overall defects in cell function and integrity. B[a]P is first oxidized at the bay region by Phase I CYP1A1 into B[a]P-7,8 epoxide, which through hydration by epoxide hydrolase is metabolized to B[a]P-7,8-dihydrodiol (BPD). This BPD either serves as a substrate for a second CYP dependent oxidation reaction and generates the metabolite B[a]P-7,8-dihydroxy-9.10-epoxide (BPDE) (Kim and Guengerich, 2005) or it is converted into B[a]P-7,8-dione (B[a]P *ortho*-quinone, BPQ) in the presence of aldo-ketoreductase1C1 (Burczynski and Penning, 2000). Both BPDE and BPQ are genotoxic due to their ability to interact with DNA and form stable and depurinating DNA adducts (Shimada, 2006; Uno and Makishima, 2009) (Figure 1.12).

Another alternative B[a]P metabolic pathway is production of phenols such as 3-hydroxy-B[a]P and 9-hydroxy-B[a]P by other CYP enzymes. These phenols are then converted into quinones like B[a]P-1,3-, 1,6-, and 3,6-quinones. These metabolites are converted into B[a]P diols and induce the production of ROS thereby causing oxidative stress (Shimada, 2006; An *et al*, 2011) (Figure 1.12).

Among all of the metabolites produced by B[a]P activated metabolism, BPDE forms DNA adducts most effectively and is identified as a putative carcinogen (Miller and Ramos, 2001). BPDE contains an epoxide ring within the bay region making it highly susceptible to bind with DNA. The amount of B[a]P that binds to DNA through BPDE increases with exposure time. The conversion of BPDE-DNA starts with the induction of CYP 450 1A1 by B[a]P (Kim *et al*, 1998) which increases the metabolism of B[a]P to its ultimate carcinogen.

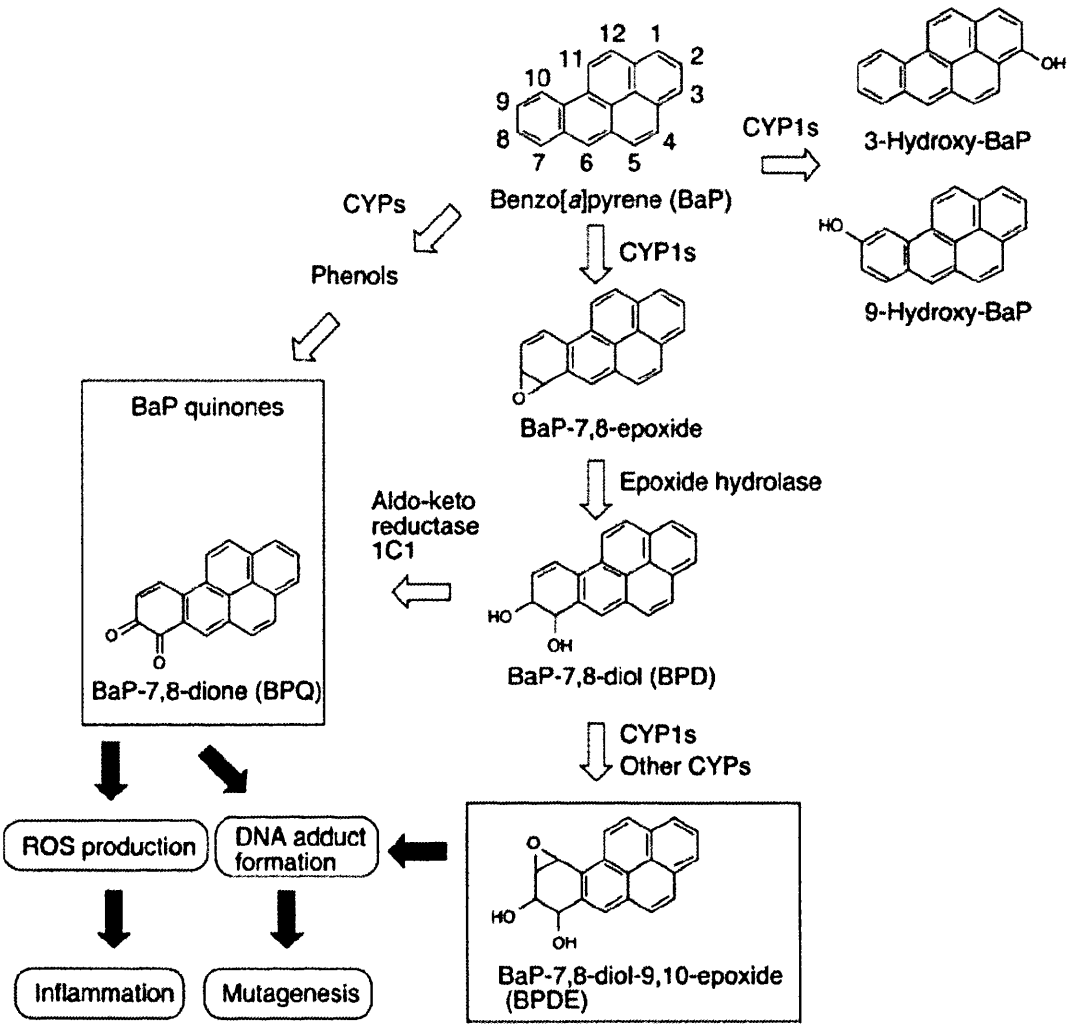

Figure 1.12 B[a]P is metabolized into genotoxic forms B[a]P-7,8-diol-9,10-epoxide (BPDE) and B[a]P *o*-quinone (BPQ) due to their reactivity with DNA, and form bulky DNA adducts to exert mutagenesis; BPQ production can also lead to reactive oxygen species (ROS) production, resulting inflammation in cells. Modified from Uno and Makishima (2009).

Detoxification of B[a]P

In spite of the formation of intermediates that promote cellular damage and toxicity, metabolism of B[a]P is also undergo detoxification and elimination pathway. Phenols and diols become conjugated to water-soluble compounds by either UGT or SULT respectively (Phase II enzymes).

1.10 Heterocyclic aromatic amines

Heterocyclic aromatic amines (HAAs) are a class of toxic chemicals formed during the heating process of organic products containing nitrogenous compounds, mainly proteins (Alaejos *et al*, 2008). HAAs are formed at temperatures between 100 and 300°C and are

generated from the reaction of free amino acids, creatine and hexoses. So far 30 different HAAs have been identified and named (Alaejos *et al*, 2008). A few are presented in Figure 1.14.

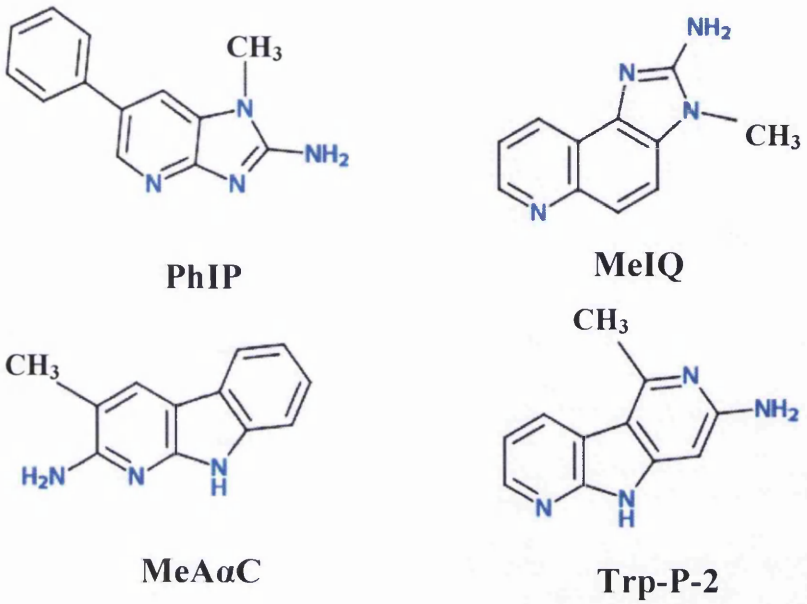

Figure 1.14 Some Heterocyclic aromatic amines (HAAs); PhIP: 2-Amino-1-methyl-6-phenylimidazo(4,5-b)-pyridine, MeIQ: 2-Amino-3,4-dimethyl-imidazo(4,5-f)-quinoline, MeAαC: 2-Amino-3-methyl-9H-pyrido(2,3-b) indole and Trp-P-2: 3-Amino-1-methyl-5H pyrido(4,3-b) indole. Structures drawn using freeware at www.emolecule.com.

Many HAAs are formed from high temperature cooking, frying and grilling of meat, fish and poultry (Sugimura *et a*l, 2004; Turesky, 2007; Turesky and Marchand, 2011). HAAs are also detected in processed food flavourings, high-temperature burning of tobacco, wine, beer, environmental particulates, surface water, diesel exhaust, etc. (Manabe *et al*, 1993; National Toxicology Program, 2011). The HAA levels in cooked meat vary from below 1 to about 500ng/g (from 0.001 to 0.5ppm), (Wakabayashi *et al*, 1992; Sinha *et al*, 1995) and according to the National Toxicology Programme (2011, US) the exposure of HAAs through diet was estimated to range from less than 1 to 17ng/kg of body weight per day. Similarly, Müller *et al*, (2006) reported safe daily PhIP intake of 1.5µg/day (1500ng) over a life time or up to 120µg/day (12000ng/day) in one month and suggested these doses to be used as Threshold Toxicological Concern (TTC), thus any intake above these limits could pose genotoxic risks.

The formation of HAAs in cooked meat is dependent upon the method of cooking, variety of meat being cooked, temperature and duration of cooking. The prolonged cooking time and high temperature cooking surfaces produce the highest quantities of HAAs, depending on the presence of particular amino acids, e.g. 2-amino-3-methylimidazo[4,5-f]quinoline (IQ) formation needs the mixture of glycine, serine and proline, while PhIP formation requires

phenylalanine and leucine (Knize *et al,* 1994). The meats prepared for domestic use have very low concentrations of HAAs (low parts-per-billion (ppb) range) as compared to well-done cooked meats or poultry (Skog *et al*, 1998) or grilled or pan-fried scraping used for gravies (as high as 500ppb) (Skog *et al*, 1998; Gross *et al*, 1993), and fumes arising from cooking oils (Yang *et al*, 1998).

To date, more than 25 HAAs have been isolated and characterized as potent mutagens in the Ames test using *Salmonella* strains (Sugimura and Sato, 1983; Schut and Snyderwine, 1999; Zhang *et al*, 2013), and more have been identified from cooked foods. Oral administration of almost all of these HAA are carcinogenic and induce tumours at multiple sites like the oral cavity, liver, stomach, lung, colorectum, prostate and mammary glands, in laboratory animals such as rodents (Sugimura *et al*, 2004). HAAs are mutagenic in bacteria and mammalian cells and produce chromosomal aberrations and sister chromatid exchanges in cultured cells (Alaejos *et al*, 2008). Epidemiological studies have reported that in humans they induce colon (Sinha *et a*l, 1999), stomach (Ward *et al*, 1997), lung (Sinha *et al*, 1998), breast (Sinha *et al*, 2000) and prostate cancer (Tang *et al*, 2007). The toxicity data reviewed by the International Agency for Research on Cancer (1993) listed HAAs as "probable or possible human carcinogens" (Group 2A) and the 11th edition (2005) of the *Report on Carcinogens* have concluded that prevalent HAAs are "reasonably anticipated" to be human carcinogens. Considering the worldwide meat consumption coupled with globalization of food industry the potential exposure and health risks of these HAA has increased.

Metabolism of HAAs

HAAs undergo extensive metabolism in experimental animals and in humans. Enzymes involved in the metabolic activation of HAA are polymorphic in nature thus leading to variability in an individual's ability to metabolise HAA (Turesky, 2002). HAAs require metabolic activation for DNA adduct formation (Schut and Snyderwine, 1999; Turesky, 2007) and their metabolism is most actively mediated by CYP1A2 in the liver. The pathway starts with the metabolic activation of HAAs with the N-hydroxylation of the exocyclic amino group, catalysed by the Phase I enzymes CYP1A1 or CYP1A2 (Turesky, 2007). This oxidation reaction is also catalyzed by CYP1A1 and CYP1B1 in extrahepatic tissues (King *et al*, 2000). The N-hydroxyarylamine derivatives either directly react with DNA or require second metabolic activation by Phase II enzymes such as N-acetyltransferases (NATs), sulphotransferase (SULTs) etc. to form highly unstable esters that react with DNA to form adducts as summarized in Figure 1.15.

Sinha, (2002) reported the presence of basal and inducible CYP1A2 activity in humans, whereby inducible activity increased with consumption of well-done meat containing high levels of HAAs, increasing the risk of breast cancer. There is a large inter-individual variation in CYP1A2 activity. CYP1A2 mRNA expression varied as much as 15-fold (Schweikl *et al*, 1993) and CYP1A2 protein varied by 25-fold in human liver between individuals (Turesky *et al*, 1998) thus indicating variability in the ability to metabolize HAA within the human population.

NATs (NAT1 and NAT2) are critical enzymes involved in the genotoxicity of HAAs. NAT2 is involved in *N*-acetylation of aromatic amines and *O*-acetylation of the N-hydroxylated derivatives. *N*-acetylation is a detoxification mechanism whereas the *O*-acetylation is an activation step. Several SULTs also bio-activate HAAs, but SULT1A1 is reported to be the most active isoform to catalyse *N*-hydroxy-PhIP and *N*-hydroxy-MeAαC (Glatt *et al*, 2004; Wu *et a*l, 2000). The activated esters lead to the formation of DNA-adducts. The reaction of the esterified *N*-hydroxy-HAAs and the C-8 atom of deoxyguanosine (dG) produces dG-C8-HAA adducts, which is believed to involve reactive nitrenium ion as an intermediate (Schut and Snyderwine, 1999; Turesky and Vouros, 2004). In relatively fewer cases, DNA adducts also form at the N^2 group of dG and at the C-5 atom of the heterocyclic ring structures, indicating charge delocalization of the nitrenium ion over the heteronuclei of these HAAs (Turesky and Vouros, 2004). Some metabolites can be conjugated by sulphation and glucuronidation mechanisms and form polar products that are not reactive and are excreted by the urine.

Molecular epidemiological studies do not show a consistent pattern between cooked meat consumption and cancer development in the general population (Sachse *et al.*, 2003), however, these studies concluded that carcinogenicity related to cooked meat consumption increases among people who have a higher frequency of cooked meat consumption and have the ability to metabolise HAA rapidly (Le Marchand *et al*, 1994).

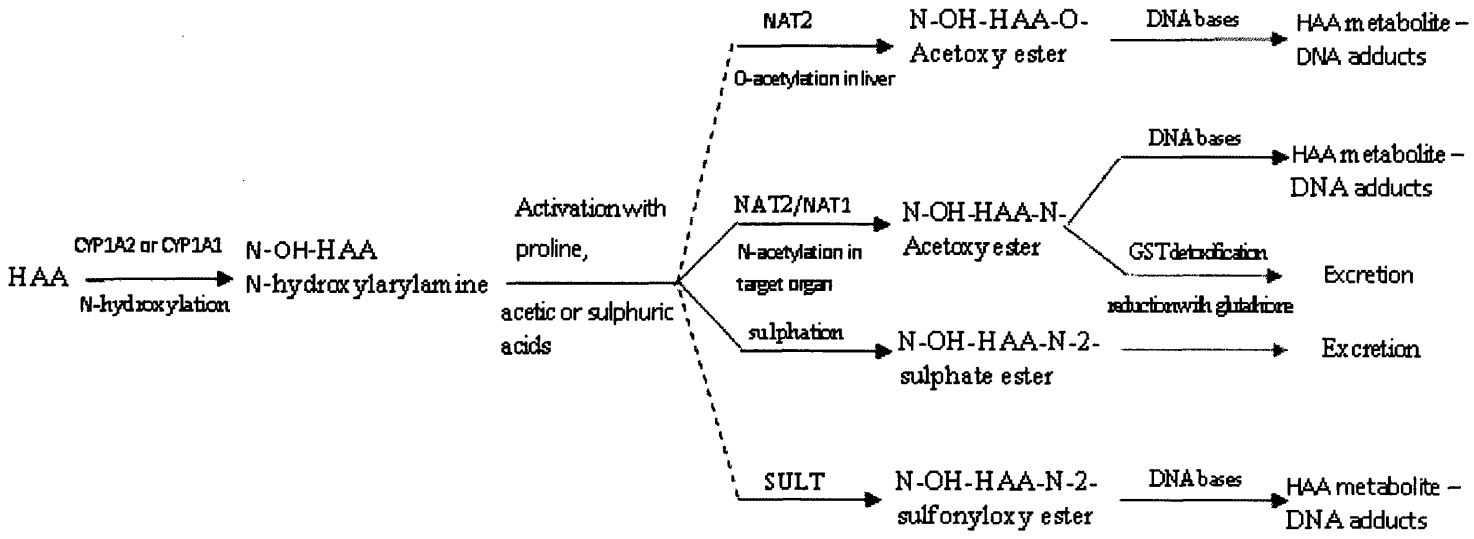

Figure 1.15 Scheme presentation of the metabolism of Heterocyclic Aromatic Amines (HAAs). Image adapted from Alaejas *et al*, (2008).

1.10.1 2-Amino-1-methyl-6-phenylimidazo (4, 5-b) pyridine (PhIP)

2-Amino-1-methyl-6-phenylimidazo (4, 5-b) pyridine (PhIP) is the most abundant HAA formed during the cooking of protein rich food like meat and fish at high temperature (Figure 1.16) (Felton *et al*, 2007; Knize *et al*, 1999). PhIP has been identified in smoke condensates from frying of meat (Thiebaud *et al*, 1995), detected from the air-borne particles, diesel-exhaust particulates and incineration ash from garbage-burning plants and also found in cigarette smoke (Manabe *et al*, 1993). PhIP is also a urinary mutagen in smokers of black tobacco (Peluso *et al*, 1991).

According to IARC (1997) PhIP has been found in grilled beef, pork, chicken and fish products at concentrations up to 70ng/g. To estimate the PhIP intake, Keating *et al*, (2007) and Sinha *et al*, (2005) established a HAAs database in which they suggested that the estimated mean daily intake of PhIP is between 43 and 110ng/day. It is also found in mainstream cigarette smoke (level up to 23ng/cigarette), beer and wine (Manabe *et al*, 1993; Hecht, 2002). Its concentration is measured as low as 0.1ppb in cooked meat and chicken and up to 500ppb in well-done flamed-grilled chicken (Ni *et al*, 2008). The following table (Table 5.1) shows that the amount of PhIP produced from cooked food is highly dependent on the type of meat and its portion, variety of different cooking methods and severity of cooking (rare, medium, well-done and very well-done). Several factors such as presence of anti-carcinogen e.g. fibre or chlorophyllin, which directly bind to PhIP and prevent absorption, flavonoids that are known to inhibit metabolic activation, and substances that prevent formation of the carcinogen during cooking influence exposure of PhIP to individuals.

The formation of PhIP can be reduced by decreasing the temperature and length of cooking time. PhIP formation can be reduced by marination with herbs such as garlic, rosemary, basil, mint, sage, savoury, marjoram, oregano, olive oil and cherries; and vitamin E has been shown to reduce its formation. Recently, Hansol *et al*, (2014) reported significant reduction in the concentration of proline, valine, methionine, and phenylalanine which are the building block of PhIP, in marinated meat. Similarly pre-heating of meat in the microwave have been shown to remove creatine which is a building block in the formation of PhIP (Felton *et al*, 1994; Salmon *et al*, 1997).

PhIP and its metabolites have been reported in colon tissue, blood, lymphocytes and in urine of individuals following consumption of cooked meat (Boobis *et al*, 1994; Dingley *et al*, 1999; Magagnotti *et al*, 2003; Fede *et al*, 2009). In other studies, PhIP has been linked with carcinogenic affects, therefore, it is considered as a dietary risk factor for cancer of the colon,

breast, stomach and prostrate (Ito *et al*, 1991; De Stefani *et al*, 1998; Tang *et al*, 2007; Choudhary *et al*, 2012).

Table 1.2 PhIP concentrations depend on different meat types and variation in cooking. Modified table from Norrish *et al*, (1999).

Meat Type	Cooking variation	PhIP ng/g
Beef (1.5cm thick)	Fried- medium rare (51°C)	0.29
	Fried- well-done (63°C)	0.73
	Fried- very well-done (74°C)	7.33
Lamb chop	Fried- medium (75°C)	0
	Fried- well-done (85°C)	2.4
Pork (2cm thick)	Fried-medium (63°C)	0.37
	Fried- well-done (83°C)	7.82
Minced beef patty (2cm thick)	Fried- medium (51°C)	0
	Fried-well-done (58°C)	3.96
Chicken (2.5cm, no skin)	Fried- lightly browned (63°C)	0.2
	Fried- well-done (79°C)	17.54
Sausage	Fried- lightly browned (42°C)	0
	Fried- well browned (70°C)	0.61
Bacon, middle	Fried- lightly cooked	0.11
	Fried- well cooked	1.93

Metabolism of PhIP

Like many other HAAs chemical carcinogens, PhIP requires metabolic activation for DNA adduct formation and genotoxicity (Kato and Yamazoe, 1987; Thompson *et al*, 1987; Snyderwine *et al*, 1992). In humans, PhIP is metabolically activated via Phase I CYP 1A2 mediated N-hydroxylation to N-hydroxy-PhIP (Crofts *et al*, 1998; Zhao *et al*, 1994) followed by esterification of the N-hydroxy-PhIP into derivatives that can bind covalently at the C-8 position of guanine to form the DNA adduct N-(Deoxyguanosin-8-yl)-2-amino-1-methyl-6-phenylimidazo[4,5-β]pyridine (dG-C8-PhIP) (Schut and Snyderwine, 1999), both *in vivo* and *in vitro* (Turesky, 1994; Pfau *et al*, 1997).

PhIP toxicity- DNA adducts

The PhIP-adducts are reported to be critical in inducing carcinogenesis of the mammary gland (Ghoshal *et al*, 1995) The formation of PhIP-adducts bring structural changes in DNA and also induces mutations in genes controlling cell proliferation that leads to tumour formation (Nagaoka *et al*, 1992).

Three activated intermediate metabolites have been reported to form DNA-adducts; *N*-hydroxy PhIP and its *O*-acetyl and sulphate conjugates (Patterson *et al*, 2010) (Figure 1.17).

These esterified intermediates can covalently bind to DNA at the C-8 atom of 2′-deoxyguanosine (dG) to form DNA adducts, N-(deoxyguaunosin-8-yl)-2-amino-1-methyl-6-phenylimidazo (4,5- b) pyridine (dG-C8-PhIP) (Lin *et al*, 1992; Felton *et al*, 1997; Turesky 2007), causing the generation of predominantly G→T transversion mutations in mammalian cells through mis-pairing of the adducted guanine base with adenine (Wu *et al*, 1995; Shibutani *et al*, 1999).

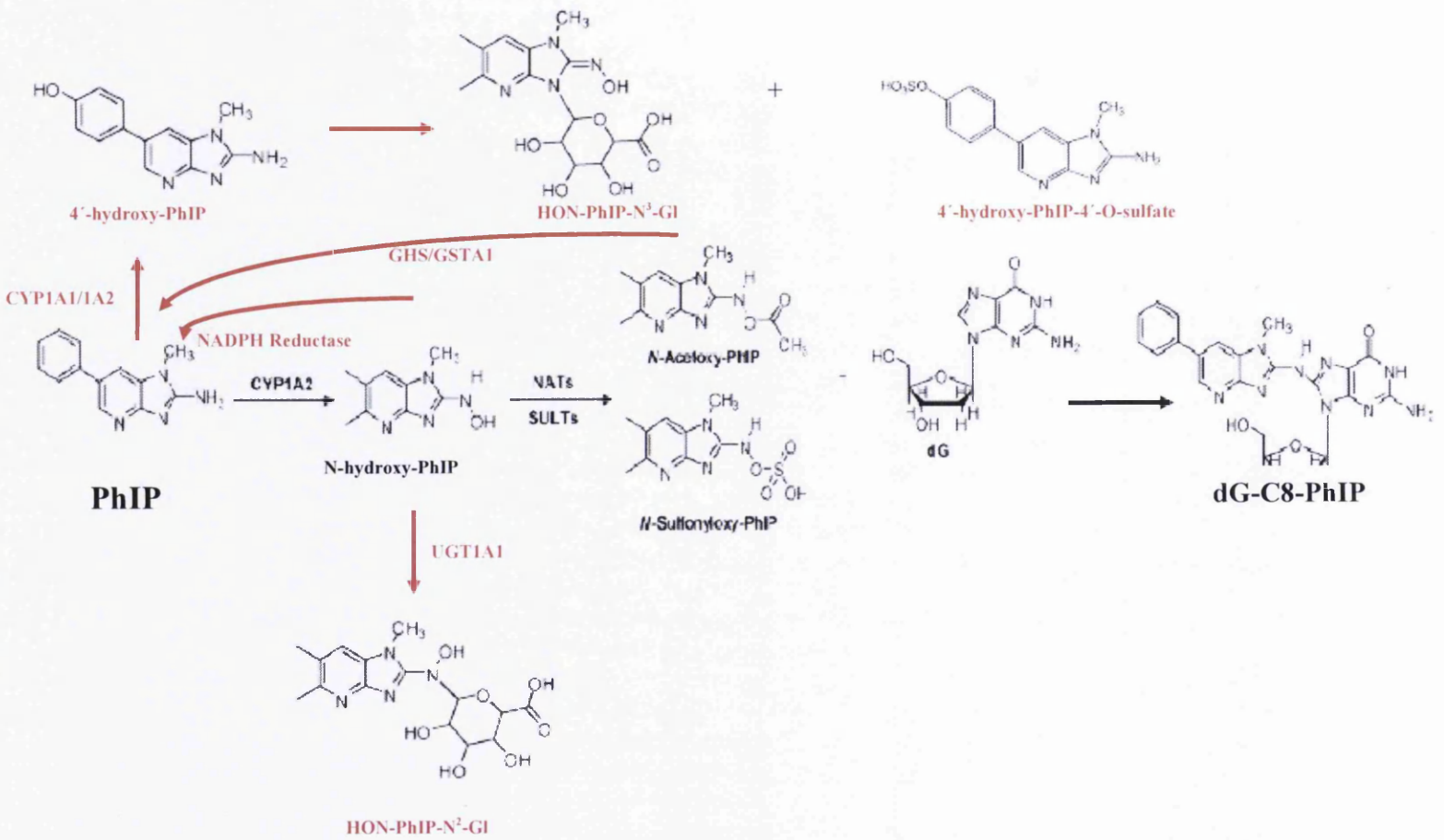

Figure 1.17 Major PhIP metabolic pathways in experimental animals and humans. Black arrows showed the toxification pathway and red arrows showed the detoxification pathway of PhIP. Modified image from Turesky (2007) and Gooderham *et al*, (2001).

PhIP detoxification

PhIP also undergoes a parallel detoxification pathway, producing metabolites by glucuronidation (through Phase II enzymes) of N-hydroxy-PhIP, 4'hydroxylation of PhIP and subsequent sulphate conjugation (Figure 1.18). The UDP-glucuronosyl-transferase 1A1 (UGT1A1) is the most active enzyme in the glucuronidation process (Malfatti and Felton, 2004). N2-(β-1-glucosiduronyl-2-(hydroxyamino)-1-methyl-6-phenylimidazo (4,5-b) pyridine (HON-PhIP-N2-Glu) is the major PhIP metabolite excreted in human urine (Malfatti *et al*, 2006). N-hydroxy–PhIP may also undergo detoxification by NADPH reductase and be converted back to PhIP (King *et al*, 2000). The *N*-Acetoxy-PhIP (ester of *N*-hydroxy-PhIP) is detoxified mostly by the active enzyme gltutathione S-transferase (GST1) through unstable glutathione (GSH) conjugate (Lin *et al*, 1994; Coles *et al*, 2001).

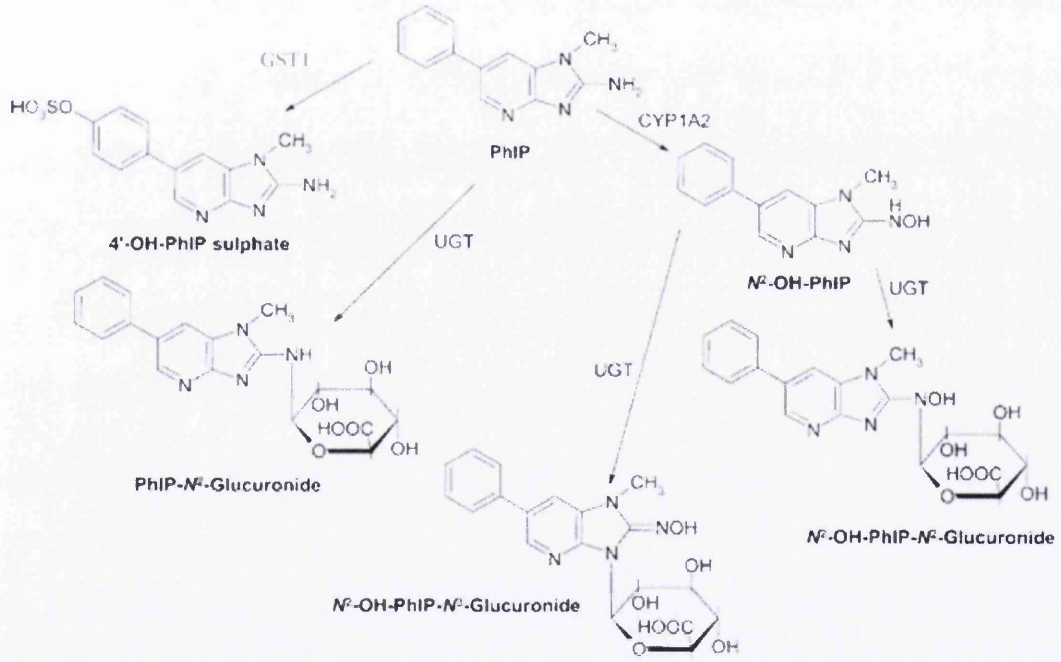

Figure 1.18 Detoxification pathways of PhIP metabolism in humans. PhIP is metabolized by CYP1A2 and (UGT) and (GST1) enzymes. Modified image from Walters *et al*, (2004).

Expression variation in genes involved in PhIP metabolism and exposure to PhIP play an important role in DNA adduct formation therefore, DNA adducts can be used as an effective biomarker to study genetic variation in PhIP metabolism (Bendaley, 2009).The most frequent mutational signatures reported to be induced by PhIP are single base substitutions which are predominantly GC→TA transversions, a high percentage of -1G frameshift mutations and a preference for 5'-GGA-3' motifs (Gooderham *et al*, 1997). DNA damage following exposure

to activated PhIP is the first step (Zhu *et al*, 2000) which could either lead to the cells demise by apoptosis or retention of the damage as a mutated gene.

Wild and Kerder, (1998) reviewed results generated from different studies involving different tests such as HPRT assay, Ames and tests for sister chromatid exchange (SCE test) in mammalian cells and concluded that PhIP is a highly potent genotoxin. They explained that genotoxicity of PhIP is dependent on the host organism's metabolic activity to generate reactive DNA-binding PhIP intermediates (nitrenium ions). These studies suggest that the ability to transform PhIP to electrophilic nitrenium ions is more likely to induce genotoxicity rather than the quantity of PhIP present in the diet. The DNA-binding potency of nitrenium ions is related to their electrophilic reactivity and mutagenic potency. PhIP nitrenium ions bind preferentially to guanine nucleotides in DNA, such as the mononucleotide, deoxyguanosine-3′ - phosphate (dGp).

PhIP metabolism varies within and among species e.g. rodent CYP450 enzymes are involved in detoxification process through 4'-hydroxylation whereas human processes involve the production of *N*- hydroxy metabolites that leads to esterification and production of active electrophilic metabolite (Cheung *et al*, 2005). This variability makes it difficult to rely on laboratory experiments while assessing human risk to PhIP exposure. Turesky (1998a) also noted a differences in the amount of CYP1A2 in human and rodent liver, with its expression up to 10 -fold greater in human liver as compared to that of rodents (Turesky *et al*, 1998a). Among humans, metabolic processes such as variability in levels of CYP1A2 determine the risk of carcinogenicity to HAAs (Hammans *et al,* 1997). To better understand the human risk of PhIP induced mutagenicity, it is important to consider interspecies variability in catalytic activity and expression levels of CYP1A2. PhIP metabolism represents a competing process between activation of PhIP and detoxification process. Whether PhIP undergoes activation or detoxification is dependent on PhIP dose and metabolic activity of the individual.

1.11 Cell lines

The following cell lines having different metabolic competencies were used in this study conducted at Swansea University.

AHH-1 TK+/- (Suspension cells)

The human lymphoblastoid cell line AHH-1 cell line was developed by Crespi and Thilly and originally derived from RPMI-1788. It is free of mycoplasma and has Aryl Hydrocarbon Hydrolase (AHH) activity for xenobiotic metabolism (Crespi and Thilly, 1984, Crespi *et al*, 1991; Freedman *et al*, 1979). AHH-1 is a human lymphoblastoid cell line, transformed by an

Epstein Barr virus (EBV) that expresses high level of CYP1A1 (Crespi *et al*, 1993; Crespi and Thilly, 1984) responsible for the oxidation of many chemicals present in our environment (Gonzalez *et al*, 1991). AHH-1 cells do not contain any detectable microsomal epoxide hydrolase (mEH) activity (Penman *et al*, 1994). AHH-1 cells have a heterozygous transition mutation (C→T) in the *p*53 locus at the codon 281/282 interface within exon 8 (Guest and Parry, 1999), yet despite this express phosphorylated-p53 and p-21 (Doak *et al*, 2008) and are capable of apoptosis (Zair *et al*, 2011). AHH-1 TK+/- can be used in chromosome aberration tests and in studying the induction of gene mutations at both the thymidine kinase (*tk*) locus and the hypoxanthine guanine phosphoribosyl transferase (*hprt)* locus. The population doubling time of AHH-1 cells is 22-24h. These cells were purchased from American Type Culture Collection (ATCC, Middlesex, UK).

MCL-5 (Suspension cells)

MCL-5 cells are derived from L3 cells, a subpopulation of AHH-1 cells transfected with two plasmids; one containing two copies of CYP3A4 complementary DNA (cDNA) and one copy of CYP2E1 cDNA and a second plasmid containing one copy of each CYP1A2, CYP2A6 and microsomal epoxide hydrolase (mEH) (Crespi *et al*, 1991). These cells also carry a hygromycin B resistance gene and like AHH-1 cells, carry a heterozygous mutation in the p53 locus at codon 282 (Guest and Parry, 1999).

MCL-5 cells stably express all five cDNAs and has increased levels of CYP1A1 as compared to AHH-1 cells. Therefore, MCL-5 cells have shown to be more sensitive than AHH-1 TK+/- to the mutagenic properties of many pro-mutagens and procarcinogens and direct acting agents (Crespi *et al*, 1991, Doherty *et al*, 1996). The population doubling time of MCL-5 cells is 22-24h. MCL-5 cell lines were purchased from American Type Culture Collection (ATCC, Middlesex, UK).

TK6 (Suspension cells)

The human lymphoblastoid cell line TK6 is a derivative of the Wil-2 cell line. The cells have a stable genome, heterozygosity at the *tk* locus and contain functional wild-type *p53* gene. TK6 cells were purchased from the European Collection of Cell Cultures (ECACC, Salisbury, UK). The population doubling time of TK6 cells is 18h.

HepG2 (Adherent cells)

These cell lines were isolated by Aden *et al*, in 1997 from a primary hepatoblastome of an 11-year old Argentine boy. HepG2 have epithelial-like morphology which resembles liver parenchymal cells and retain many of the specialized functions in culture such as secretion of major plasma proteins (Knowles *et al*, 1980; Aden *et al*, 1979). HepG2 cells have chromosomal number of 52 and range of 48-54 chromosomes per cell (Natarajan and Darroudi, 1991). The population doubling time of HepG2 is longer (20-28h) than that of lymphoblastoid cell lines (AHH-1 and MCL-5) (Natarajan and Darroudi, 1991). HepG2 cell line expresses a wide range of Phase I and Phase II enzymes which play an important role in the activation and detoxification of genotoxic pro-carcinogens.

HepG2 cells are used to detect cytotoxic and genotoxic substances by using the different genotoxicity assays. HepG2 cells have also been used for anti-mutagenic studies (Mersch-Sundermann *et al*, 2004). This cell line was purchased from the European Collection of Cell Cultures (ECACC, Salisbury, UK).

These cell lines are stable in expressing cytochrome P450 except TK6 and thus serve as a good tool to investigate the role of P450 enzymes in assessing the genotoxicity of chemicals that require metabolic activation. The stable expression system also helps to understand the process from metabolic activation of test compounds to the appearance of toxicological consequences entirely in the same intact cells. We used these cell lines to investigate the effect of two pro-carcinogens B[a]P and PhIP on these cell lines in order to gain a better understanding of the variability in metabolic potential and genotoxic effects caused by these agents.

1.12 Cytokinesis-block micronucleus assay (CBMN) and its application in research

The CBMN assay was initially developed to study chromosomal damage in human lymphoblastoid cells (Fenech and Morley, 1985) but now it is successfully applied for population monitoring of genetic damage, screening of chemicals for genotoxic potential and for the prediction of the radiosensitivity of tumurs. The *in vitro* CBMN method has an ability to measure both clastogenic (structural) and aneugenic (numerical) chromosomal changes. It is being used successfully for human lymphocytes (Fenech, 2000), fibroblasts (Heddle *et al*, 1990), keratinocytes (He and Baker 1989), nucleated bone marrow cells (Odagiri 1994) and primary tumour cell cultures (Masunaga *et al*, 1991).

In the CBMN assay, cells that have passed through one mitosis, are prevented from undergoing cytokinesis by using cytochalasin-B (Cyto-B) exposure to the cells in culture.

Cyto-B is a metabolite of the fungus *Helminthosporium dematioideum* that blocks cytokinesis but not karyokinesis and results in the formation of binucleated cells that have undergone one nuclear division (Carter, 1967). Cyto-B binds high molecular complexes in the plasma membrane to inhibit formation of daughter cells by preventing induction of actin polymerisation and resultant formation of microflilaments and increases the sensitivity and consistency of the experiment (Figure 1.20).

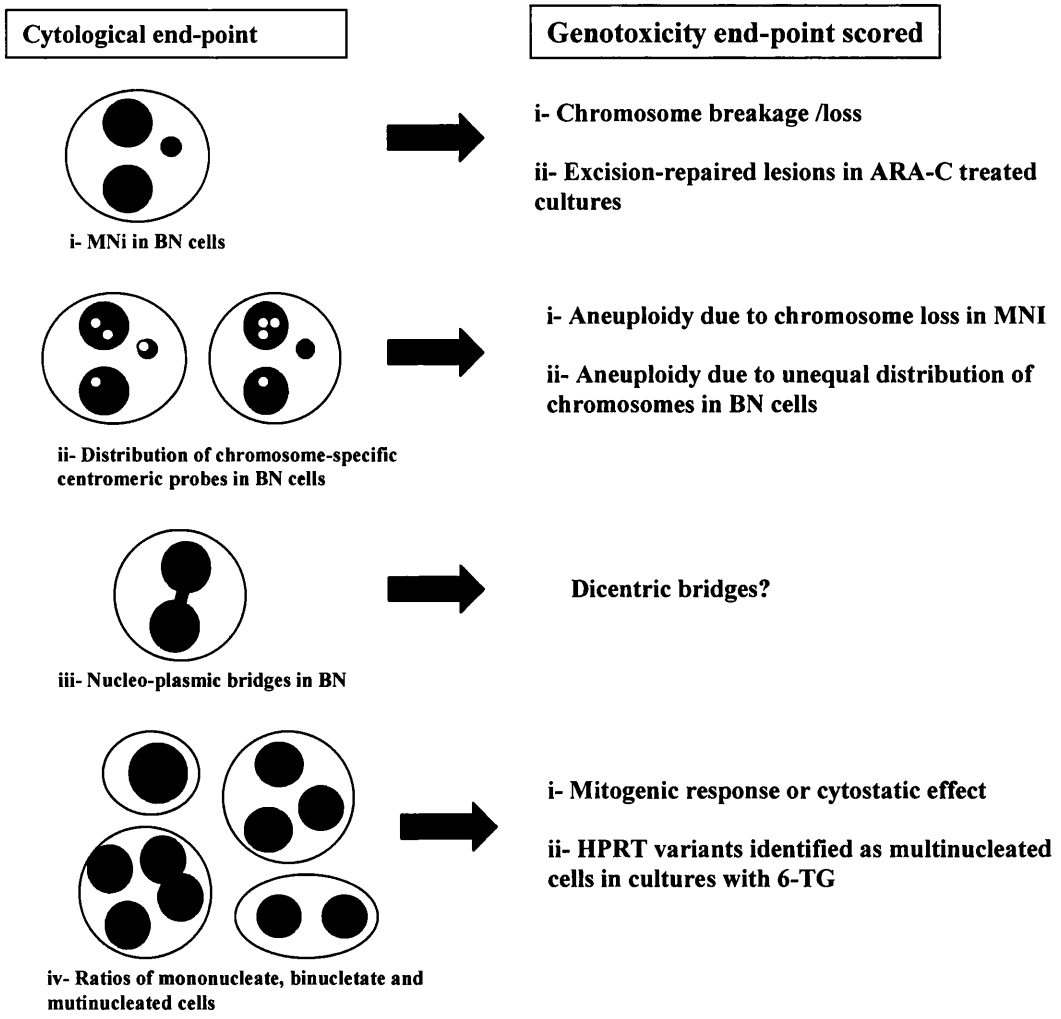

Figure 1.20 A schematic diagram showing the end-points that can be scored with the CBMN assay. Figure modified from Fenech, 1997.

Thus studying micronuclei levels in binucleated cells offers the opportunity to assess the level of DNA damage in cells that have undergone division after exposure with the test chemical (Figure 1.21) (Fenech, 2000), as it enables cells that are not dividing to be distinguished from dividing cells within the cell population. It also provides reliable comparison of chromosome damage between cell populations that may differ in their cell division kinetics (Fenech, 2000).

This test system also offers the possibility of detecting dicentric bridges as well as chromosome loss and non-disjunction events (Fenech, 1997).

OECD 487 guideline (2007) provides well established guidelines to perform the CBMN assay. The scoring criteria was established and validated by Human MicroNucleus (HUMN) international collaborative project (http://www.humun.org). CBMN assay has an ability to detect both clastogenic and aneugenic events (Fenech, 2000) and these events can be achieved at low doses of mutagen exposure (Vral *et al*, 1997; Touil *et al*, 2002).

The efficiency of cyto-B inhibition of cytokinesis is dependent on the concentration used. It might be causing micronuclei induction in binucleated cells but many studies have confirmed that there is no dose-response effect for micronucleus induction over the concentration of 1-6μg/ml (Fenech, 1997).

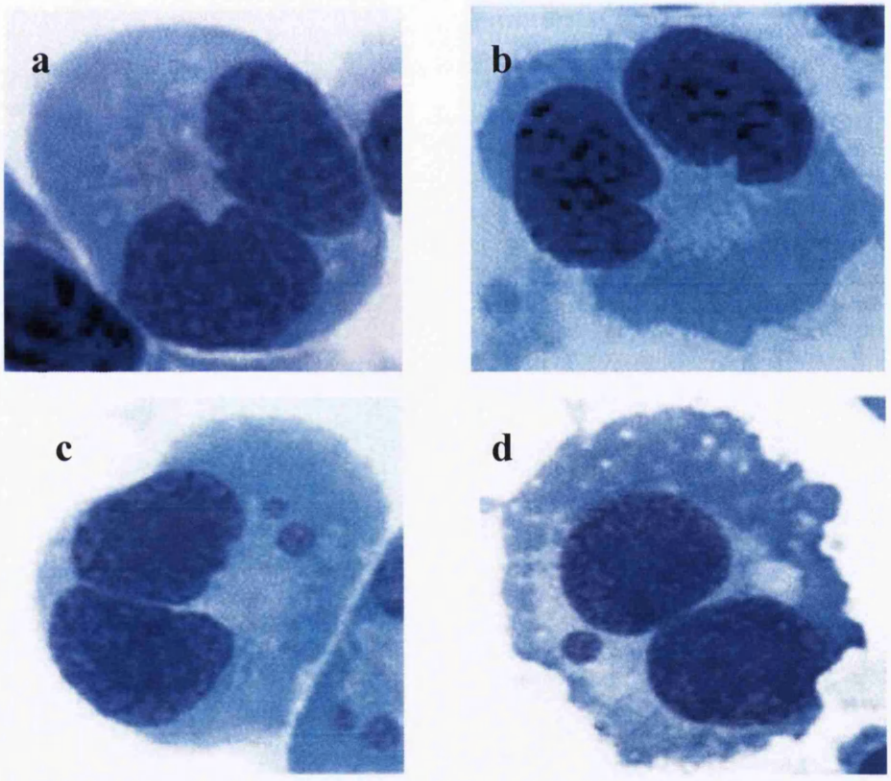

Figure 1.21- Photomicrographs of binucleated cells (a,b) and binucleated cells with micronuclei (c,d) (Fenech *et al*, 2003).

CBMN assay has been widely used, for example, to study spontaneous micronucleus frequency in gender and individual susceptibility (Fenech *et al*, 1994) and for assessing the effect of nutritional deficiency such as homosyteine and Vitamin C (Fenech, 2004). Micronucleus levels have also been a good indicator of cancer. For example, lymphocytes of cancer patients and patients with certain syndromes have increased micronucleus frequency (Duffaud *et al*, 1997; Rudd *et al*, 1988), deficiency of vitamin folate in blood associated with

increased risk for some cancers (Blount *et a*l, 1997; Fenech, 1998) and diagnosis of early stages of cervical carcinogenesis in women (Olaharski *et al*, 2006).

1.13 Hypoxanthine guanine phosphoribosyl transferase H(G)PRT

Monitoring point mutations at the genetic level in humans is a useful biomarker to evaluate the cancer risk from exposure to environmental mutagens (Au, 2007). Several assays which detect DNA damage have been developed for use in human cells, such as hypoxanthine guanine phosphoribosyl transferase H(G)PRT –Forward Mutation Assay (Crespi and Thilly, 1984). The HPRT assay is a very common and sensitive method to examine the point mutations induced by mutagen exposure at low doses. Indeed, the HPRT assay has well established regulatory guidelines (OECD guideline 476, 1997) these well validated protocols exist for its use in mutation research. Parry *et al*, (2005) and Albertini (2001) have utilised the HPRT assay for human bio-monitoring. In this assay both HPRT $^{+}$ and HPRT $^{-}$ cells can grow in the simple selective media. After exposure to the chemical of interest, cells deficient in the HPRT gene are selected by resistance to the cellular poison 6-thioguanine (6-TG). The experimental end point is expressed in the form of Mutation Frequency (MF) which is the frequency of HPRT mutant cells among the cell population in the medium. This assay has been widely used to screen mutagens or carcinogens and to study mutagenicity expressed in the form of DNA base pair substitutions, small base deletions or frameshifts in the *HPRT* gene. Many mammalian cell lines have been used successfully for the HPRT assay such as mouse lymphoma cells, Chinese hamster cell lines (CHO and V79) (OECD, 1997; Tindal and Srankowski, 1989), and the human lymphoblastoid cells AHH-1, MCL-5 and TK6 (Crespi *et al*, 1991; Crespi and Thilly, 1984; Parry *et al*, 2005). The *HPRT* loci is located on the X chromosome, therefore, it is also used to study mutagenic effects in primary male cell lines (Tates *et al*, 1994; van Dam *et al*, 1992). However, this method is not suitable to detect the mutagenicity of chemicals that cause X chromosome lethality (Johnson, 2012).

1.13.1 *HPRT* assay and the study of mutations

The HPRT assay was used by DeMarini *et al*, (1989) for the detection of gene mutations in the mammalian cells. *HPRT* gene is located on the long arm of X chromosome at position Xq26-27 (Pai *et al*, 1980) in mammalian cells and is hemizygous in male i.e. a single copy of the gene in male cells (Stout and Caskey, 1985). It has 47542 base pairs (bp) and a protein-coding region of 657bp over 9 exons, which are spliced together forming 1435bp of mRNA (Figure 1.22). Human *HPRT* gene mutations happen due to alterations in splicing of the

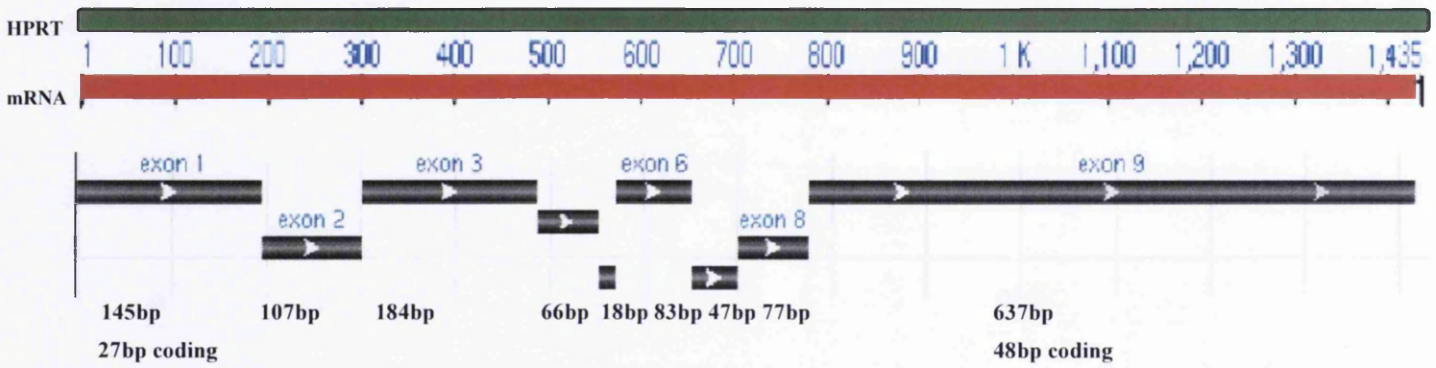

Figure 1.22 *HPRT* gene with exon organisation. Modified from http://www.ncbi.nml.nih.gov. Values taken from O'Neil *et al* (1998).

mRNA and most of these mutations have been found in all eight splice sequences (O'Neil *et al*, 1998). HPRT deficiency in humans can cause a biochemical defect called Lesch-Nyhan syndrome (Caskey and Kruch, 1979).

The *HPRT* gene encode the hypoxanthine-guanine phosphoribosyltransferase enzyme (HPRT, EC 2.4-2.8), which is in a soluble form and present in the cytoplasm of all cells. Each monomer of *HPRT* protein contains 217 amino acids and has a molecular weight of 24,470 kDa (Wilson *et al*, 1983). The HPRT enzyme plays an important role in the purine salvage pathway involved in DNA synthesis. There are two pathways involved in the production of purines for DNA and RNA biosynthesis. These are:

The *de novo* pathway:

It is a complex and energy-expensive pathway, involving eleven enzymatic steps to form inosine monophosphate (IMP) nucleotide. The pathway starts with the synthesis of 5-phosphoribosyl-1-pyrophosphate (PRPP) from ribose-5-phosphate and ATP (Figure 1.23). After IMP nucleotide is formed it then converts to either AMP (adenosine monophosphate) or GMP (guanosine monophosphate) by using the purine bases adenine hypoxanthine or guanine, respectively (Zaharevitz *et al*, 2004). This is the default pathway which is compensated by the salvage pathway. Purine synthesis is important for DNA synthesis, therefore it is extensively studied for chemotherapeutic purposes (Jancso *et al*, 2001) as blocking salvage pathway (with nucleoside analogues) can halt cancer cell growth. In the absence of the HPRT enzyme, the concentration of PRPP will increase, resulting in an increase in the rate of purine biosynthesis by the *de novo* pathway (Natsumeda *et a*l, 1984). This over-production of purines is responsible for HPRT deficiency syndrome (Lesch-Nyhan syndrome) leading to build up of urate in all body fluids causing severe gout and kidney problems (Camici *et al*, 2010).

Salvage Pathway: This is a recycling biochemical pathway that converts degraded DNA bases into useful purine nucleotides for re-use in synthesis. It is an energy saving pathway and 90% of free purines in mammalian cells are recycled (Lehninger, 1978). Erythrocytes are deficient in the *de novo* pathway for the synthesis of purine and therefore use the salvage pathway (Fontele and Henderson, 1969). The HPRT enzyme in the presence of Mg^{+2} uses PRPP as a substrate and catalyzes the transfer of 5-phosphoribosyl group to the 9 position of

purine bases hypoxanthine and guanine to form IMP and GMP respectively for DNA or RNA synthesis (Figure 1.23) (Torres and Puiq, 2007).

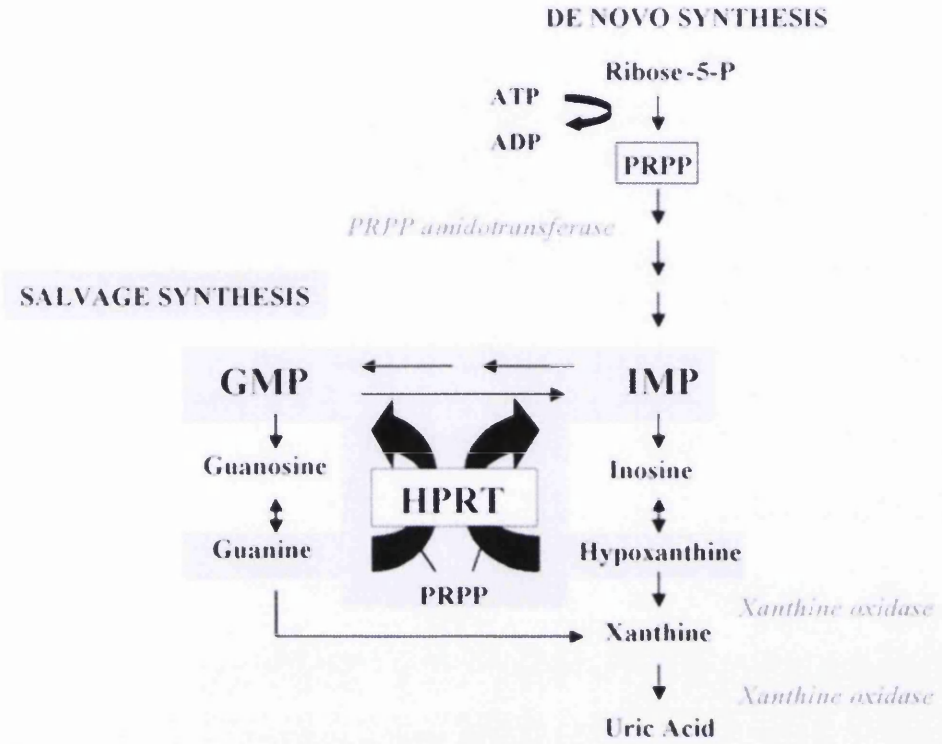

Figure 1.23 Recycling of purine through salvage pathway. Image modified from Torres and Puiq, 2007.

1.14 Selection for ($HPRT^+$) wild type and ($HPRT^-$) deficient cells

1.14.1 ($HPRT^+$) wild type

HPRT mutants are always removed in the beginning of the HPRT assay to increase the sensitivity of the assay to chemical mutagenesis. Wild type ($HPRT^+$) cells are selected using HAT media (hypoxanthine, aminopterin and thymidine) as a supplement in tissue culture media. HAT blocks *de novo* purines for DNA synthesis and so forces the cells to use other pathways or results in cell death in $HPRT^-$ cells (Caskey and Kruh, 1979). Cells can sometimes, due to the loss of heterozygosity mutations (deletions), become deficient in HPRT, and in HAT media are unable to synthesise purines so undergo apoptosis through an unknown mechanism possibly involving *c-myc* proto-oncogene expression (Chung *et al*, 2001). The aminopterins in HAT inhibit the enzyme dihydrofolate reductase (DHFR) which is important in the *de novo* nucleotide synthesis (Figure 1.24). DHFR converts folic acid into intermediates such as dihydrofolate (DHF) and tetrahydrofolate (THF). THF is then converted by formate-tetrahydrofolate ligase (FTL) into 10-formyl tetrahydrofolate (10-formyl THF),

which donates formyl (CHO) groups to intermediates of the *de novo* purine biosynthesis pathway (Figure 1.24) (Huennekens *et al*, 1963; Zaharevitz *et al*, 2004). Without 10-formyl THF purine biosynthesis only occurs through HPRT and the salvage pathway. As a result of inhibition of DHFR, depletion of intracellular pools of nucleotides occurs, affecting DNA strand synthesis during S phase of the cell cycle and limiting the cell's capacity to divide (Tsurusawa *et al*, 1990). In present study the cells were transferred from HAT media to HT media (rescue media) which provide purines and pyrimidine to overcome the effects of residual intracellular aminopterin. Cells were grown in HT media until *de novo* biosynthesis pathway were reestablished.

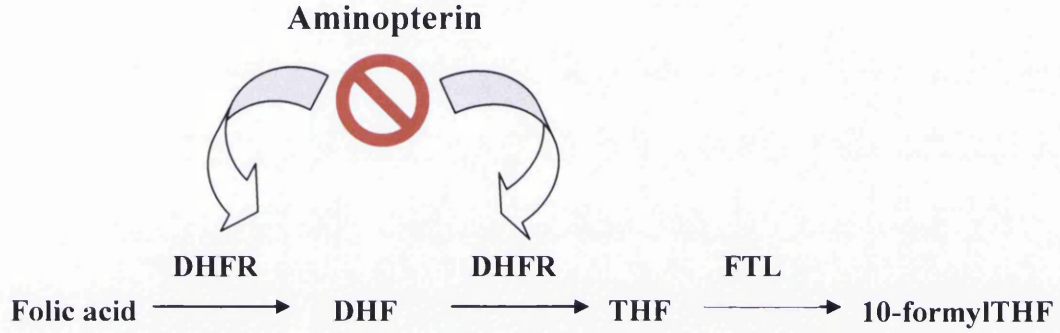

Figure 1.24 Aminopterin inhibits the conversion of folic acid into 10-formylTHF by blocking the enzyme DHFR. 10-formylTHF is an essential intermediate of the *de novo* purine biosynthesis pathway. DHFR: Dihydrofolate reductase, DHF: dihydrofolate, THF: tetrahydrofolate, FTL: formate-tetrahydrofolate ligase. Constructed from Lightfoot *et al* (2005).

1.14.2 ($HPRT^-$) deficient cells

The mutant cells deficient in HPRT ($HPRT^-$) are selected through use of the guanine analogue, 6-thioguanine (6-TG) which is toxic only to cells having functional HPRT. Previously, 8-azaguanine was used as a guanine analogue for selecting HPRT mutants, which later proved to be a poor substrate for HPRT (Arlett *et a*l, 1975; van Diggelen *et al*, 1979). Cellela *et al* (1983) discovered that wild type HPRT has a higher affinity for 6-TG and thus 6-TG provides precise mutant selection. Wild type HPRT cells convert 6-TG to 6-thioguanine monophosphate (6TGMP), this analogue blocks purine synthesis through inhibition of amidophosphoribosyl and IMP dehydrogenase (Figure 1.27) (Aubrecht *et al,* 1997). These processes increase the probability of 6TGMP incorporation into nucleic acid and its subsequent incorporation into DNA (Nelson *et al*, 1976). Incorporation of 6-TG into DNA is believed to be involved in the development of single strand DNA breaks due to replacement of guanine by thioguanine and also results in blockage of strand extension because of the

inefficiency of thioguanine to act as a substrate for DNA polymerase and DNA ligase (Ling *et al*, 1992). Hence, 6-TG kills dividing cells. Balajee and Geard (2004) proposed that an accumulation of Replication Protein A (RPA p34) and γ-H2AX foci (double strand break binding factor) at the site of replication blockage which are responsible for double stranded breaks (DSBs) are as a result of 6-TG. Yan *et al* (2003) observed a significant increase in single stranded DNA breaks in mismatch repair (MMR) proficient cells and suggested a role of 6-TG in triggering apoptosis through MMR processes. These mechanisms enable counter selection of wild type or HPRT mutant strains and provide an effective tool in determining the mutagenic effect of a test chemical.

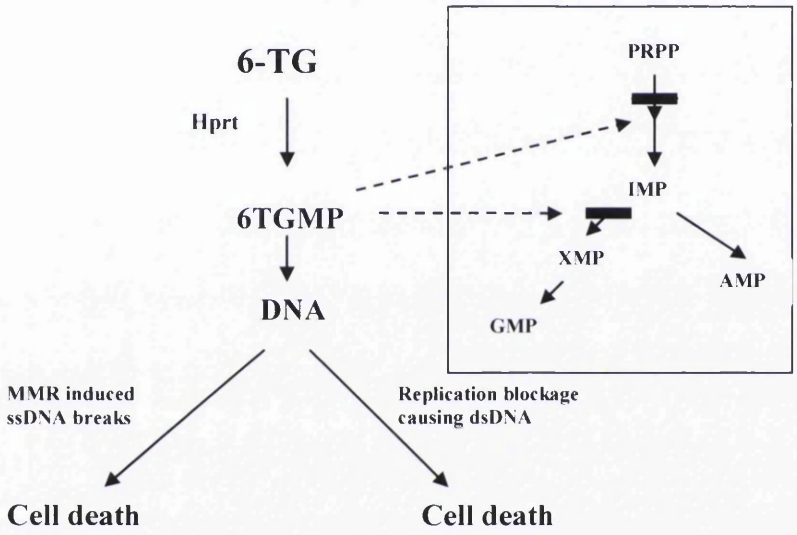

Figure 1.25 Metabolism of 6-thioguanine (6-TG) in $HPRT^+$ cells where 6-TG is converted into 6-thioguanine monophosphate (6-TGMP) by HPRT, which inhibits *de novo* purine synthesis and therefore purine incorporation into DNA resulting to cell death. In HPRT deficient cells 6-TG will not metabolise and cell will survive. Modified from Aubrecht *et al* (1997).

1.15 HPRT assay methodology

The HPRT assay has been described by Crespi and Thilly (1984) in the AHH-1 cell line. It has three important stages; i. HPRT mutant cleansing, ii. Treatment with mutagen, and iii. mutant's selection and quantification.

i HPRT mutant cleansing

To reduce the mutation background i.e. the mutation frequency in untreated cells, media is supplemented with HAT which blocks *de novo* purine synthesis; thus only cells that can use

the salvage pathway for purine synthesis can grow in this media. Selection allows growth of HPRT+ cells and lead to a reduction in HPRT $^-$ mutant cells to background levels of 1-100 mutant cells in a population of 10^5 cells. Cells are then maintained under normal conditions for 3 days to achieve the required cell count for treatment exposure.

ii Test compound treatment and sub-culturing

Cells are then treated with different concentrations of test compound as per OECD guideline 476 (1997). The test compound is then removed and cells are cultured in normal media for 13 days. Initial cell divisions result in permanent mutations, with the possibility of changing the structure and function of the resulting HPRT proteins. The mutated proteins accumulate and then change the phenotype of the cells with respect to HPRT function (the salvage pathway). Subsequent culture growth over 13 days allows mutant HPRT to replace the wild type HPRT within the cell to HPRT $^-$. Cultures are diluted with fresh media on alternating days to replenish nutrients. Depending upon cell type, maximum mutation frequency is achieved 4-9 days post treatment and remains stable up until 17 days (Diamond *et al*, 1982; Grosovsky and Little, 1983).

iii Mutation selection and quantification

At 13 days post treatment, the culture consists of a mixture of $HPRT^+$ and $HPRT^-$ cells. To isolate $HPRT^-$ cells for propagation and colony counting, cells are diluted and pipetted into 96 well plates in the presence of 6-TG which becomes toxic when catalysed by HPRT in $HPRT^+$ cells. Each well represents an independent count and a higher number of counts are recommended for statistical threshold analysis (Doak *et al*, 2007). Each $HPRT^-$ colony derives from a single mutated cell and thus represents one colony.

1.16 Alternative mutation assays

Other biological tests are available as alternatives to the HPRT assays. These alternatives include Ames, Pig-a and Thymidine kinase (TK) assays.

- Ames is a bacterial reverse mutation assay which uses amino acid-dependent strains of *Salmonella typhimurium* and *Escherichia coli* that carry mutations in the genes required for histidine synthesis (Ames *et al*, 1973). The test measures the reverse mutations to form histidine biosynthesis capability in the absence of histidine or in histidine free culture media. Mutagens cause an increase in the number of revertant colonies as compared to that of spontaneous reversions. The Ames test has been used in initial screening of the genotoxicity of chemicals and has well defined OECD

guidelines. It is widely used in a battery of mutation tests for regulatory purposes (COM guidelines, 2000). Limitations of the assay include reliance on bacterial cells which therefore does not represent a perfect model for humans.

- Pig-a is a flow cytometry based assay that detects mutations in *Pig-a*, a gene whose product is essential for the synthesis of glycosylphosphatidylinositol (GPI) anchors. In the absence of these anchors, surface markers (CD58, 59) will not be expressed. The assay measures the frequency of cells without these surface markers. It is a rapid screening assay that can also be used *ex vivo*, however, it has not been validated by OECD. Another limitation of the assay is that it does not identify the sources of Pig-a mutation.
- The TK assay is used to detect mutations at the thymidine kinase locus involved in pyrimidine biosynthesis. Mutant cells, lacking in TK are resistant to the cytotoxic effect of pyrimidine analogues such as trifluorothymidine (TFT) (Clive and Spector, 1975). An increase in the number of mutant cells represents mutagenicity of the test chemical. This assay can detect recombinations, non-disjunctions and larger deletions but it has a higher background than the HPRT assay (Doak *et al*, 2007).

1.17 Construction of mutation spectrum

Mutation spectra are recognised as sequence maps that represent the types and distributions of initial lesions caused by exposure to mutagens. They also reflect the characteristics of DNA replication and repair mechanisms present in the cell lines involved (Rogozin *et al*, 2003). Nowadays, there is a growing interest in identifying the correlation between exposure to certain carcinogens and the risk of cancer induced by alterations in mutated genes. Mutation spectra in cancer genes have already been examined in various studies in *in vivo* (Burkhart-Schultz *et al*, 1993; Boyiri *et al*, 2004) and *in vitro* experimental systems (Chan 2002; Gottschalg *et al*, 2007) shedding some light on the mechanisms involved in carcinogenesis (Dogliotti *et al*, 1998).

It is possible to construct the mutation spectra of *HPRT* mutants by DNA sequence analysis. Mutation spectra provide the information about the location and frequency of mutations in a DNA sequence. In the present study, the *HPRT* gene was used to build the mutation spectra induced by B[a]P.

The mutation spectra are useful to understand the mechanisms of mutation in single cell organisms, and causes of genetic changes in human organs (Chen and Thilly, 1996). Kohler,

et al (1991) used the *lacI* gene to construct the spectra of spontaneous and mutagen-induced mutations in transgenic mice exposed to ENU and B[a]P, and concluded that the pattern of mutation induction was mutagen specific (Chen and Thilly, 1996). Therefore, mutation spectra can provide the information of mutation induction caused by different mutagens, define mutation hotspots (Casciano *et al*, 1999), can compare mutation induction *in vivo* and *in vitro* in repair deficient and proficient cells ((Tomita-Mitchell *et al*, 2003; Chen *et al*, 1992; Yang *et al,* 1994) and aid in understanding the molecular nature of spontaneous mutations (Zhang *et al*, 1992; Lewis *et al,* 2001).

1.18 DNA sequencing

DNA sequencing is the process to determine the actual order of nucleotides within DNA. Sanger in 1977 developed a rapid DNA sequencing method. Recently many methodologies have been developed based on Sanger's method but with automation to achieve better results with less cost. The method employed in the current study used four dideoxynucleotides (ddATP, ddCTP, ddGTP and ddTTP), each ddNTP with a different fluorescent tag, were mixed with sample DNA. The ddNTP's contain a hydrogen group (H) instead of a hydroxyl group (OH), and as such once incorporated into the DNA strand during synthesis, block the addition of further nucleotides and terminate the DNA chain into the growing DNA strand. The result is a mixture of oligonucleotide fragments of varying sizes. The fragments are then separated by size and fluorescence emission. It is important to sequence the genomic DNA to define the exact mutation present within the *HPRT* gene.

1.19 Quantitative Real- time Polymerase Chain Reaction (qRT-PCR)

qRT-PCR was first described in the mid- 1990 and is the variation of the standard PCR technique. It is an efficient, sensitive and robust method of detecting and quantifying gene expression (Bustin, 2009). This technique allows detection and quantification in real time during each cycle and removes the need for post PCR product processing. It uses a similar principle to PCR, however, it relies on detection and quantification of a fluorescent reporter which is directly proportional to the amount of amplicon being generated (Ginzinger, 2002). There are two common methods to quantify the amount of DNA in real time.

1. The first method involves the use of non-specific fluorescent dyes such as SYBR Green that binds to any double stranded DNA (Morrison *et al*, 1998; Schmittgen *et al*, 2000). SYBR Green binds to the minor grooves of the DNA double helix and can be

used to detect any double stranded target including primer dimers. To improve the specificity of SYBR Green based qRT-PCR, PCR reactions must be optimized to reduce primer dimers and amplification of non-specific products (Bustin, 2000). The only disadvantage of using DNA binding dyes is that they will bind to all DNA present in a sample.

2. The second method relies on DNA probes that transmit fluorescence upon binding to sequence specific DNA (Bustin, 2000). The most commonly used probes include hybridisation probes, molecular beacons and hydrolysis probes such as TaqMan probes. These probes are sequence specific thus only bind to target DNA and increase specificity. These probes can also be used in the presence of non-specific DNA or to amplify more than one target in a multiplex reaction. Due to their high sequence specificity, these probes can only be used for one target, and thus requires design and optimization of a new probe for each target (Bustin, 2000).

Quantification of real time PCR can either be done using an absolute or a relative quantification method. The absolute method involves the use of a standard curve generated from a known product to quantify the amount of unknown target in samples (Bustin, 2000). A standard curve is obtained by a serially diluted standard solution Relative expression is based on expression levels of a target gene against a housekeeping gene and thus is considered to be the most adequate method of investigating physiological changes in gene expression (Livak, 2001, Bonetta, 2005)

In ordered to obtain a standard curve a housekeeping gene such as Beta-actin (β- actin) is used. With a housekeeping gene as a standard it is therefore possible to measure increase or decrease in required gene copy number relative to housekeeper.

1.20 Aims of Thesis

The aim of this thesis were to

- Understand the *in vitro* dose response relationship of two pro-carcinogens B[a]P and PhIP at low doses using cell lines with different metabolic potential.
- Determine whether these pro-carcinogens follow linear or nonlinear dose-responses as there is no evidence of genotoxic thresholds for these chemicals. .
- Understand the underlying mechanisms in the metabolic activation dependant mutagenesis of B[a]P and PhIP,
- Determine genetic mutations caused by B[a]P and PhIP to analyze mutation spectra to understand the types of mutations caused by these chemicals.
- Determine the effect of B[a]P and PhIP on CYP450 expression in cell lines with varying level of metabolic activity.

Chapter 2

General Materials and Methods

2.1 Tissue culture

All tissue culture was carried out in sterile Biological Safety Cabinets (Scanlaf Mars Pro class2, VWR International Ltd, Leicestershire, UK) pre-cleaned with 70% ethanol and UV sterilisation. The equipment and media used were sprayed with 70% ethanol before placing in the safety cabinets. When handling toxic chemicals appropriate safety precautions including lab coat, goggles and over-arm gloves were used.

2.1.1 Cell lines

AHH-1, MCL-5 , TK6 and HepG2 cell lines were used in this study.

2.1.2 Cell culture

MCL-5, AHH-1 and TK6

All cells were cultured in RPMI 1640 (GIBCO®, Paisley, UK) supplemented with 10% horse serum (GIBCO®, Paisley, UK) and 1% L-Glutamine (GIBCO®, Paisley, UK). In addition MCL- 5 cells were supplemented with hygromycin B (final concentration 200μg/ml, see Appendix I, A) at each passage to ensure plasmid retention (Crespi *et al*, 1991).

All cells were cultured in growth media in humidified atmosphere at 37°C, 5% CO_2. Mycoplasma testing was carried out routinely by using MycoAlert® mycoplasma detection kit (Lonza, Slough, UK). The cell concentrations were maintained between 1-3 x 10^5cells/ml and sub-cultured every 2 days, when cell populations reached confluency, which was confirmed by microscopic examination under x100 objective on a Ziess Axiovert 25 light microscope. For sub-culturing, cells were centrifuged at 113 x g (1200 rpm) for 10 minutes and then re-suspended in a volume of 50ml culture medium in 75 cm^2 flasks. The cells were counted with a haemocytometer (Hawksley, Sussex, UK) or the Z1 Coulter Particle Counter (Beckman Coulter Inc., High Wycomb, UK) and diluted to a final concentration of 1.5 x 10^5cells/ml in 50ml media. MCL-5 and AHH-1 cell lines have a cell cycle time of 22-24h and TK6 cells have 18h cell cycle.

HepG2

HepG2 cell line was cultured in DMEM (GIBCO®, Paisley, UK) supplemented with 10% foetal bovine serum (FBS, GIBCO®, Paisley, UK). Sub-culturing or processing of HepG2 cells was performed by trypsinisation with trypsin/EDTA solution (0.05%) (GIBCO®, Paisley, UK). Firstly, the old media was discarded and cells were washed twice with phosphate buffered saline (PBS, GIBCO®, Paisley, UK) to remove traces of media. Then cells were washed twice with warm trypsin. Finally a sufficient amount of trypsin was added to cover the whole surface of cells, and the flask left for 6-8 minutes, after which the flask was gently tapped to dislodge cells from its surface. Once the cells were lifted they were transferred to a multipurpose container (Greiner bio-one) using a syringe with a 1G needle (BD Microlance 3) and 5ml of PBS was added to dilute the trypsin. Cells were then centrifuged at 113 x g (1200rpm) for 10min, the supernatant discarded, and washed with PBS and 5 ml growth media.

Cells were counted with a haemocytometer (Hawksley, Sussex, UK) or the Z1 Coulter Particle Counter (Beckman Coulter Inc., High Wycomb, UK) and diluted to a final concentration of 1.5 x 10^5cells/cm^2 in 15ml of media in a 75 cm^2 flask (Cellstar). These cells were cultured in growth media in humidified atmosphere at 37°C, 5% CO_2. Mycoplasma testing was carried out routinely by using MycoAlert® mycoplasma detection kit (Lonza, Slough, UK). The cell concentrations were maintained between 1-3 x 10^5cells/ml or cm^2 and sub-cultured every 5 days, until they reached confluency, with microscopic examination under x 40 objective on a Ziess Axiovert 25 light microscope.

2.1.3 Measurement of cell concentration

The amount of cells per ml of culture media was measured by either the haemocytometer or the Z1 Coulter Particle Counter.

Haemocytometer

For the haemocytometer 10µl of cell suspension was taken from the culture flask after gentle shaking and spread on the haemocytometer slide. The number of the cells were scored from each of the four large corner counting chambers (each comprised of 16 small squares), averaged and multiplied by 1x10^4 to obtain the final cell number per ml of media (Figure2.1)

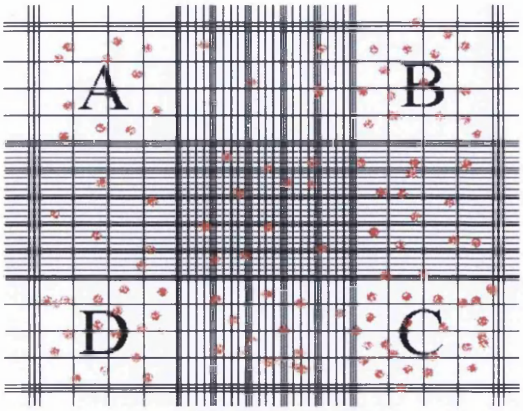

Figure 2.1 Diagram of a haemocytometer grid. Cells (red dots) were counted from A, B, C and D labelled squares, averaged and multiplied by $1x10^4$ to get final cell number per ml of media. Modified from home.c.c.umanitoba.ca.uk.

Z1 Coulter particle counter

For the Z1 Coulter Particle Counter 100µl of cell suspension was taken from culture flask after gentle shaking and poured into a cuvette containing 10ml of dilute conducting liquid (Coulter Isoton). The particles passed through an aperture of defined size and cell number is displayed on a screen as cells per ml of media (Figure 2.2).

Figure 2.2 Z1 Coulter Particle Counter. Cell suspension was mixed into Coulter Isoton in the cuvette and the particles passed through the aperture their number displayed on screen. Image derived from www.bioniquest.com.uk.

The following equation was used to calculate the appropriate cell concentration for all experiments.

$$C_1 x V_1 = C_2 x V_2$$

Therefore,

$$V_2 = \frac{(C_1 x V_1)}{C_2}$$

Where

C_1= Concentration needed (cells/ml)

V_1= Volume needed (ml)

C_2= Culture concentration (cells/ml)

V_2= Volume of stock (ml)

For example; dilute a cell stock of $1.3x10^6$cells/ml to 50ml at $1.2x10^5$cells/ml.

$$V_2 = \frac{(1.2x10^5 x 50)}{1.3x10^6}$$

V_2= 4.6ml

Therefore,

4.6ml (from stock) + 45.4ml growth media will give 50ml at $1.2x10^5$cells/ml.

2.1.4 Cell freezing for long term storage

Cell stocks were stored at an ultra-low temperature by cryopreservation process. Confluent cell suspension was poured into a multipurpose container (Greiner bio-one) and centrifuged at 113 x g (1200rpm) for 10minutes. The supernatant was discarded and the pellet was re-suspended in 4ml of horse serum containing 10% v/v dimethyl sulfoxide (DMSO, Fisher Scientific). Subsequently, 1.5ml of cell suspension was aliquoted into cryovials®(Elkay Laboratories products) and then did gradual freezing by placing overnight into -80°C freezer (New Brunswick Freezer) in Biofreezing vessels (Bicell) and then cryovials were transferred to liquid nitrogen at -196°C for long term storage.

To use the frozen cells, the cryovial® was removed from the liquid nitrogen and thawed rapidly at 37°C using water bath (Grant) before transferral to 50ml growth media.

2.2 Preparation of chemical stocks for experiments

All toxic chemicals were handled inside an allocated sterile Biological Safety Cabinet (Scanlaf Mars Pro class2, VWR International Ltd, Leicestershire, UK) pre-cleaned with 70% ethanol and UV sterilisation. All pieces of equipment were also sterilized prior to use. To prevent the leaching of plastics, stocks were prepared and diluted in glass vials (Sigma, Gillingham, UK) using appropriate solvents (Table 2.1). All the toxic waste material was carefully disposed of in plastic containers intended for incineration.

Table 2.1 Chemicals and their stock information

Chemical name	Solvent	Stock concentration	Final concentration in media	Storage after reconstituted (°C)
Benzo-a-pyrene (B[a]P)	DMSO	1M	**Refer to Table 3.1**	4 for 2weeks
N-Cyclohexyl-N'-dodecylurea (NCND)	Methanol	10mM	170nM	-20 up to 3 months
2-Amino-1-methyl-6-phenylimidazo 4,5-b)pyridine (PhIP)	DMSO	1M	**Refer to Table 5.1**	Discarded after use
6-thioguanine (6-TG)	1M sodium hydroxide (NaOH)	1.5µg/ml	0.6µg/ml	-20

2.2.1 Benzo[a]pyrene (B[a]P)

Benzo[a]pyrene (B[a]P)(Sigma. UK)

Catalogue Number: B1760

Molecular Formula: $C_{20}H_{12}$

Molecular weight: 252.32g/ml

CAS Number: 50-32-8

2.2.2 Soluble Epoxide Hydrolase Inhibitor, N-Cyclohexyl-N-dodecylurea (NCND)

(Calbiochem, EMD Chemicals Inc. an affiliate of Merk KGaA, Darmstadt, Germany)

Catalogue Number: 324813

Molecular formual: $C_{19}H_{38}N_2O$

Molecular weight: 310.5g/ml

CAS Number: 402939-18-8

2.2.3 2-Amino-1-methyl-6-phenylimidazo 4, 5-b) pyridine (PhIP)

2-Amino-1-methyl-6-phenylimidazo (4,5-b) pyridine(PhIP) (Santa Cruz Biotechnology, Inc)

Catalogue Number: 1530

Molecular Formula: C13H12N4

Molecular weight: 224.26/ml

CAS Number: 105650-23-5

2.2.4 6-thioguanine (6-TG)

The 1x stock of 6-TG was prepared in 0.1M sodium hydroxide solution (NaOH. Appendix I, B) from 30x stock (4.5mg/ml; Sigma), and filter sterilized by 0.2μM filter. To minimize freeze and thaw cycles, 5ml working stocks at 0.15mg/ml (1x) aliquots were prepared and kept at -20°C. To get a final concentration of 0.6μg/ml, 40μl of 1x 6-TG was added to 10ml of culture flask. One stock of 6-TG was used for all HPRT assays. The quality of stock was checked by determining the absorbance ratio of 320/260nm and reliable stock has >2.5 ratio. The stock used here had a 4.8 (0.708/0.149) ratio.

2.3 Assessing cytotoxicity using relative population doubling (RPD)

Relative population doubling (RPD) toxicity measure was used to calculate the cytotoxicity of the chemical in the absence of cytochalasin B (Lorge *et al*, 2004). RPD was determined by counting the number of cells before and after treatment. For each cell line 10ml cell suspensions per dose were seeded at 1 x 10^5cells/ml (AHH-1, MCL-5 and TK6) or 1.2 x 10^5 cell/cm^2 (HepG2) for 24h at 37°C, 5% CO_2. Each treatment flask of HepG2 was counted on day of seeding. After 24h each flask (AHH-1, MCL-5 and TK6) was gently shaken and 100μl culture media was pipetted out and mixed with 10ml Isoton diluent (Beckman) and the cell number was counted using the Beckman coulter counter. Each flask was treated with appropriately diluted chemical and incubated for 4h or 24h at 37°C, 5% CO_2. After different incubation times the flasks were washed twice with growth media (without supplements) and re-suspended in 10ml growth media. Again 100μl was sampled and counted to obtain 24h post-treatment counts. Cytotoxicity analysis was performed in triplicate. All three pre- and post-counts were averaged and used for calculating relative population doubling by using the following formula:

$$\text{RPD} = \frac{\text{Number of population doubling (PD) in treated cultures}}{\text{Number of population doubling (PD) in control cultures}} \times 100$$

Where,

$$\text{PD} = \frac{[\log(\text{24h Post-treatment cell number/Initial cell number})]}{\text{Log2}}$$

2.4 The *in vitro* Cytochalasin-Blocked Micronucleus (CBMN) Assay

The semi-automated scoring protocol, using the Metafer-System (MetaSystems, Altlussheim, Germany) was performed in this study (Decordier *et al*, 2009).

2.4.1 Initiation of the assay

To analyse the levels of chromosomal damage induced by a chemical, 10ml cell suspensions per dose were seeded at 1 x 10^5cells/ml (AHH-1, MCL-5 and TK6) or 1.2 x 10^5 cell/cm^2 (HepG2) for 24h at 37°C, 5% CO_2 into 25cm^2 flasks. Each was dosed with appropriately diluted test chemical (Table 3.1; Table 5.1) for different time points (4h and 24h). After a set time point the suspensions (from AHH-1, MCL-5 and TK6) were transferred to labelled tubes. The cells (AHH-1, MCL-5 and TK6) were spun down for 10min at 113 x g (1200rpm) and washed twice with growth media (without supplement) to remove any residual chemical. The media with chemical was pipetted out. from HepG2 flasks . The cells were washed with PBS twise. Cells were again re-suspended in 10ml of growth media and transferred to 25cm^2 flasks. Then 40µl (4µg/ml, AHH-1, MCL-5 and HepG2) or 20µl (2µg/ml, TK6) depending on the cell line, cytochalasin B (Merk) was added to the flasks for one cell cycle. HepG2 cells were trypsanised and then wash with PBS.

2.4.2 Cell harvesting and slide preparation

For semi-automated scoring, cells were prepared as described by Verga *et al*, (2004). After washing the cells with PBS (Lonzo, Blackley, UK), the cells were treated with 0.56% KCl solution, centrifuged for 10min at 800rpm and supernatant was discarded. Cells were then fixed with methanol/acetic acid/ 0.09% NaCl (5:1:6) solution for 10 min. Centrifuged at 124 x g (800rpm) for 10min at 4°C (Centrifuge 5810R, Eppendorf) and the supernatant was discarded. Next, a second fixation step was performed by adding methanol/acetic acid (5:1) for 10mins, centrifuged for 10min (124 x g or 800rpm) at 4°C, and the supernatant discarded. This second fixation wash was repeated four times. Cells were incubated in fixative 2 for 16hours at 4°C.

The fixed cells were dropped across the length of labelled slides and mounted in Vectashield anti-fading solution containing 4',6-diamidino-2-phenylindole (DAPI) stain (Vector) and covered with a cover-slip (25 x 60mm, VWR International).

2.4.3 Scanning and scoring

The slides were scanned at 10x magnification with the Metafer 4 master station, coupled to an Olympus BX50 fluorescent microscope (Carl Zeiss), a Dell computer hub loaded with the Metafer 4 Version 3.8.5 software and a high resolution megapixel charge coupled device (CCD) camera (Axiocam; Carl Zeiss) for image capture. A number of grid positions evenly distributed across the scan area determined the plane of focus and a predetermined scan area

was used for all slides. Classifiers developed by Metasystem were modified to detect binucleated cells. The search definition classifiers were used to define the size and shape of nuclei and micronuclei (MN) (Table 2.2).

Table 2.2 Classifier settings on the Metafer-System to define binucleated cells and micronuclei (MN)

	Binucleated cells	
	Nuclei	**MN**
Object threshold	30%	8%
Minimum area	20μm^2	1.5μm^2
Maximum area	400μm^2	55μm^2
Maximum relative concavity of depth	0.9	0.9
Maximum aspect ratio	1.5	4
Maximum distance between	30μm	25μm
Maximum area asymmetry	70%	-

The detection and scoring process for the Metafer-system was done in three steps: firstly the slides were scanned and binucleated cells detected. Secondly MN-positive binucleated cells were validated microscopically and finally manual confirmation of the MN was performed in the image gallery (Figure 2.3). A minimum of 10,000 or 6000 binucleated cells per dose were scored for B[a]P and PhIP respectively.

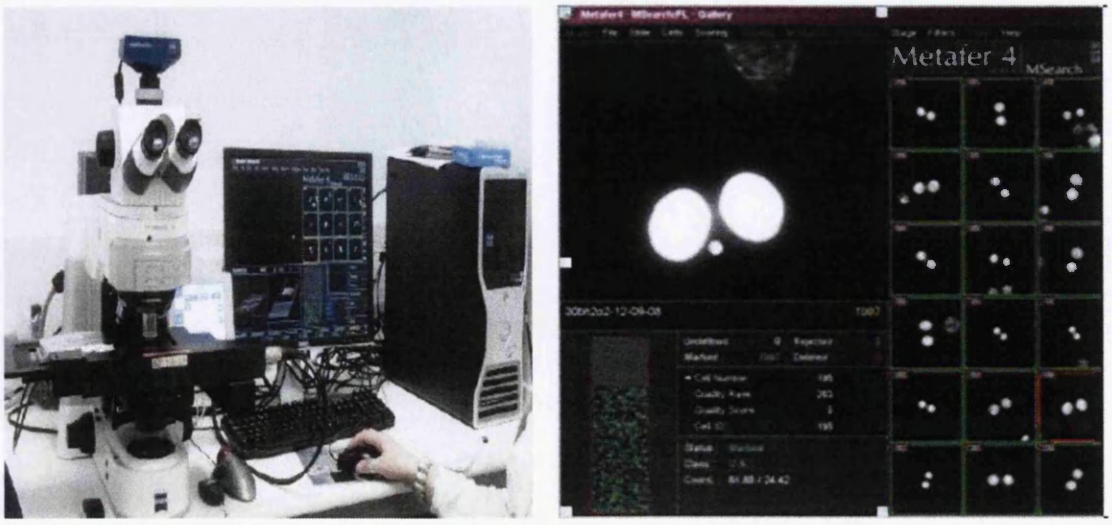

A B

Figure 2.3 Metafer 4 master station (A) and Metafer image gallery showing a binucleated cell with micronuclei (B)

2.5 The mammalian cell HPRT assay

The hypoxanthine phosphoribosyl transferase (HPRT) is a gene mutation assay which detects mutations that destroy the functionality of the HPRT gene or protein by positive selection (Johnson *et al*, 2012).

2.5.1 Mutant cleansing stage

This first step was necessary to establish a HPRT mutant free cell stock, and involved adding 1ml of hypoxanthine-aminopterin-thymidine (50x HAT, Invitrogen, Paisley, UK) to 49ml AHH-1 or MCL-5 cultures ($4x10^5$ cells/ml), which were then grown for 3days. After that the cells were centrifuged at 113 x g (1200rpm) for 10min, washed with PBS and re-suspended in 49ml fresh growth media supplemented with 1ml HT (HAT media without aminopterin, 50xHT, Invitrogen, Paisley, UK) for appropriate cell sub-culturing. Cells were grown in the presence of HT for 24h, washed with PBS and re-suspended in 100ml normal growth media for 2days. Cells were then frozen according to the method outlined in Section 2.1.4.

2.5.2 Treatment protocol

After the mutant cleansing stage the cells were revived as mentioned in section 2.1.4 and grown in normal growth media for 2 days. 10ml cell cultures were established into $25cm^2$ flasks at a concentration of $4x10^5$ cells/mland incubated at 37°C, 5% CO_2. The cell cultures were then treated with the appropriate test chemical for a set time period (4h or 24h). After treatment time the chemical was washed off with growth media (without supplements), the cells re-suspended in 50ml growth media in $75cm^2$ flasks and left to grow for thirteen days at 37°C, 5% CO_2 to enable expression of a mutant HPRT (HPRT$^-$) phenotype. The day treatment was removed was counted as day 0 and sub-culturing took place on days 1, 3, 5, 7, 9 and 11. On day 7, during the mutant expression period, some cultures were frozen down in liquid nitrogen for further analysis. Upon revival, cells were designated day 7 and sub-cultured on day 9. After the phenotypic expression period at day 13, cell suspensions were transferred to 96 well plates (100µl per well).

For mutation frequency (MF) analysis, cell cultures with a concentration of $4x10^5$ cells/ml in 60ml were treated with 240µl of 6-TG (0.6µg/ml) for selection. Ten or five plates per dose were loaded with 100µl of cell suspension in each well ($4x10^4$cells/well). HPRT $^+$ cells incorporate 6-TG into the DNA and die, where as HPRT$^-$ cells cannot incorporate the toxic analogue into their DNA and consequently survive (Johnson, 2012).

For plating efficiency (PE), 200cells/ml (20cells/well) in 100µl non-selective media were added into each well of 5 plates per dose.

All plates were incubated at 37°C, 5% CO_2 for 14 days before cell colonies scored. Only 60 wells per plate were scored; the perimeter wells were excluded because the media partially evaporated. Colonies having >20cells in diameter with a smooth and shining outer boundary and a light colour were identified as positive mutants. The experiment was carried out in triplicate.

2.5.3 Equations for mutation frequency and plating efficiency

Percentage Plating Efficiency (%PE) = $-\text{Ln}\,(X_o/N_o) \times 100$

$$\text{Cell Viability (\%)} = \frac{\text{PE}}{\text{PE of control}} \times 100$$

$$\text{Mutation Frequency (MF)} = \frac{-\text{Ln}\,(X_s/N_s)}{-\text{Ln}\,(X_o/N_o)} \times \text{DF}$$

$$\text{DF} = \text{Dilution factor} = \left[\frac{\text{(No. of initial cells per well) Non-selective conditions}}{\text{(No. of initial cells per well) selective conditions}}\right]$$

X_s = No. of wells without colonies
N_s = Total no. of wells
} Selective conditions

X_o = No. of wells without colonies
N_o = Total no. of wells
} Non-selective conditions

2.5.4 Enumeration of mutant colonies

At the end of the HPRT assay, colonies from the solvent control and selected dose plates were aspirated and transferred to 24 well plates (Nunc, ThermoScientific, Loughborough, UK) containing 2ml growth media per well. The colonies were grown for sufficient RNA yield. The plates were left to grow at 37°C, 5% CO_2 for 5 days and then individual cell colonies were carefully aspirated using a 300µl pipette, mixed with 5 volumes (1.5ml) RNA protect® cell reagent (Qiagen, Sussex, UK) and stored at -20°C for RNA extraction.

2.6 RNA extraction

2.6.1 RNA extraction from cultured cell lines

Total RNA was extracted using the RNeasy Mini Kit® (Qiagen, Sussex, UK) according to the manufacturer's instructions. All surfaces and equipment were wiped with RNAzap® (Applied Biosystems, Warrington, UK) to remove RNAses. All the centrifugation was done at 25°C for 15sec at 9503 x g (10,000rpm) in (BIOFUGE Fresco, Heraeus) a centrifuge with a radius of 85mm, unless stated otherwise. Cells in the RNA protect® cell reagent were defrosted at room temperature and pelleted by centrifuging at 275 x g (1700rpm) for 3mins (Centra CL 3 R) and re-suspended in 350µl RLT cell lysis buffer. The cells were homogenized by passing the lysate 5 to 6 times through a 20G needle (0.9 x 40mm, BD Microlance 3) fitted to a 2ml syringe. Next an equal volume (350µl) of 70% ethanol was added, which binds RNA to the spin column, the sample was mixed thoroughly and applied to the spin column. The column was centrifuged and the flowthrough discarded. The column was washed with 350µl RW1, centrifuged and flowthrough discarded. Genomic DNA was digested using the RNase-free DNA set (Qiagen, Sussex, UK). For each column 80µl DNase mix (10µl DNaseI+70µl RDD buffer) was applied and incubated at room temperature for 15mins, followed by another washing step with 350µl wash buffer RW1. Then 500µl buffer RPE was added to the column and the sample centrifuged. A second 500µl buffer RPE wash was performed but centrifuged for a longer time (2min) to dry the column from ethanol present in the buffer RPE. The column was then transferred to a new collection tube; 30µl water was added directly to the column and incubated at room temperature for 10mins. Finally RNA was eluted by centrifugation.

2.6.2 Quantification and storage of RNA

The concentration of RNA and its purity (A_{260}:A_{280}) was determined with a NanoDrop (ND-1000 Spectrophotometer, Labtech International, Uckfield, UK). Nucleic acids absorb at 260nm and contaminating proteins and other material absorb at 280nm. RNA was considered suitably pure for use if the A_{260}/A_{280} ratio was greater than 1.6.

To calculate 1µl RNA for cDNA synthesis following formula was used.

$$\text{Volume (µl) of sample to give 1µg RNA} = \frac{1000(\text{ng})}{\text{Amount of RNA (ng/µl)}}$$

For example, if the amount of RNA in sample is 350ng/µl then 2.85µl of sample would give 1µg for cDNA synthesis

The samples were divided into two aliquots and stored at -80°C (New Brunswick freezer). The first RNA aliquot was used for end-point PCR and mutation detection through sequencing and the second aliquot to confirm mutations in the same samples.

2.6.3 Complementary DNA (cDNA) synthesis for end-point PCR

RNA samples were converted into cDNA using RETROscript® kit (Applied Biosystems, Warrington, UK). The cDNA synthesis reactions were set-up on ice within a purifier vertical clean bench (Labconco, USA) pre-cleaned with RNAzap®. The volumes of reagents used per reaction are given in Table 2.4.

Table 2.4 Reagents per sample for cDNA synthesis

Reagents	Volume (µl)
RT Buffer	1
Oligo (dT)	1
dNTP	2
RNase inhibitor	0.5
MMLV-reverse transcriptase enzyme	0.5
RNA template	1µg
Nuclease-free water	= 5 – volume of RNA
Total volume	**10**

The icycler (Bio-Rad, Hemel Hemstead, UK) was used to run the reaction at 44°C for 60min followed by 10min at 90°C to inactivate the reverse transcriptase enzyme. cDNA was stored at -20°C until further use.

2.6.4 End-point PCR

Oligo (dT) primers targeted all mRNA transcripts from the total RNA extracted from cells while β-actin is an abundant target with optimised primers. Therefore, β-actin primers were used to amplify the β-actin cDNA which clarifies the success of the cDNA reaction. The master mix was prepared for this reaction from reagents listed in Table 2.5. All the reagents used to prepare the master mix were purchased from Promega (Southampton, UK) and β-actin forward and reverse primers were synthesized by MWG Eurofins (Germany) with instructions for reconstitution of lyophilized primers to 100µM (pmol/µl) with nuclease free water. The primer master stock was further diluted to 1:10 (10µl stock + 90µl water) to 10µM working stock in nuclease-free water and frozen (-20°C) as single use (10µl) aliquots.

Table 2.5 Components for master mix to amplify β-actin cDNA

Reagents	Final concentration	Volume (µl) in β-actin master mix
5x Go Taq® Flexi Buffer	1X	5
10mM dNTP mix	0.2mM each	0.5
25mM Magnesium Chloride	2mM	1.5
β-actin forward primer	0.2µM	0.5
β-actin reverse primer	0.2µM	0.5
GoTaq® DNA polymerase (5u/µl)	1.5U	0.15
cDNA template	-	1
Water	-	15.85
Total	-	**25**

The conditions used in the icycler (Biorad, Hemel Hemstead, UK) for the amplification of β-actin mRNA are shown in Table 2.6.

Table 2.6 Thermo-cycling conditions for β-actin mRNA amplification

Steps	Temperature (°C)	Time	Number of cycles
Initial denaturation	93	2min	1
Denaturation	93	10sec	25
Annealing	60	20sec	
Extension	72	10sec	
Preservation	4	Infinity	-

Upon reaction completion, samples were stored at -20°C until required for gel electrophoresis and DNA sequencing.

HPRT cDNA was amplified by using two pairs of overlapping primers (D and K) to obtain 83% gene coverage. The oligonucleotide sequence for each primer is listed in Table 2.7 and their location on the *HPRT* gene is shown in Figure 2.4.

Table 2.7 Primers name and sequences used for the amplification of β-actin and HPRT cDNA

Primer Name	Sequence (5′ – 3′)	Product size (bp)
β-actin Forward	GATGGCCACGGCTGCTTC	100
β-actin Reverse	TGCCTCAGGGCAGCGGAA	
D Forward (HPRT NF2 S-M)	GAACCTCTCGGCTTTCCC	537
D Reverse (HPRT NR2 MS)	TGCCAGTGTCAATTATATCTTCC	
K Forward (HPRT NF3)	GATGATCTCTCAACTTTAACTGG	715
K Reverse(HPRT Inner Reverse)	CTTACTTTTCTAACACACGGTGG	

```
   1 GGCGGGGCCT GCTTCTCCTC AGCTTCAGGC GGCTGCGACG AGCCCTCAGG CGAACCTCTC
  61 GGCTTTCCCG CGCGGCGCCG CCTCTTGCTG CGCCTCCGCC TCCTCCTCTG CTCCGCCACC
 121 GGCTTCCTCC TCCTGAGCAG TCAGCCCGCG CGCCGGCCGG CTCCGTTATG GCGACCCGCA
 181 GCCCTGGCGT CGTGATTAGT GATGATGAAC CAGGTTATGA CCTTGATTTA TTTTGCATAC
 241 CTAATCATTA TGCTGAGGAT TTGGAAAGGG TGTTTATTCC TCATGGACTA ATTATGGACA
 301 GGACTGAACG TCTTGCTCGA GATGTGATGA AGGAGATGGG AGGCCATCAC ATTGTAGCCC
 361 TCTGTGTGCT CAAGGGGGGC TATAAATTCT TTGCTGACCT GCTGGATTAC ATCAAAGCAC
 421 TGAATAGAAA TAGTGATAGA TCCATTCCTA TGACTGTAGA TTTTATCAGA CTGAAGAGCT
 481 ATTGTAATGA CCAGTCAACA GGGGACATAA AAGTAATTGG TGGAGATGAT CTCTCAACTT
 541 TAACTGGAAA GAATGTCTTG ATTGTGGAAG ATATAATTGA CACTGGCAAA ACAATGCAGA
 601 CTTTGCTTTC CTTGGTCAGG CAGTATAATC CAAAGATGGT CAAGGTCGCA AGCTTGCTGG
 661 TGAAAAGGAC CCCACGAAGT GTTGGATATA AGCCAGACTT TGTTGGATTT GAAATTCCAG
 721 ACAAGTTTGT TGTAGGATAT GCCCTTGACT ATAATGAATA CTTCAGGGAT TTGAATCATG
 781 TTTGTGTCAT TAGTGAAACT GGAAAAGCAA AATACAAAGC CTAAGATGAG AGTTCAAGTT
 841 GAGTTTGGAA ACATCTGGAG TCCTATTGAC ATCGCCAGTA AAATTATCAA TGTTCTAGTT
 901 CTGTGGCCAT CTGCTTAGTA GAGCTTTTTG CATGTATCTT CTAAGAATTT TATCTGTTTT
 961 GTACTTTAGA AATGTCAGTT GCTGCATTCC TAAACTGTTT ATTTGCACTA TGAGCCTATA
1021 GACTATCAGT TCCCTTTGGG CGGATTGTTG TTTAACTTGT AAATGAAAAA ATTCTCTTAA
1081 ACCACAGCAC TATTGAGTGA AACATTGAAC TCATATCTGT AAGAAATAAA GAGAAGATAT
1141 ATTAGTTTTT TAATTGGTAT TTTAATTTTT ATATATGCAG GAAAGAATAG AAGTGATTGA
1201 ATATTGTTAA TTATACCACC GTGTGTTAGA AAAGTAAGAA GCAGTCAATT TTCACATCAA
1261 AGACAGCATC TAAGAAGTTT TGTTCTGTCC TGGAATTATT TTAGTAGTGT TTCAGTAATG
1321 TTGACTGTAT TTTCCAACTT GTTCAAATTA TTACCAGTGA ATCTTTGTCA GCAGTTCCCT
1381 TTTAAATGCA AATCAATAAA TTCCCAAAAA TTTAAAAAAA AAAAAAAAAA AAAAA
```

Figure 2.4 Sequence of *HPRT* mRNA or gene, with colour coded primer locations; red- D forward, green- K forward, blue-D reverse and pink-R reverse.

The *HPRT* primers were designed using Beacon 2 software (Premier Biosoft) and synthesized by MWG Eurofins (Germany) with instructions for reconstitution of lyophilized primers to 100µM (pmol/µl) with nuclease free water. The primer master stock for *HPRT* amplification was further diluted to 1:10 (10µl stock + 90µl water) to 10µM working stock in nuclease-free water and stored as single use (10µl) aliquots at -20°C. All the reagents used to prepare master mix were from Promega (Southampton, UK). Two master mixes (D and K) were prepared for each primer pair according to the volumes (0.2µM) shown in Table 2.8.

Table 2.8 Components of each master mix to amplify HPRT mRNA.

Reagents	Final concentration	D Master mix	K Master mix
		Volume (µl)	Volume (µl)
5x Go Taq® Flexi Buffer	1X	10	10
10mM dNTP mix	0.2mM each	1	1
25mM Magnesium Chloride	2mM	4	4
D forward primer	0.2µM	1	0
D reverse primer	0.2µM	1	0
K forward primer	0.2µM	0	1
K reverse primer	0.2µM	0	1
Go*Taq* DNA polymerase (5u/µl)	1.5U	0.3	0.3
cDNA template	-	2	2
Water	-	30.7	30.7
Total	-	**50**	**50**

Both master mixes were run in the icycler (Biorad, Hemel Hempstead, UK) machine simultaneously under the conditions given in Table 2.9. After completion of the reaction, samples were stored at -20°C until required for gel electrophoresis.

Table 2.9 Thermo-cycling conditions for amplification of HPRT cDNA with D and K primers.

Steps	Temperature (°C)	Time	Number of cycles
Initial denaturation	93	2min	1
Denaturation	93	10sec	30
Annealing	52.6	20sec	
Extension	72	10sec	
Preservation	4	Infinity	-

2.7 Visualising PCR products

2.7.1 6% Polyacrylamide Gel Electrophoresis (PAGE) preparation

Vertical 6% PAGE gel were used to verify the success of PCR amplification. The reagents and their volumes used for the preparation of two 6% PAGE gels (7.5cm x 9cm in size) are listed in Table 2.10.

Table 2.10 Reagents for the preparation of two 6% PAGE gels.

Reagent	Supplier	Volume
Distilled water	-	16ml
10x TBE (Tris/Borate/EDTA)	Sigma	2.3ml
10% APS (Ammonium per sulphate)	Sigma	110µl
30% Acrylamide/Bis acrylamide	Bio-Rad	4ml
N,N,N',N'- Tetramethylethylenediamine (TEMED)	Sigma	22.5µl

One litre of 10xTBE and 10% APS were prepared as mentioned in Appendix I, D. Stock 10xTBE was autoclaved for 20min. Gels were constructed as follows; 1.5mm glass plates were wiped with 70% ethanol and assembled in the casting stand. The reagents in Table 2.10 were mixed in a glass beaker and added to the casts. A 15 well comb was inserted in each gel and the gel left to polymerise for 30min at room temperature. The reservoir between the two plates was filled with 1x TBE buffer. The 10µl of each sample was mixed with 2µl loading dye (RETROscript® cDNA synthesis kit). The 1µl of 100 base pair (bp) DNA ladder (Promega, Southamptom, UK) was mixed with 2µl loading dye. The combs were removed carefully and samples/ ladder were carefully loaded into wells using a pipette. The whole gel apparatus was put into a tank filled with 1x TBE buffer and the gel was run at 170V for 30min using a mini protean® 3 cell kit and a power pac 300 (Biorad, Hemel Hempstead, UK). The product bands were visualized by silver nitrate staining.

2.7.2 Silver nitrate staining of gels

The silver stain was prepared and developed within a fume hood (Clean Air limited) according to methods stated in Appendix I, D. Gels were immersed in silver nitrate for 8min at room temperature on agitator at low speed. Then gels were washed twice with distilled water and then incubated at room temperature in developing solution with gentle agitation until the bands were visible. The photographs were taken using Biorad Universal Hood II (Biorad).

2.8 Preparation of HPRT samples for sequencing

The remaining 40µl of PCR product was purified using a PCR purification kit® (Qiagen, Sussex, UK) according to the manufacturer's instructions. Briefly, 200µl (5x volume) of buffer PE, with pH indicator was added to the reaction mixture. The solutions were applied to the provided Qiaquick spin columns and centrifuged for 1min at 16060 x g (13,000rpm) in a Heraeus

Biofuge Fresco centrifuge and the flowthrough were discarded. The 750µl of wash buffer was added with repeat centrifugation and the flowthrough was discarded. The columns were centrifuged to remove ethanol, present in the wash buffer. Finally 30µl of nuclease-free water was added, incubated for 1min at room temperature and eluted by centrifugation.

The samples were sent to Genome Enterprise Limited (Norwich, UK) for sequencing. According to the instructions of Genome Enterprise Limited, 20µl of each sample were put into PCR tubes (Fisher Scientific, Loughborough, UK) in supplied sequencing boxes for shipping. The 1.5µM D forward, D reverse, K forward and K reverse primers were also added into separate tubes in sufficient volume to run 5µl per sequencing reaction. Mutations were identified using mutation surveyor software (3.3). Any mutations found were confirmed by repeat processing of the second aliquot of RNA.

2.9 Construction of mutation spectrum

Mutation spectra were constructed using iMARS software, kindly provided by Dr Paul Lewis at Swansea University (Morgan and Lewis, 2006).

The whole HPRT assay methodology is represented in the form of flow chart in Figure 2.5

2.10 Reverse Transcription-Polymerase Chain Reaction (RT-PCR)

For evaluating the induced expression of CYP1A1, CYP1B1 and CYP1A2 in human cell lines AHH-1, MCL-5, TK-6 and HepG2, RT-PCR was performed. The doses of B[a]P and PhIP treatment selected were based upon the LOEL dose obtained as a result of cytokinesis block micronucleus assay (Table 3.1 in Section 3.4 for B[a]P and Table 5.1 in Section 5.4 for PhIP). All four cell lines were treated with B[a]P and PhIP for 24h.

2.10.1 Genomic DNA (gDNA) elimination reaction

Firstly, the genomic DNA (gDNA) elimination reactions were prepared by using QuantiTect® Reverse Transcription kit (Qiagen). The reactions were prepared using the reagents in Table 2.11.

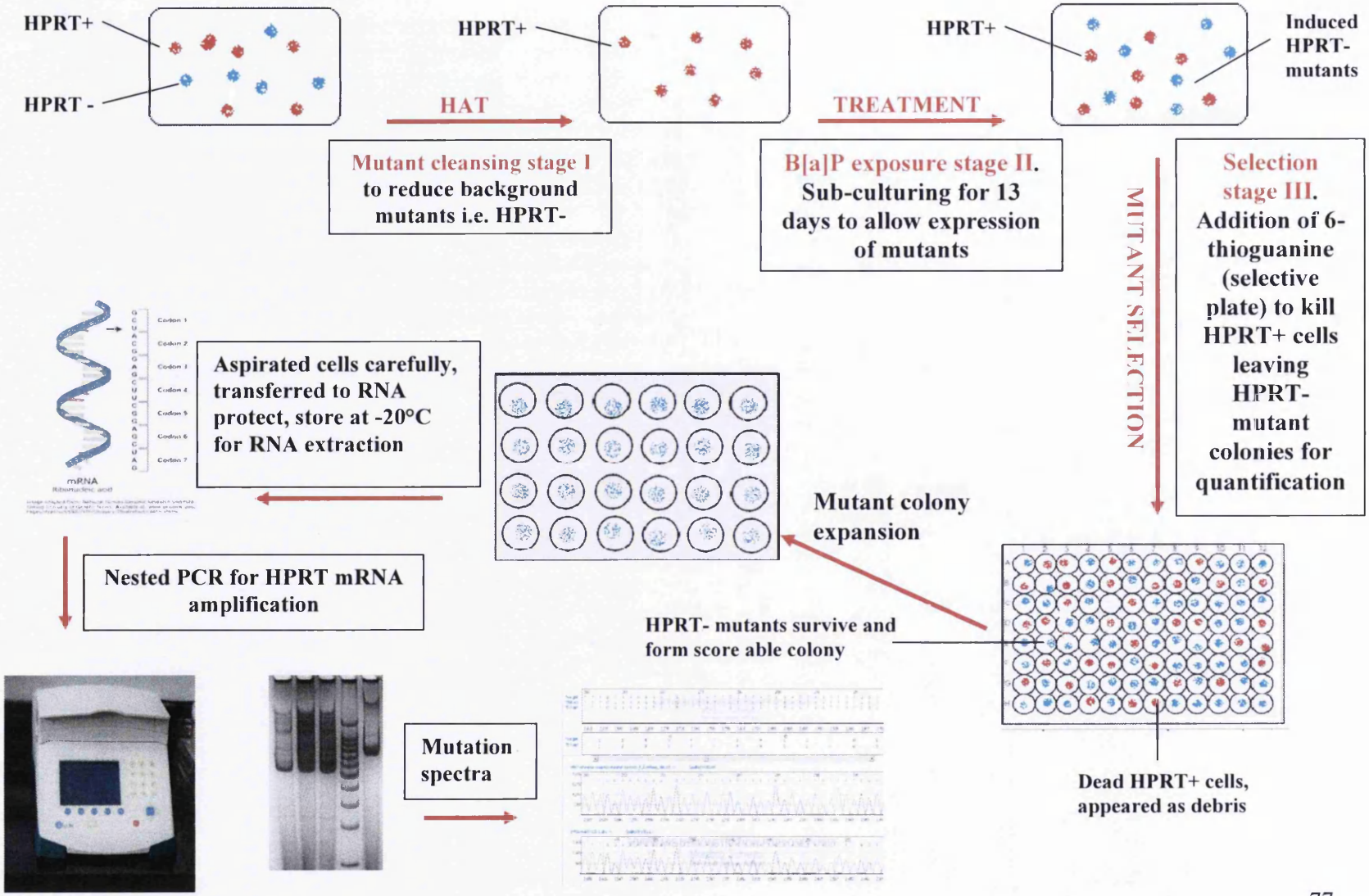

Figure 2.5 Representation of HPRT assay methodology to quantify mutagenic potential of Benzo-a-pyrene on the basis of hypoxanthine guanine phosphoribosyl transferase (HPRT) mutant colony formation in a treated cell population.

Table 2.11 Components for the elimination of genomic DNA from RNA samples.

Reagent	Volume per reaction
gDNA wipeout buffer, 7x	2µl
Template RNA	1µg
Rnase-free water	Make total volume upto
Total	**14µl**

The reagents were vortexed and centrifuged and then incubated for 2min at 42°C on an Thermal Cycler (BIO-RAD T100™, Hampstead, UK). After the completion of the reaction, sample tubes were immediately placed on ice.

2.10.2 cDNA synthesis reaction

Following gDNA elimination, the reverse-transcription master mix for multiple reactions was prepared using reagents listed in Table 2.12. The 6µl of this reverse transcription master mix was added into each genomic DNA elimination reaction tube.

Table2.12 Components for cDNA synthesis reaction.

Component	Reagent	Volume per reaction (µl)
Reverse-transcription master mix	Reverse transcriptase	1
	RT Buffer, 5x	4
	RT Primer Mix	1
Template RNA	Entire genomic DNA elimination reaction	14
Total		**20**

The tubes were vortexed, centrifuged and again incubated for 15min at 42°C followed by 3min at 95°C in a thermal cycler (BIO-RAD T100™, Hampstead, UK) to inactivate the Quantiscript reverse transcriptase. On completion the tubes were stored on ice.

2.10.3 End-point PCR

The master mix was prepared for this reaction from reagents listed in Table 2.13. All the reagents used to prepare master mix were from the GoTaq® Flexi DNA Polymerase kit (Promega, Southampton, UK) and all forward and reverse primers for respective genes listed in Table 2.15 were synthesized by Sigma-Aldrich (UK) with instructions for reconstitution of lyophilized primers to 100µM (pmol/µl) with nuclease free water. The primer master stock was further diluted to 1:10 (10µl stock + 90µl water) to 10µM working stock in nuclease-free water and stored as single use (10µl) aliquots at -20°C until further use.

Table 2.13 Components of master mix to amplify cDNA of CYP1A1, CYP1A2 and β-actin.

Reagents	Final concentration	CYP1A1 master mix Volume (µl)	CYP1A2 master mix Volume (µl)	β-actin master mix Volume (µl)
5x Go Taq® Flexi Buffer	1X	5	5	5
10mM dNTP mix	0.2mM each	0.5	0.5	0.5
25mM Magnesium Chloride	2mM	1.5	1.5	1.5
Forward primer	0.2µM	0.5	0.5	0.5
Reverse primer	0.2µM	0.5	0.5	0.5
Go*Taq* DNA polymerase (5u/µl)	1.5U	0.15	0.15	0.15
cDNA template	-	1	1	1
Nuclease-free water	-	15.85	15.85	15.85
Total	-	**25**	**25**	**25**

The oligonucleotide sequence for each primer is shown in Table 2.14. After completion of the reaction, samples were stored at -20°C until required for gel electrophoresis.

Table 2.14 Primer names and their sequence to amplify the cDNA.

Primer name	Sequence (5′ – 3′)	Product size (bp)
CYP1A1 Forward primer	ATCCTTGTGATCCCAGGCTCC	76
CYP1A1 Reverse primer	TAGGGATCTTGGAGGTGGCTGA	
CYP1A2 Forward primer	CCAACGTCATTGGTGCCATG	262
CYP1A2 Reverse primer	GTGATGTCCCGGACACTGTTC	
β-actin Forward primer	GATGGCCACGGCTGCTTC	100
β-actin Reverse primer	TGCCTCAGGGCAGCGGAA	

All the master mixes were run simultaneously under the conditions given in Table 2.15 using an Thermal cycler (BIO-RAD T100^{TM}, Hampstead, UK).

After the reaction completion, samples were stored at -20°C awaiting 6% PAGE gel electrophoresis.

Table 2.15 Thermo-cycling conditions for amplification of cDNA.

Steps	Temperature (°C)	Time	Number of cycles
Initial denaturation	94	2min	1
Denaturation	94	30sec	34
Annealing	60	30sec	
Extension	72	30sec	
Final extension	72	20sec	
Preservation	12	Infinity	-

2.10.4 Visualizing PCR product

The PCR product was vusualized using 6% polyacrylamide gel followed by silver staining
A photographic record was kept using a Biorad Universal Hood II (Biorad).

2.11 Quantitative Real-time Polymerase Chain Reaction (Real-time PCR)

cDNA was prepared as mentioned in Section 2.11.2 and 2.11.3. Real-time PCR was performed immediately after cDNA synthesis. The expression analysis was performed using QuantiFast™ SYBR® Green PCR Kit (Qiagen, Sussex, UK).

The reactions were set up in the PCR hood under sterile conditions. The components of each reaction are listed in Table 2.16

Table 2.16 Components of each well of a 96-well plate for Real-time PCR.

Components	Volume per reaction (96 well plate) (µl)
2xQuantifast SYBR Green PCR Master Mix	12.5
Primer A	0.25
Primer B	0.25
cDNA template	1.5
RNase-free water	10.5
Total	**25**

Firstly, master mix for each sample was prepared by mixing QuantiFast SYBR® Green Master mix, primers and water to ensure that the same reagents were present in each reaction well. Then 4.5µl sample cDNA (1.5µl per reaction) was added into each master mix. From each master mix 25µl was aliquoted into wells of a sterile 96-well PCR plates (Multiplate™ PCR plate, white, BIORAD, UK). In all experiments the housekeeping gene β-actin was used as a standard to compare gene expression change. Standard samples and negative controls were also included for each primer pair. In negative controls the cDNA was replaced with water.
The plates were sealed after loading all the reactions into the wells with Microseal B Adhesive sealer (MSB-1001, BIORAD, UK). The plates were briefly centrifuged to bring all the contents to the bottom of the wells and placed in the CFX Connect™ Real-Time System (Biorad, Hertfordshire, UK) and run under the following thermocycling conditions:

1. 95°C for 5min
2. 95°C for 10sec
3. 60°C for 30sec

} x 40

4. 65°C for 0.05sec

5. 55°C for 1min
6. 10sec at each 0.5°C increase in temperature from 55°C to 95°C to generate a melt curve

The first step activates the HotStarTaq *Plus* DNA polymerase. Step 2 and 3 represent the PCR reaction, while steps 4 to 6 enable melt curve analysis.

From the amplification reaction the fluorescent data was collected at step 3 as well as analysed in real-time. The melt curve analysis was done by collecting the data from step 6 and analysed in real time.

2.11.1 Data analysis

The CXF Manager Software (Biorad, Herdfordshire, UK) was used to analyse the data. Each sample was analysed individually.

The melt curve of all the samples were analysed for the specificity of the PCR reaction product. If the melt temperature was incorrect for any sample, this sample was removed from the analysis.

For the relative quantification of gene expression the standard curve method was used. Standard samples with known template amounts were defined in the "sample setup" view. Therefore stock cDNA samples were diluted (10-fold dilutions with the dilution values: 1, 10, 100, and 1000). The results from wells defined as Standards were used to generate a standard curve. The crossing points (C_Ts) were plotted against the log of the template amount, resulting in a straight line. Threshold cycle (C_T) values for these samples and the standard curve were then used to calculate the amount of starting template in the experimental samples.

The samples were normalized by their respective endogenous control results to calculate a normalized target value:

$$\text{Normalized target} = \frac{\text{Target}}{\text{Endogenous control}}$$

The normalized target values were then divided by one another to calculate the fold difference in target quantity:

$$\text{Fold difference in Target} = \frac{\text{Normalized target (treated sample)}}{\text{Normalized target (untreated control)}}$$

N-fold differences observed were considered as change in gene expression if <0.5 or >1.5 as defined by Doak et al, (2004) and statistical analysis was conducted.

2.12 DNA extraction from cultured cell lines for *TP53* gene

All TK6, AHH-1, MCL-5 and HepG2 cell lines ($5x10^6$) were centrifuged at 9503 x g (10,000rpm) for 10min at 4°C. The supernatant was discarded and the cells were resuspended in ice cold PBS and recentrifuged. The cell pellet was again resuspended in ice cold PBS and centrifuged at 300 x g (1800rpm) for 10min at 4°C. The supernatant was then removed and DNA was extracted using the DNeasy Blood and Tissue Kit® (Qiagen, Sussex, UK) according to the manufacturer's instructions. All the centrifugation was done at 25°C in (BIOFUGE, Fresco, Heraeus). The cell pellet was resuspended in 200µl PBS and 20µl proteinase K. Then 4µl RNase A was added (to get RNA-free genomic DNA) mixed by vortexing and left for 2min incubation at room temperature. Then 200µl Buffer AL was added and mixed thoroughly by vortexing and incubated again at 56°C for 10min. Afterwards 200µl ethanol (96-100%, Fisher Scientific) was added and mixed by vortexing. The mixture was pipetted into the DNeasy Mini spin column placed in a 2ml collection tube, centrifuged at 6000 x g (8000rpm) for 1min. The flow-through and collection tube was discarded. The spin column was placed in a new 2ml collection tube and 500µl Buffer AW1 added centrifuged for 1min at 6000 x g (8000rpm) and again discarded the flow-through. The spin column was again placed into new 2ml collection tube and 500µl Buffer AW2 was added, centrifuged for 3min at 20,000 x g (14,000rpm) to dry the membrane. The flow-through and tube was discarded. Finally the spin column was placed in clean 1.5ml centrifuge tube and 200µl Buffer AE was added onto the DNeasy membrane and incubated at room temperature for 10min and DNA was eluted by centrifugation for 1min at 6000 x g (8000rpm).

The concentration of DNA and its purity was determined as mentioned in Chapter 2 Section 2.7.2. The samples were divided into two aliquots and stored at -20°C.

2.12.1 Polymerase chain reaction

The GoTaq® Flexi DNA Polymerase Kit (Promega) was used for PCR reaction. The volumes of the reagents used per reaction are given in Table 2.17. The *TP53* forward and backward primers used were synthesized by Sigma (UK). Their name and sequence are listed in Table 2.18.

Table 2.17 Components for master mix to amplify *TP53* cDNA.

Reagents	Final concentration	Volume (µl) in master mix
5x Go Taq® Flexi Buffer	1X	5
10mM dNTP mix	0.2mM each	0.5
25mM Magnesium Chloride	2mM	1.5
Forward primer	0.2µM	0.5
Reverse primer	0.2µM	0.5
Go*Taq* DNA polymerase (5u/µl)	1.5U	0.15
DNA template	-	0.7µg
Nuclease-free water	-	To makeup total volume
Total	-	**25**

Table 2.18 The *TP53* primers and sequences used for the amplification of *p53* DNA.

Primer name	Sequence (5′-3′)	Product length (bp)
Forward primer	TTGGGAGTAGATGGAGCCT	445
Reverse primer	AGTGTTAGACTGGAAACTTT	

The conditions used for the icycler (Biorad, Hemel Hemstead, UK) for the amplification of *p53* DNA were shown in Table 2.19.

Table 2.19 Thermo-cycling conditions for *p53* DNA amplification.

Steps	Temperature °C	Time	Number of cycles
Initial denaturation	92	2min	1
Denaturation	94	30sec	34
Annealing	60	30sec	
Extension	72	5sec	
Final extension	72	20sec	
Preservation	12	Infinity	

The PCR product was then loaded on 6% ployacrylamide gel, stained with silver staining to visualize.

2.12.2 Sample preparation for sequencing and construction of mutation spectra

Samples were purified using PCR purification kit ® (Qiagen, Sussex, UK). For detailed methodology see Chapter 2 Section 2.9. Samples were sent to Source Bioscience, Sanger sequencing (Rochdale, UK) for sequencing. Mutation spectra was constructed using iMARS software, kindly provide by Dr Paul Lewis at Swansea University (Morgan and Lewis, 2006).

Chapter 3

Investigation of the Genotoxic Potential of Benzo[a]pyrene in Human Cells With Differing Metabolic Activation Capacity

3.1 Introduction

B[a]P is considered to be a "probably carcinogenic to humans", categorized as Group 2A by IARC 1987 (IARC, 1987). USEPA in 2001 concluded B[a]P was a "probable human carcinogen" (B2), on the basis of sufficient evidence of its carcinogenicity in laboratory animals in 1992 and other data generated from genotoxicity assays. B[a]P has been used as a model compound to study carcinogenic effects (Phillips, 1983). Due to the unavoidable human exposure it is a serious threat to carcinogenicity. B[a]P is known to cause lung, head-and-neck cancers as well as other diseases such as atherosclerosis (Miller and Ramos, 2008; Shimada and Fujii-Kuriyama, 2004).

Upon exposure to cells, different pathways attempt to detoxify and eliminate B[a]P from the cell but this process also results in the formation of intermediate products that are able to bind with DNA to form DNA adducts. In the absence of DNA repair mechanisms, it could lead to permanent mutations and carcinogenic process (Hoeijmakers, 2001). Earlier research on B[a]P focussed on evaluating carcinogenetic activities of different B[a]P products, for example, Levin *et al* (1976) showed a higher tumour formation in response to B[a]P- 7,8-diol than B[a]P- 7,8-oxide whereas in another study Kapitulnik *et al* (1977) injected newborn mice with B[a]P, B[a]P- 7,8-diol, and BPDE and reported a higher incidence of cancerous growth in different organs. This study also showed that B[a]P- 7,8-diol was more carcinogenic than B[a]P; and BPDE was highly mutagenic to bacterial and mammalian cells and considered as the ultimate carcinogen.

Studies performed *in vitro* have demonstrated that CYP1A1 and mEH are involved in the metabolic activation of B[a]P into reactive intermediates, and is responsible for B[a]P-mediated mutation and cancer (Millar and Ramos, 2001). Among the various forms of P450 determined so far, CYP1A1 and CYP1B1 have been shown to be the most important human P450 enzymes in the metabolic activation of PAHs and PAH dihydrodiols (Shimada *et al*,

2002). Deutsch-Wenzel *et al*, (1983) studied rats and indicated higher carcinogenic effects of B[a]P than the benzofluoranthenes or indeno(1,2,3-cd)pyrene. Although other PAH such as dibenz(a,h)anthracene, 5- methylchrysene, and dibenzo(a,i)pyrene are substantially stronger lung tumourigens than B[a]P in mice or hamsters, but their concentration in cigarettes are relatively lower, therefore, they have not been studied as extensively as B[a]P (Nesnow *et al*, 1995; Sellakumar and Shubik, 1974). B[a]P is thought to be responsible for a reproductive toxic effect as well. For example Neal *et al*, (2008) found high levels of B[a]P from the follicular fluid of women exposed to mainstream smoke.

As discussed in chapter 1, several factors such as the nature of the chemical and its interaction with the target, variability in cells, tissues and cell protective mechanisms etc. influence dose dependant responses (Jenkins *et al*, 2005). Therefore, it is important to consider these factors while determining threshold of any genotoxins.

These considerations become even more complex if the genotoxin involved is a pro-carcinogen that requires metabolic activation to initiate genotoxicity. As compared to direct acting agents, little is known about the threshold of pro-carcinogenic agents and further studies are required to understand the dose dependant response of chemicals that require metabolic activation to cause carcinogenetic effects. This chapter deals with the genotoxic thresholds at low doses caused by B[a]P and the potential mechanisms behind the threshold dose response to such pro-carcinogens.

Over recent years OECD developed several guidelines for the testing of chemicals (OECD, 2005). Those guidelines are internationally accepted and used by government, industry and independent laboratories. The data produced from studies following the guidelines are accepted by all OECD member countries (Cimino, 2006). Therefore, the present study is focuses on testing of chemicals using the *in vitro* cytokinesis-block micronucleus (CBMN) assay guided by OECD (2005) for the hazard characterization that can be used in risk assessment. This test is used in genotoxicity testing as an initial screening for mutagenicity and carcinogenesis.

3.1.1 Aims of the study

As already mentioned above, much work has been done to find out the genotoxic threshold of chemicals that interact with DNA directly, with the potential to form DNA adducts and exert carcinogenicity. Currently there is no evidence of genotoxic thresholds for chemicals requiring metabolism to form products that are capable of binding to DNA, forming DNA adducts and leading to mutation. Considering this, the aim of this study was to identify the

existence of a potential threshold for B[a]P, which is one of the extensively studied clastogenic PAHs. The results obtained from this study will tell whether there is

1. A differential genotoxicity of B[a]P in different human cell lines based on their metabolic capacity and
2. An exhibited threshold for genotoxicity for B[a]P after metabolic activation at low doses.

The study utilised the *in vitro* CBMN assay, in the human lymphoblastoid cell lines AHH-1, MCL-5, TK6 and human hepatoma line HepG2, which are known to have differential expression of CYP450 enzymes, to evaluate the dose related responses by the induction of micronuclei.

3.2 Materials and Methods

3.2.1 Cell lines

AHH-1, MCL-5 and HepG2 cells were used for both 4h and 24h B[a]P exposure studies. TK-6 cells were used in 24h B[a]P exposure studies only.

3.2.2 Cell culture

Cell culture was performed as described in Chapter 2 Section 2.1.2.

3.2.3 Test chemical B[a]P and dosing regime

All the flasks were seeded at $1x10^5$cells/ml (10ml/flask, MCL-5) and $1.2x10^5$ cells/cm^2 (10ml flask, HepG2) before treatment with the chemical for 24h or 4h at 37°C, 5% CO_2. Satellite flasks were also prepared for each dose for cytotoxicity analysis.

The 1M stock solution of B[a]P was prepared by dissolving 0.050g of B[a]P powder (Sigma, UK) into 200µl DMSO. This stock was kept at 4°C for 2weeks for further use. For each replicate a new working stock was prepared. Working stocks of B[a]P were prepared by dissolving the 1M stock further in DMSO+RPMI1640 (1:2) to obtain the required working stocks. These working stocks were added into 10ml cell culture to get the desired concentrations mentioned in Table 3.1 and incubated for different time points e.g. 4h or 24h. After treatment time the chemical was washed off using growth media (without supplements).

Table 3.1 Range of B[a]P doses and amount of two working stocks used

Doses (µM)	1mM working stock	10mM working stock
	Volume (µl)	Volume (µl)
1	10	-
2	20	-
3	30	-
4	40	-
5	50	-
10	100	-
25	-	25
30	-	30
50	-	50
70	-	70

3.2.4 Cytotoxicity Assay

The Relative Population Doubling (RPD) toxicity measure was used to calculate the cytotoxicity of the chemical in the absence of cytochalasin B as described by Lorge *et al*, (2008). Briefly, the satellite flasks for suspended cells (TK6, AHH-1 and MCL-5) were counted one hour before dosing using a Coulter counter (Z1-Coulter Particle Counter, Beckman Coulter, Inc). HepG2 cells were counted on the day of seeding. After each treatment time, 4h or 24h, cells were incubated for another 24h in fresh media and counted again as described in Chapter 2 Section 2.3. The experiment was repeated three times.

3.2.5 Micronucleus Assay

Cytochalasin B was added as described in Chapter 2 Section 2.4.1. The cells were washed with 0.56% KCl, fixed with fixative 1 and 2 and harvested onto slides as described in Chapter 2 Section 2.4.2. Cells were stained with DAPI+Vectorshield solution and then scanned for binucleated cells on the Metafer system (Chapter 2 Section 2.4.3). Binucleated cells with positive micronuclei were validated microscopically using a 100x objective and then manual confirmation of the micronuclei was done by visualizing the gallery images.

3.2.6 Scoring

The CBMN assay slides were scored using the criteria described in Chapter 2 Section 2.4.3. To increase the confidence on the Metafer system and the statistical power of the test, the experiment was run in triplicate and 10,000 binucleated cells were checked for the presence of micronuclei per dose.

3.2.7 Pre-treatment of MCL-5 with NCND before B[a]P 24h exposure for micronucleus induction

Soluble epoxide hydrolase inhibitor NCND (Calbiochem, EMD Chemicals Inc., Germany) was used to inhibit the activity of microsomal epoxide hydrolase (mEH) in the MCL-5 cell line. The data sheet stated an IC50 (Inhibition concentration 50) at 85.2nM for recombinant human mEH, and therefore, a two-fold concentration of NCND (170nM) was used to incubate MCL-5 cells with for 2h before B[a]P treatment for 24h.

The 10mM stock solution of NCND was prepared by dissolving 0.031g of NCND powder into 10ml methanol (Sigma). Aliquots (100µl) were prepared and the stock was kept at -20°C for 3 months for further use. For each replicate a new working stock was prepared by diluting the 10mM stock in methanol+RPMI1640 (1:2).

All the flasks were seeded at $1x10^5$cells/ml (10ml/flask) for 24h The IC_{50} value is 85.2nM for recombinant human sEM (soluble Epoxide Hydrolase) therefore we used 170nM to gain IC_{100}. This concentration was used to treat MCL-5 cells for 2h prior to 70μM B[a]P exposure for 24h and then proceed as mentioned in Chapter 2 Section 2.4.

3.2.8 Statistical analysis

A one-way ANOVA followed by Dunnett's post-hoc test (2-tailed) was used to compare all treatment data from control data using IBM SPSS software (version 19). A confidence limits of 95% ($p<0.05$), 99.9% ($p<0.01$) and 99.99% ($p<0.001$) were applied. The hockey stick modelling software, provided by Lutz and Lutz (2009) and implemented in the R package (version 2.9.1), was used to estimate a threshold dose.

3.2.9 RNA extraction

Total RNA was extracted from the human cell lines TK6, AHH-1, MCL-5 and HepG2 from control and 24h post B[a]P treatment. The doses of B[a]P treatment selected were based upon the LOEL dose obtained as a result of CBMN assay (Table 3.2 in Section 3.4.1). Details of method are described in Chapter 2 Section 2.6.1.

3.2.10 Reverse Transcription with elimination of genomic DNA and cDNA synthesis

The reverse transcription reactions and cDNA synthesis are described in detail in Chapter 2 Section 2.10.1 and Section 2.10.2. This experiment was repeated three times.

3.2.11 -End-point PCR

This procedure was performed to study the expression of CYP1A1 and CYP1A2 in cDNA from different treated and untreated cell lines. d method described in detail in Chapter 2 Section 2.10.3 and Section 2.10.4.

3.2.12 Real-time PCR

The detailed method was described in Chapter 2 Section 2.11 and 2.11.1.

3.3 Results

To determine the cytotoxic and genotoxic effects of B[a]P on cell lines with different levels of metabolic activity, MCL-5, AHH-1, TK6 and HepG2 were exposed to different doses of B[a]P and dose-responses were assessed utilising the CBMN assay. Micronucleus frequency was used to assess the levels of chromosomal aberration. Soluble epoxide hydrolase (sEH) inhibitor, NCND was also used to determine the importance of microsomal epoxide hydrolase (mEH) in the metabolism of B[a]P and determined its effect on the induction of micronuclei in the MCL-5 cell line. The RT-PCR was used to evaluate the difference in basal and induced expression of CYP1A1 and 1A2 in all four cell lines (treated with LOEL dose of B[a]P for 24h obtained as a result of CBMN assay).It is important to note LOEL doses varied for each cell line, therefore, in this study each cell line was treated with different B[a]P doses i.e. its respective LOEL dose. These different doses were selected to compare the effect of B[a]P on CYP1A1 and CYP1A2 expression at doses where micronucleus induction become significant in the respective cell line. The difference in CYP1A1 and CYP1A2 expressions were quantified by real-time PCR.

3.3.1 Cytotoxicity and genotoxicity of B[a]P after 24h exposure

All four cell lines TK6, AHH-1, MCL-5 and HepG2 were treated with B[a]P for 24h using a dose range of 1-70μM B[a]P. These doses were chosen to represent a range of doses as described in previous studies. Relative Population Doubling (%RPD) and average percentage of binucleated cells that contained micronuclei (%Mn/Bn) was used to assess cytotoxicity and genotoxicity, respectively (Table 3.2). For all cell lines, average cytotoxicity and genotoxicity (from three replicates) in response to different doses of B[a]P is shown in Table 3.2 and individual results are discussed below for each cell line.

Table 3.2 A summary table showing the average results of cytotoxicity (%RPD) and average percentage of binucleated cells that containing micronuclei (%Mn/Bn) with 24h benzo[a]pyrene treatment in all four cell lines.

Dose	TK6		AHH-1		MCL-5		HepG2	
(μM)	%RPD	%Mn/Bn	%RPD	%Mn/Bn	%RPD	%Mn/Bn	%RPD	%Mn/Bn
0	100.00	0.91	100.00	1.35	100.0	1.51	100.00	0.65
1	101.55	0.82	104.95	1.33	72.8	1.67	84.42	0.77
2	104.63	0.87	104.36	1.36	71.0	1.81	77.99	0.89
3	102.73	0.84	102.42	1.42	65.8	2.05*	77.73	1.03*
4	106.68	0.8	96.13	1.5**	63.98	2.18***	61.45	1.13***
5	109.02	0.82	95.46	1.57***	60.41	2.2***	53.60	1.38***
10	101.62	0.75	91.57	1.72***	55.78	2.32***	38.04	1.50***
25	107.63	0.71	83.20	1.81***	52.72	2.42***	17.47	
30	112.82	0.78	81.78	2.05***	41.04	2.76***	-17.86	
50	101.76	0.79	81.06	2.1***	38.25	2.96***	-32.38	
70	85.70	0.74	61.48	2.23***	16.03	3.38***	-43.52	

*, **, *** Indicates a statistically significant difference compared to control ($p<0.05$, $p<0.01$ and $p<0.001$ respectively)

3.3.1.1 TK6 cells

B[a]P did not show any significant effect in TK6 cell line at any of the doses tested. Relative population doubling and micronuclei induction values varied non-significantly between the untreated control and any of the B[a]P dose which ranged from 0-70μM (Table 3.2, Fig. 3.1, Raw data in Appendix II, Table A.1). Since the TK6 cell line has minimal CYP 450, there is little cellular mechanism to metabolize B[a]P in these cells. These results are in line with earlier reports that metabolic activation of B[a]P is required to cause genotoxicity (Gelboin, 1980).

Figure 3.1 Relative population doubling (% RPD) and average percentage of binucleated cells that contained micronuclei (%Mn/Bn) with 24h benzo[a]pyrene treatment in TK6 cells. *Points*: mean of 3 replicates, *Bars*: standard error.

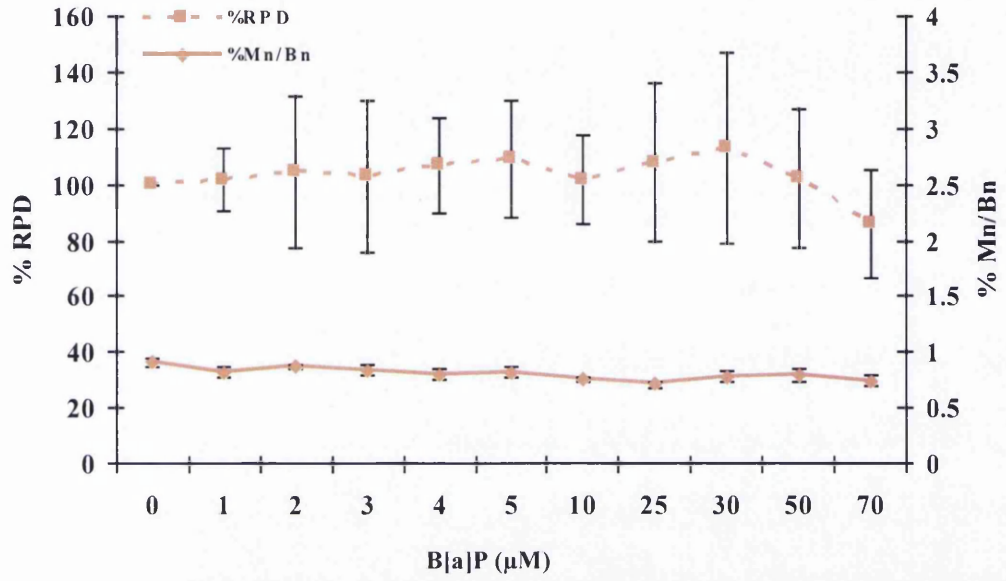

3.3.1.2 AHH-1 cells

In contrast to TK6 cells, AHH-1 cells showed a reduction in %RPD values with increasing doses of B[a]P but overall these responses did not vary significantly with that of the untreated control (Table 3.2, Figure 3.2, Raw data in Appendix II, Table A. 2). There was a slight increase in cytotoxicity observed over the whole dose range (1µM to 70µM) but 50% cytotoxicity was not achieved even at the highest dose (70µM). AHH-1 cells showed increasing gentoxocity with increasing dose of B[a]P. A linear dose-response was observed in AHH-1 cells and the frequency of Mn/Bn cells was significantly increased from 1.5% to 2.23% at 4µM ($p<0.01$) to the top dose of 70µM ($p<0.001$), respectively.

The result of the Hockey stick model for estimation of the dose-response relationship revealed that B[a]P exhibited a linear dose response in AHH-1 after 24h exposure and a threshold model was rejected (Figure 3.3).

Figure 3.2 Relative population doubling (% RPD) and average percentage of binucleated cells that contained micronuclei (%Mn/Bn) with 24h benzo[a]pyrene treatment in AHH-1 cells. *Points*: mean of 3 replicates, *Bars*: standard error, **, *** Indicates a statistically significant difference in %Mn/Bn compared to control ($p<0.01$ and $p<0.001$ respectively)

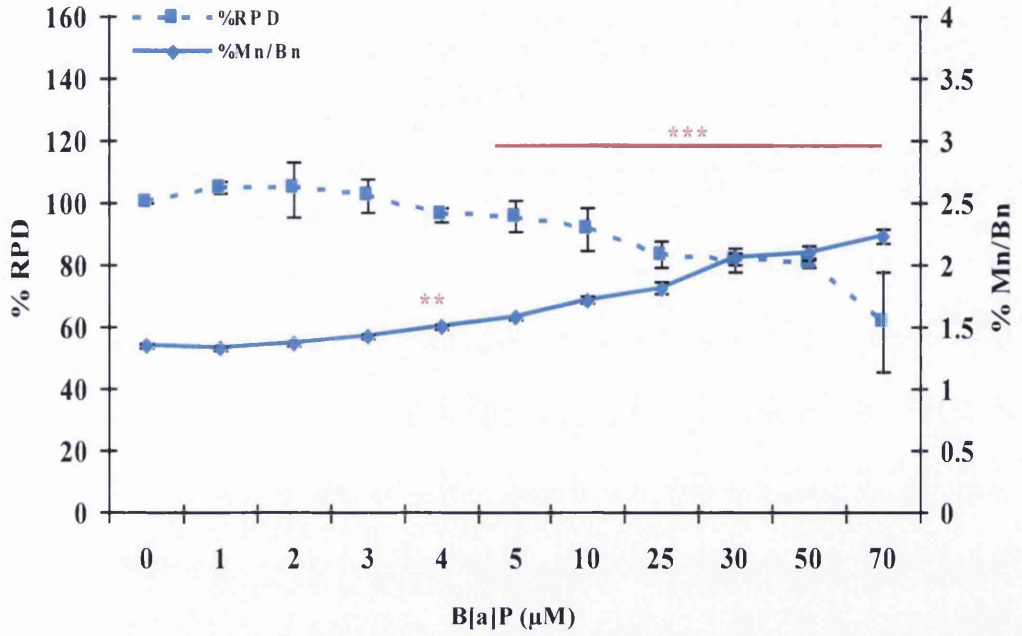

Figure 3.3 Graph generated by the Hockey stick threshold model using the Lutz approach for the analysis of dose-response relationship in AHH-1 cells to benzo[a]pyrene.

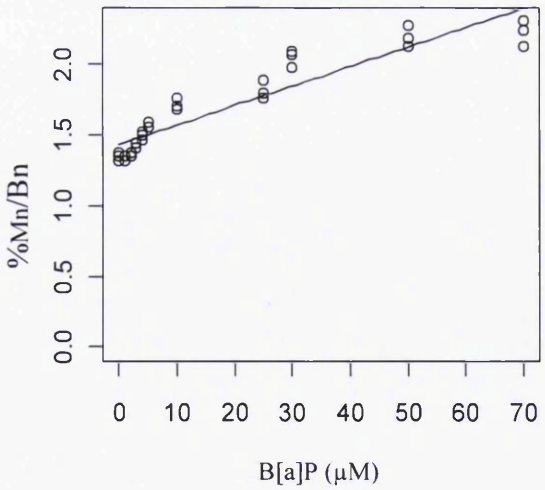

3.3.1.3 MCL-5 cells

MCL-5 cells showed a linear increase in cytotoxicity with B[a]P dose and 50% cytotoxicity was achieved between the dose ranges of 25-70µM B[a]P (Figure 3.4, Raw data in Appendix II, Table A.3). At 25µM, RPD was 52.72% and decreased to 16.03% at 70µM. A linear genotoxic dose-response was observed in MCL-5 cells treated over the 1µM to 70µM dose

range of B[a]P. The frequency of Mn/Bn cells was significantly increased from 2.05% to 3.38% at 3μM ($p<0.05$) to the top dose of 70μM ($p<0.001$).

The result of the Hockey stick model for the estimation of dose-response relationship revealed that B[a]P exhibited a linear dose response in MCL-5 cells after 24h exposure (Figure 3.5) and no threshold dose was found.

Figure 3.4 Relative population doubling (% RPD) and average percentage of binucleated cells that contained micronuclei (%Mn/Bn) with 24h benzo[a]pyrene treatment in MCL-5 cells. *Points*: mean of 3 replicates, *Bars*: standard error, **, *** Indicates a statistically significant difference in %Mn/Bn compared to control ($p<0.01$ and $p<0.001$ respectively)

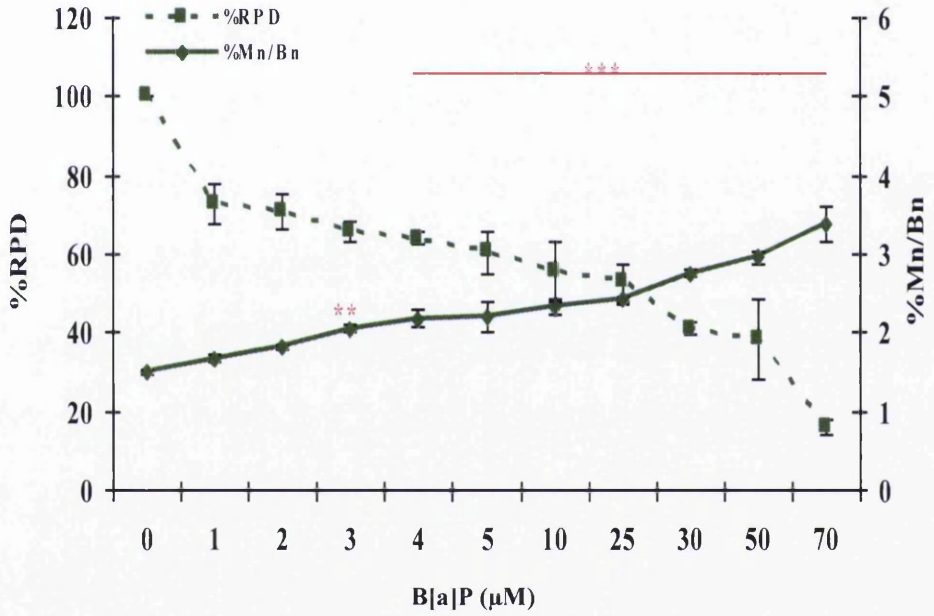

Figure 3.5 Graph generated by the Hockey stick threshold model using the Lutz approach for the analysis of dose-response relationship in MCL-5 cells to benzo[a]pyrene.

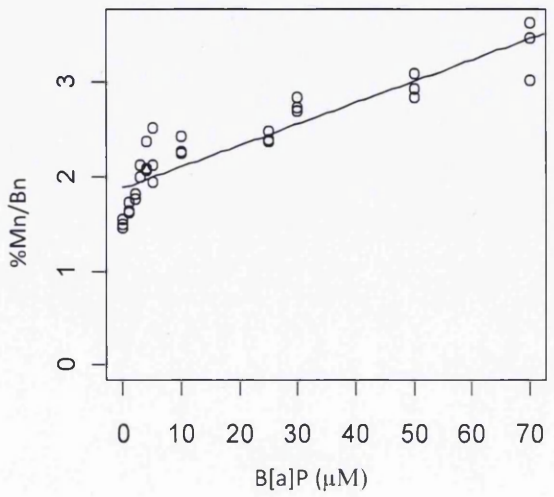

3.3.1.4 HepG2 cells

B[a]P treated HepG2 cells showed a linear increase in cytotoxicity with increasing dose and 50% cytotoxicity was achieved at 5μM (Figure 3.6, Raw data in Appendix II, Table A. 4). Cell viability (RPD) dropped to 17.48% at 25μM and at 70μM reached -43.52% indicating a strong cytotoxic effect. It is important to note, the HepG2 cells showed increased sensitivity to B[a]P over the other cell lines. For example, at concentrations of 25μM of B[a]P and above, cytotoxicity caused HepG2 cells numbers to decrease below the original seeded concentration, a phenomenon not observed in the other cell lines. Due to the high cytotoxicity of B[a]P, HepG2 cell were not tested for doses above 10μM for micronuclei frequency. A linear genotoxic dose-response was observed in HepG2 cells treated with a 1μM to 10μM dose range of B[a]P. A significant increase in the frequency of Mn/Bn cells was observed at 3μM which is 1.04% ($p<0.05$) and this reached to 1.50% at 10μM ($p<0.001$).

The result of the Hockey stick model for estimation of the dose-response relationship revealed that B[a]P exhibited a linear dose response in HepG2 cells after 24h exposure to B[a]P (Figure 3.7) and again no threshold dose was found.

Figure 3.6 Relative population doubling (% RPD) and average percentage of binucleated cells that contained micronuclei (%Mn/Bn) with 24h benzo[a]pyrene treatment in HepG2 cells. *Points*: mean of 3 replicates, *Bars*: standard error, *, *** Indicates a statistically significant difference in %Mn/Bn compared to control ($p<0.05$, and $p<0.001$ respectively)

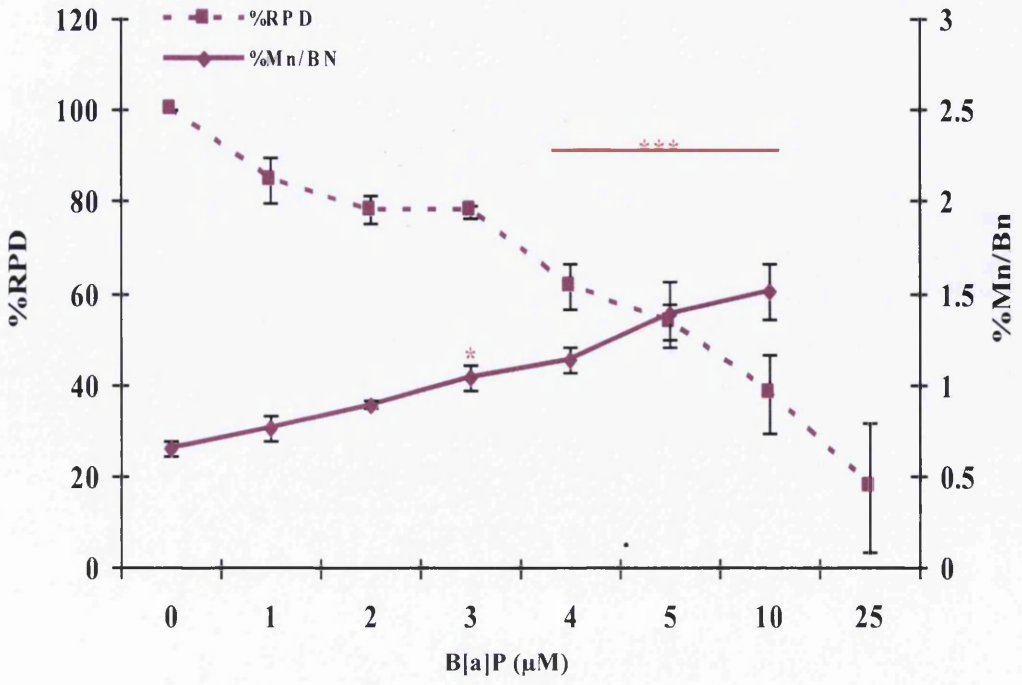

Figure 3.7 Graph generated by the Hockey stick threshold model using the Lutz approach for the analysis of dose-response relationship in HepG2 cells to benzo[a]pyrene.

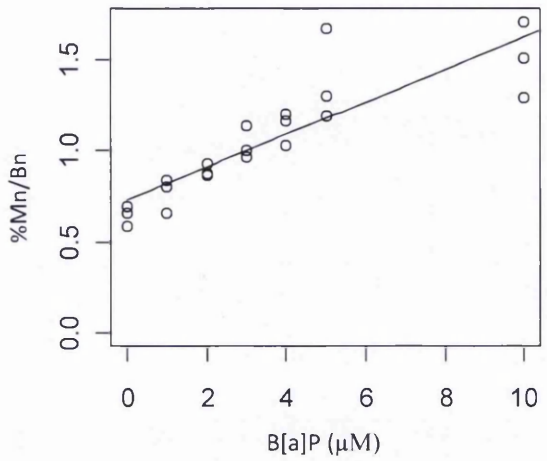

3.3.2 Cytotoxicity and genotoxicity of B[a]P after 4h treatment

As 24h exposures to B[a]P caused significant cytotoxic and genotoxic effects (apart from in TK6 cells), a shorter exposure to B[a]P was performed. TK6 cells have minimal ability to metabolically activate B[a]P and thus did not show any cytotoxicity and genotoxicity after 24h exposure to B[a]P as such, a 4h exposure to B[a]P in TK-6 cells was not included in the study. AHH-1, MCL-5 and HepG2 cell were treated with B[a]P for 4h using a dose range of 10-70μM. The average results of cytotoxicity and genotoxicity are shown in Table 3.3. The table shows the dose of B[a]P (μM), the average percentage of %RPD and the average percentage of binucleated cells that contained micronuclei (%Mn/Bn) for all three cell lines. Individual results were discussed below for each cell line.

Table 3.3 A summary table showing the average results of cytotoxicity (%RPD) and average percentage of binucleated cells containing micronuclei (%Mn/Bn) with 4h benzo[a]pyrene treatment in all three cell lines.

Dose	AHH-1		MCL-5		HepG2	
(μM)	%RPD	%Mn/Bn	%RPD	%Mn/Bn	%RPD	%Mn/Bn
0	100.00	1.32	100.00	1.44	100.00	1.10
10	122.31	1.37	86.01	1.46	52.25	1.15
20	107.43	1.36	80.66	1.53	41.00	1.47*
30	108.23	1.32	67.57	1.56	32.75	1.38*
40	98.04	1.30	67.34	1.75*	35.05	1.57***
50	96.55	1.41	60.42	1.84**	29.59	1.85***
60	107.16	1.43	56.90	2.01***	9.46	2.11***
70	92.02	1.54	45.18	2.26***	7.20	2.49***

*, **, *** Indicates a statistically significant difference compared to control ($p<0.05$, $p<0.01$ and $p<0.001$ respectively)

3.3.2.1 AHH-1 cells

AHH-1 cells showed little change in the cytotoxicity level with increasing B[a]P dose. Cytotoxicity decreased from 122.31% at 10μM B[a]P to 92.02% at 70μM B[a]P. Similarly, a small non-significant elevation in genotoxicity was observed from 1.37% to 1.54% as the tested dose range increased (Table 3.3, Figure 3.8, Raw data in Appendix II, Table A. 5).

The Hockey stick model for estimation of the dose-response relationship was not applied as there was no significant increase in the genotoxicity observed.

Figure 3.8 Relative population doubling (% RPD) and average percentage of binucleated cells that contained micronuclei (%Mn/Bn) with 4h benzo[a]pyrene treatment in AHH-1 cells. *Points*: mean of 3 replicates, *Bars*: standard error.

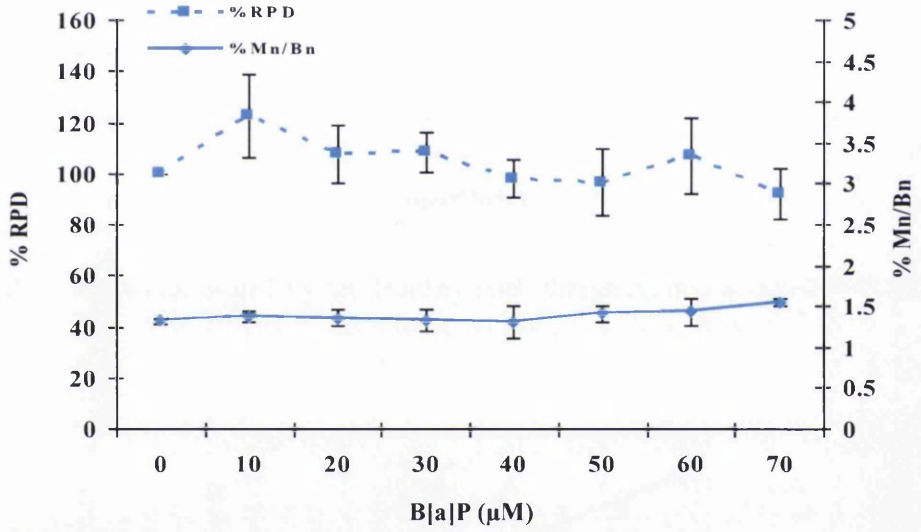

3.3.2.2 MCL-5 cells

MCL-5 cells showed no significant change in cytotoxicity until the top dose of 70μM was reached and RPD values dropped from 86.01% to 45.15%. A non-linear increase in genotoxic dose-response was observed in MCL-5 cells across the dose range of B[a]P. The frequency of %Mn/Bn cells significantly increased from 1.44% in untreated controls to 1.75% at 40μM ($p<0.05$) and reached up to 2.26% at 70μM ($p<0.001$) (Table 3.3, Figure 3.9, Raw data in Appendix II, Table A).

The result of the Hockey stick model for estimation of the dose-response relationship revealed that B[a]P exhibited a non-linear dose response in MCL-5 cells after 4h exposure and thus a threshold dose exists for B[a]P induced chromosome breakage in these cells (Figure 3.10). The estimated threshold dose (IP) was 25.46μM. The lower limit of 90% confidence interval (CI) is 14.60μM (indicated by broken line) at $p<0.002$.

Figure 3.9 Relative population doubling (% RPD) and average percentage of binucleated cells that contained micronuclei (%Mn/Bn) with 4h benzo[a]pyrene treatment in MCL-5cells. *Points*: mean of 3 replicates, *Bars*: standard error, *, **, *** Indicates a statistically significant difference in %Mn/Bn compared to control ($p<0.05$, $p<0.01$ and $p<0.001$ respectively).

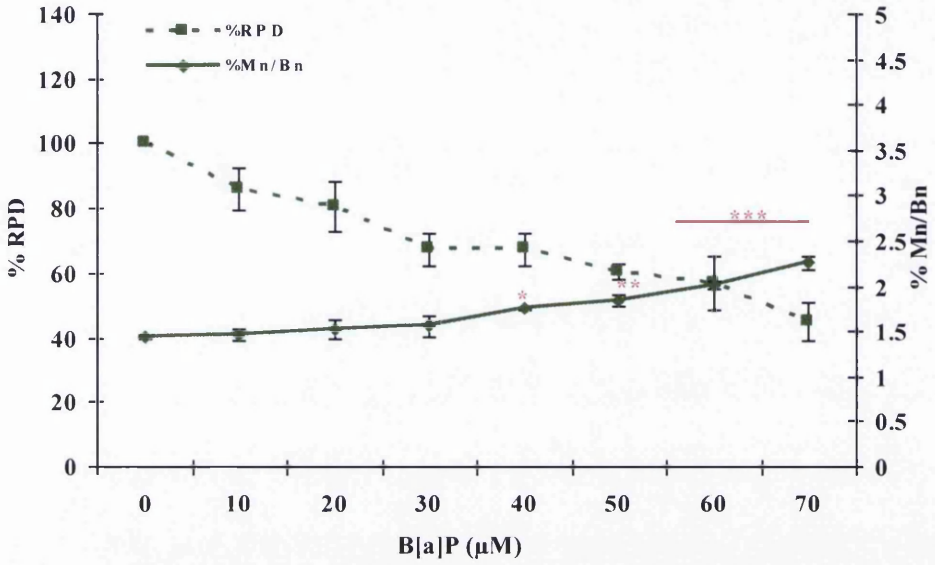

Figure 3.10 Graph generated by the Hockey stick threshold model using the Lutz approach for the analysis of dose-response relationship in MCL-5 cells treated with benzo[a]pyrene for 4h.

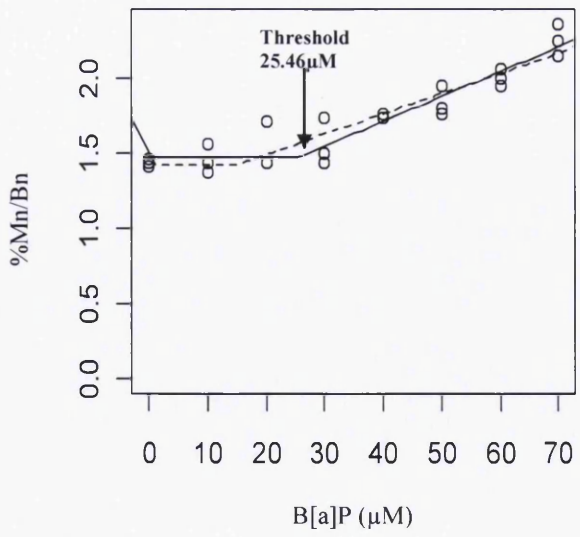

3.3.2.3 HepG2 cells

HepG2 cells showed a linear increase in cytotoxicity and 50% cytotoxicity was recorded at 10µM B[a]P. Cytotoxicity was 47.75% at 10µM and at 70µM it decreased by 92.8% (7.20% RPD). An increasing genotoxic response was observed in HepG2 cells across the 10µM to

70μM dose range of B[a]P. A significant increase in frequency of %Mn/Bn cells was first observed at 20μM where 1.47% ($p<0.05$) genotoxicity was observed, and reached to 2.49% at 70μM ($p<0.001$) (Table 3.3, Figure 3.11, Raw data in Appendix II, Table A).

The result of the Hockey stick model for estimation of the dose-response relationship after 4hrs exposure to B[a]P, favoured a linear model and rejected a threshold model despite showing a non-linear dose curve in HepG2 cells (Figure 3.12).

Figure 3.11 Relative population doubling (% RPD) and average percentage of binucleated cells that contained micronuclei (%Mn/Bn) with 4h benzo[a]pyrene treatment in HepG2 cells. *Points*: mean of 3 replicates, *Bars*: standard error, *, *** Indicates a statistically significant difference in %Mn/Bn compared to control ($p<0.05$ and $p<0.001$ respectively).

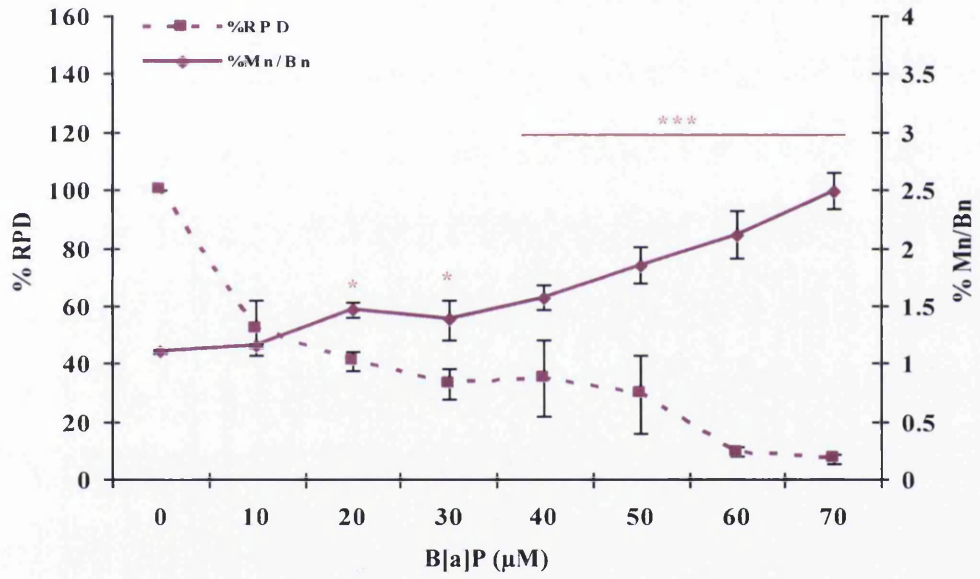

Figure 3.12 Graph generated by the Hockey stick threshold model using the Lutz approach for the analysis of dose-response relationship in HepG2 cells treated with benzo[a]pyrene for 4h.

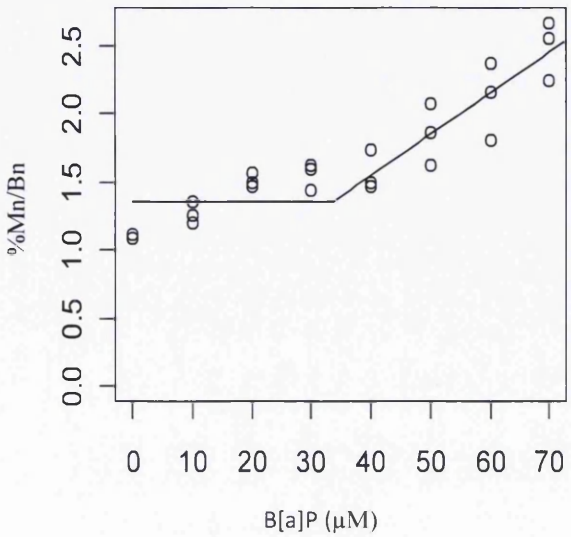

3.3.3 Effect of NCND on micronuclei induction in MCL-5 cells

In order to investigate the role of the metabolising enzyme microsomal epoxide hydrolase (mEH) in the metabolism of B[a]P and its resultant genotoxicity, an inhibitor of this enzyme was used. The average results of cytotoxicity and micronucleus induction in MCL-5 cells pre-treated with NCND for 2h prior to B[a]P (70μM) exposure for 24h are represented graphically in Figure 3.13. There was non-significant difference in cytotoxicity between control and NCND treated MCL-5 cells (t-test). However, cytotoxicity was significantly higher in B[a]P treated cell as compared to control ($p<0.001$) and NCND+B[a]P ($p<0.001$) (Figure 3.13, Raw data in Appendix II, Table A. 8). There was no significant difference in %MnBn between control and NCND only treated cells. B[a]P treatment of cells pre-treated with NCND induced statistically significant higher %Mn/Bn cells ($p<0.01$) when compared to the negative control, however, it was significantly lower than the cells treated with B[a]P alone. MCL-5 cells without pre-treatment exposed to B[a]P also showed significantly higher levels of %Mn/Bn cells ($p<0.001$) when compared to the control. Percentage Mn/Bn frequency in B[a]P only treated cells was 3.15% as compared to NCND-treated plus B[a]P treated cell which was 1.93%, thus represent 1.63 fold increase in % Mn/Bn frequency in B[a]P only treated cells (Figure 3.13).

Figure 3.13 Effect on micronucleus frequency in MCL-5 cells pre-treated with soluble epoxide inhibitor, NCND before benzo[a]pyrene exposure for 24h. *Points*: mean of 3 replicates, *Bars*: standard error, *, *** Indicates a statistically significant difference compared to control ($p<0.05$ and $p<0.001$ respectively)

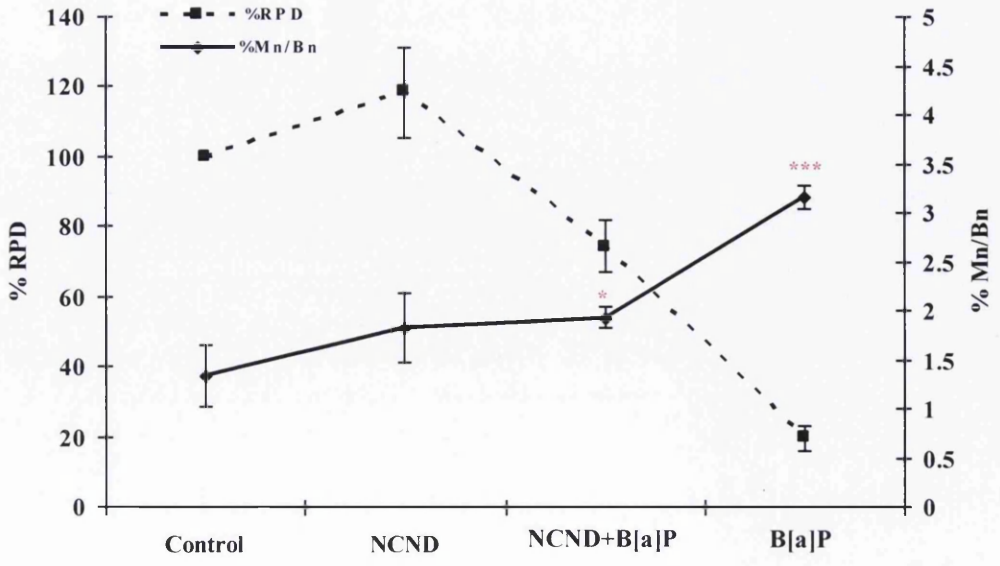

3.3.4 Basal and induced expression of CYP1A1 and CYP1A2 enzymes

Expressions of CYP1A1 and 1A2 enzymes in MCL-5, AHH-1, TK6 and HepG2 cells were determined by RT-PCR. There was a difference in basal and induced expressions of CYP1A1 for all cell lines at different doses of B[a]P evaluated. It was confirmed by measuring the intensity of each band by intensitometry method using Chemidot software (For figures see Appendix III, Figure A. 1) and further confirmed by Real-time PCR . Induction of CYP1A1 expression was 2.9-fold in MCL-5 and 1.28 fold in AHH-1 cell line observed when compared to LOEL dose. In TK6 and HepG2 cell lines, induced CYP1A1 increased by 1.2-folds and 2.3-fold respectively (Figure 3.14 A) For CYP1A2, expression was 3.2-fold and 2-folds increase in MCL-5 and HepG2 cell lines respectively. While in TK6 and AHH-1 cell lines no fold increase in CYP1A2 expression was observed (Figure 3.14 B)

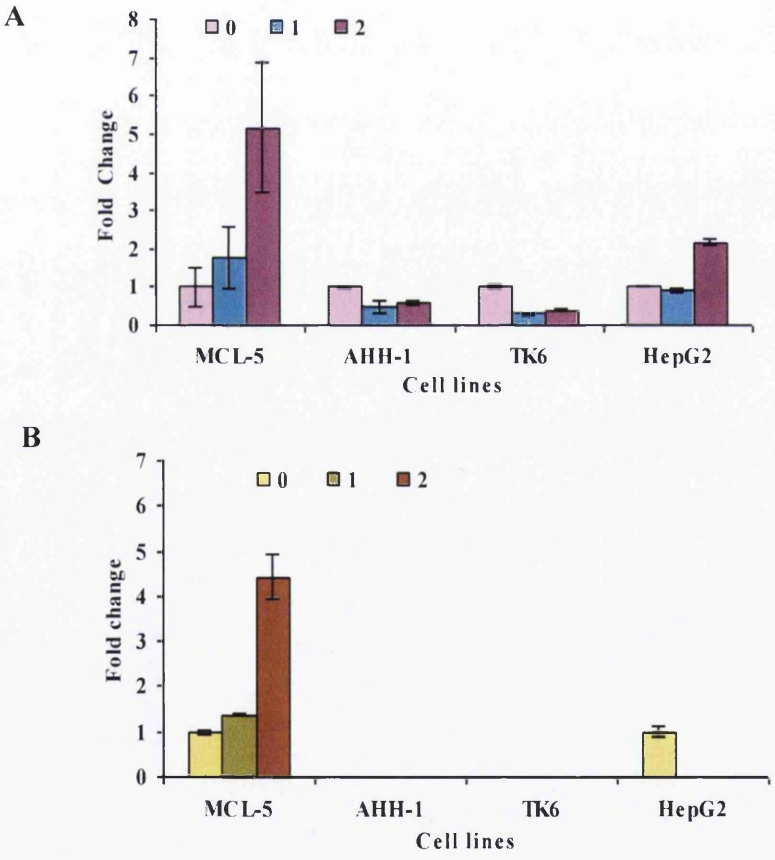

Figure 3.14 Fold change in (A) CYP1A1 and (B) CYP1A2 expressions vs. β-actin after 24h B[a]P exposure in MCL-5- (0) Untreated control, (1) 3μM, (2) 4μM, AHH-1 - (1) 4μM, (2) 5μM, TK6-(1) 5μM, (2) 10μM, HepG2- (1) 3μM, (2) 4μM

3.4 Discussion

This chapter describes the genotoxic effect of B[a]P on cultured human cell lines expressing different levels of the metabolising enzymes CYP450s. B[a]P itself is not DNA reactive, but when absorbed in the human body, it is metabolised by cytochrome P450 enzymes, especially CYP1A1, into its genotoxic and carcinogenic intermediates that bind to DNA and lead to the formation of BPDE (Kim and Guengerich, 2005). Studies were aimed at determining the effect of B[a]P dose and exposure time on the cytotoxicity and formation of micronuclei in response to varying metabolic potential of selected cell lines. Cytotoxicity data is represented as a measure of reduction in relative population doubling following exposure to B[a]P for either 4h or 24 h. Genotoxicity data is represented as dose-related responses of chromosomal damage in the form of micronucleus induction. Since B[a]P requires metabolic activation to cause genotoxic effects therefore metabolically competent cell lines, MCL-5, AHH-1 and HepG2, and with minimal CYP450 activity the cell line TK6 were used as *in vitro* models for studying the cytotoxicity and genotoxicity of B[a]P at different exposure times and doses. Indeed studies confirmed varying levels of basal and induced CYP enzymes in cell lines evaluated here. MCL-5 and HepG2 showed highest basal and induced CYP1A1 and CYP1A2 while AHH-1 showing lower activity. TK6 cells had least CYP1A1 and no CYP1A2 activity.

3.4.1 B[a]P cytotoxicity and genotoxicity in different cell lines

While determining genotoxicity of a compound, it is also important to determine cytotoxicity of the compound to understand its effects on cell growth and cell replication. It was observed in present study that cell cycle of the cell lines tested ranged from 22-24h, therefore differences observed in micronucleus formation were due to the effect of B[a]P rather than the difference in cell growth patterns and/or its cell cycle. Furthermore, we used B[a]P doses that showed less than 50% cytotoxicity and this dose selection was in accordance with OECD guidelines (2007) that recommend that studies aimed at determining genotoxicity of a compound should include a dose range that produces a low level of cytotoxicity and a maximum of 50$\pm$5% cytotoxicity.

Human thymidine kinase heterozygote TK6 cells were used in this study because they express wild-type p53, grow rapidly in suspension (population doubling time of 18h), and are routinely used in genetic toxicology studies. Results of our study showed non-significant effects of B[a]P on either cytotoxicity or genotoxicity of TK6 cell lines (Figure 3.1). The TK6 cell line had low expression of CYP1A1, and therefore, is unable to metabolize B[a]P. There was no significant difference in MN frequency between untreated and B[a]P treated TK6 cells

therefore, the cell line was excluded from studies aimed at determining the effect of B[a]P exposure for 4h.

Results of this study with metbolically competent cells confirm that the differences in the expression of CYP1A1 and the presence of microsomal epoxide hydrolase (mEH) play an important role in the metabolic activation of B[a]P, leading to the formation of te carcinogenic metabolite BPDE. Indeed unlike TK6 cells, B[a]P exposure gave significant increases in %Mn/Bn frequencies in AHH-1, MCL-5 and HepG2 cell lines at concentrations giving less than 50±5% cyotoxicity (as measured by RPD). The results of this comparative study have shown that B[a]P has a potential to induce cytotoxic and genotoxic effects in AHH-1, MCL-5 and HepG2 at both 24h and 4h exposure times (Figure 3.15 and 3.16). In particular, MCL5 and HepG2 cells showed strong genotoxic responses to B[a]P, which was less apparent in AHH-1 cells. These difference appeares to be due to the difference in CYP1A1 induction in these cell lines. The study on CYP1A1 expression showed that induction of CYP1A1 in response to B[a]P is higher for MCL-5 and HepG2 as compared to AHH-1 (Figure 3.14).

Figure 3.15 Comparision of average percentage of binucleated cells containing micronuclei (%Mn/Bn) in TK6, AHH-1, MCL-5 and HepG2 cells after treatment with benzo[a]pyrene for 24h. *Points*: mean of 3 replicates, *Bars*: standard error*, **, Indicates a statistically significant difference compared to control ($p<0.05$ and $p<0.01$ respectively).

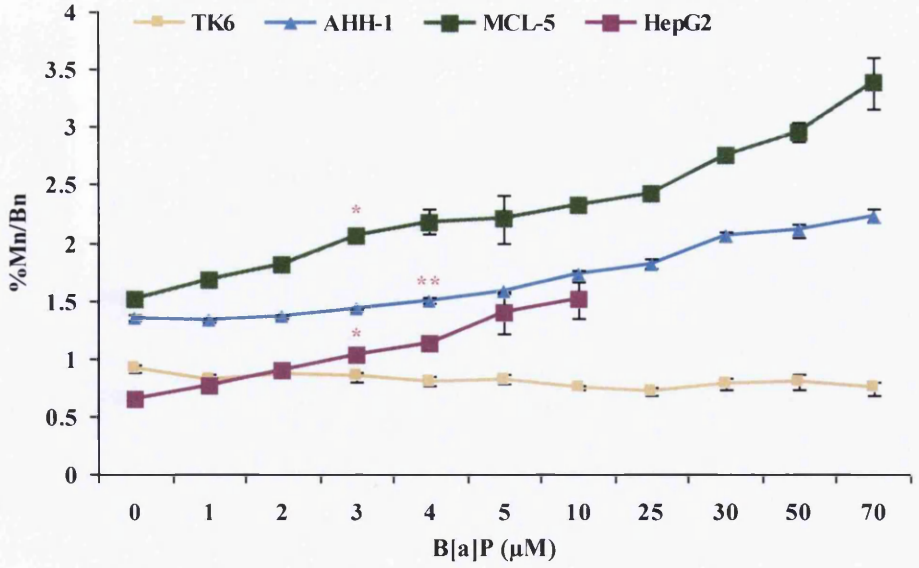

3.4.2 Effect of differential metabolic competency on micronucleus frequencies after 24h exposure

The AHH-1 cells express high levels of native CYP1A1 (Crespi *et al*, 1990). MCL-5 cells were developed from a subpopulation of AHH-1 cells by transfection of cDNAs of the human

CYP 450s, such as CYP1A2, CYP2A6, CYP2E1, CYP3A4, CYP1A1 and microsomal epoxide hydrolase (mEH) (Crespi *et al*, 1991). CYP450 cloned in MCL-5 are native in HepG2 cells and it also has several other CYP enzymes (Knasmuller *et al*, 1998) and mEH. It should be noted that a dose dependant response was represented after a B[a]P exposure for 24h for all cell lines, however, the dose range for AHH-1 and MCL-5 is 0 to 70μM whereas for HepG2 dose ranges from 0 to 10μM. Differences in metabolic competencies may explain why MCL-5 and HepG2 display a greater genotoxic response after B[a]P exposure as compared to AHH-1 cells. For example, at 24h B[a]P exposure, in AHH-1 cells the first significant increase in micronuclei induction using Dunnett's posthoc test, was observed at 4μM ($p<0.01$), whereas it was a lower concentration of 3μM ($p<0.05$) in both MCL-5 and HepG2 cells (Figure 3.4). Further analysis of the data using fold change in micronucleus frequency was also comparatively higher in MCL-5 and HepG2 cells than that of AHH-1. For example at a B[a]P dose of 10μM, MCL-5 and HepG2 showed 1.5 and 2.3-fold increase in micronucleus frequency respectively as compared to the untreated control, however fold increase in micronucleus frequency at 10μM was only 1.27 in AHH-1. A similar trend was observed at higher doses (70μM) where MCL-5 showed far more increase in micronucleus frequency (2.23 fold) than in AHH-1 (1.65 fold) (Figure 3.17). Due to higher cytotoxicity of B[a]P in HepG2, studies were restricted to 10μM of B[a]P. It should be noted that even at this dose the fold increase in micronucleus formation was significantly higher than the micronucleus formation observed in AHH-1 at 70μM dose (Figure 3.15).

Further analysis of AHH-1, MCL-5 and HepG2 micronucleus data using hockey stick statistical modeling confirmed a linear (non-thresholded) dose-response at 24h exposure to B[a]P for all the metabolically competent cell lines (Figures 3.3, 3.5 and 3.7). These findings may be explained by the potent formation of stable DNA adducts at N2-guanosine residues (Lin *et al*, 2001) which if left unrepaired, might block replication and transcription. Even a single BPDE-DNA adduct can effectively block expression of a reporter gene (Koch *et al*, 1993) and has been linked to mutations in multiple genes includes *TP53* and *Kras*, thus causing severe damage to cell integrity, function and replication (Denissenko *et al*, 1996; Yoon *et al*, 2003).

3.4.3 Effect of differential metabolic competency on micronucleus frequencies after 4h exposure

The studies at a shorter exposure time allow to compare all cell lines including HepG2 to doses ranging from 0 to 70μM. Micronuclei induction in the cell lines following 4h exposure

to B[a]P showed a similar trend to that observed following B[a]P exposure for 24h (Figure 3.16). Following 4h exposure, no significant difference in cytotoxicity or micronucleus frequency was observed in AHH-1 (Figure 3.8). These findings are in line with our studies at B[a]P exposure of 24 hours as well as earlier reports that B[a]P required a longer exposure time for efficient metabolic activation to cause genotoxic effects (Yamakage *et al*, 1998). The results of this study indicate that metabolic activity in AHH-1 cells was unable to activate B[a]P even at the highest dose of 70μM in 4h (Table 3.3), however, at a longer exposure of 24h it is capable of activating B[a]P at doses 4μM and above (Table 3.2). These findings also indicate that lower levels of CYP1A1 and absence of mEH in AHH-1 cells were unable to convert enough B[a]P into mutagenic intermediates. Differences in the dose dependent response at 4h and 24h exposure provides further evidence of the role of CYP1A1 and mEH in converting B[a]P to its mutagenic metabolites. These findings indicate that B[a]P conversion to its mutagenic intermediates in cells devoid of mEH and with lower CYP1A1 levels is slow and thus requires more time to convert similar quantities of B[a]P into its intermediate products at a level or concentration that is required to cause a genotoxic effect.

In the case of MCL-5 at 4h B[a]P exposure, the first significant increase in micronuclei induction was observed at 40μM ($p<0.05$, Dunnett's posthoc test) (Figure 3.9). In HepG2 cells micronuclei induction was significantly different from the untreated control and 20μM ($p<0.05$) was the lowest concentration observed to cause a statistically significant effect in micronuclei induction (Figure 3.11) and the increase in the frequency of micronuclei was dose dependent.

Figure 3.16- Average percentage of binucleated cells containing micronuclei (%Mn/Bn) of AHH-1, MCL-5 and HepG2 cells after treatment with benzo[a]pyrene for 4h. *Points*: mean of 3 replicates, *Bars*: standard error, * Indicates a statistically significant difference compared to control ($p<0.05$).

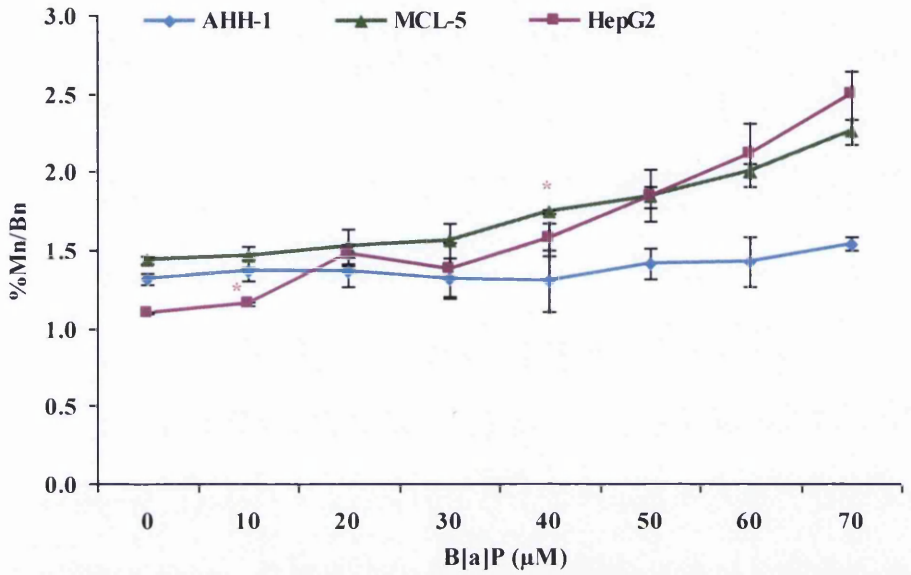

The statistically significant difference in micronucleated cell frequency between 0 and 70µM at 4h B[a]P doses was 1.16 fold in AHH-1, 1.6 fold in MCL-5 and 2.26 fold in HepG2 cells. (Figure 3.17).

Figure 3.17 Comparision of fold increase in micronuclei induction in AHH-1, MCL-5 and HepG2 cells at 10µM and 70µM benzo[a]pyrene doses following 24h and 4h exposure time. HepG2 was not tested at 70µM dose due to very high cytotoxicity.

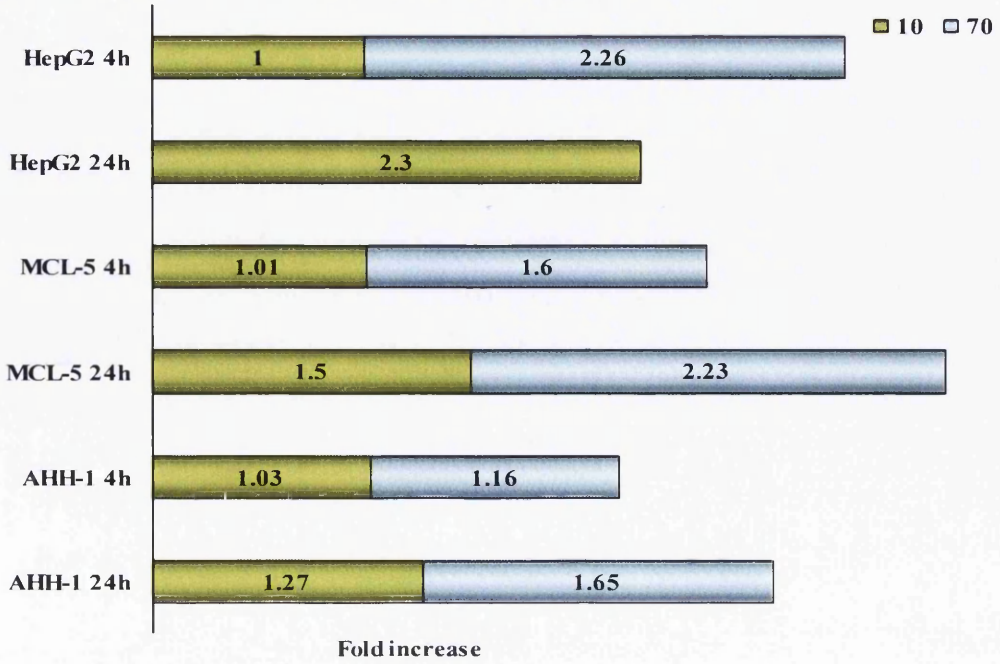

According to the CBMN data for both time exposures, the cell lines were ranked in the following order according to their metabolic competancy: HepG2 > MCL-5 > AHH-1 > TK6. These results clearly indicate that micronucleus induction appeared to link with the levels of CYP450 and the exposure to B[a]P. It is worth mentioning that the dose dependent genotoxic response is also linked with exposure time indicating a slow conversion rate in these cells (Fig. 3.17).

3.4.4 Presence of genotoxic threshold in MCL-5 cell line

The presence of a genotoxic threshold in MCL-5 cells treated for 4h with 20μM of B[a]P suggested the role of metabolic activation of B[a]P in its ability to cause genotoxic effects. Following a B[a]P exposure for 4h, the MCL-5 cell line appeared to be incapable of activating B[a]P to induce genotixicity. With shorter exposure time of 4 h, B[a]P could not induce genotoxicity untill a 40μM dose, however, at 24h exposure even a lower dose of 3μM was capable of inducing genotoxicity. These findings suggest that longer exposure times allows the cells to metabolize B[a]P which could results in accumulation of higher dose of its intermediate products that are capable of inducing genotoxicity.

Metabolism of pro-mutagenic compounds may influence dose responses for DNA mutation and as such, lack of metabolism may contribute to thresholded dose responses (Jenkins *et al*, 2005). At lower doses of the toxin, DNA repair mechanisms are also able to repair DNA damage and remove DNA adducts from cells at a relatively faster rate as compared to the number of DNA adducts formed, and a NOEL will be observed (Doak *et al*, 2007). Earlier studies by Lutz (1998) have shown that the level of toxicity depends on the availibility of DNA repair mechanisms, therefore, we can assume that B[a]P toxicity is a reflection of both cellular capacity for B[a]P metabolism as well as the absence or failure of cell mechanisms to remove metabolites of B[a]P from cells. We did not measure DNA repair enzyme levels or activity here and so cannot comment on the relative role of metabolism and repair.

3.4.5 Effect of microsomal epoxide inhibitor (NCND) on micronucleus induction in MCL-5 cells.

The previous and present study strongly suggested a role for CYP1A1 in the metabolism of B[a]P to induce chromosomal damage appearing as micronuclei in binucleated cells. A further study with MCL-5 cell line was done to confirm the importance of microsomal epoxide hydrolase (mEH) which is responsible for inducing increased genotoxic potential in MCL-5and HepG2 as compared to AHH-1 cells. N-Cyclohexyl-N'-dodecylurea (NCND), is an

effective inhibitor for microsomal epoxide hydrolase (Davis *et al*, 2002) and was used in this study. The results (Figure 3.13) showed that the frequency of binucleated cells having micronuclei decreased when MCL-5 cells were pre-treated for 2h with NCND (dose 170nM) and then exposed to 70μM B[a]P for 24h as compared to cells without this pre-treatment. For example, 1.6-fold decrease in %Mn/Bn frequency was observed between MCL-5 cells pre-treated with NCND and without NCND pre-treatment. Increased micronuclei in MCL-5 without NCND pre-treatment suggests that mEH along with CYP1A1 play an important role in the conversion of B[a]P to compounds that induce chromosomal damage (Figure 3.3). Our results correspond with studies performed by Pelkonen and Nebert (1982) and Johnson *et al*, (2010) which also observed higher micronucleus frequencies in MCL-5 cells as compared to AHH-1 cell lines. AHH-1 cells did not contain detectable activity of epoxide hydroxylase (Penman *et al*, 1994) therefore, the number of micronucleated cells were relatively low.

In conclusion this study shows that TK6 cells have minimal ability to metabolise B[a]P and thus did not show any cyotoxicity nor genotoxicity, suggesting that B[a]P is non-toxic without metabolic conversion. Higher levels of genotoxicity and cytotoxicity observed in AHH-1, MCL-5 and HepG2 cell lines with higher metabolic activity further confirms that bi-products of B[a]P metabolism are involved in its toxicity.

CYP1A1 enzyme and mEH play an important role in the metabolic activation of B[a]P and the subsequent observed cytotoxicity and genotoxicity. The combined presence of CYP1A1 and mEH caused MCL-5 and HepG2 cells to yield more binucleated cells with micronuclei as compared to AHH-1 cell as AHH-1 are devoid of mEH. At 24h exposure, there is a dose dependent linear increase in the %Mn/Bn frequency observed in AHH-1, MCL-5 and HepG2 cells. The linear dose-response confirms that there is no safe exposure level for B[a]P in metabolically competent cell lines exposed for extended periods to B[a]P. At 4h exposure AHH-1 cells did not show a significant induction of cytotoxicity or genotoxicity, whereas HepG2 cells showed a linear increase in the frequency of %Mn/Bn cells. Only MCL-5 cells are able to produce a thresholded response at 25.46μM following a shorter exposure time of 4h.. At lower doses with shorter exposure, MCL-5 may not appear to metabolically activate sufficient quantities of B[a]P to its genotoxic form, therefore, no stable adduct formation was observed. At longer exposure time of 24 h, MCL-5 was able to transform even lower dose of 3μM to its genotoxic forms.

These findings showed that metabolic activation of B[a]P plays an important role in activating B[a]P to compounds that have the potential to induce genotoxicity. Considering the human exposure to B[a]P through cigarete smoking, results of this study support previous reports of a

link between cigarette smoking and risk of developing cancer. B[a]P concentration is reported to be about 9ng (0.035μM) per cigarette in a full flavoured cigarettes (Chepiga *et al*, 2000). Fowles (2000) reported B[a]P concentrations of 0.0099 and 0.0141μg in main and sidestream respectively (Fowles 2000), therefore, a single cigarette could potentially pose a carcinogenic risk among individuals with high metabolic activity. Similarly, regular smoking i.e higher and continous exposure to B[a]P may therefore be considered as a relatively higher risk factor, however, further *in vivo* studies are needed to confirm this corelation of cigarette smoking and cancer risk.

Chapter 4

Investigation of Point Mutations Induced by Benzo[a]pyrene in Human Cell Lines

4.1 Introduction

B[a]P is one of the most well-known combustion products in vehicle exhausts, cigarette smoke and ambient air. B[a]P acts as a substrate for the oxidative reactions carried out by CYP450 (Conney, 1992). The metabolic intermediates, hydroxyl and epoxide are highly electrophilic and bind covalently to macromolecules to form bulky hydrophobic adducts (Guo *et al*, 2002). BPDE is the major genotoxic product formed from B[a]P metabolism. B[a]P is metabolized into four different stereoisomers of BPDE. The (+)-anti-BPDE [(+)-anti-7R,8S-diol-9S,10R-epoxide of B[a]P] is formed in great excess, both *in vivo* and *in vitro*, as compared to the others. This bay region diol epoxide (BPDE) has greatest tumorigenicity *in vivo* (Buening *et al*, 1978) and it covalently reacts at the N_2 position of 2-deoxyguanosine (dG) in DNA to form two different adducts: (+)-trans-anti-BPDE-N_2-dG and (+)-cis-anti-BPDE-N_2-dG (Figure 4.1). The (+)-trans-anti-BPDE-N_2-dG is the most abundant and major adduct formed, and if not repaired can induce mutations such as G→T base pair transversions during DNA replication (Luch, 2005).

The mutation profile induced in the *HPRT* gene of mammalian cells by B[a]P has been reported to be dose dependent. For example, the proportion of G→T transversions increased from 42% to 69% from 10-480nM dose range of B[a]P (Wei *et al*, 1991; Wei *et al*, 1993).

B[a]P mutagenesis has also been reported in other genes. Among them, the *TP53* gene is the most studied gene, mainly because of its vast number of mutation sites (nearly 300 sites) (Daya-Grosjean *et al*, 1995) and mutations have already been observed in many of its codons (5 to 8) (Fares *et al*, 2007). B[a]P causes mutations in the *p53* gene in lung cancer (Denissenko *et al*, 1996). In lung cancer ~ 40-51% of the mutations are G→T transversions (Greenblatt *et al*, 1994: Yoon *et al*, 2001: Pfeifer *et al*, 2002).

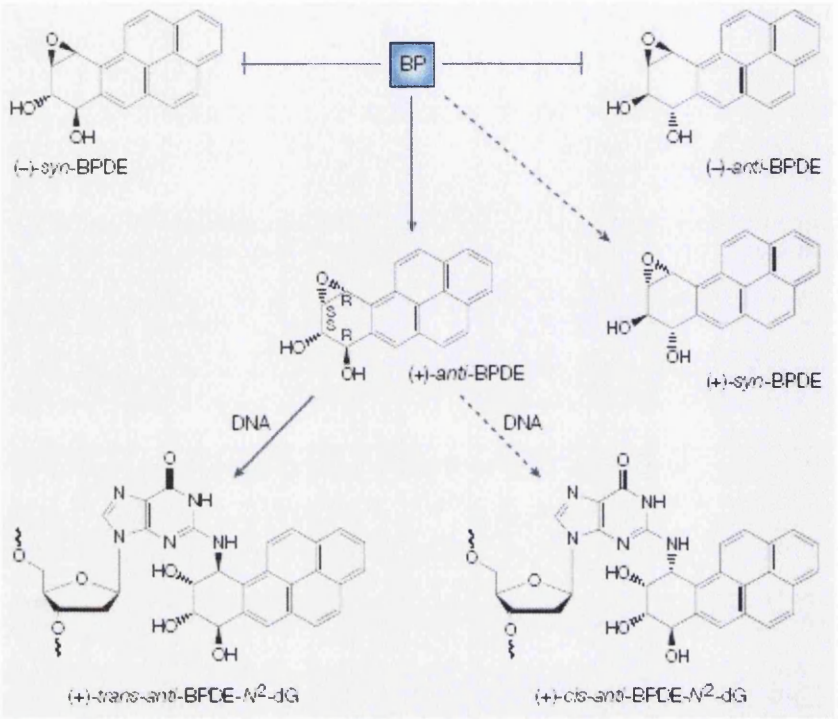

Figure 4.1 Four different stereoisomers of benzo[a]pyrene diol epoxide after metabolic activation. (+)-trans-anti-BPDE-N_2-dG is the most potent product. Modified from Luch (2005).

The *supF* gene in *Escherichia coli* has also been used for the detection of DNA damage induced by B[a]P, where Rodriguez and Loechler (1993b) showed that the metabolised form of B[a]P, (+)-anti–BPDE induced 45% base substitutions, 24% frame shifts, 23% insertions and 8% deletions. Where base substitutions occurred significantly they were observed at G:C base pairs; with GC→TA (57%), GC→AT (23%) and GC→CG (20%) reported. Similarly, Yoon *et al*, (2001) found a 42% induction of G→T transversions in *supF* gene by BPDE and further analysis of embryonic mouse fibroblasts from BigBlue mouse embryos, has shown the *cII* and *lacI* genes to have 56% and 68% BPDE-induced G→T transversion mutations, respectively.

4.1.1 Aim of the study

The aim of this chapter was to determine the mutagenicity caused by low doses of B[a]P following a 24h and 4h exposure times in AHH-1 and MCL-5 cell lines. The second part of the study focused on the construction of B[a]P-induced mutation spectra for both cell lines to determine how differences in metabolic capabilities affect the spectrum of B[a]P-induced mutation at 10μM and spontaneous mutation in solvent control after 24h exposure. There are conflicting reports regarding mutations in the *p53* gene of AHH-1 and MCL-5, therefore, we

conducted further studies to analyse basal mutations in the *p53* gene of AHH-1, MCL-5, TK6 and HepG2 cell lines.

4.2 Materials and Methods

4.2.1 Cell lines used and their maintenance

AHH-1 and MCL-5 cell lines were selected to study the *in vitro* effect of B[a]P exposure (following 24h and 4h time period) at the genetic level.

Cell culture was performed as described in Chapter 2 Section 2.1.2.

4.2.2 Test chemical B[a]P

Further details in Chapter 3 Section 3.2.3.

4.2.3 HPRT assay

The HPRT assay has three important stages as detailed in Chapter 2 Section 2.5

I HPRT mutant cleansing stage: to reduce the (HPRT-) mutant cells from the AHH-1 and MCL-5, cell populations of $5x10^{-5}$ cells / ml were grown for 3 days in $2x10^{-4}$ mol/L HAT (hypoxanthine aminopterin thymidine) media followed by 24h HT (hypoxanthine thymidine) media. Cells were then grown for 3 days in normal media to achieve sufficient cell numbers for treatment.

II Treatment with chemical and sub-culturing stage: Cells were seeded at $4x10^5$ ml (10 ml) in $25cm^2$ flasks. Untreated control and solvent control flasks were also prepared. The experiment was repeated three times and treated with freshly prepared stock solution of B[a]P from the purchased product following the dose regime mentioned in Chapter 3 Table 3.1. The cells were washed with RPMI media (without supplements) twice and then incubated for 13 days. The cells were diluted in fresh media on days 1, 3, 5, 7, 9, and 11, to replenish the nutrients to repopulate the culture. Half of the doses were cryogenically frozen down on day 7. The other halves of the doses were incubated for a further 13 days before proceeding on to the third stage.

III Mutant selection stage: At this stage the cells were diluted at concentration 4 $x10^4$ cells/well in a 96 well plate (NUNC) and the $HPRT^-$ cells isolated by using 6-TG (0.6µg/ml) which is toxic for HPRT+ cells, from AHH-1 and MCL-5 cell populations. In addition, plates without selection containing 20 cells/well were also prepared to measure the plating efficiency (PE). All plates were incubated for another 14 days at 37°C in a humidified incubator with 5% CO_2, for colony formation. Five plates were prepared for each dose from selective and non-selective media. Sixty wells per plate were scored (avoiding perimeter wells due to the partial evaporation of media in these wells).

4.2.4 Scoring of colonies

Colonies were only scored from wells (from plates with and without 6-TG selection) containing 20+ cells in diameter (a criteria established and used in our laboratory) and colonies clearly separated from each other. Each well represented one observation. The colonies were counted using a light microscope and the number of colonies observed used to determine the mutation frequency (MF) of each dose as described in Chapter 2 Section 2.5.3.

4.2.5 Statistical analysis

A one-way ANOVA followed by Dunnett's post-hoc test (2-tailed) was used to compare all treatments with control using IBM SPSS statistic software (version 19). Confidence limits of 95% ($p<0.05$), 99.9% ($p<0.01$) and 99.99% ($p<0.001$) were applied. The hockey stick modelling software, provided by Lutz and Lutz (2009) and implemented in the R package (software 2.9.1), was used to estimate a threshold dose.

The t-test was used to assess whether the means of two groups were statistically different from each other in untreated and solvent control. The Confidence limit of 95% ($p<0.05$) was applied.

4.2.6 Clonal expansion of mutants

Untreated control, solvent control and 10μM B[a]P treated HPRT mutant colonies were transferred to 24 well plates containing 2ml growth media per well and grown for 5 days at 37°C, 5% CO_2, after which cells were carefully mixed with 1.5 ml RNA protect® (Sigma) and stored at -20°C for RNA extraction.

4.2.7 RNA extraction

For a detailed description of RNA extraction methodology see Chapter 2 Section 2.6.

4.2.8 Complementary DNA (cDNA) synthesis from HPRT mRNA

For a detailed description of methodology see Chapter 2 Section 2.6.3.

4.2.9 End-point PCR

A detailed description of methodology and primers used in present study was given in Chapter 2 Section 2.6.4.

4.2.10 6% PAGE gel and Silver nitrate staining

Detailed procedures of gel preparation, gel loading, and silver nitrate staining were given in Chapter 2 Section 2.7.1 and 2.7.2.

4.2.11 Preparation of samples for sequencing

For detailed methodology see Chapter 2 Section 2.8. Samples were sent to Genome Enterprise Limited (Norwich, UK) for sequencing.

4.2.12 Construction of mutation spectra

Mutation spectra was constructed using iMARS software, kindly provide by Dr Paul Lewis at Swansea University (Morgan and Lewis, 2006).

4.3 Results

4.3.1 B[a]P mutation dose–response using the HPRT assay

The HPRT assay was performed with suspension cell lines, AHH-1 and MCL-5 to study the low dose effect of 24h and 4h exposures of B[a]P at the genetic level. TK6 and HepG2 cell lines were not included here as TK6 cell line did not show any response to B[a]P in MN data and minimal CYP450 expression. HepG2 cells are adherent cells and they did not form colonies, that we have to count at the end of HPRT assay to calculate MF. Doses selected for this study were low doses including the dose that produced the first significant increase in the %Mn/Bn frequency in Chapter 3 i.e. 4μM for AHH-1 ($p<0.01$) and 3μM for MCL-5 cells ($p<0.05$) after 24h exposure and 20μM for MCL-5 ($p<0.05$) after 4h exposure of cells (Chapter 3 Section 3.3.1 and 3.3.2).

4.3.1.1 Mutation frequency of B[a]P after 24h exposure

In the HPRT assay the plating efficiency (PE) of treated cultures was used to measure the toxicity. Plating efficiency was based on colony forming ability of cells when inoculated into a 96 well plate without 6-thioguanine (non-selective conditions). The colonies grown in non-selective conditions and selective conditions were counted to assess the mutant frequency (MF). In selective conditions, MF ($MFx10^{-5}$) is the frequency of the HPRT mutants in a population of cells. PE plates were grown alongside MF plates to assess mutant frequency.
DMSO was used to dissolve the B[a]P, therefore, it was used as solvent control for both cell lines. It was observed that the MF of the cells in solvent control was not statistically different from the cells in untreated control in both cell lines by using t-test statistical analysis (Table 4.1, .Raw data in Appendix IV, Table A. 9 and 11).

Table 4.1 Comparison of mutation frequency $x10^{-5}$ and % cell viability in control and solvent control in AHH-1 and MCL-5 cell lines

Cell lines	B[a]P (μM)	$MFx10^{-5}$	St. error	t test	% Cell viability	St. error	t test
AHH-1	Untreated control	0.26	0.03		96.93	1.86	
	Solvent control (0)	0.18	0.03	0.08	100.00	0.00	0.11
MCL-5	Untreated control	2.39	0.13		99.98	1.16	
	Solvent control (0)	2.2	0.15	0.26	100	0.00	0.98

These studies showed that DMSO is non-mutagenic for both cell lines and as such can be used to represent the spontaneous HPRT MF in AHH-1 and MCL-5 cell lines.

Both cell lines, AHH-1 and MCL-5, were treated with B[a]P for a 24h exposure using a dose range of 1-10μM. The average % cell viability and MF ($x10^{-5}$) from the triplicates in response to different doses of B[a]P is shown in Table 4.2 and individual results are discussed below for each cell line.

Table 4.2 A summary table showing the average results of % cell viability and average mutation frequency (MF$x10^{-5}$) with 24h benzo[a]pyrene treatment in AHH-1 and MCL-5 cells.

B[a]P (μM)	AHH-1		MCL-5	
	%Cell viability	MF ($x10^{-5}$)	%Cell viability	MF ($x10^{-5}$)
0	100.00	0.18	100.00	2.20
1	99.49	0.63	100.92	13.77
2	103.45	1.03	99.70	22.96**
3	97.86	1.71	94.99	28.23***
4	98.26	3.14*	93.58	40.67***
5	93.73	4.42**	84.89	52.27***
10	91.93	5.52***	74.65	137.00***

*, **, *** Indicates a statistically significant difference compared to control ($p<0.05$, $p<0.01$ and $p<0.001$, respectively)

4.3.1.1.1 AHH-1 cells

The AHH-1 cell viability decreased with increasing dose of B[a]P but overall the responses did not vary significantly with that of the solvent control (Table 4.1 and Figure 4.2, Raw data in Appendix IV, Table A. 10). The cell viability was 99.49% at 1μM and was reduced to 91.93% at 10μM. Despite low toxicity levels, AHH-1 cells showed increased MF with increasing B[a]P dose, for example, MF was significantly increased from 3.14 $x10^{-5}$ at 4μM ($p<0.05$) to 5.52 $x10^{-5}$ at the top dose of 10μM ($p<0.001$). When MF from treated samples was compared to the spontaneous frequency of the solvent control 17.4 and 30.6 fold increases in MF were observed at 4μM and 10μM doses respectively (Figure 4.2).

The increase in MF was observed as a linear dose-response, as confirmed by the result of the Hockey stick model for estimation of the dose-response relationship for 24h B[a]P exposure in AHH-1 cells (Figure 4.3).

Figure 4.2 Average mutation frequency (MF $x10^{-5}$) and average % cell viability in AHH-1 cells after 24h benzo[a]pyrene treatment. *Points*: mean of 3 replicates, *Bars*: standard error, *, **, *** Indicates a statistically significant difference compared to control ($p<0.05$, $p<0.01$ and $p<0.001$, respectively)

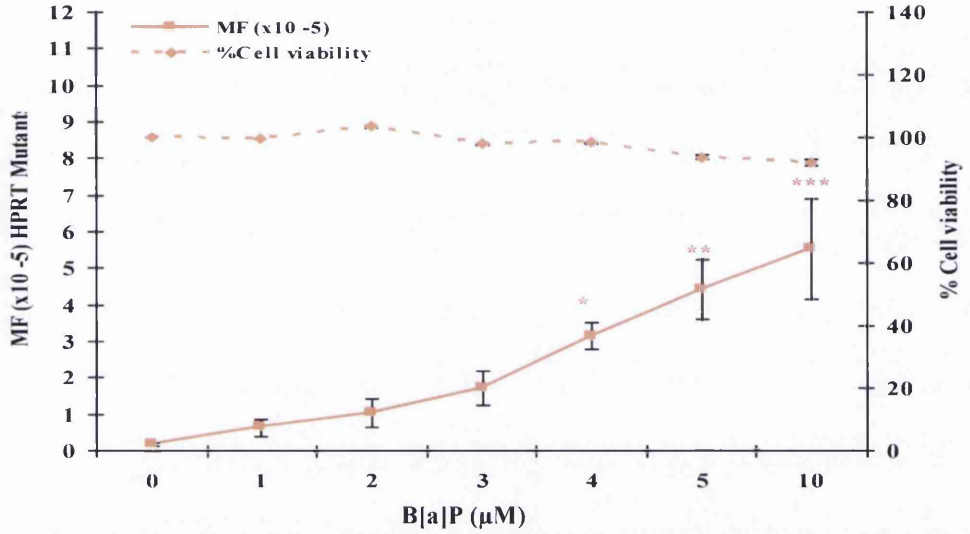

Figure 4.3 Graph generated by the Hockey stick threshold model using the Lutz approach for the analysis of dose-response relationship in AHH-1 cells to benzo[a]pyrene.

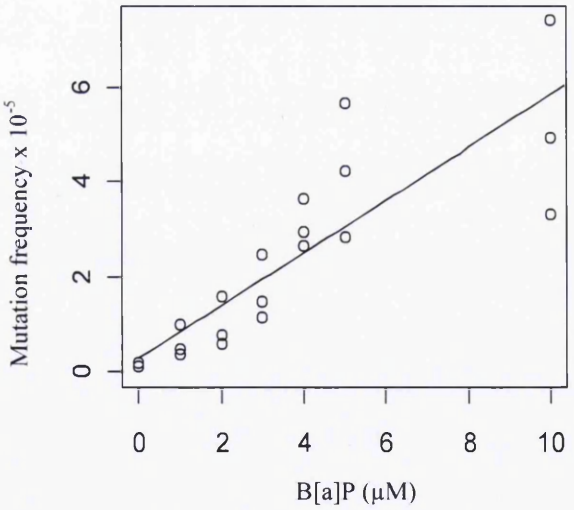

4.3.1.1.2 MCL-5 cells

When dosed with B[a]P for 24h, the % cell viability was not affected in MCL-5 cells until the 3µM dose, after which a steady linear decrease in % cell viability was observed. At 10µM the cell viability was still 74.65% (approximately 25% toxicity) compared to 100% in the solvent control (Table 4.2 and Figure 4.4). A linear increase in MF was observed over the 1-5µM dose range, which was followed by a sharp increase in MF at the 10µM dose. Statistically significant increases in the MF were shown at 2µM (22.96 $x10^{-5}$; $p<0.01$) and all of the doses above ($p<0.001$). For example, there were 10.43, 12.83, 18.48, 23.75 and 62.27 fold increases

found over the spontaneous frequency at 2μM. 3μM, 4μM, 5μM and 10μM doses respectively (Figure 4.4, Raw data in Appendix IV, Table A.12). MCL-5 was observed to be more sensitive than AHH-1 to comparative doses of B[a]P.

The Hockey stick modelling for estimation of the dose-response relationship revealed that B[a]P exhibited a linear dose-response in MCL-5 cells after 24h exposure (Figure 4.5) and no threshold dose was found.

Figure 4.4 Average mutation frequency (MF $x10^{-5}$) and average % cell viability in in MCL-5 treated with benzo[a]pyrene for 24h. *Points*: mean of 3 replicates, *Bars*: standard error, **, *** Indicates a statistically significant differencein MF compared to control ($p<0.01$ and $p<0.001$, respectively).

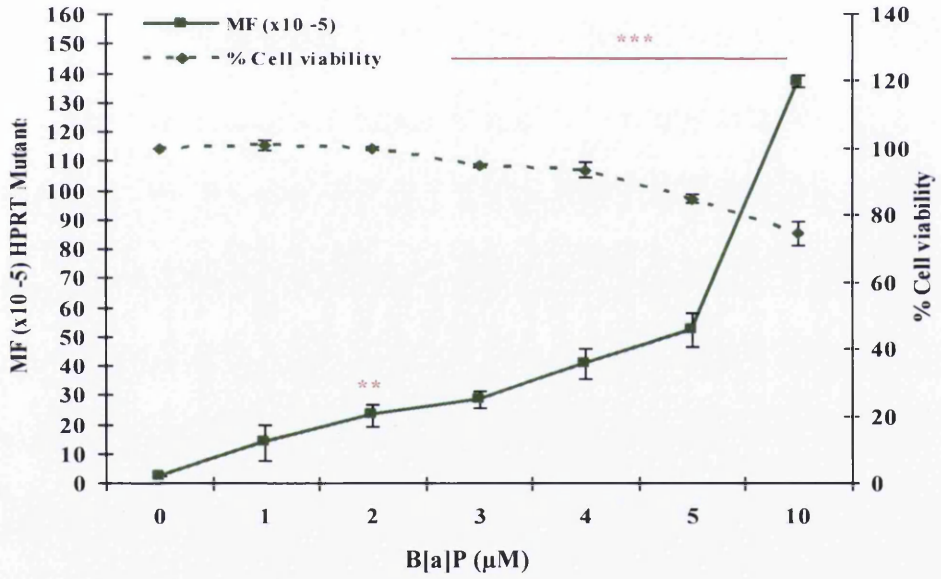

Figure 4.5 Graph generated by the Hockey stick threshold model using the Lutz approach for the analysis of dose-response relationship in MCL-5 cells to benzo[a]pyrene.

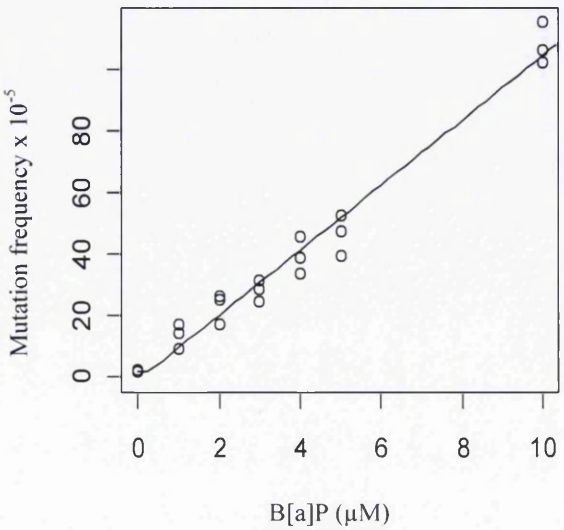

4.3.1.2 Mutation frequency of B[a]P after 4h exposure

As extended period of 24h exposures to B[a]P caused significant genetic mutations (expressed as increases in MF), a shorter (4h) exposure to B[a]P was performed with both cell lines. Both cell lines, AHH-1 and MCL-5, were treated with B[a]P for 4h exposure using a dose range of 10-50μM and 5-50μM, respectively. These doses were selected on the basis of previous experiments (Chapter 3) that showed that at 4h exposure required higher doses of B[a]P to cause any significant effect. Mean cell viability and MF ($x10^{-5}$) from three replicates in response to different doses of B[a]P is shown in Table 4.3 and individual results are discussed below for each cell line.

Table 4.3 A summary table showing the average results of % cell viability and average mutation frequency (MF$x10^{-5}$) after 4h benzo[a]pyrene treatment in AHH-1 and MCL-5 cells.

B[a]P (μM)	AHH-1		MCL-5	
	% Cell viability	MF ($x10^{-5}$)	% Cell viability	MF ($x10^{-5}$)
0	100.0	0.38	100.00	3.70
5	-	-	100.40	6.70
10	111.25	0.91	91.86	13.09**
15	-	-	88.50	12.13**
20	100.58	1.25	84.61	20.03***
25	100.55	1.48	83.36	22.1***
30	94.22	1.56	80.03	28.05***
50	95.64	1.60	77.52	29.2***

*, **, *** Indicates a statistically significant difference compared to control ($p<0.05$, $p<0.01$ and $p<0.001$ respectively). Dashed line: dose not tested.

4.3.1.2.1 AHH-1 cells

AHH-1 cells showed little change in % cell viability with increasing B[a]P dose. The cell viability reduced to 95.64% at the highest dose of 50μM B[a]P (Table 4.3). Similarly, a non-significant increase in MF was observed from 0.91 $x10^{-5}$ to 1.60 $x10^{-5}$ as the tested dose range increased (Figure 4.6, .Raw data in Appendix IV, Table A. 14).

The Hockey stick model for estimation of the dose-response relationship was not applied as no significant increase in the MF was observed.

Figure 4.16 Average mutation frequency (MF $x10^{-5}$) and average % cell viability in AHH-1 cells treated with benzo[a]pyrene for 4h. *Points*: mean of 3 replicates, *Bars*: standard error.

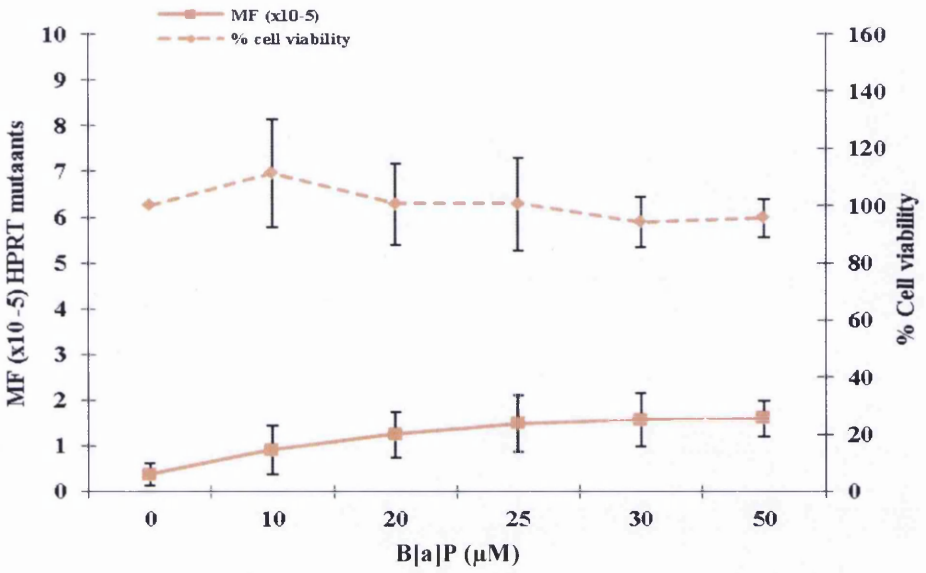

4.3.1.2.2 MCL-5 cells

MCL-5 cells showed a gradual decrease in % cell viability with increasing dose of B[a]P (5-50µM). For example, the cell viability dropped to 77.52% at the highest dose of 50µM from 100.40% at the lowest dose of 5µM (Table 4.3 and Figure 4.7). This represents a 23% toxicity level which is significantly lower than the maximum toxicity testing limits of 50±5% (OECD 2007). A linear increase in MF was observed in MCL-5 cells across the range of B[a]P doses. For example, MF was 3.70% in untreated control which varied non-significantly with B[a]P dose of 5µM, however at 10µM, MF was significantly ($p<0.01$) higher than the untreated control. MF continue to increase with increasing B[a]P dose reaching to 29.2% at 50µM ($p<0.001$). When compared to the spontaneous MF in the solvent control, fold increases of 3.53 to 7.89 MF were induced by B[a]P exposure (Figure 4.7, Raw data in Appendix IV, Table A.16).

The result of the Hockey stick model for estimation of the dose-response relationship revealed that B[a]P exhibited a linear dose response in MCL-5 cells after 4hrs exposure and thus proves that there is no safe exposure to B[a]P in these metabolically competent cells. Thus, low doses of B[a]P are capable of inducing gene mutations in these cells (Figure 4.8).

Figure 4.7 Average mutation frequency (MF $x10^{-5}$) and average % cell viability in MCL-5 cells treated with benzo[a]pyrene for 24h. *Points*: mean of 3 replicates, *Bars*: standard error, **, *** Indicates a statistically significant difference in MF compared to control ($p<0.01$ and $p<0.001$, respectively).

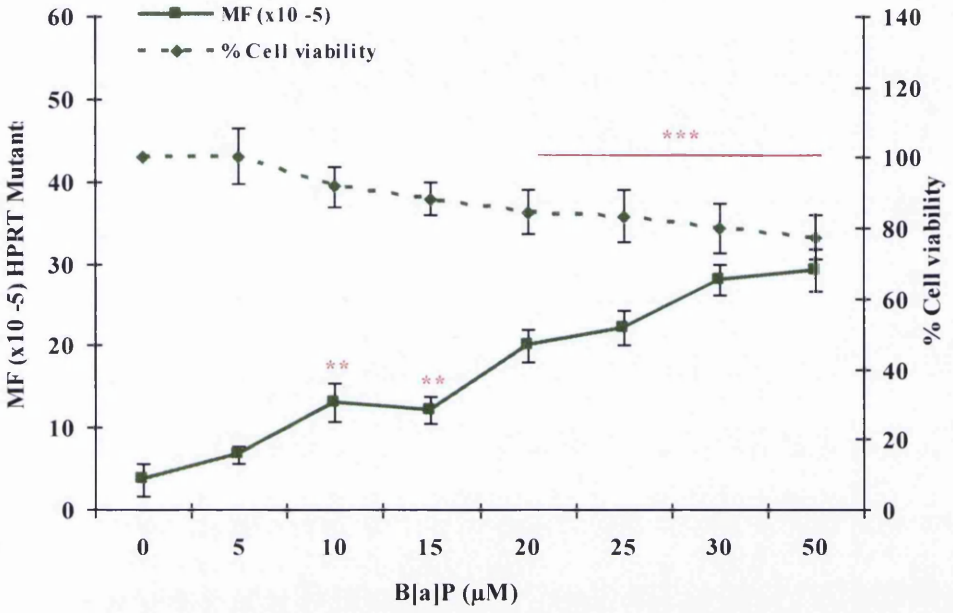

Figure 4.8 Graph generated by the Hockey stick threshold model using the Lutz approach for the analysis of dose-response relationship in MCL-5 cells to benzo[a]pyrene.

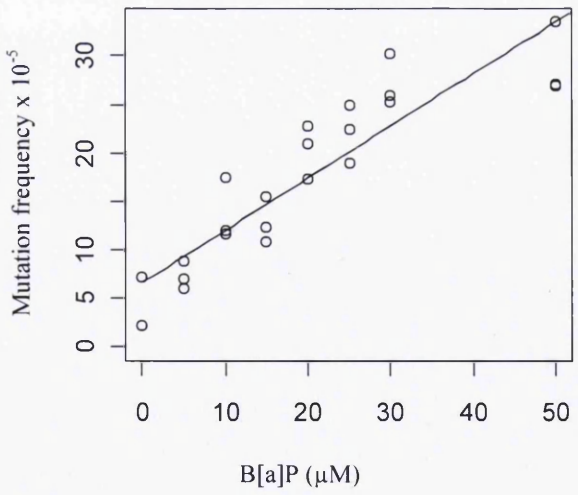

4.3.2 Sequence analysis of HPRT mutants

Mutation spectra were constructed to investigate the type of mutations induced by B[a]P in AHH-1 and MCL-5 mutants. Since no significant difference in mutation frequency in AHH-1 was observed at 4h B[a]P exposure, mutants for further studies were selected from the 24h experiment. Mutant cells for further studies were selected that were exposed to 10μM B[a]P

for 24h as well as mutants obtained from the solvent control (Sections 4.3.1.1.1 and 4.3.1.1.2) to further study B[a]P-induced mutations and spontaneous mutations respectively. These mutants were isolated and propagated at the end of the HPRT assay for sequence analysis. In the AHH-1 cell line 20 mutants were observed for spontaneous mutations and 20 mutants were used for B[a]P-induced mutations. Spontaneous mutations were examined in 20 mutants of the solvent control and 28 mutants treated with B[a]P in MCL-5 cells. The percentages of all the mutations resulting from B[a]P exposure and solvent control in both cell lines are shown in Table 4.4.

Table 4.4 Percentages of spontaneous and benzo[a]pyrene-induced mutations (10μM dose, 24h) at the *HPRT* locus in AHH-1 and MCL-5 mutants.

Type of Mutations	AHH-1 Sol. control	AHH-1 B[a]P treated	MCL-5 Sol. control	MCL-5 B[a]P treated
Base substitutions	0	11	5	20
Transitions				
G → A				
T → C		2 (11%)		1 (4%)
Transversions				
C → A				
G → C		1 (5.5%)	4 (30%)	1 (4%)
T → A				
G → T		8 (44.4%)	1 (8%)	18 (72%)
% Transversion mutations	0%	9/18 (50%)	5/13 (38%)	19/25 (76%)
Tandem Mutations	1 (7%)		1 (8%)	
Deletion/Insertion				
Deletions	13 (93%)	6 (33%)	7 (54%)	5 (20%)
Insertions		1 (5.5%)		

In the AHH-1 solvent control, a total of 14 mutations with different mutations were found from 20 mutants, whereas mutation spectra of the remaining 6 mutants showed mixed colony traces, therefore, were excluded them for further analysis. The most dominant spontaneous mutations were deletions, constituting 93% of the spontaneous mutation spectra. The other

7% of mutations represented a single tandem mutation (TG285/6AT) (Table 4.4, Appendix V, screen shot A, Figure A.3, A) involving a T→A and G→T mutation at exon 2 of the HPRT gene (Table 4.5). Among the 13 deletions, 80bp deletions (Exon 4) and 76bp (Exon 7) deletions occurred 7 and 3 times respectively (Table 4.5 Appendix V, screen shot A, Figure A. 2, B).

Table 4.5 Spontaneous and benzo[a]pyrene-induced mutational spectrum at the *HPRT* locus in the AHH-1 cell line.

Treatments	Mutations		Sequence	Exon
Solvent control	Tandem mutations			
	1	AT →TA	TCATGGA	284
		GC → TA	TCATGGA	285
	Deletions			
	1	-106 bp	GTG <>GAC	195 <> 301
	1	-1 bp G	GAG <>CCA	343
	7	-80 bp	ATG <>TTA	490 <> 570
	3	-76 bp	TGT <>CAG	700 <> 776
	1	-16 bp	AAT <>TGA	777 <> 793
B[a]P Treated	Single bp substitutions			
	1	CG → AT	GCTGAGG	255
	1	AT → CG	GACTAAT	289
	1	GC → TA	AAGGAGA	333
	1	AT → CG	CCCTCTG	361
	6	CG → AT	AAGGGGG	375
	1	CG → GC	CAGGGAT	767
	Insertions			
	1	+1 bp G	GGG <>CTA	379 <> 380
	Deletions			
	5	-2 bp TG	GTG <> CTC	367 <> 368
	1	-46 bp	AGC <> TTG	653 <> 699

Following treatment with 10μM B[a]P for 24h, from 20 AHH-1 mutants 11 point mutations, 6 deletions and 1 insertion were observed. The mutation spectra of remaining 2 mutants showed mixed colony traces, therefore, were excluded them for further analysis. The predominant B[a]P-induced point mutations were G→T transversions which was observed in 9 mutants thus representing 50% of the total 18 mutation spectra analysed, (Table 4.4, Appendix V, screen shot A, Figure A. 2, A). Out of 11 different point mutations, the G375T substitution occurred 6 times while the others appeared only once (Table 4.5). Other mutations such as GC→AT transitions (11%), insertion of 1 base pair i.e. G (5.5%) (Appendix IV, screen shot A, Figure A. 2, B), and deletions (33%) were also observed (Table 4.4). Of the deletions observed base pair (TG) deletions occurred in 5 instances (Table 4.5, Appendix V, screen shot A, Figure A. 2, C). The ratio of transitions to transversions was 0 for spontaneous and 2:9 for B[a]P-induced mutations. The proportion of G→T transversion mutations was higher as compared to other single base pair substitution types.

In the MCL-5 solvent control, 20 mutants were processed and only 13 mutation spectra were analysed as mutation spectra of remaining 7 mutants showed mixed colony traces. The mutational spectrum constituted of 54% deletions and 38% transversion mutations (Table 4.4). Among 5 point mutations G648C appeared four times (Appendix V, screen shot B, Figure A. 4, A) and a TG285/6AT tandem mutation occurred once (Appendix V, screen shot B, Figure A. 4, B). Deletions of 1 (n=3), 9 (n=2) and 76 (n=2) base pairs appeared repeatedly as spontaneous mutations in MCL-5 mutants (Table 4.6) (Appendix V, screen shot B, Figure A. 4, C).

Following treatment with 10μM B[a]P for 24h exposure, 25 different mutations were observed from 28 MCL-5 mutants. The predominant B[a]P-induced point mutations were GC→TA transversions, constituting 76% of the mutation spectra (Table 4.4). Out of 20 different point mutations (Appendix V, screen shot B, Figure A. 5, A), G306T (n=6), G378T (n=3) and G 767T (n=2) substitutions occurred frequently (Table 4.6). Other mutations such as GC→TA transitions (4%) and deletions (20%) (Appendix V, screen shot B, Figure A. 5, B) were also observed (Table 4.4). The ratio of transitions to transversions was 0:5 for spontaneous and 1:19 for B[a]P-induced mutations. Among all the point mutations, the proportion of G→T transversion mutations was higher as compared to other single base pair substitution types.

Table 4.6 Spontaneous and benzo[a]pyrene-induced mutational spectrum at the *HPRT* locus in the MCL-5 cell line.

Treatments	Mutations		Sequence	Exon
Solvent control	**Single bp substitutions**			
	1	**CG → AT**	**AAGGGGG**	**375**
	4	**GC → CG**	**GTCGCAA**	**648**
	Tandem mutation			
	1	**AT → TA**	**TCATGGA**	**284**
		GC → TA	**TCATGGA**	**285**
	Deletions			
	2	**- 9 bp**	**TGT<>GTG**	**356 <> 365**
	3	**- 1 bp T**	**CTT <> GCT**	**604**
	2	**- 76 bp**	**TGT <> CAG**	**700 <> 776**
B[a]P treated	**Single bp substitutions**			
	1	**CG → AT**	**GATGAAC**	**207**
	1	**CG → AT**	**CATGGAC**	**285**
	1	**GC → TA**	**ATGGACA**	**297**
	6	**CG → AT**	**ACTGAAC**	**306**
	3	**CG → AT**	**GGGGGCT**	**378**
	1	**GC → TA**	**CTGGCAA**	**586**
	1	**CG → AT**	**CCACGAA**	**675**
	1	**GC → TA**	**CCAGACT**	**696**
	1	**GC → CG**	**TAGGATA**	**736**
	1	**CG → AT**	**TCAGGGA**	**766**
	2	**GC → TA**	**CAGGGAT**	**767**
	Deletions			
	1	**- 5 bp**	**GTG <>TGA**	**195 <> 199**
	1	**-1 bp G**	**CAG <>ACT**	**302**
	1	**- 4 bp**	**GTG <>ATA**	**567 <> 570**
	1	**- 46 bp**	**AGC <>TTG**	**653 <> 699**
	1	**- 20 bp**	**CTT <> ACA**	**700 <> 720**

4.3.2.1 Mutation spectra present on the *HPRT* gene sequence

The spectrum of spontaneous and point mutations along the HPRT mRNA sequence in AHH-1 and MCL-5 cell lines are presented in Figures 4.9 and 4.10, respectively. The sequence of mRNA used in the present study, is identical to the non-transcribed /anti-sense strand. Therefore the mutations identified in the mRNA indicate mutagenesis in the non-transcribed strand of the double helix which is the transcription-associated mutagenesis. In the non-transcribed strand there was no spontaneously occurring GC→AT transitions found in both cell lines spectrum. In the presence of B[a]P all AT→CG transitions where T→C change in the non-transcribed strand. A clear difference was seen in the distribution of mutations along the HPRT target sequence between the solvent control and B[a]P-induced mutants in both cell lines. The mutational spectra of AHH-1 mutants from the solvent control (Figure 4.9 A) showed deletions of a number of base pairs and most of them occurred at exon 6 and 7 and no mutation due to base substitutions was observed. However, B[a]P-induced mutation spectra showed mutations due to deletions, insertions and single base pair substitutions (Figure 4.9 B). The most dominant mutations were observed to be G→T transversions, present at exon 2 and exon 3 on the HPRT sequence. Other point mutations such as T→C and G→C also appeared at exon 2 and exon 7, respectively. The insertion of one base (G) and deletions of two bases (TG) took place at exon 3 and another 46bp deletion appeared at exon 6.

As seen in AHH-1, the mutational spectra of 20 MCL-5 mutants from the solvent control (Figure 4.10 A) also showed deletions of a number of base pairs and other point mutations distributed at exons 3, 6 and 7. Among spontaneous mutations (solvent control) more deletions were observed as compared to point mutations. The base substitution G→C occurred 4 times at exon 6 and 7 as compared to G→T base pair substitution which appeared once at exon 3. The B[a]P-induced mutation spectra of 25 mutants showed a mixture of mutations such as deletions, insertion and single base pair substitutions (Figure 4.10 B). The most dominant mutations were observed to be G→T transvertions, which were present at exons 2, 3, 6 and 7 on HPRT sequence. Other point mutations such as C→T and G→C were also observed at exon 6 and exon 7, respectively. The deletions were distributed all over the HPRT sequence, but the majority were located at exon 6 and 7. In the case of both cell lines most of the point mutations were GC→TA transversions, with exon 3 of the HPRT sequence being the prominent hot spot for mutations to arise.

Tandem mutations at 284-285 base pair were similar in solvent control of both cell lines where 1 mutant from each cell line showed this mutation. Solvent control also showed similar

deletion at 700-776 in both cell lines, however, 3 mutants from AHH-1 and 2 mutants from MCL-5 showed these deletions.

There were two similar mutations observed in B[a]P treated AHH-1 and MCL-5 cell lines. The G→T transversion at 767 base pair was common in both cell lines but it appeared only once in AHH-1 and twice in MCL-5 cell line. One mutant from each cell line showed deletion of 46 bp at 653-699.

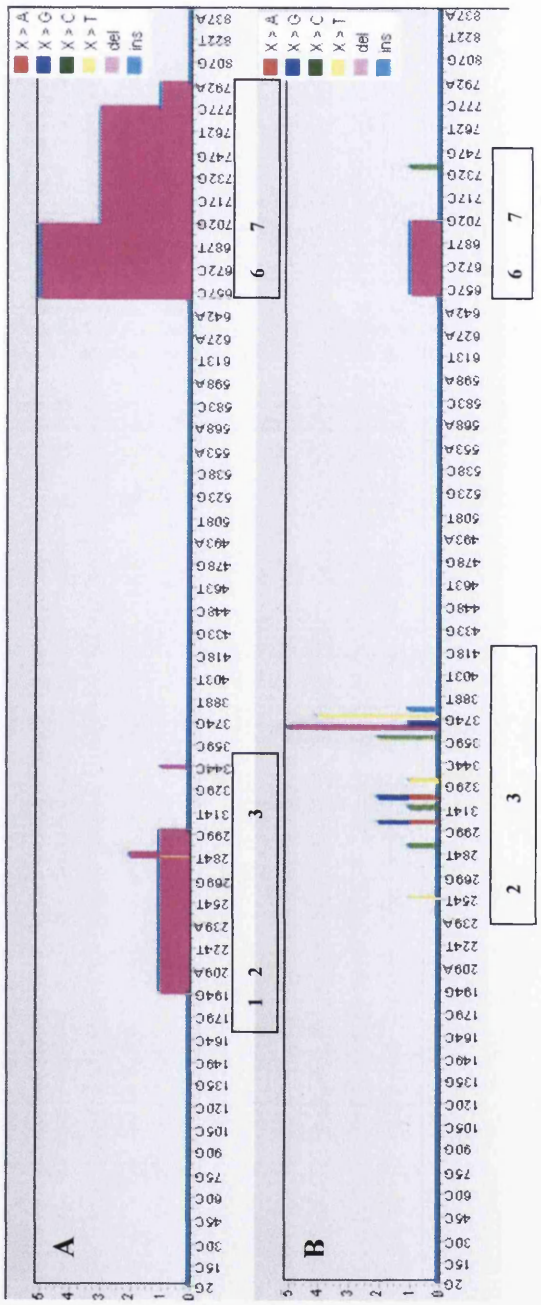

Figure 4.9 Mutation spectra (A) spontaneous and (B) benzo[a]pyrene-induced in the HPRT gene in AHH-1 mutants. Each base and its number on the HPRT sequence are presented on the *x-axis*. The number of mutations is portrayed on the *y- axis*. Each base alteration is colour coded where the letter X stands for the 4 bases; A, C, G or T determined by the position on the sequence. Numbers in the rectangular boxes represent the hotspot on exons.

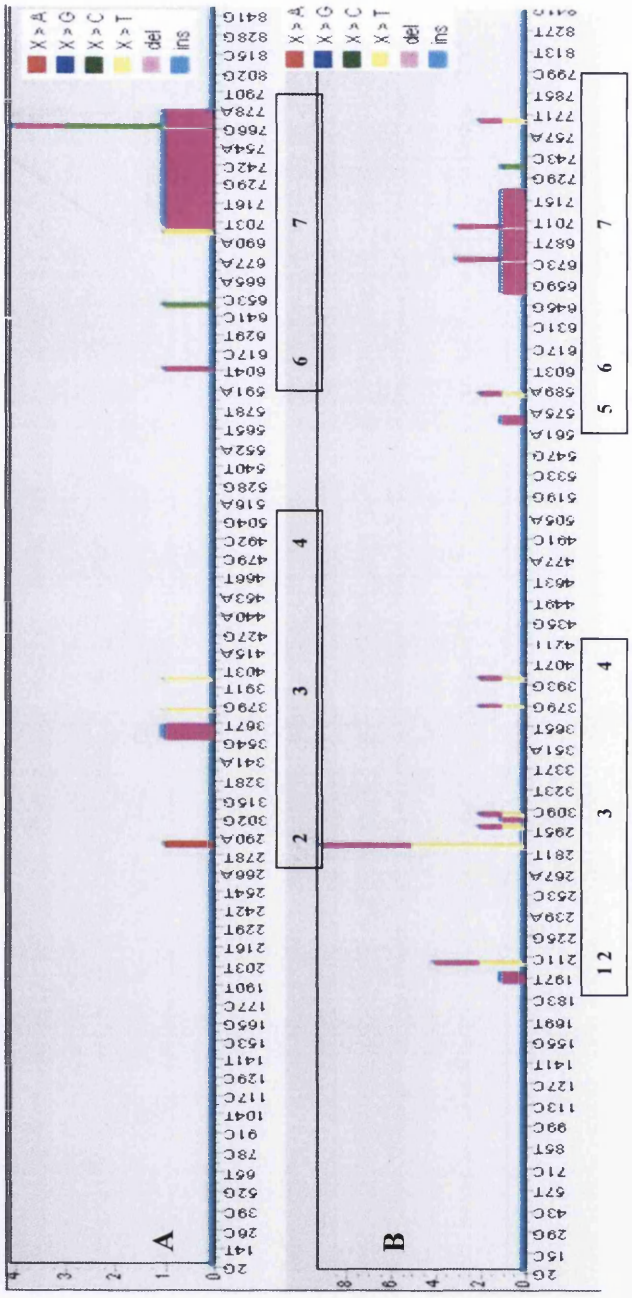

Figure 4.10 Mutation spectra (A) spontaneous and (B) benzo[a]pyrene-induced in the HPRT gene in MCL-5 mutants. Each base and its number on the HPRT sequence are presented on the *x-axis*. The number of mutations is portrayed on the *y- axis*. Each base alteration is colour coded where the letter X stands for the 4 bases; A, C, G or T determined by the position on the sequence. Numbers in the rectangular boxes represent the hotspots on exons.

4.3.3 Mutation spectra of *TP53* gene

The section of TP53mRNA spectrum is shown for MCL-5 and AHH-1 cell lines in Figure 4.11 A and B respectively. Sequence analysis of the *TP53* gene product showed a partial CCGG to TTGG transition at codon 281, 282 in exon 8 in both cell lines MCL-5 and AHH-1

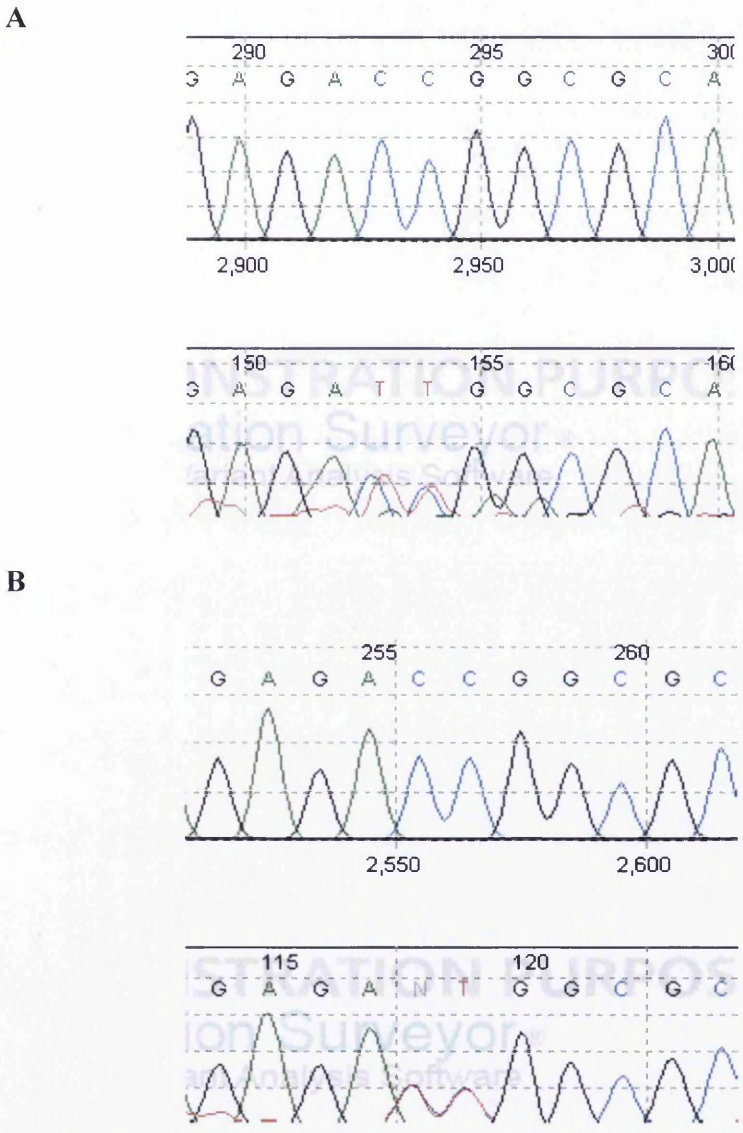

Figure 4.11 DNA sequence of (A) MCL-5 and (B) AHH-1 cell lines shows a partial CCGG to TTGG transition mutation at codon 282 in exon 8 of the *TP53* gene.

4.4 Discussion

The methodology of the HPRT assay has been standardised by OECD guidelines (OECD 486, 1997) for testing and identifying chemicals that may induce DNA mutations. In the present study, the HPRT assay was used to elucidate the dose-response relationship of gene mutations induced by B[a]P and also to analyse the spontaneous and induced mutational spectra of HPRT mutations in 6-TG resistant human cell lines. B[a]P was shown here to be genotoxic and have the potential to induce gene mutations in both AHH-1 and MCL-5 cells. B[a]P had an increased mutagenic effect in the MCL-5 cell lines compared to AHH-1 cell line (Figures 4.4 and 4.8) at both 24h and 4h time exposures, probably because of the difference in the metabolic capabilities of these cell lines. The present studies on *TP53* gene analysis showed that mutations in exon 8 of *TP53* gene are heterozygous in MCL-5 and AHH-1 cell lines. Earlier studies by Guest & Parry (1999) have shown that these heterozygous mutations do not influence the ability of AHH-1 and MCL-5 to undergo DNA damage induced cell death. These findings confirmed that genotoxicity observed in our study is not due to mutations in *TP53* genes.

4.4.1 Response of 24h exposure of B[a]P on mutation frequency

I observed that long-term, low doses exposure (24h at 1-5μM and 10μM doses) of the metabolically competent MCL-5 cell line to B[a]P, produces significant increases in mutation frequencies (Table 4.2) as compared to short-term, high-doses (4h at 5-25μM) exposure (Table 4.3). The reasons for lower mutation frequencies in short-term exposures in both cell lines are probably due to the lower metabolic activity to activate lower doses of B[a]P to produce mutations. This is consistent with the observations that in MCL-5 cells at 5 and 10μM the MF were only $6.70x10^{-5}$ and $13.09x10^{-5}$ ($p<0.01$) after 4h exposure (Table 4.3) as compared to 24h where the MF were $52.27x10^{-5}$ and $137x10^{-5}$ at 5μM and 10μM respectively (Table 4.2). In the case of AHH-1 cells, which are less metabolically competent cell line, non-significant increases in MF were observed at high-doses for a short exposure time (Table 4.3). In contrast low doses exposure for a longer time produced significant increases in MF at $4.42x10^{-5}$ ($p<0.01$) and $5.52x10^{-5}$ ($p<0.001$) at 5 and 10μM observed respectively (Table 4.2). Again probably reflecting time needed for efficient metabolism of B[a]P to mutagenic metabolites.

There was a linear dose-response observed for B[a]P exposed for 24h in AHH-1 and MCL-5 cell lines for the induction of gene mutations. The lowest doses that induced a statistically significant increase in MF were 4μM with $3.14\ x10^{-5}$ ($p<0.05$) and 2μM with $22.96x10^{-5}$

values ($p<0.01$) in AHH-1 and MCL-5 cell lines respectively. A non-significant increase in MF was observed at lower doses when compared to solvent control and these indicate that the presence of B[a]P even at lower level has a potential to induce genetic mutations in these cell lines after 24h exposure. Indeed the Lutz modelling rejected a non-linear response and supported linear increases in mutation frequency.

4.4.2 Response of 4h exposure of B[a]P on mutation frequency

Unlike 24h exposure of B[a]P, which caused significant increase in MF in both AHH-1 and MCL-5 cell lines at lower doses, a 4h exposure only showed significant increase in MF with MCL-5 cells at low doses (Figure 4.7). The first statistically significant increase in MF was 13.09 $x10^{-5}$ at 10μM ($p<0.01$) observed in MCL-5 cell line and a linear dose-response was observed. Non-significant increases in MF were observed from 0.91 $x10^{-5}$ to 1.60 $x10^{-5}$ as the tested dose range increased with AHH-1 cell line (Figure 4.6). This means that dose response for B[a]P is highly dependent on metabolic competency and exposure duration. At both exposure times and in both cell lines (Table 4.2 and Table 4.3) the first statistically significant increases in MFs observed occurred at concentrations where cell viability was not statistically decreased, therefore, increases in mutation frequencies observed were not induced via cytotoxicity related mechanisms. This lack of observed cell death means that viable mutant cells are present, which correlate with increased concern for *in vivo* tumorgenic potential.

4.4.3 Effect of metabolic competency on occurrence of mutation frequency

At both, 24h and 4h exposure times MCL-5 cells showed dose-dependent increases in mutation frequencies. MCL-5 cells were 25 to 14-folds more sensitive than AHH-1 to B[a]P induced mutation (10μM) at 24h and 4h respectively. These findings were similar to Crespi *et al*, (1990) where MCL-5 cells were about 833-fold more sensitive than AHH-1 cells in comparison to the control. MCL-5 cells are derived from L3 cells, a sub-population of AHH-1 cells expressing only CYP1A1 and are devoid of mEH activity (Penman *et al*, 1994). Thus, MCL-5 cells have CYP1A1 but have also been transfected with a plasmid which expresses other metabolic enzymes such as CYP1A2, CYP2A6, CYP2E1 and CYP3A4 and mEH (Crespi *et al*, 1991). Therefore, MCL-5 cells express all five enzymes and also have higher expression of CYP1A1 as compared to AHH-1 cells, and thus produce more B[a]P metabolites than AHH-1 following B[a]P exposure. Therefore, this difference in metabolic potential is potentially responsible for the difference in the mutation frequencies of AHH-1 and MCL-5 cell lines. These observations are consistent with CYP1A1 and mEH being

primarily involved in activating B[a]P in addition to suggesting a role for other transfected CYP enzymes.

B[a]P is an extensively studied compound among the group of PAH's and is present at low levels (10-50ng/cigarette) in cigarette smoke (Hecht, 1999). Indeed, the PAH's (like B[a]P) present in smoke are believed to be responsible for the link between smoking and lung cancer. B[a]P from cigarette smoke has been linked with lung cancer, and studies by Dennisenko *et al* (1996) have reported distribution of BPDE adducts along exons of the *TP53* gene in BPDE-treated HeLa cells and bronchial epithelial cells. This study further showed adduct formation at guanine positions in codons 157, 248, and 273, which are believed to be major mutational hotspot in human lung cancer. B[a]P induces gene mutations by forming bulky nucleotide adducts; mainly through BPDE (Singer and Grunberger, 1983; Xue and Warshawsky, 2005). The B[a]P adduct that induces point mutations is associated with the level of Benzo[a]pyrene-7,8-diol-9,10-epoxide (BPDE) adduct which binds covalently at the N2 position of guanine in genomic DNA (BPDE-N^2-dG) and produces predominantly G:C to T:A transversion mutations (Yoon *et al*, 2001). B[a]P also inefficiently form BPDE- N^6-dA adducts in the DNA (Jeffrey *et al*, 1979) which have different conformation and arrangement of DNA complex than the BPDE-dG adducts (Geacintov *et al*, 1997). BPDE-N^2-dG is present in (+)-trans and (+)- cis forms (Mocquet *et al*, 2007). (+)- trans- BPDE- N^2-dG is the most abundant and major adduct identified *in vivo* (Weinstein *et al*, 1976) and was detected in 45% of smokers' lungs (Boysen and Hecht, 2003).

At low doses, the rate of adduct repair is probably faster than its rate of formation, resulting in NOEL (Doak *et al*, 2007). BPDE-DNA adducts are recognized and repaired mainly by nucleotide excision repair (NER) (Hess *et al*, 1997; Meschini *et al*, 2008). Hess *et al* (1997) described that the rate of repair of BPDE- N^2-dG depends on their different steriochemical configurations. For example, NER lesion recognition complex XPC-HR23B recognized the adducts differentially and repaired the *cis*-adduct of dG more rapidly than the (+)-*trans*-BPDE- N^2-dG adducts (Macquet *et al*, 2007). Chen *et al*, (1992) and Denissenko *et al*, (1998) showed that through transcription-coupled repair, the repair of BPDE-DNA adducts occurs much faster in the transcribed strand than in the non-transcribed strand of *HPRT* or *TP53* genes.

4.4.4 Mutation spectra

Mutation spectra were constructed to find out the difference in mutations induced by B[a]P in AHH-1 and MCl-5 cell lines at the *HPRT* locus. Mutations of the human *HPRT* gene are

responsible for a wide spectrum of diseases. The most severe form of disease is known as Lesch-Nyhan syndrome due to point mutation along the HPRT gene (Jinnah *et al*, 2000). As shown in Figure 4.11 single base substitutions that are responsible for causing this disease are spread throughout the 9 exons of the *HPRT* gene.

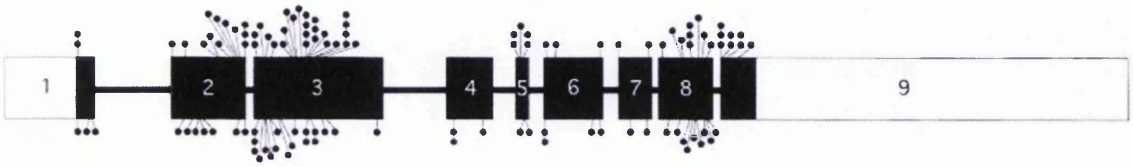

Figure 4.11 Single base substitutions are spread along the protein-coding region (black boxes) of *HPRT* gene and represent the locations of point mutations appeared as Lesch-Nyhan syndrome. Taken from Jinnah *et al* (2000)

Spontaneous mutations occur in the normal cells without any exposure to exogenous genotoxins in the environment. In the present study, DMSO was used as a solvent control and was included in this study as an untreated control, to determine the spontaneous mutations and to compare them with B[a]P-induced specific mutations. The MF of DMSO is therefore similar to untreated control. There is no evidence suggesting that DMSO exerts any mutagenesis in animal cells, and indeed is known to be a scavenger of reactive oxygen species (ROS) which are capable of DNA reaction and mutagenesis (Yu and Quinn, 1994). The mechanism responsible for spontaneous deletions in *HPRT* mRNA is the splicing at intron-exon junctions during pre-mRNA maturation prior to translation (O'Neill *et al*, 1998). The sources of spontaneous mutations are;

- DNA adduction by ROS as a result each nucleotide is susceptible to oxidative damage and cause multiple substitutions (Wiseman and Halliwell, 1996)
- Replication over abasic sites from chemically unstable bases, which causes transversions and transitions.
- Spontaneous deamination of 5-methylcytosine at CpG sites leading to GC→AT transitions.
- Error in replicating polymerase in DNA synthesis (Tippin *et al*, 2004).
- Transition associated mutagenesis, causing GC→AT, TA→GC and AT→TA substitutions (Hudson *et al*, 2003).

The present study showed that 93% and 54% of the spontaneous mutations were due to deletions at different exons of the *HPRT* locus in AHH-1 and MCL-5 cell lines (Table 4.4). In AHH-1 cell line, 93% of the deletion mutations were found on exon 1, 3 and 7, whereas in the MCL-5 cell line, 54% of spontaneous events were deletions observed in exon 2 and 3 of the *HPRT* gene. It was also observed that there is a variation in spontaneous mutation between

cell types possibly due to the difference in genotypic variations in cellular mechanisms. Earlier studies by Lewis and Parry (2002) confirmed variability among different cell types in expressing spontaneous mutations at *SupF* locus. Variability in culture age, handling conditions and differences between laboratories can also contribute towards spontaneous mutations; therefore, these factors should be taken into consideration when interpreting results of mutation spectra. Similarly it is important to standardize the culture and working conditions to minimize inter-laboratory variation.

Analysis of mutation spectra between solvent controls and B[a]P treated cell lines showed differences in type of mutations. Mutation spectra of solvent control for both cell lines, AHH-1 (Figure 4.9A) and MCL-5 (Figure 4.10A) mainly consist of deletions whereas B[a]P treated cell lines mutation spectra shows a range of mutations (Figures 4.9B and 4.10B), mostly G to T (implicating N2-dG adduct). These findings indicate the influence of B[a]P in inducing mutations rather than the induction of mutations resulting from one of the factors responsible for spontaneous mutations. Similarly B[a]P treated cell lines showed mutations at different exons compared to solvent control thus further indicating that mutations observed in B[a]P treated cells are independent of the factors associated with spontaneous mutations. It was observed that all the B[a]P induced mutations target guanine on the transcribed strand of the *HPRT* gene in all of the mutants sequenced.

Results of this study suggest the potential of B[a]P in causing cancer through DNA adduct formation and mutation. Mutational patterns observed in B[a]P treated cell lines was consistent with earlier reports where frequent G to T transversions were observed in the smoking associated mutational spectra of human lung cancer (Denissenko *et al*, 1996; Pfeifer *et al*, 2002). These findings provide further evidence that DNA adducts and mutational pattern caused by B[a]P are similar to those observed among smoking associated lung cancers (Pfiefer *et al*, 2002). Furthermore cigarette smoking provides optimum conditions for the absorption and metabolism of B[a]P in lungs leading to DNA adduct formation and mutations. Pfiefer *et al*, (2002) also reported a high incidence of G to T transversions in *p*53 in lung samples as compared to larynx and the oral cavity of smoking associated cancers. These finding indicate a link between absorption and metabolism of B[a]P and incidence of mutational patterns. The present study has also shown a similar pattern and assumed that higher DNA adduct formation was taken at higher doses. Similarly its prevalence was relatively higher in MCl-5 cell line that represents metabolic activity. Furthermore, B[a]P treated mutational patterns observed in present study are consistent with those observed in cancers associated with smoking.

Chapter 5

Investigation of the Genotoxic Potential of 2-Amino-1-methyl-6-phenylimidazo (4, 5-b) pyridine in Human Cells With Differing Metabolic Activation Capacity

5.1 Introduction

IARC (1997) classified PhIP as a Group 2B carcinogen, "possibly carcinogenic to humans". The U.S. Department of Health and Human Services National Toxicology Program (2011) has concluded that PhIP is "reasonably anticipated to be a human carcinogen". PhIP is formed when creatine or creatinine (found in muscle meats), amino acids and sugars are reacting together at high temperatures. The formation of PhIP depends upon the type of meat, temperature, duration and method of cooking (Cross and Sinha, 2004).

Various *in vivo* and *in vitro* studies have concluded that PhIP is a potent mutagen and causes multi-organ tumours in laboratory rodents. Low doses of PhIP have been shown to induce colon and mammary tumours in F344 rats through diet (Fukushima *et al*, 2004; Ito *et al*, 1991). Also PhIP induces chromosomal abnormalities in Chinese hamster cells *in vitro*. *In vivo* PhIP formed DNA adducts in both rats and monkeys (Carthew *et al*, 2010). Epidemiological studies also revealed that there is a correlation between high intake of well-done meat and high HAAs exposure with cancer of the colorectum, breast, prostate, pancreas, lung, stomach and oesophagus in humans (Zheng and Lee, 2009; Shirai *et al*, 1997).

PhIP is a strong rodent carcinogen and induces tumours at multiple sites during long-term feeding studies with mice and rats (Sugimura *et al*, 2004). Lauber *et al* (2004) have shown recently that PhIP can possess oestroagenic activity but can also invoke a mitogenic response at very low doses (10^{-9} to 10^{-11}M). Benford and her team in 2009 used a margin of exposure (MOE) approach, based on the benchmark lower confidence limit (BMDL), to study the prostate and mammary cancer induced by PhIP and concluded that there is no dose of PhIP without carcinogenic effect.

PhIP is a strong mutagen causing DNA adduct formation and mutations. These adducts have been found in exposed tissues and organs like colon. For example, Dingley (1999) used accelerator mass spectrometry (AMS) and observed DNA and protein adducts in colon tissues and blood of humans when a dose of PhIP equivalent to that found in very well-done chicken was administered through capsules, but these adducts were unstable and declined over a 24h period. Fukushima *et al*, (2009) investigated dose dependant carcinogenicity of PhIP in 6-week old F344 male rats by administering PhIP at different doses in the diet for 16 weeks. They noted that only higher doses of 50 to 400ppm were able to induce aberrant crypt foci (ACF), a surrogate marker of prenoplastic lesions in colon, however, an increased DNA adduct formation was observed at low doses of 0.01ppm and higher. These findings suggest that even low doses of PhIP are capable of inducing or initiating processes that could lead to carcinogenic activity. Adducts are only a marker of exposure of PhIP and they are not necessarily linked to mutation that lead to cancer. They can be repaired and not induce mutants at all.

PhIP requires metabolic activation to form DNA adducts. CYP enzyme's activity is central to metabolic activation and MCL-5 expresses this activity. Activated PhIP causes adduct formation and induced mutations which are mainly at Guanine base pair. Previous studies have shown correlation between mutations and DNA adduct formation, however, most of these studies were conducted at higher doses of PhIP. This study uses MCL-5 and HepG2 cell lines to determine the effect of lower doses on DNA adducts formation and mutations.

5.1.1 Aims of the study

2-Amino-1-methyl-6-phenylimidazo (4, 5-b) pyridine (PhIP), is a heterocyclic aromatic amine and its metabolic activation is catalyzed by CYP1A2 enzyme through oxidation. As compared to direct acting carcinogens, very little is known of low dose exposures to chemicals that require metabolic activation.

This study aims

- to determine the effect of low doses of PhIP on different cell lines
- to investigate the influence of varying metabolic activity particularly the variation in the expression of CYP1A1 and CYP1A2 on PhIP dose responses

5.2 Materials and Methods

5.2.1 Cell lines

Only MCL-5 and HepG2 cells were used for both 4h and 24h exposure studies. AHH-1 cell line lacks mEH and did not expressing CYP1A2, while TK6 did not expressed any of the CYP enxyme efficiently.

Cell culture was performed as described in Chapter 2 Section 2.1.2.

5.2.2 Treatment with test chemicalPhIP and dosing regime

All the flasks were seeded at $1x10^5$cells/ml (10ml/flask, MCL-5) and $1.2x10^5$ cells/cm^2 (10ml flask, HepG2) before treatment with the chemical for 24h or 4h at 37°C, 5% CO_2. Satellite flasks were also prepared for each dose for cytotoxicity analysis.

The 10mM stock of PhIP was prepared by adding 4.46ml of DMSO with a syringe into a glass bottle containing 10mg PhIP powder (Santa Cruz, Biothecnology, Inc). The 100µl aliquots were prepared and stored at 4°C for single use. For each replicate a new working stock was prepared by further diluting the 10mM stock of PhIP in DMSO+RPMI1640 (1:2) The chemical doses were then added to the flasks containing the cells according to Table 5.1 and incubated for different time points e.g. 4h or 24h. After treatment time the chemical was washed off using growth media (without supplements).

Table 5.1 Range of PhIP doses and amount of two working stocks used.

Doses (µM)	1mM working stock	10mM working stock
	Volume (µl)	Volume (µl)
2.5	25	-
5	50	-
7.5	75	-
10	100	-
15	-	15
20	-	20
25	-	25
35	-	35
50	-	50
100	-	100

5.2.3 Cytotoxicity assay

As described in Chapter 2 and Section 2.3. The experiment was repeated three times.

5.2.4 Micronucleus assay

As described in Chapter 2 Section 2.4. Cells were stained with DAPI + Vectorshield solution and then scanned for binucleated cells on the Metafer system.

5.2.5 Scoring

The CBMN assay slides were scored using the criteria described in Chapter 2 Section 2.4.3. After getting confidence on the Metafer system and the statistical power of the test this experiment was run in triplicate and 6000 binucleated cells were checked for the presence of micronuclei per dose.

5.2.6 Statistical Analysis

A one-way ANOVA followed by Dunnett's post-hoc test (2-tailed) was used to compare all treatments including untreated control data using SPSS software (version 19). Confidence limits of 95% ($p<0.05$), 99.9% ($p<0.01$) and 99.99% ($p<0.001$) were applied. The Hockey stick modelling software provided by Lutz and Lutz (2009) and implemented in the R package (software 2.9.1), was used to estimate a threshold dose.

5.2.7 RNA extraction

Total RNA was extracted from the human lymphoblastoid cell line MCL-5 and hepatoma cell line HepG2, from control and after 24h PhIP treatments. The doses of PhIP treatment selected were based upon the LOEL dose obtained as a result of CBMN assay (Table 5.2 in Section 5.4.1). Details of methods are described in Chapter 2 Section 2.6.1.

5.2.8 Reverse Transcription with elimination of genomic DNA and cDNA synthesis

The reverse transcription reactions and cDNA synthesis are described in detail in Chapter 2 Section 2.10.1 and Section 2.10.2. This experiment was repeated three times.

5.2.9 End-point PCR

This procedure was performed to study the expression of CYP1A1 and CYP1A2 in cDNA from different treated and untreated cell lines. The GoTaq® Flexi DNA Polymerase kit (Promega, Southampton, UK) was used for experiments and the method is described in detail in Chapter 2 Section 2.10.3 and Section 2.10.4.

5.2.10 Real-time PCR

The expression analysis was performed using QuatiFast™ SYBR® Green PCR Kit (Qiagen, Sussex, UK). The detailed method was described in Chapter 2 Section 2.11 and 2.11.1.

5.3 Results

MCL-5 and HepG2 cell lines were used in this study as these express high levels of CYP 450 enzymes. AHH-1 cell line was not used because it have very low expression of CYP1A2 which is required for metabolic activation of PhIP and lacks mEH (Wu *et al*, 2000). TK6 cells were not used as they are non-responsive to B[a]P due to the low CYP expressions (See Chapter 3). Both MCL-5 and HepG2 cell lines were exposed to different doses of PhIP for 24h and 4h. The *in vitro* dose-responses were assessed utilising the CBMN assay. Micronucleus frequency was used to assess the levels of chromosomal aberration. The Reverse Transcription-Polymerase Chain Reaction (RT-PCR) was used to evaluate the difference in induced expression of CYP1A1 and 1A2 in MCL-5 and HepG2 cell lines (treated with LOEL dose of PhIP for 24h obtained as a result of CBMN assay) and the expressions were quantified by Real-time PCR. It is important to note LOEL doses varied for each cell line, therefore, in this study each cell line was treated with different PhIP doses i.e. its respective LOEL dose. These different doses were selected to compare the effect of PhIP on CYP1A1 and CYP1A2 expression at doses where micronucleus induction become significant in the respective cell line

5.3.1 Cytotoxicity and genotoxicity of PhIP after 24h exposure

MCL-5 and HepG2 were treated with PhIP for 24h using a dose range of 2.5-100μM. These doses were chosen from previously published studies (Hewitt *et al*, 2007; Majer *et al*, 2004). Relative population doubling (%RPD) and average percentage of binucleated cells that contained micronuclei (%Mn/Bn) was used to assess cytotoxicity and genotoxicity respectively. For cell lines, average cytotoxicity and genotoxicity (6000 cells were scored from three replicates) in response to different doses of PhIP are shown in Table 5.2 and individual results are discussed below for both cell lines.

Table 5.2 A summary table showing the average results of cytotoxicity (%RPD) and average percentage of binucleated cells that contain micronuclei (%Mn/Bn) with 24h 2-Amino-1-methyl-6-phenylimidazo(4,5-b) pyridine treatment in MCL-5 and HepG2 cell lines.

PhIP dose (μM)	MCL-5		HepG2	
	%RPD	%Mn/Bn	%RPD	%Mn/Bn
0	100	1.45	100	0.9
2.5	99.96	1.33	98.11	0.9
5	98.32	1.3	94.2	0.92
7.5	98.55	1.28	90.15	1.02
10	99.04	1.23	89.72	1.2*
15	95.35	1.45	87.69	1.27***
20	94.45	1.52	83.05	1.33***
25	85.47	1.6	82.4	1.42***
35	78.52	1.85*	64.89	1.58***
50	54.13	2.27***	17.93	1.67***
100	30.40	2.03***	-16.81	0.90***

*, *** Indicates a statistically significant difference compared to control ($p<0.05$, and $p<0.001$ respectively).

5.3.1.1 MCL-5 cells

When compared to untreated control, PhIP treated MCL-5 cells showed no difference in cytotoxicity with increasing dose until more than 20μM PhIP. The cell viability (RPD) observed at the low dose range of 2.5-20μM, was 99.96% to 94.45% respectively when compared to 100% RPD of untreated control. The RPD was 85.47% (14.53% cytotoxicity) at 25μM PhIP, reaching to 30.4% (64.6% cytotoxicity) at the highest dose of PhIP (100μM) after 24h exposure (Table 5.2, Figure 5.1). At the dose range 2.5-10μM the micronucleus frequency ranged from 1.33-1.23% which was non-significantly lower as compared to 1.45% observed in the untreated control. A significant increase in micronucleus frequency was observed at 35μM (1.85%, $p<0.05$) and this reached to 2.27% at 50μM ($p<0.001$) and then dropped to 2.03% at 100μM ($p<0.001$) due to higher cytotoxicity levels (Figure 5.1, Raw data in Appendix VI, Table A.17).

The result of the Hockey stick model for estimation of the dose-response relationship revealed that PhIP exhibited a non-linear dose response in MCL-5 cells after 24h exposure and thus a threshold dose exists for PhIP induced chromosome breakage in these cells (Figure 5.2). The 100 μM dose was not included for the estimation of dose-response relationship because of the drop in RPD value to 30.40% (70% toxicity) which is below the 50±5% level suggested by OECD guidelines (2007). The estimated threshold dose (IP) was 23.69μM. The lower limit of 90% confidence interval (CI) was 20.5μM (indicated by broken line) at $p<0.001$.

Figure 5.1 Relative population doubling (%RPD) and average percentage of binucleated cells that contain micronuclei (%MnBn) in 2-Amino-1-methyl-6-phenylimidazo(4,5-b)pyridine 24h treated MCL-5 cells. *Points*: mean of 3 replicates, *Bars*: standard error, *, *** Indicates a statistically significant difference compared to control ($p<0.05$, and $p<0.001$ respectively).

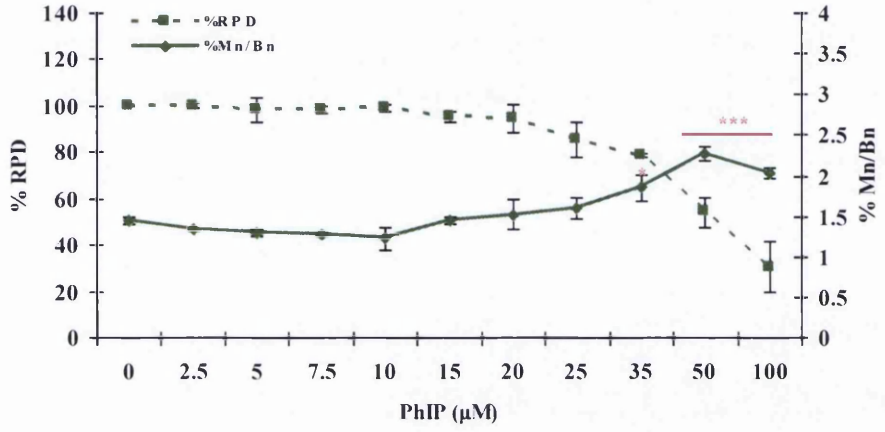

Figure 5.2 Graph generated by the Hockey stick threshold model using the Lutz approach for the analysis of dose-response relationship in MCL-5 cells to 2-Amino-1-methyl-6-phenylimidazo(4,5-b)pyridine.

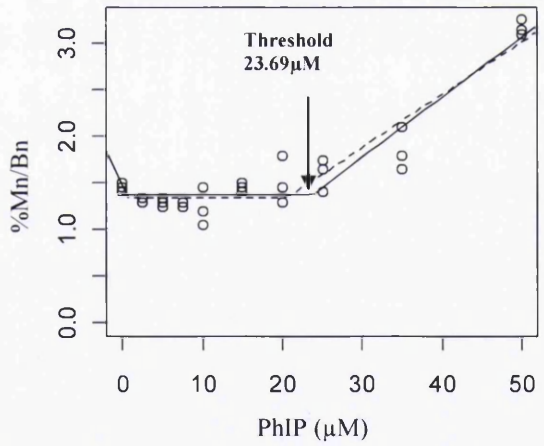

5.3.1.2 HepG2 cells

PhIP treated HepG2 cells showed a very small increase in cytotoxicity with increasing dose and 50% cytotoxicity was achieved at 50µM (Table 5.2, Figure 5.3). Cell viability (RPD) dropped to 17.93% at 50µM and at 100µM reached -16.81% indicating a strong cytotoxic effect. HepG2 cells exhibited increased sensitivity to PhIP over the MCL-5 cell line, for example at concentrations of 50µM of PhIP and above where HepG2 cell numbers decrease below the original seeded concentration, a phenomenon not observed in MCL-5 cell line. The background micronucleus frequency in HepG2 cells was lower (0.9%) as compared to MCL-5 cells (1.45%). At lower doses 2.5 and 5µM the micronucleus frequency was similar to that of

the untreated control. A linear genotoxic dose-response was observed in HepG2 cells treated with the 7.5μM to 50μM dose range of PhIP. A significant increase in the frequency of %Mn/Bn cells was first observed at 10μM which was 1.2% ($p<0.05$) and this reached 1.67% at 50μM ($p<0.001$). At the 100μM dose due to strong cytotoxic effects the %Mn/Bn frequency dropped to 0.9% (Figure 5.3, Raw data in Appendix VI, Table A.18)..

The result of the Hockey stick model for estimation of the dose-response relationship revealed that PhIP exhibited a linear dose response in HepG2 cells after 24h exposure to PhIP (Figure 5.4) and no threshold dose was found. The 100μM and 50μM doses were not included for the estimation of dose-response relationship because of the drop in RPD values to 17.93% (82% toxicity) and -16.81% respectively.

Figure 5.3 Relative population doubling (%RPD) and average percentage of binucleated cells that contain micronuclei (%MnBn) in 2-Amino-1-methyl-6-phenylimidazo(4,5-b)pyridine 24h treated HepG2 cells. *Points*: mean of 3 replicates, *Bars*: standard error, *, *** Indicates a statistically significant difference compared to control ($p<0.05$, and $p<0.001$ respectively)

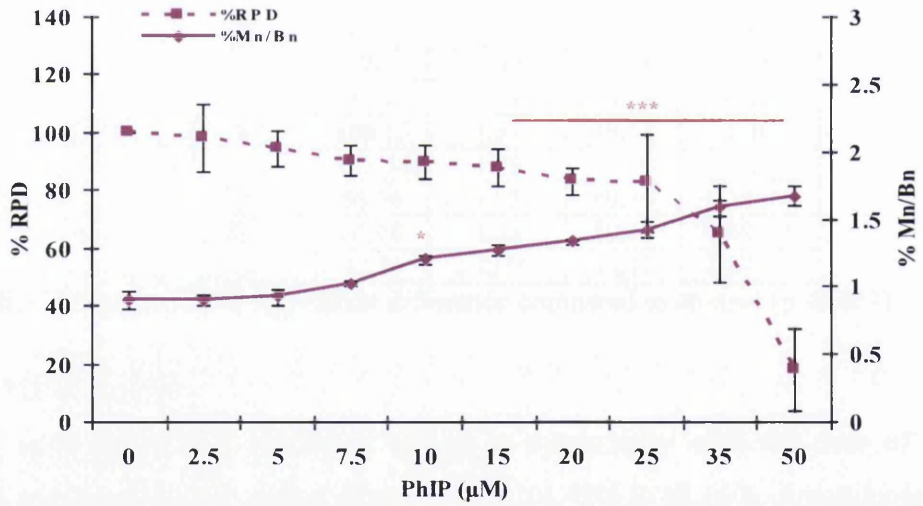

Figure 5.4 Graph generated by the Hockey stick threshold model using the Lutz approach for the analysis of dose-response relationship in HepG2 cells to 2-Amino-1-methyl-6-phenylimidazo(4,5-b)pyridine.

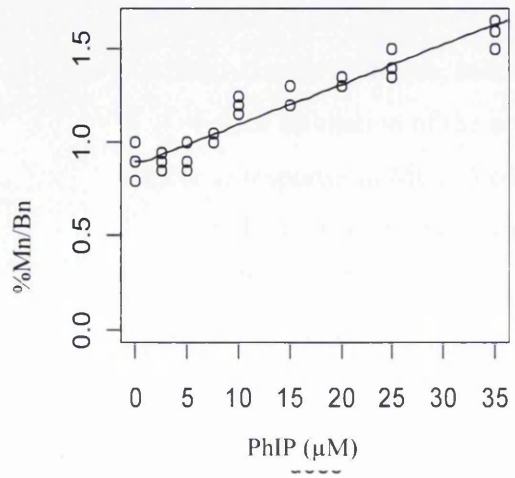

5.3.2 Cytotoxicity and genotoxicity of PhIP after 4h treatment

As 24h exposures to PhIP caused significant cytotoxic and genotoxic effects, a shorter exposure to PhIP was performed. MCL-5 and HepG2 cell were treated with PhIP for 4h using a dose range of 2.5-120μM for cytotoxicity and genotoxicity. The average results of cytotoxicity and genotoxicity are shown in Table 5.3. The table shows the dose of PhIP, the average percentage of relative population doubling (%RPD) and the average percentage of binucleated cells that contained micronuclei (%Mn/Bn) for both cell lines. Individual results are discussed below for both cell lines.

Table 5.3 A summary table showing the average results of cytotoxicity (%RPD) and average percentage of binucleated cells contain micronuclei (%Mn/Bn) with 4h 2-Amino-1-methyl-6-phenylimidazo(4,5-b)pyridine treatment in MCL-5 and HepG2 cell lines.

PhIP dose (μM)	MCL-5		HepG2	
	%RPD	%Mn/Bn	%RPD	%Mn/Bn
0	100	1.48	100	0.97
2.5	101.42	1.45	101.09	0.65
5	109.2	1.40	90.58	0.78
7.5	111.16	1.43	89.39	0.93
10	108.15	1.37	79.52	1.10
25	122.54	1.25	83.39	1.15
50	95.16	1.53	80.30	1.35***
100	67.68	1.75	50.49	1.48***
120	43.56	2.72***	34.17	1.87***

*** Indicates a statistically significant difference compared to control ($p<0.001$)

5.3.2.1 MCL-5 cells

MCL-5 cells showed no significant change in cytotoxicity until the dose of 50μM was reached when cytotoxicity values dropped from 101.42% to 95.16%. A nonlinear increase in micronucleus induction was observed in MCL-5 cells across the dose range of PhIP. The frequency of micronuclei non-significantly reduced from 0μM to 25μM (as seen in the 24hr data, Table 5.2), but then increased at higher doses (50-120μM) to a statistically significant 2.72% at 120μM ($p<0.001$) (Figure 5.5, Raw data in Appendix VI, Table A. 19). The dose range 140-180μM was toxic for MCL-5 cells therefore, not included in genotoxicity testing.

The result of the Hockey stick model for estimation of the dose-response relationship revealed that PhIP exhibited a non-linear dose response in MCL-5 cells after 4hrs exposure and thus a threshold dose exists for PhIP induced chromosome breakage in these cells (Figure 5.6). The estimated threshold dose (IP) was 97.71μM. The lower limit of 90% confidence interval (CI)

is 92.55μM (indicated by broken line) at $p<0.001$. It should be noted that estimated threshold was 23.69μM at 24h exposure time.

Figure 5.5 Relative population doubling (%RPD) and average percentage of binucleated cells that contain micronuclei (%MnBn) in 2-Amino-1-methyl-6-phenylimidazo(4,5-b)pyridine 4h treated MCL-5 cells. *Points*: mean of 3 replicates, *Bars*: standard error, *** Indicates a statistically significant difference compared to control ($p<0.001$)

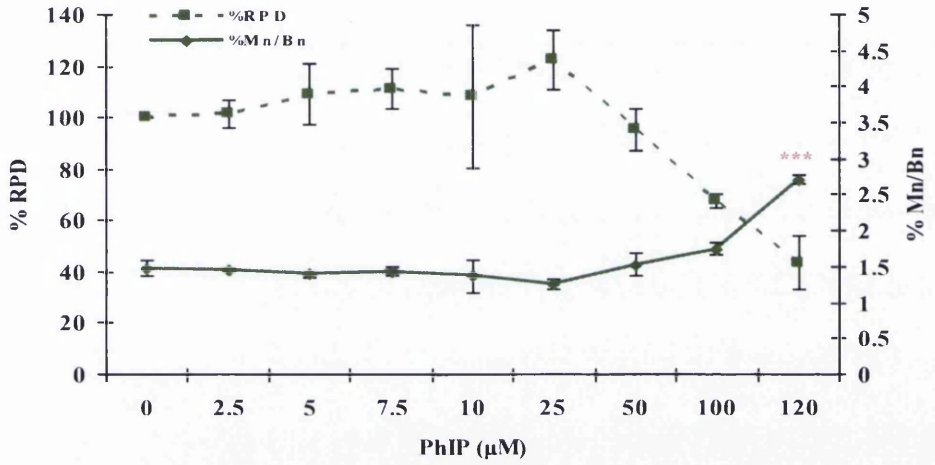

Figure 5.6 Graph generated by the Hockey stick threshold model using the Lutz approach for the analysis of dose-response relationship in MCL-5 cells treated with 2-Amino-1-methyl-6-phenylimidazo(4,5-b)pyridine for 4h.

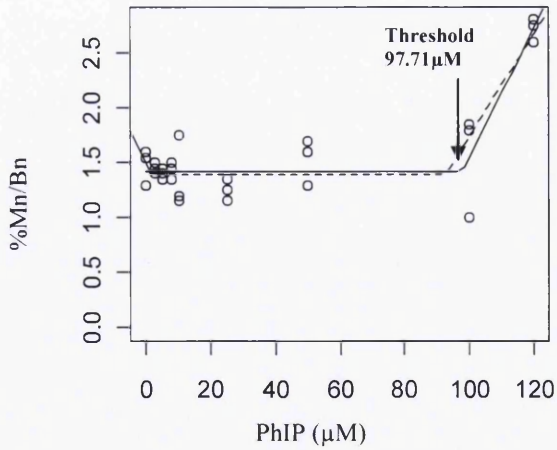

5.3.2.2 HepG2 cells

HepG2 cells showed increases in cytotoxicity across the dose range and 50.49% cytotoxicity was reached at the 100μM dose. At the higher dose 34.17% RPD was observed for 120μM (Table 5.3). A non-linear increase in genotoxic dose-response was observed in HepG2 cells across the dose range of PhIP. A reduction in %Mn/Bn frequency compared to untreated control was observed at lower doses until 7.5μM which had a Mn frequency of 0.93%. The

frequency of Mn/Bn cells was significantly increased at 50μM to 1.35%, reaching 1.87% ($p<0.001$) at 120μM (Figure 5.7, Raw data in Appendix VI, Table A. 20).

The result of the Hockey stick model for estimation of the dose-response relationship after 4hrs exposure to PhIP, favoured a linear model and rejected a threshold model despite showing a non-linear dose curve in HepG2 cells (Figure 5.8) which is similar to the 24h data. The PhIP dose 120μM was not included for the estimation of the dose-response relationship as %PRD value was dropped to 34.17% (66% toxicity).

Figure 5.7 Relative population doubling (%RPD) and average percentage of binucleated cells that contain micronuclei (%MnBn) in 2-Amino-1-methyl-6-phenylimidazo(4,5-b)pyridine 4h treated HepG2 cells. *Points*: mean of 3 replicates, *Bars*: standard error, *** Indicates a statistically significant difference compared to control ($p<0.001$).

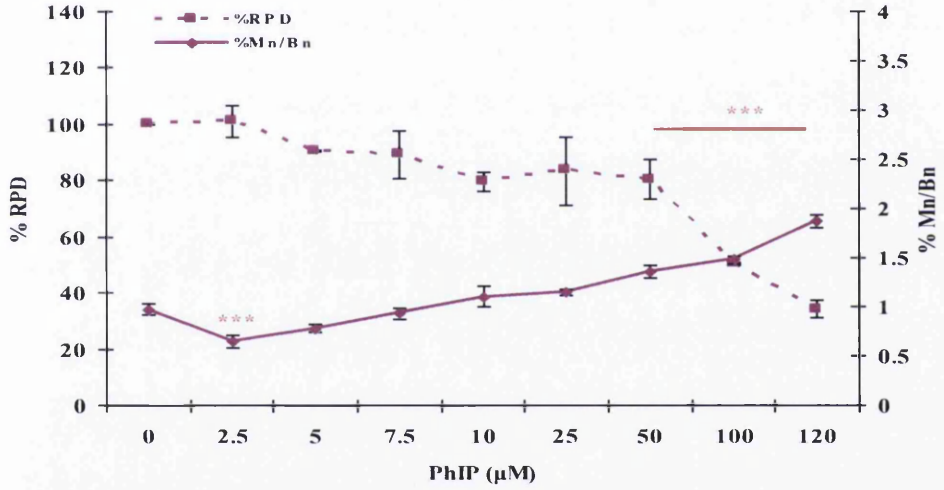

Figure 5.8 Graph generated by the Hockey stick threshold model using the Lutz approach for the analysis of dose-response relationship in HepG2 cells treated with 2-Amino-1-methyl-6-phenylimidazo(4,5-b)pyridine for 4h.

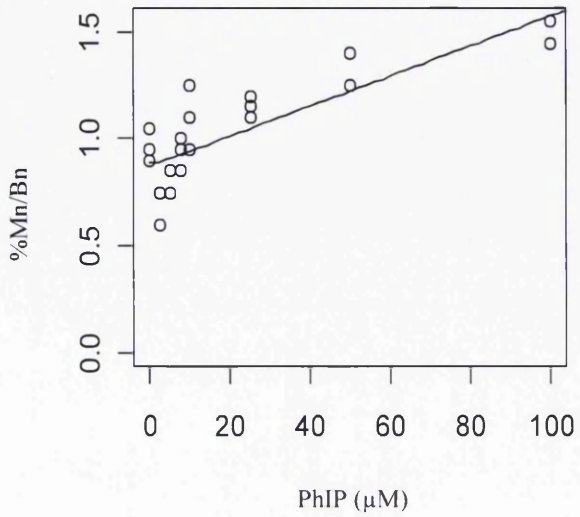

5.3.3 Basal and Induced expression of CYP1A1 and 1A2 enzymes

Expressions of CYP1A1 and 1A2 enzymes in MCL-5 and HepG2 cells were determined by RT-PCR. The intensity of each band was measured by intensitometry method using Chemidot software (Appendix VII, Figure A. 8) and further confirmed by Real-time PCR. There was a difference in basal and induced expressions of CYP1A1 and 1A2 for both cell lines at different doses. The CYP1A1 induction expression was significantly ($p<0.001$) higher in HepG2 cell line as compared to MCL-5 (Figure 5.9 A). Similarly CYP1A2 induction expression was 2.8-fold and 8.3-fold ($p<0.01$) in MCL-5 and HepG2 cell lines respectively (Figure 5.9 B).

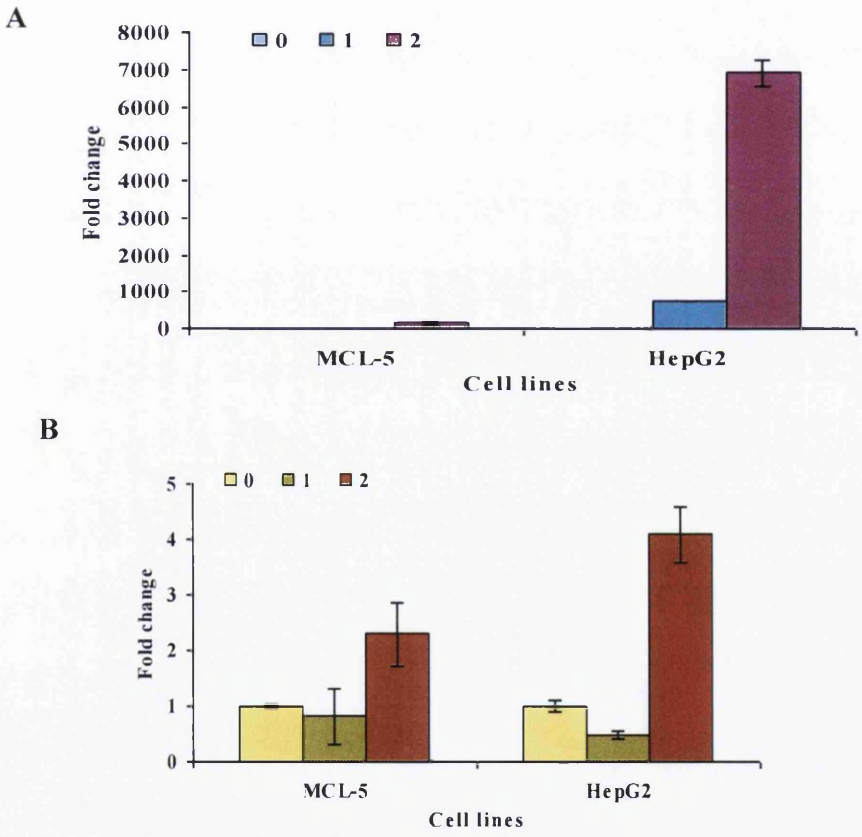

Figure 5.9 Fold change in (A) CYP 1A1 and (B) CYP1A2 expressions vs. β-actin after 24h PhIP exposure in (0) Untreated control, MCL-5, (1) 35μM, (2) 50μM and HepG2, (1) 10μM, (2) 15μM

5.4 Discussion

2-amino-1-methyl-6-phenylimidazo(4,5-b)pyridine (PhIP) is a mutagenic substance formed during the high temperature cooking of meat, fish, poultry and cigarette smoke (Wakabayashi *et al*, 1992; Sugimura *et al*, 2004; Hecht, 2002). Recently it has been found to be the most abundant carcinogen consumed by human populations (Snyderwine *et al*, 2003; Layton *et al*, 1995). Initially it was described as a rodent carcinogen (Ito *et al*, 1991). However, its presence in well-done cooked meat and cigarette smoke make it an environmental risk factor for development of diet associated cancer in humans such as breast, prostate and colon (Manabe *et a*l, 1991; Sinha *et al*, 2000). In this context, Zhu and co-workers studied the genotoxic effect of PhIP in humans and they found PhIP-specific DNA adducts in the mammary gland samples of women aged from 25-50 years (Zhu *et a*l, 2003).

After human exposure, PhIP undergoes metabolic transformation to become carcinogenic. This process requires CYP 450 enzymes, which effectively cause *N*-oxidation of PhIP; an essential step in the bioactivation of PhIP. The *N*2-hydroxy metabolite is further metabolised by conjugation through acetylation or sulfonation to form electrophilic intermediates which are capable of covalently binding to DNA and exerting genotoxic effects (Minchin *et al*, 1992; Zhao *et al*, 1994; Chou *et al*, 1995; Turesky, 2007). *In vitro* studies by Croft (1998) have shown that CYP1A2 has been most closely associated with PhIP metabolism into the N^2-hydroxy PhIP intermediate than CYP1A1 and CYP1B1 (Croft *et al*, 1998). Differences in the expression of CYP 450 enzymes may play an important role in the differential metabolic activation of PhIP and formation of carcinogenic metabolites and thus overall genotoxicity exerted.

In the present study, cytotoxic and genotoxic effects of PhIP were examined in the metabolically competent human cell lines MCL-5 and HepG2, in order to compare their sensitivity to PhIP at low doses. MCL-5 cells are a human lymphoblastoid line that constitutively expresses high level of CYP1A1 and also have been transfected with other human CYP enzymes including CYP1A2, 2A6, 3A4, 2E1 and epoxide hydrolase (Crespi *et al*, 1991; Schut and Snyderwine, 2004). HepG2 cells are a useful model human hepatoma cell line and express many functional Phase I and Phase II CYP450 metabolizing enzymes (Hewitt and Hewitt, 2004; Knasmüller *et al*, 1999, 2004; Majer *et al*, 2004). Recently it has been shown that HepG2 cells possess glutathione-S-transferase (GST) and N-acetyltransferase 1(NAT1) activity and NAT 2 is lacking; sulfotransferase isozymes SULT1A1 and SULT1A3 were found active but CYP1A2 and CYP2E1 were not detectable (Majer *et al*, 2004), the glucuronosyltransferase (UGT 1) activity was detectable and that of UGT 2 was below the

detection limit (Uhl *et al*, 2003a). Although CYP1A2 is important for the bioactivation of aromatic amines and despite its absence in HepG2 cells, such compounds were able to induce genotoxic effects due to the presence of CYP1A1 (Knasmüller *et al*, 1999). Westerink and Schoonen (2007) showed that HepG2 cells have low levels of cytochromes (CYPs) 1A1 and 1A2 but normal levels of Phase II enzymes with the exception of UDP-glucuronosyl transferases.

5.4.1 Cytotoxic effect of PhIP

The results of this study have shown that PhIP has a potential to induce a dose–dependent cytotoxic effect in both cell lines after 24h and 4h exposure (decrease in % RPD value) (Table 5.2 and 5.3). MCL-5 cells showed less sensitivity to PhIP as compared to HepG2 cells in terms of cytotoxicity which is in line with the expression of CYP1A1 and CYP1A2 (Figure 5.9). For example, at 50μM PhIP produced 46% cytotoxicity in MCL-5 while HepG2 cells showed more cytotoxicity, i.e. 82.07%. Again in HepG2 cells cytotoxicity was higher (-116.81%) in comparison with MCL-5 cells 70% cytotoxicity after 24h exposure at 100μM (Table 5.2, Figure 5.1 and Figure 5.3). Similarly after 4h exposure to PhIP at the 120μM dose MCL-5 and HepG2 cells showed 56% and 66% cytotoxicity respectively (Table 5.3, Figure 5.5 and Figure 5.7). In the HepG2 cell line the dose-dependent increase in cytotoxicity was observed earlier (5μM) as compared to MCL-5 cells (50μM). Therefore, HepG2 cells showed more cytotoxicity and genotoxicity to PhIP due to the presence and expression of a greater number of Phase I and Phase II CYP enzymes that bioactivate PhIP. In the case of CYP1A1, MCL-5 expressed less CYP1A1 as compared to HepG2 cells. Similarly, HepG2 cells induced more CY1A2 after PhIP exposure. There was no difference in CYP1A1 and CY1A2 basal expressions in both cell lines (Figure 5.9).

5.4.2 Genotoxic effect of PhIP

The comparative study results have shown that at both 24h and 4h exposure times, PhIP has the potential to induce genotoxic effects in both cell lines with HepG2 exhibiting higher micronucleus frequency than MCL-5. The increased sensitivity to PhIP in HepG2 cells reflect the differences in bioactivation capacities within the cell lines or function of PhIP used. In MCL-5 cells it was observed that the micronucleus induction was not statistically significant from the control at lower doses (2.5μM to 25μM). The HepG2 cell line showed more micronuclei induction as compared to the MCL-5 cell line after PhIP exposure (Table 5.2 and 5.3). For instance, micronucleus frequency in MCL-5 cells was seen to increase by 1.56-fold

as compared to the control after 24h exposure to 50μM of PhIP, while it increased by 1.9-fold in HepG2 cells at the same dose, therefore, HepG2 cells produced 0.34-fold more binucleated cells containing micronuclei (Mn/Bn) as compared to MCL-5 cells (Table 5.2, Figure 5.1 and Figure 5.3). The highest dose of PhIP used in the CBMN assay, (100μM) was too toxic for the analysis of binucleated cells in the HepG2 cell line population due to the high number of necrotic cells (Table 5.2, Figure 5.3). Similarly, after 4h exposure of PhIP a higher level of genotoxicity was observed in HepG2 cells in comparison to MCL-5 cells. For example, at 120μM PhIP the micronucleus frequencies were 1.83-fold and 1.92-fold observed in MCL-5 and HepG2 cells, respectively when compared to control micronuclei frequency (Table 5.3 Figure 5.5 and Figure 5.7). Indeed, micronucleus induction was 0.09-fold more in the HepG2 cell line than MCL-5 cells. Even at non-toxic doses such as 25μM, the micronucleus frequency was 0.34-fold more in HepG2 cell line as compared to MCL-5 cell line.

The experiments are in agreement with other studies examining the effects of PhIP. *In vitro* studies have shown that a 2-fold increase in micronulei induction was observed at 35.7μM in the HepG2 cell line (Majer *et al*, 2004) and a 25-50μM concentration range was the lowest effective micronuclei inducing dose reported by Knasmuller *et al*, (1999). Pfau (1999) used a 100μM dose to produce micronuclei in the MCL-5 cell line. A positive dose response was observed in Chinese hamster lung male V79 cells in a dose range from 50 to 900μM (Perez *et al*, 2002). In *in vivo* experiment with Male Balb/c mice, there was a significant dose-response relationship observed in the induction of MN in erythrocytes up to 36 mg/kg body weight (Durling and Abramsson-Zetterberg, 2005).

5.4.3 Difference in CYP 1A1 and 1A2 expressions

The differences observed in micronucleus induction are due to the differential metabolic capabilities of both cell lines. The expression of Phase II enzyme such as N-acetyltransferases (NATs) is known to be involved in the metabolism of PhIP (Turesky and Marchand, 2011) and converts it to its ester intermediate that is capable of binding with DNA and causing a genotoxic effect. The expression of CYP1A1 in MCL-5 was lower in comparison to HepG2 cell line and there was no change in expression observed after 24h PhIP treatment. Similarly no difference in basal and induced CYP1A2 expression was noticed in MCL-5; however, in HepG2 cell line the induced expression was more as compared to basal (Figure 5.9). It showed that in MCL-5 other enzyme system unrelated to CYP1A2 may be responsible for PhIP metabolism. The high induction of micronuclei in HepG2 cells is likely to be due to the Phase II enzyme *N*-acetyltransferase (NATs). This assumption is in agreement with a previous

study by Otsuka (1996) with human and Chinese Hamster cells in which the micronuclei induction was increased when Chinese Hamster lung (CHL) cells were transfected with *N*-acetyl-transferase gene (Otsuka, *et al*, 1996).

5.4.4 Dose- response to PhIP

It is important to obtain the knowledge of a chemical's dose-response relationship, because if a threshold dose exists then there is a non-linear dose response and safe levels of exposure can be calculated. If the dose-response is linear then there is perhaps no safe exposure level. From the data described here, in MCL-5 cells the dose-response relationship of PhIP was non-linear and a threshold dose was calculated after both 24h and 4h exposure times (Figure 5.2 and Figure 5.6). The estimated threshold doses of PhIP for MCL-5 cells were 23.69μM and 97.7uM at 24h and 4h, respectively. This represents a 4 fold increase in estimated threshold doses at 4h exposure when compared to 24h PhIP exposure. (Figure 5.2 and Figure 5.6), using Hockey stick statistical modelling. In MCL-5 PhIP doses below 15μM at 24h and 50μM at 4h exposures also showed a significant reduction in the micronucleus frequencies compared to control levels and the dose-response resembles to some extent a J-shaped curve. This type of dose-response curve is indicative of a phenomenon termed hormesis, where the lower doses have the opposite effect to higher doses (Davis and Svendsgaard, 1990). At such lower doses, when DNA damage was induced the DNA defence processes were stimulated either for repairing the DNA damage or for removal of the damaged cells through apoptosis (Kinoshita *et al*, 2006). Indeed before threshold doses (23.69μM and 97.7μM) there was no statistically significant micronucleus induction observed in comparison to control and PhIP failed to induce any toxicity (Figure 5.2 and Figure 5.5) in the MCL-5 cells after 24h and 4h exposure. At low doses PhIP may have initiated different cellular responses in human lymphoblastoid MCL-5 cells and at high doses it induced DNA damage and influence cell signalling processes involved in the cell proliferation. (Gooderham *et al,* 2007).

The results with HepG2 cells with regards to their genotoxic dose-response relationship showed that PhIP exhibited a linear dose-response after 24h and 4h exposure and no threshold dose was determined (Figure 5.4 and Figure 5.6) using hockey stick statistical modelling. Therefore, no safe exposure level for HepG2 at both time exposures was observed. Statistically significant increases in micronucleus frequencies were observed at 10μM ($p>0.05$) and 50μM ($p>0.001$) doses of PhIP at both 24h and 4h, respectively (Figure 5.3 and Figure 5.7). As the HepG2 cells are primary liver cells they are considered to be very

sensitive towards PhIP and considered a valuable *in vitro* model to identify compounds that are potentially toxic to humans.

Turteltaub (1999) observed that oxidative metabolism of PhIP is different in humans and rodents. Both activate and detoxify PhIP whereas humans predominantly convert PhIP to its reactive genotoxic metabolites. PhIP metabolism in rodents involves predominantly oxidation in the ring system followed by conjugation, however, in humans *N*2-hydroxylation to the proximate mutagen *N*2-hydroxy- PhIP is the major metabolic pathway for PhIP followed by glucuronidation (Turteltaub *et al*, 1999). Due to these differences between rodents and humans, it is difficult to extrapolate results from animal to determine health risks to humans.

This study shows that PhIP dose response are highly dependent on exposure time and metabolic competency, therefore, it represents relatively higher risks for individuals with higher metabolic activity and greater exposure to PhIP. Furthermore, a prolonged exposure to low doses of PhIP has the potential to cause DNA damage and act as a tumour initiator.

Chapter 6

Investigation of Point Mutations Induced by 2-Amino-1-methyl-6-phenylimidazo(4, 5-b)pyridine in Human Cell Lines

6.1 Introduction

Induction of DNA adducts and mutations following PhIP exposure have been widely reported in a wide range of exposed tissues and organs such as colon, liver, lung, pancreas, stomach, prostate, and breast (Dingley, 1999; Zheng and Lee, 2009; Shirai *et al*, 1997). PhIP induced DNA adducts have also been reported in organs and sites where tumour formation usually does not occur, such as kidney. The most frequent cause of PhIP exposure in humans is through the consumption of cooked meat. For example, a "well-done" cooked chicken contains a very small dose of PhIP which is capable of inducing DNA adducts in colon and blood cells. However, these adducts are unstable and decline over a 24 hour period (Dingly 1999). A gas chromatography / mass spectrometry (GC/MS) assay was used to analyse 100μg of DNA of colorectal mucosae from a number of individuals and long-lived lymphocytes of colorectal cancer, this study detected several dG-C8-PhIP adducts per 10^8 DNA bases (Friesen *et al*, 1994; Magagnotti *et al*, 2003). Turesky (2007) reported dG-C8-PhIP DNA adduct formation in about 30% of the human population with levels of adduct varying up to 10 fold between lowest to highest levels. These findings suggest that either quantity of PhIP consumption or differences among individuals in their ability to activate PhIP is involved in adduct formation. However, dG-C8-PhIP adduct levels were not observed at significantly higher levels in smokers or heavy consumers of meat than in individuals who ate meat less frequently (<5 servings per week); yet, the individual extent of exposure to PhIP was not known.

Gorlewska-Roberts (2002) used the ^{32}P-postlabeling method and detected a mean value of 4.7 dG-C8-PhIP adducts/10^7 nucleotides in the exfoliated epithelial cells from 30 milk samples of lactating mothers. Similarly dG-C8-PhIP adduct was identified by an immunohistochemical method from the section of human breast tissues at levels of >1 adduct per 10^7 bases (Zhu *et al*, 2003).

Glaab (2000) reported mutations in cell lines defective of mismatch repair (MMR) following an exposure to 10 μM PhIP using the HPRT assay. Most mutations induced contained G:C to T:A transversion mutations, which is consistent with the pro-mutagenic adduct of PhIP at the C8 position of guanine miscoding with adenine. This study also showed a hotspot for mutation in a run of six guanines in *HPRT* exon 3, where a total of 23 (27%) of all PhIP-induced mutations occurred. These mutations consisted of transversions, transitions, and frameshift mutations. Similarly, Yadollahi-Farsani and his team (2002) identified PhIP-induced mutations involving G:C base pairs in a Chinese hamster cell line (XE Mh1A2-MZ) at the *HPRT* locus (Figure 6.1). The mutations were predominantly GC→TA transversions but a -1G frameshift in a 5'-GGGA sequence was also observed. Exon 3 was reported as the hot spot for mutations.

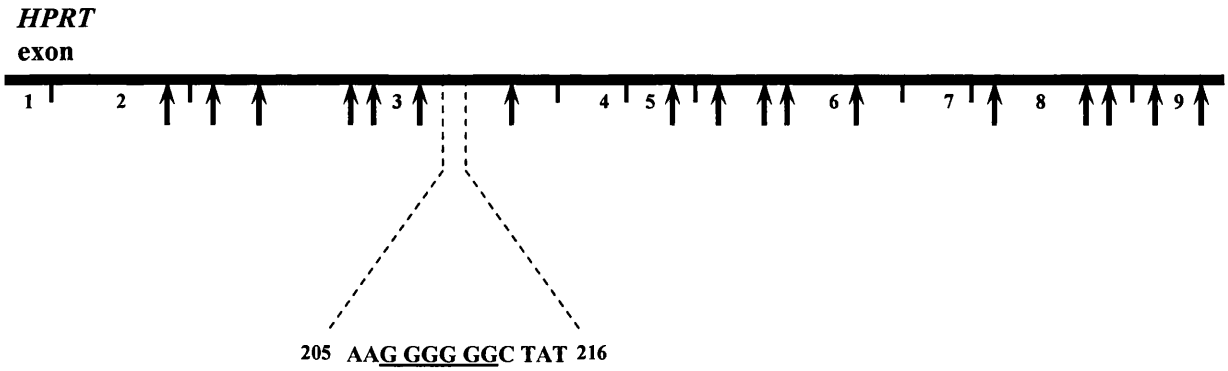

Figure 6.1 Locations of PhIP induced mutations in the coding region of Chinese hamster *HPRT* gene. Arrowheads show mutations. Modified from Yadollahi-Farsani *et al*, (2002).

PhIP was also found to be mutagenic in a mammalian assay using repair-deficient CHO cells versus *Salmonella*, and in *in vivo Dlb-1* locus mutation assay in the mouse small intestine (Thompsom *et al*, 1987; Brooks *et al*, 1994). Carothers and co-workers (1994) found PhIP induced mutations in the dihydrofolate reductase (DHFR) gene of Chinese hamster ovary cell line (UA21) and found 75% GC→TA transversions along with deletion of entire locus and -1 frameshift mutations. These induced mutations targeted the guanine on the non-transcribed stand of the gene in all of the mutants sequenced and confirm the presence of the dG-C8-PhIP adduct in DNA (Carothers *et a*l, 1994). The *cII* gene in the colon of male rats and mice was reported to have highest mutation frequencies induced by PhIP consisting of G:C to A:T transitions, G:C to T:A transversions and –G frameshifts in runs of guanine bases around the nucleotide 179 –(G:C) (Stuart *et al*, 2000). Transversion mutations occurred more frequently at the human *HPRT* gene, where PhIP forms adducts with dG (dG-C8-PhIP) which can mis-

base pair with adenine. Similarly A-G frameshift mutation in the 5/-GGGA-3/ sequence is a frequent signature mutation of PhIP in the *HPRT* gene as well as the *APC* tumour suppressor gene (Yadollahi-Farsani *et al*, 1996). One of the hotspots of PhIP induced GC base pair deletion in 5'-GTGGGA-3' around codon 653 in the rat is conserved in the human *Apc* gene and represent a signature mutation of PhIP in human colon cancer (Nagao et al, 1997) PhIP showed a dose–dependent increase in the mutations at the *hprt* locus in modified Chinese hamster (V79) cells (XEMh1A2) (Wolfel *et a*l, 1992), with a high percentage of G to T transversions along with significant number of -1G:C base pair deletions. Most of these guanine-based mutations occurred on the non-transcribed strand (Yadollahi-Farsani *et a*l, 1996). Similar mutations were identified *in vivo* in the *lacZ* transgene of the Mutamouse® when 20mg/kg per day PhIP was administered orally for 4 days (Lynch et al, 1998) and in the *lacI* transgene isolated from the colon of Big Blue® mice (Okonogi *et a*l, 1997; Stuart *et al*, 2000).

PhIP requires metabolic activation to form DNA adducts. CYP enzyme's activity is central to metabolic activation and MCL-5 expresses this activity. Activated PhIP causes adduct formation and induced mutations which are mainly at Guanine base pair. Previous studies have shown correlation between mutations and DNA adduct formation, however, most of these studies were conducted at higher doses of PhIP. This study uses MCL-5 cell line to determine the effect of lower doses on DNA adducts formation and mutations.

6.1.1 Aims of the study

The aim of this study was to determine the mutagenicity of low doses of PhIP at 24h exposure time in MCL-5 cell lines. A gene mutation study was carried out using the *in vitro* HPRT assay. The second part of the study focused on the construction of PhIP-induced mutation spectra for the MCL-5 cell line to determine the type and position of mutations caused by lower dose of PhIP.

6.2 Materials and Methods

6.2.1 Cell line used and their maintenance

Only MCL-5 cell line was selected to study the *in vitro* effect of 24h PhIP exposure at the genetic level after metabolic activation. The HepG2 cells are adherent cells and they did not grow in the form of colonies. In HPRT assay the live colonies are counted to calculate the MF.

Cell culture was performed as described in Chapter 2 Section 2.1.2.

6.2.2 Test chemical

2-Amino-1-methyl-6-phenylimidazo (4, 5-b) pyridine (PhIP) (Santa Cruz Biotechnology, Inc)

See Chapter 5 Section 5.2.3 for further details.

6.2.3 HPRT assay

Further details in Chapter 4 Section 4.2.3

6.2.4 Scoring of colonies

Further details in Chapter 4 Section 4.2.4

6.2.5 Statistical analysis

A one-way ANOVA followed by Dunnett's post-hoc test (2-tailed) was used to compare all treatments with control using IBM SPSS statistic software (version 19). Confidence limits of 95% ($p<0.05$), 99.9% ($p<0.01$) and 99.99% ($p<0.001$) were applied. The hockey stick modelling software, provided by Lutz and Lutz (2009) and implemented in the R package (software 2.9.1), was used to estimate a threshold dose.

The t-test was used to assess whether the means of two groups were statistically different from each other in untreated and solvent control. The Confidence limit of 95% ($p<0.05$) was applied.

6.2.6 Clonal expansions of mutants

Untreated control, solvent control and 25μM PhIP treated HPRT mutant colonies were transferred to 24well plates containing 2ml growth media per well and grown for 5 days at 37°C, 5% CO_2, after which cells were carefully mixed with 1.5 ml RNA protect (Sigma) and stored at -20°C for RNA extraction.

6.2.7 RNA extraction

For a detailed description of RNA extraction methodology see Chapter 2 Section 2.6.

6.2.8 Complementary DNA (cDNA) synthesis from HPRT mRNA

For a detailed description of methodology see Chapter 2 Section 2.6.3.

6.2.9 End-point PCR

A detailed description of methodology and primers used in present study was given in Chapter 2 Section 2.6.4.

6.2.10 % PAGE gel and Silver nitrate staining

Detailed procedures of gel preparation, gel loading, and silver nitrate staining were given in Chapter 2 Section 2.7.1 and 2.7.2.

6.2.11 Preparation of samples for sequencing

For detailed methodology see Chapter 2 Section 2.8. Samples were sent to Genome Enterprise Limited (Norwich, UK) for sequencing.

6.2.12 Construction of mutation spectra

Mutation spectra was constructed using iMARS software, kindly provide by Dr Paul Lewis at Swansea University (Morgan and Lewis, 2006).

6.3 Results

6.3.1 PhIP mutation dose–response using the HPRT assay

The HPRT assay was performed with MCL-5 cells to study the low dose effect of PhIP at the base-pair level after 24h exposure to PhIP. Earlier studies showed similar metabolic activity and response to PhIP for HepG2 and MCL-5. Secondly, HepG2 are adherent cells thus making it difficult to conduct the HPRT assay. In contrast, the MCL-5 cell line is easy to handle and provides a reproducible human system and therefore, only MCL-5 cells were used to study PhIP-induced damage at DNA level.

The 24h exposure dose range of PhIP used for this study in MCL-5 cells (0-50μM) was the same used to calculate the %Mn/Bn frequency in a previous chapter (Chapter 5 Section 5.4.1). The dose range chosen here was 0-50μM selected as the first significant genotoxic effect was observed at 35μM.

6.3.1.1 Mutation frequency of PhIP after 24h exposure in MCL-5 cells

In the HPRT assay the plating efficiency (PE) of treated cultures was used to measure the toxicity. Toxicity studies were based on colony forming ability of cells when inoculated into a 96 well plate without 6-thioguanine (non-selective conditions). The PhIP exposed and untreated control colonies grown in non-selective conditions and selective conditions were counted to access the mutant frequency (MF). In selective conditions, MF ($MFx10^{-5}$) is the frequency of the HPRT mutants in a population of cells. PE plates were grown alongside MF plates to assess mutant frequency.

DMSO was used to dissolve the PhIP, therefore, it was used as an solvent control. It was observed that the MF of the solvent control was not statistically different from the untreated control by using t-test statistical analysis (Table 6.1, Raw data in Appendix VIII, Table A. 21). It showed that DMSO is non-mutagenic and as such can be used to represent the spontaneous HPRT MF in MCL-5 cell line.

Table 6.1 Mutation frequency $x10^{-5}$ and % cell viability in control and solvent control in the MCL-5 cell line.

Cell line	PhIP (μM)	$MFx10^{-5}$	St. error	t test	% Cell viability	St. error	t test
MCL-5	Untreated control	2.08	0.65		100	0.00	
	Solvent control (0)	1.99	0.43	0.89	101.09	1.47	0.499

The MCL-5 cell line was treated with PhIP for 24h exposure using a dose range of 2.5- 50μM. OECD guidelines (1997) recommend using a maximum of 10,000μM for HPRT experiment thus our doses were within the recommended range. The average % cell viability and MF ($x10^{-5}$) from the triplicates in response to different doses of PhIP is shown in Table 6.2 and Fig 6.2 and the data are discussed below.

Table 6.2 A summary table showing the average results of % cell viability and average mutation frequency ($MFx10^{-5}$) with 24h 2-Amino-1-methyl-6-phenylimidazo (4, 5-b)pyridine treatment in MCL-5 cells.

PhIP (μM)	MCL-5	
	%Cell viability	MF ($x10^{-5}$)
0	101.09	1.99
2.5	105.34	1.88
5	107.90	1.82
7.5	102.26	2.11
10	92.40	3.89***
20	95.88	4.83***
25	91.18	5.23***
35	85.51	6.95***
50	77.38	9.98***

*** Indicates a statistically significant difference compared to control ($p<0.001$).

When dosed with PhIP for 24h, the % cell viability of MCL-5 cells did not vary significantly with that of the solvent control (0) except the highest dose (50μM) (Table 6.2 and Figure 6.2). MCL-5 cells showed non-significant decreases in MF at lower doses as compared to the control, for example in the control the MF was $1.99x10^{-5}$ and this decreased to $1.88x10^{-5}$ and $1.82x10^{-5}$ at 2.5μM and 5μM PhIP, respectively. A statistically significant increase in MF was observed from 10μM which was $3.89x10^{-5}$ ($p<0.001$) and all the doses above ($p<0.001$) using Dunnett test (2-tailed). There were 1.95, 2.42, 2.62, 3.49 and 5.0 fold increases found over the spontaneous frequency at 10μM, 20μM, 25μM, 35μM and 50μM PhIP, respectively (Table 6.2 and Figure 6.2, Raw data in Appendix VIII, Table A. 22).

The result of the Hockey stick model for estimation of the dose-response relationship revealed that PhIP exhibited a non-linear dose response in MCL-5 cells after 24h exposure and thus a threshold dose exists for PhIP induced DNA damage in these cells (Figure 6.3). The estimated threshold dose (IP) was 4.02μM. The lower limit of 90% confidence interval (CI) was 0.5μM (indicated by broken line) at $p<0.05$.

Figure 6.2 Average mutation frequency (MF $x10^{-5}$) and average % cell viability in MCL-5 cells after exposure to different doses of 2-Amino-1-methyl-6-phenylimidazo (4, 5-b) pyridine for 24h. *Points*: mean of 3 replicates, *Error Bars*: standard error, *** Indicates a statistically significant difference of MF compared to control ($p<0.001$).

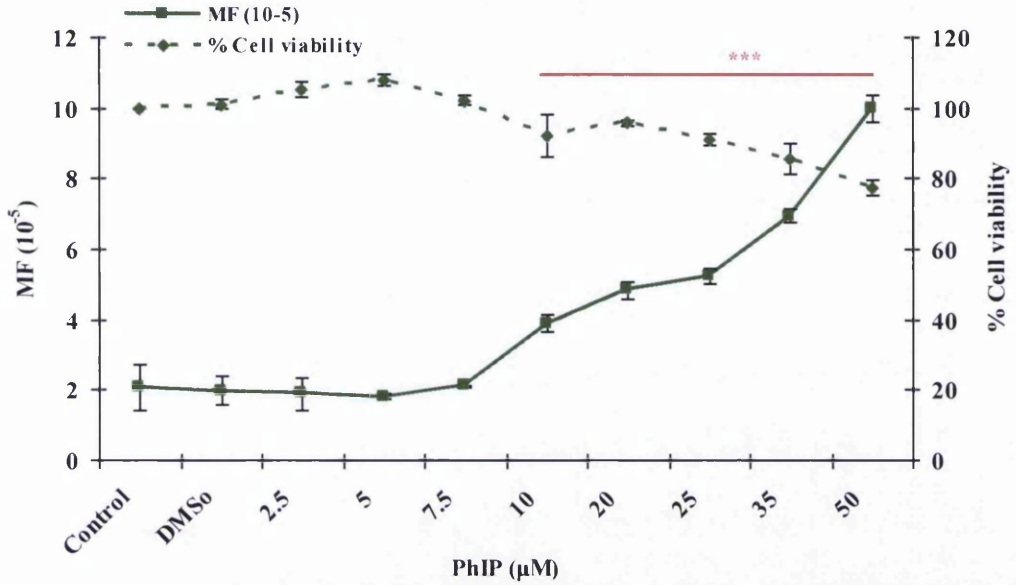

Figure 6.3 Graph generated by the Hockey stick threshold model using the Lutz approach for the analysis of dose-response relationship in MCL-5 cells after 24h exposure to 2-Amino-1-methyl-6-phenylimidazo (4, 5-b)pyridine.

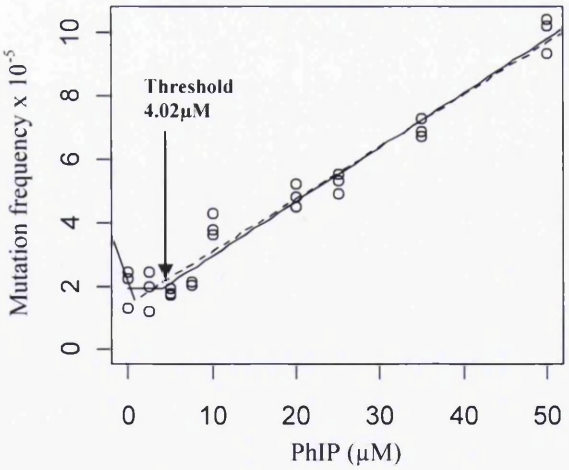

6.3.2 Sequence analysis of HPRT mutants

A mutation spectrum was constructed to investigate the type and location of mutations induced by PhIP in MCL-5 mutants. The mutants exposed to 25µM PhIP for 24h and mutants obtained from the solvent control were selected to further investigate PhIP-induced mutations and spontaneous mutations, respectively. These mutants were isolated and propagated at the end of the HPRT assay for sequence analysis. Mutations in the coding region were identified from the sequencing of cDNA of the *HPRT* gene products obtained by RT-PCR.

In the MCL-5 cell line 15 mutants were analysed for spontaneous mutations and 20 mutants were used for PhIP-induced mutations. The percentages of all the mutations resulting from PhIP exposure and solvent control in both cell lines are shown in Table 6.3.

Table 6.3 Mutation types and percentages of spontaneous and 2-Amino-1-methyl-6-phenylimidazo (4, 5-b)pyridine-induced mutations (25μM dose, 24h) at the *HPRT* locus in 15 solvent control and 20 treated MCL-5 mutants.

Type of Mutations	MCL-5 Solvent control	MCL-5 PhIP treated
Base substitutions	7	8
Transitions		
G → A		2 (25%)
T → C	3 (43%)	
Transversions		
C → A		
C → G	2 (29%)	
G → C	1(14%)	
G → T	1(14%)	6 (75%)
Tandem mutation	2 (17%)	
Deletion/Insertion		
Deletions	3 (25%)	11 (58%)
Insertions		

In the MCL-5 solvent control, 15 mutant colonies were processed and 12 mutations were observed from 12 colonies. In the remaining 3 mutant colonies a translocation of 25 bp (TCTTGATTGTGGAAGATATAATTGA) was observed at position 489 on the transcribed strand (See Appendix IX, Figure A. 9, A). At the *HPRT* locus 25% deletions, 58% point and 17% tandem mutations appeared spontaneously. Among the point mutations (See Appendix X, Figure A. 9, B) due to base substitutions, 43% transition and 57% transversion mutations were observed (Table 6.3). G375T (14%) and C653G (29%) transversion mutations and TG285/6AT (17%) tandem mutations each appeared twice; whereas G648C (14%) transversion and T370C (43%) transition appeared once and three times respectively. Deletions of 1 (n=1), and 13 (n=2) base pairs appeared as spontaneous mutations in MCL-5 mutants also (Table 6.3 and Table 6.4. See Appendix IX, Figure A.9, C).

Following treatment with 25μM PhIP for a 24h period, 19 different mutations were observed from 20 MCL-5 individual mutant colonies. The PhIP-induced mutations on the *HPRT* locus of MCL-5 were deletions (58%) and point mutations (42%). Point mutations (See Appendix IX, Figure A. 10, A) observed due to base substitutions, were represented by 25% transition and 75% transversions (Table 6.3). Transition mutations G376A (25%) appeared twice whereas G264T (75%) transversion was found six times in different mutant colonies. Deletions of 36 (n=3), 45 (n=2), 17 (n=3) and 29 (n=2) base pairs appeared at the HPRT locus as PhIP induced mutations in MCL-5 mutants (Table 6.3 and Table 6.4. See Appendix IX, Figure A. 10, B). One mutant colony showed a deletion of 58bp (GAAAGAATAGAAGTGATTGAATATTGTTAATTATACCACCGTGTGTTAGAAAAG TAAGA) from position 1182-1239 and translocated at position 776 on the mutant *HPRT* locus (See Appendix IX, Figure A. 10, C). The ratio of transitions to transversions was 3:4 for spontaneous- and 2:6 for PhIP-induced mutations. Among all the point mutations recorded, the proportion of G→T transversion mutations was higher in treated MCL-5 mutant colonies as compared to solvent control mutant colonies.

Table 6.4 Spontaneous and 2-Amino-1-methyl-6-phenylimidazo (4, 5-b)pyridine (PhIP) - induced mutational spectrum at the *HPRT* locus in MCL-5 cell line.

Treatments	Mutations		Sequence	Positions
Solvent control	Single bp substitutions			
	1	G → T	AAGGGGG	375
	3	T→ C	GCTCAA	370
	1	G → C	GTCGCAA	648
	2	C→ G	AAGCTTG	653
	Tandem mutation			
	2	T → A	TCATGGA	284
		G → T	TCATGGA	285
	Deletions			
	2	- 13 bp	AAT<>TCC	432 <> 445
	1	- 1 bp T	CTT <> GCT	604
PhIP treated	Single bp substitutions			
	6	G → T	TTGGAAA	264
	2	G → A	AGGGGGG	376
	Deletions			
	3	- 36 bp	TGG<>GGC	548<>584
	2	- 45 bp	TGG<>ATG	548<>593
	3	- 17 bp	AAG<>GAT	552<>569
	2	- 29 bp	TGG<>TGA	548<>577
	1	-438 bp	AAT<>CCA	776<>1239

6.3.2.1 Location of mutation spectra present on the *HPRT* gene sequence

The spectrum of spontaneous and point mutations along the *HPRT* mRNA sequence in MCL-5 cell line are presented in Figure 6.4. The sequence of mRNA used in the present study, is identical to the non-transcribed /anti-sense strand. Therefore the mutations identified in the mRNA indicate mutagenesis in the non-transcribed strand of the double helix which is the

transcription-associated mutagenesis. There was spontaneously occurring GC→AT transitions where T→C change in the non-transcribed strand found in spectrum. In the presence of PhIP all GC→AT transitions where G→T change in the non-transcribed strand. This is the indicative of the mode of action of the PhIP (Zhang *et al*, 2001) and is not the effect of transription-coupled repair as this strand biased was independent of transcriptional status (Palombo *et al*, 1991) A clear difference was seen in the distribution of mutations along the *HPRT* target sequence between the solvent control and PhIP-induced mutants in MCL-5. Spectra for spontaneous mutations showed mutations due to deletions and single base pair substitutions. The mutational spectra of 12 MCL-5 mutants from the solvent control showed deletions of a number of base pairs and other point mutations distributed at exon 2, 3, 4 and 6 (Figure 6.4 A). Base substitutions were observed more frequently than deletions for solvent control. Tandem mutations were found twice at exon 2. G→T base pair substitution appeared once and T→C appeared three times at exon 3. The base substitutions C→G and G→C occurred 2 times and one time respectively at exon 6. Among deletions, 13 base pair deletions were observed in two mutant colonies at exon 4 and one base (T) was deleted from one colony at exon 6 (Figure 6.4 A).

PhIP-induced mutation spectra in MCL-5 also showed mutations due to deletions and single base pair substitutions (Figure 6.4 B). The most dominant mutations were observed to be G→T transversions, present at exon 2 on the *HPRT* sequence. Other point mutations such as G→A transition appeared at exon 3. The deletions were distributed all over exon 5 of the *HPRT* sequence, but in one mutant, exon 7 and 12 were partially deleted and exons 8, 9, 10 and 11 were completely deleted due to the PhIP exposure (Figure 6.4 B). All mutation observed whether for solvent control or PhIP treated cells were observed on transcribed strand.

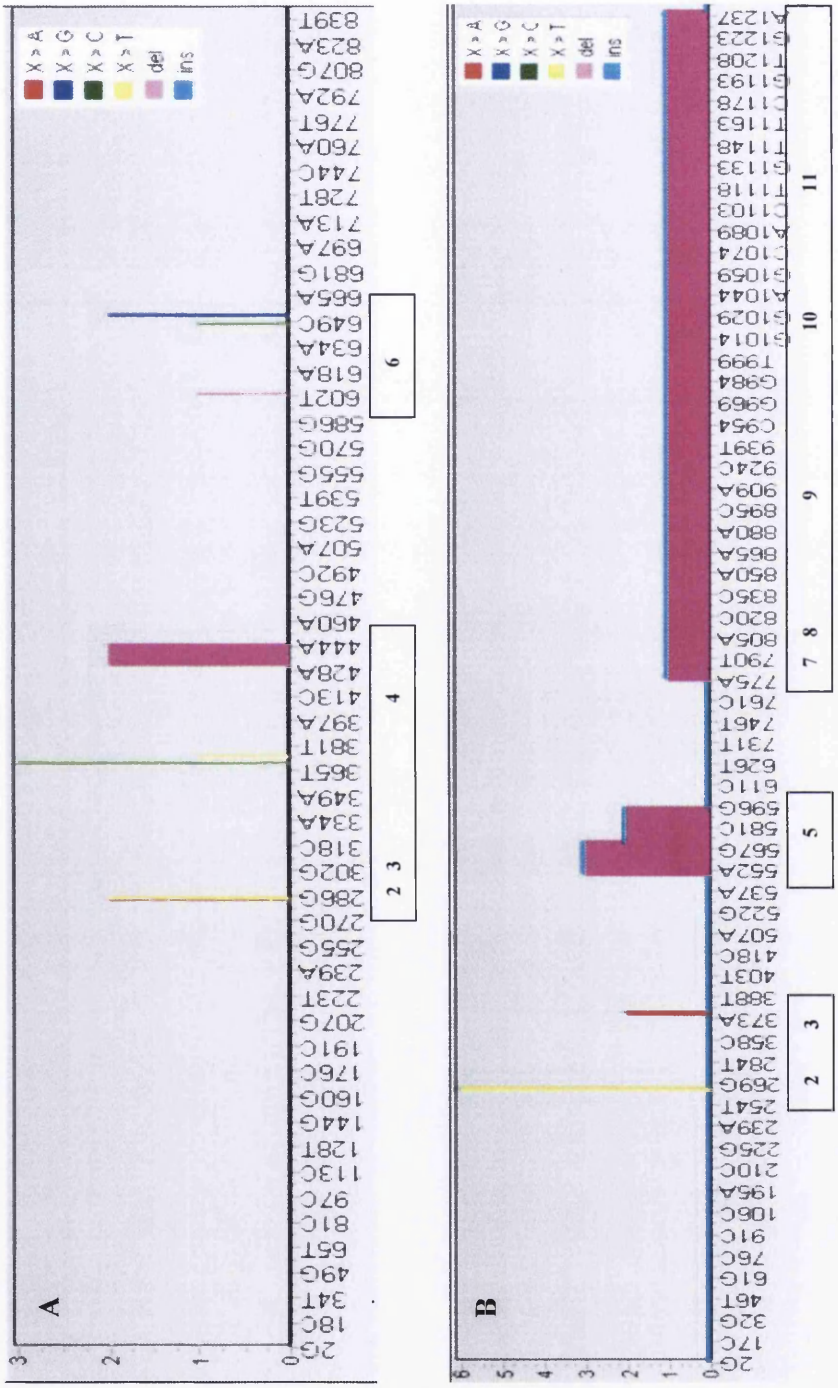

Figure 6.4 Mutation spectra (A) spontaneous and (B) 2-Amino-1-methyl-6-phenylimidazo (4, 5-b)pyridine (PhIP)-induced in the *HPRT* gene in MCL-5 mutants. Each base and its number on the HPRT sequence are presented on the *x-axis*. The number of mutations is portrayed on the *y- axis*. Each base alteration is colour coded where the letter X stands for the 4 bases; A, C, G or T determined by the position on the sequence. . Numbers in the rectangular boxes represent the hotspots on exons.

6.4 Discussion

Cooking food at high temperatures is responsible for the production of genotoxins that have adverse effect of human health. The consumption of red meat and human cancer are positively correlated (Sinha *et al*, 2005). Among many HAA, PhIP is extensively bioavailabile to humans in the form of cooked meat and 0.1-15μg PhIP per day has been consumed. PhIP is readily activated by CYP1A1 and 1A2 to produce DNA damage (Zhao *et al*, 1994). It is rodent carcinogens and in rats induces cancer of prostate, colon and mammary glands (Sugimura, 1997; Ito *et al*, 1991). This study was aimed at determining the ability of low doses of PhIP to induce gene mutations in the MCL-5 cell line using the HPRT assay. Our earlier studies showed that PhIP is capable of causing genotoxicity (significant increase in micronucleus frequency was observed at doses 35μM and above). This study focussed on understanding the effect of PhIP in inducing gene mutations at low doses as well as to compare the level and type of mutation induced by PhIP to those mutations that are observed spontaneously without PhIP. The MCL-5 cell line has a high expression of the CYP1A2 enzyme (Figure 5.10), and is capable of metabolizing PhIP in to its active form following 24h exposure, and therefore, serves as a good cell line to determine mutagenic activity of PhIP.

6.4.1 Genetic mutations induced by PhIP

Cell viability assays revealed that PhIP affected cell viability non-significantly at lower doses. Only highest test dose of 50μM caused significant reduction in cell viability after 24h. exposure. (Table 6.2, Figure 6.2). These results and studies reported in Chapter 5 indicate that lower doses of PhIP do not inhibit cell multiplication.

Results of mutation assays, however, showed higher sensitivity to PhIP as significant differences in mutation frequency were observed at a dose of 10μM. The results showed that at PhIP doses of 2.5μM, 5μM, and 7.5μM ($1.88x10^{-5}$, $1.82x10^{-5}$, and $2.11x10^{-5}$, respectively) mutation frequencies did not differ significantly from the solvent control ($1.99x10^{-5}$). The first significant increase in the mutation frequency was noted at the 10μM PhIP dose which was $3.89x10^{-5}$ ($p<0.001$) and all doses above that ($p<0.001$) using Dunnett's test (2-tailed) in MCL-5 cell line. A non-linear dose-response and threshold dose was recorded by using Lutz R analysis. The MF thresholded dose was 4.02μM for PhIP induced DNA damage in MCL-5 cell line (Figure 6.3). Threshold dose for micronucleus assay was 23.69μM therefore it indicates that HPRT assay is more sensitive than MN assays.

Similar toxicity and mutagenicity of PhIP in TK6 cells was noted by Margenthaler and Holzhäuser in 1995 who found that exposure to 2.5μg/ml (11μM) PhIP for 4h was not

significantly toxic for TK6 cells growing in the presence of exogenous activating enzyme (10% rat liver S9). At highest dose of 5μg/ml (22μM) PhIP, 70% survival and a significant increase in mutant fraction ($x10^{-6}$) was observed. Similarly, Lauber and his team (2004) reported an increase in mutation frequency (24±9 and 173±46 mutant colonies per 10^6surviving cells ($p< 0.01$)) at higher concentrations of PhIP (10^{-5} M to 10^{-4} M)) after 24h incubation period in the hamster fibroblast cell line V79h1A2 (has very stable karyotype and possesses a functional X-linked *hprt* locus). While lower concentrations of PhIP (10^{-7} M) had a non-significant effect on cell survival and mutation frequencies when compared to control (Lauber *et al*, 2004).

6.4.2 PhIP induced mutations

Our studies also showed that the frequency and type of mutations induced by PhIP were different to those occurring in the untreated control (referred to here as spontaneous mutations). For example, more G→T transversions were observed in mutants induced by PhIP whereas a higher number of T→C transitions and C→G transversions were observed in untreated controls (Table 6.3). Although, it might be argued that control cells had been treated with DMSO thus these does not reflect spontaneous mutations that are observed in cells without any treatment, however, we used DMSO at a final concentration of 0.01% which is not believed to be mutagenic in animal cells, therefore. DMSO mutation frequency is similar to that of untreated control.

Mutations at the *HPRT* locus occur due to the PhIP-induced DNA adduct at C8 position of deoxyguanosine (dG-C8-PhIP). This adduct can be repaired by DNA-repair processes e.g. removed by nucleotide excision repair (NER) (Schut and Snyderwine, 1999). The presence of PhIP-DNA adducts causes structural changes in the DNA and mis-pairing leading to mutations. PhIP adducts have been reported to induce mutations in genes controlling cell proliferation which can potentially lead to tumour formation (Nagaoka *et al*, 1992).

In the present study, PhIP induced a significant increase in the frequency of mutant MCL-5 colonies. The percentage of identified mutations from these colonies and their distribution are shown in Tables 6.3 and 6.4. Table 6.3 showed 12 spontaneous mutations were identified from 15 DMSO control MCL-5 mutant colonies. Among them 58% were point mutations, 25% were deletions and the remaining 17% were tandem mutations. Among the point mutations, 57% were GC→TA transversion and 43% were transitions. Nineteen mutations were identified from 20 PhIP treated MCL-5 mutant colonies. The PhIP-induced mutations on *HPRT* locus of MCL-5 were deletions (58%) and point mutations (42%). Three colonies from

DMSO and 1 from PhIP treated colony did not show any mutation probably missed as outside the sequenced area – or in introns which were not sequenced as cDNA was used in this study. The specificity of mutations induced by PhIP at the *HPRT* locus is characterized by a high percentage of GC→TA transversions (Margenthaler and Holzhäuser, 1995; Yodollahi-Farsani *et al*, 1996). Results presented in this chapter (Table 6.3) also showed predominantly GC→TA (75%) transversions (transitions were only 25%). A study on the dihydrofolate reductase gene in Chinese hamster ovary cells also showed similar mutation spectra after treatment with PhIP (Carothers *et al*, 1994). These GC→TA transversions are thought to be formed by DNA polymerases through preferential incorporation of an adenine residue across from a non-instructional base (Brown *et al*, 1989). The DNA adduct C8-dG-PhIP could also induce a conformational change leading to a purine-purine (G with A) mispair that is not recognized (Norman *et al*, 1989).

Our study (Table 6.3) shows that all the point mutations induced by PhIP in the *HPRT* locus were located at GC base pairs (G264T transversion and G376A transition) making them targeted mutations. The modified bases form the pre-mutagenic lesions preferably at the 5′ G<u>G</u> sites (underline base is mutated) (Cariello *et al*, 1992) by the formation of major DNA adduct at the C-8 position of guanine, N^2-(2′-deoxyguanosin-8-yl)PhIP, in *in vivo* and *in vitro* treatments (Margenthaler and Holzhäuser, 1995; Lin *et al*, 1992; Fukutome *et al*, 1994). Our study is in line with it and found that G→T mutation induced by PhIP in the *HPRT* locus in 6 MCL-5 mutants, in the G<u>G</u> site at 264 base pair while 2 mutants showed G→A mutations in the run of GG<u>G</u>GGG at 376 base pair (Table 6.4). This is a signature of PhIP as other chemicals such as BPDE, MNNG and ENU have strong preference for 5′ G<u>A</u> sites (Cariello and Skopek, 1993).

The mutations spectrum observed in the *HPRT* gene after PhIP exposure includes only single base substitutions at exons 2 and 3, while most of the deletions observed were loss of exon 5 and partially deletion of exon 6. One mutant colony showed a deletion of 438bp (base pair position 776 to 1239) on exon 9, resulting in the partial loss of exon 9 on the *HPRT* locus. Fifty-eight percent of mutants were found to be missing some or all of an exon, probably due to a smaller mutation that led to aberrant splicing of mRNA. Mutant mRNA differs not only in their amino acid sequence but also in their biological functions. These results are in agreement with Margenthaler and Holzhäuser (1995) who also observed 40% mutations at the *HPRT* locus due to deletion of exon 3, exon 4, exon 8 and partial loss of exon 9.

The effect of higher doses of PhIP on genotoxicity is well mentioned, whereas, very limited information is available on the concentrations that could potentially be present in humans

following consumption of a cooked meat meal (Sugimura, 1997). Similarly, very little is known on the accurate quantity of plasma PhIP after consuming a cooked meat meal as well as the chronic effects of consuming low quantities of PhIP through cooked meat (Lauber *et al*, 2004). Our study indicates the potential of PhIP in inducing mutagenicity at a threshold of 4.2μM, and according to threshold for toxicology concern (TTC) the acceptable daily intake values are 1.5ug/day (6.68μM)or 120ug/day (535μM) for ≤1 month, considered to be the safe doses (Müller *et al*, 2006). However, actual risk is dependent on several factors such as level of PhIP in tissue, exposure time, metabolism and finally DNA repair mechanisms. Cooked meat contains up to 50ng PhIP/g of meat, therefore, a potential daily intake of PhIP through meals could be as high as 50mg. PhIP is extensively absorbed, however, depending upon biological activity it could be metabolized leading to varying levels of various intermediates in blood and/or other organs and tissues. Sinha (2000) reported higher prevalence of breast cancer in women with increased PhIP consumption through dietary intake (Sinha *et al*, 2000). These reports together with results presented in this study clearly indicate the potential of PhIP in inducing mutagenic activity.

Chapter 7

General Discussion

The purpose of this project was to investigate *in vitro* low dose response relationships for the pro-carcinogens B[a]P and PhIP. B[a]P and PhIP were used to find out whether they follow linear or non-linear (thresholded) dose responses, which is important to investigate the biological significance of low dose exposure to improve health risk assessments. B[a]P and PhIP both are nontoxic themselves but known to cause genotoxicity through their highly reactive metabolites which form adducts such as dG-N^2-BPDE and dG-C^8-PhIP respectively, however, this is dependent on their metabolism (Cosman *et al*, 1992). Earlier studies have shown the role of CYP450 enzymes in the metabolic activation of B[a]P and PhIP (Guengerich, 2000; Miller, 1978). B[a]P is an environmental pollutant mainly produced by cigarette smoke and a bi-product of industrial incineration and known to cause different organ cancers (Miller *et al*, 2001; Shimada and Fujii-Kuriyama, 2004; Botteri *et al*, 2008), autoimmune (Neal *et al*, 2008) and inflammatory diseases (Klareskog *et al*, 2007). Similarly PhIP is a diet associated carcinogen, formed during the cooking of protein rich food like meat at high temperatures (Sinha *et al*, 2005; Felton *et al*, 2007). PhIP and its metabolites are considered as a dietary risk factor for cancer of the colon, breast, stomach and prostate (Tang *et al*, 2007; Choudhary *et al*, 2012). This study reports the effect of B[a]P and PhIP on human cell lines with varying metabolic abilities in response to different doses and exposure times. The semi-automated MN detection system was used to investigate the DNA damage induction at the chromosomal level. Furthermore, the mechanism of action was investigated at the genetic level by using HPRT assay and mutational spectra was used to find out the difference in spontaneous and induced mutations and their locations on the HPRT gene. Finally to correlate the difference in genotoxic effect of different cell lines, quantitative Real Time PCR studies were conducted to show difference in gene expression of CYP450 enzymes. Findings of these studies are discussed below.

Dose response thresholds for genotoxins can be used to set a safe exposure level. A threshold of genotoxic activity indicates that a compound will not produce any mutation below a critical exposure level and therefore, this reduces the risk for the induction of cancer or congenital abnormalities. The endpoints previously used for the analysis of threshold dose responses were DNA adduct formation, gene mutation and chromosomal aberration (Jenkins *et al*,

2010). In this study low dose response relationships of pro-carcinogens, B[a]P and PhIP were investigated.

7.1 Genotoxic thresholds for B[a]P on cell lines with varying metabolic activity

This study showed that B[a]P influenced cell viability (as measured by RPD) for all cell lines at dose range 0-70μM; however, the sensitivity to B[a]P reflected metabolic activation of the cell lines (Chapter 3). In the case of TK6, which has minimal ability to metabolize B[a]P, it had least cell toxicity while MCL-5 and HepG2 have highest metabolic activity thus showed over 50% of cell toxicity at 10μM following 24hr exposure. Similar response was observed for AHH-1 with relatively lower cell toxicity when compared with MCL-5 and HepG2 cell lines. These findings indicate that reactive metabolites of B[a]P interfere with cell functioning and replication, therefore, rate of metabolism is linked with cell toxicity.

Micronucleus induction was also dependant on B[a]P doses and cell metabolic activity as no significant MN induction was observed in cells with less capability to metabolize B[a]P. For example, the TK6 cell line showed little or no chromosomal damage at B[a]P dose range (0-70μM) followed by 18h with cytochalasin B. AHH-1, MCL-5 and HepG2 cells when treated with B[a]P (0-70μM) followed by 24h with cytochalasin B showed an increase in MN frequency. MCL-5 and HepG2 cell lines are relatively more metabolically competent than AHH-1 cell line therefore showed significant increase in MN frequency at lower doses (3μM) using Dunnett's test ($p<0.05$). In HepG2 cell line, MN induction was 0.23-fold more as compared to MCL-5 cell line at 3μM. The Lutz R analysis (Hockey stick model) was used for the estimation of dose-response relationship which revealed clear linear dose responses in AHH-1, MCL-5 and HepG2 cell lines, indicating that there is no safe exposure level for these cell lines when exposed to B[a]P for 24h at lower doses.

However, we extended our studies to check the response of cell lines at the same doses (0-70μM) for short exposure time (4h) followed by 24h with cytochalasin B, but we excluded TK6 from our later studies due to no metabolic activity. Similarly, our study with shorter B[a]P exposure time (i.e. 4h experiment) showed that AHH-1 cell line can tolerate higher doses as compared to doses exposed for the longer time of 24h. It was observed that AHH-1 cell line showed least cytotoxicity but over 50% cytotoxicity was observed at 30μM and 10μM for MCL-5 and HepG2 cell lines respectively. The first significant increase in MN induction was noticed at 40μM ($p<0.05$) in MCL-5 cell line as compared to 20μM ($p<0.05$) in HepG2. AHH-1 showed no increase in MN induction. A non-linear (thresholded) dose response was observed by Hockey stick model only in MCL-5 cells with an increase in MN

induction only seen at the higher dose range. The estimated threshold dose (IP) was 25.46μM and the lower limit of 90% confidence interval (CI) is 14.60μM (indicated by broken line) at $p<0.002$ (Chapter 3).

All of these results are in line with the metabolic competency of cell lines used. The metabolic activation pathway of B[a]P involves CYP1A1 and mEH. AHH-1 cell line has stable expression of only CYP1A1. Long exposure time at low dose of B[a]P could allow B[a]P metabolism into its intermediate that could result in chromosome damage and a significant increase in MN induction. MCl-5 cell line produced more MN per dose than AHH-1 due to higher expression for CYP1A1. MCL-5 also have mEH therefore it is a more competent cell line as compared to AHH-1 cell line which is devoid of mEH activity. The expression of CYP1A1 increased with higher B[a]P concentration and it was reflected by the induction of MN at higher doses of B[a]P in MCL-5 cell line. In the HepG2 cell line the dose-dependent increase in the MN frequencies was found to be higher than MCL-5 and AHH-1 after treatments making this cell line more sensitive as they express a wide range of Phase I and Phase II enzymes. The expression of CYP1A1 was also increased as the B[a]P dose increased but this increase in expression was less than MCL-5 indicating that higher MN induction may be the result of involvement of other CYP450 such as CYP1A2 or other pathway. The expression of CYP1A2 increased as B[a]P dose increased in HepG2 but in MCL-5 no difference in the expression of CYP1A2 was observed from control to high dose range. The reason for having high MN frequencies in HepG2 cell line after B[a]P exposure is perhaps due to the promising activation system of this cell line. HepG2 cells are from primary hepatoblastome and their morphology and function resembles liver therefore, when B[a]P inhaled through cigarette smoke it can cause cancer of the liver. In fact, the liver plays a central role in the mechanism of chemical bio activation and carcinogenesis and the lung represents a target organ of PAH carcinogenicity (Goldman *et al*, 2001).

Our studies showed that dose concentration, exposure time and metabolic activity are central to B[a]P genotoxicity, therefore, exposure to B[a]P through cigarette smoking poses a risk to cancer. Various studies have reported presence of B[a]P in 'full-flavoured' cigarette to about 9 -10ng per cigarette (Hoffmann and Hoffmann, 1997; Chepiga *et al*, 2000) leading to an intake of about 200ng/day for a pack-a-day cigarette smoker (Scherer *et al*, 2000). In another study Hecht (2006) reported greater uptake of PAH compounds (including B[a]P) in smokers as compared to non–smokers.

Pfeifer *et al*, (2002) reported a link between B[a]P exposure and cancer risk to oral cavity, larynx and lungs. Since exposure to cigarette smoke and B[a]P is lower in oral cavity,

intermediate in larynx and highest in lungs, it is not surprising that lung cancer risk is relatively higher than the larynx and oral cavity respectively. Our results confirm this pattern as higher genotoxicity was observed with higher dose, exposure and/or metabolic potential of the cell lines evaluated. Higher potential of carcinogenicity in lungs could also be attributed to higher absorption and metabolic activation of P450's in lung cells than B[a]P absorption and metabolism in larynx and oral cavity.

Further studies on the effect of B[a]P on induced mutation frequency also revealed similar pattern whereby mutation frequency increased with increase in B[a]P exposure time from 4h to 24h (Chapter 4). Similarly higher mutation frequency was observed in the cell line with greater metabolic activity (MCL-5) than in the AHH-1 cell line which is known to have lower metabolic activity. These studies suggest an increased risk of cancer in individuals who smoke more frequently as amount of B[a]P intake and its subsequent absorption in the body would be comparatively higher than those who smoke occasionally. Although, occasional smoking does not eliminate the chances of carcinogenic activity however, our studies indicate that an occasional smoker (lower exposure to B[a]P) would represent a comparatively lower risk than a frequent smoker. Similarly an individuals' variability in metabolic activity appears to be a vital factor in determining an individual risk to cancer following B[a]P exposure through smoking.

Studies on the effect of B[a]P on frequency and type of mutation revealed higher frequency of G to T transversion in B[a]P treated MCL-5 cells. Earlier studies have also shown that metabolic activation of B[a]P in human lung tissues take place via Ah receptor and form PAH diol epoxides–DNA adducts and cause G→T transversions that is commonly observed in the *p53* and *K-ras* tumor suppressor genes in smoking induced lung tumours (Hecht, 2000; Phillips, 2002; Tretyakova *et al*, 2002; Pfeifer *et al*, 2003; Hecht, 2006). Results of our study indicated that B[a]P is capable of inducing G→T mutations which are specific mutations that are associated with carcinogenic activity.

We also observed difference in mutation frequency in response to B[a]P exposure time and metabolic activity of the cell with higher frequency of mutation being observed in cells exposed for 24h to those exposed for 4h. Similarly, cells with higher metabolic activity (MCL-5) showed higher mutation frequency than cells with lower metabolic activity (AHH-1). It is important to mention here that metabolism of B[a]P has a dual pathway involving process that either lead to its excretion from cells or in the formation of by-products that are capable of inducing mutagenic activity. Similarly, the onset of mutagenic activity can either result in activation of DNA repair mechanisms or formation of DNA adducts. Since our

studies focussed on determining the effect of B[a]P on its mutagenic activity, evaluation of the DNA repair mechanisms were outside the scope of this study however, presence of such processes should not ignored.

7.2 Genotoxic thresholds for PhIP on cell lines with varying metabolic activity

The carcinogenicity of PhIP is associated with the metabolic activity of cells and requires CYP1A2 and other P450 enzymes for its conversion into a carcinogenic form (Lin *et al*, 1992; Gooderham *et al*, 2007) TK6 and AHH-1 cell lines were not used in this part of the study because TK6 cells showed little or no chromosomal damage due to having little metabolic activity and AHH-1 showed little expression of CYP1A2 after B[a]P treatment (Chapter 3).

Our results showed that carcinogenicity of PhIP is linked with the metabolic potential of the cell line used (Chapter 5). HepG2 cell line has been shown to have multiple metabolic pathways to metabolise PhIP as compared to MCL5. We observed higher cytotoxicity and genotoxicity in HepG2 cells following PhIP exposure which reflects its metabolic potential. The results also reflected that at the dose range (0-35μM), the cytotoxicity increased at doses more than 20μM and 50μM in both cell lines with PhIP after 24h and 4h exposures respectively.

Micronucleus induction was also dependent on PhIP doses and on cell metabolic competency. Both cell lines showed an increase in MN frequency with an increase in PhIP dose. Studies on PhIP exposure time showed a similar pattern of increased MN frequency with increasing doses, however, significantly higher MN frequency was observed at lower doses following 24h exposure as compared to 4h exposure. For example, HepG2 cell line showed significant increase in MN frequencies at 10μM ($p<0.05$) after 24h and 50μM ($p<0.001$) after 4h which is 5 times higher than the 24h exposure time. In MCL-5 cell line the significant increase was observed at 35μM ($p<0.05$) and 120μM ($p<0.001$) at 24h and 4h respectively and again about 3.5 times higher dose than the 24h treatment. At the highest dose (100μM) HepG2 cell line induced 0.34-fold more MN as compared to MCL-5 cell line. Similarly, at 120μM 4h PhIP exposure in HepG2 cell line MN frequency was 0.09-fold more than MCL-5 cell line. A non-linear (thresholded) dose-response relationship was estimated by the Lutz R analysis (Hockey stick model) and the estimated threshold dose (IP) was 23.69μM and 97.71μM for MCL-5 cell line at 24h and 4h respectively. A linear dose-response was observed in HepG2 cell line making PhIP carcinogenic for all dose ranges at both exposure times.

All of these results indicated that HepG2 cell line is metabolically more competent than MCL-5 in converting PhIP to its carcinogenic form. CYP1A2 is considered to be a "liver

specific" P450; therefore, N-oxidation of PhIP is catalyzed primarily in hepatocytes (Turesky *et al*, 2002). In study we observed that basal expression of CYP1A2 was higher in MCL-5 cells as compared to HepG2 cells, however, there was a slight increase in the inducible expression of CYP1A2 observed in HepG2 cell line at dose range as compared to basal expression. Where as, MCL-5 cell line showed no difference in the expression of CYP1A2 between treated and untreated cell lines. Only a small amount of CYP1A2 in a target cell is sufficient to start the process of bio-activation of PhIP that leads to the formation of PhIP DNA adduct and ultimately tumorigenesis (Kimura *et al*, 2003). An increase in CYIA12 expression and MN frequency in PhIP treated HePG2 cell line thus highlight the importance of metabolic potential in PhIP related carcinogenicity. We also have noticed that increased levels of CYP1A1 mRNA are B[a]P driven while PhIP is a weak inducer of CYP1A1. Thomas (2006) also observed the similar reduction in CYP1A1 expression in MCF10A breast epithelial cells treated with PhIP (Thomas *et al*, 2006).

Our studies also showed an increase in mutation frequency in MCL-5 in response of PhIP exposure compared to untreated control (Chapter 6). Similarly the type of mutation caused by PhIP was different to those observed in control (spontaneous mutations). The majority of PhIP induced mutations observed in this study were G→T transversions. These transversions could be induced by the DNA adduct C8-dG-PhIP that causes a conformational change leading to a purine-purine base pair (G with A) (Norman *et al*, 1989). Since we observed a higher MN frequency in PhIP treated cells, these results support a link between PhIP induced genotoxicity and PhIP specific mutations. Other mutations observed in the form of deletion in PhIP induced MCL-5 cell line were also in confirmation with previous reports of deletion of HPRT exon 3, 4, 8 and partial loss of exon 9 (Margenthaler and Holzhäuser, 1995).

Our results indicate that metabolic activity, dose and exposure time play an important role in PhIP induced carcinogenicity. Non existence of threshold dose for PhIP in highly metabolic cell line (HepG2) suggests that individuals with higher metabolic activity are at higher risk to PhIP induced carcinogenicity. These risks appear to the relatively lower for individuals with lower metabolic activity (as observed in MCL 5), however, an increase in PhIP dose and/or exposure time does poses a significant risk to individuals with lower metabolic potentials. Thomas *et al* (2006) reported approximately 6-20ng/kg/day of PhIP consumption through diet in western countries. Other report (Sinha et al, 2000) indicates an increasing trend in higher intake products containing PhIP which represents a higher risk of PhIP related cancers.

7.3 Limitations of my study

Like any other thesis there are points that strengthen this study along with some weaknesses. The following are some of the points that make my thesis strong, for example, I have used several cell lines to get the better picture of differences in their metabolic competency. I have used multiple end points like chromosomal damage using CBMN assay and DNA damage using HPRT assay to get the better understanding of the effect of pro-carcinogens in causing genotoxicity. I have used a wide dose range of B[A]P and PhIP that include some non-toxic doses and then performed my study along with 2 time points (24h and 4h). By using the mutation spectra I managed to identify the types and locations of mutations on DNA. Furthermore, I measured the CYP450 enzymes expressions in all cell lines that are actively involved in the metabolism of B[a]P and PhIP.

One of the weaknesses of my study is that the whole study was based on *in vitro* system. I did not use any *in vivo* system to confirm my results as we are lacking this facility in Swansea University. I found DNA damage as a result genotoxins exposure in cell lines but did not do study any mechanism that involve in DNA repair. I was not able perform any experiment where I can compare the B[a]P doses that are toxic for cell lines are in real life toxic to smoker or PhIP doses are harmful to meat eater in humans.

7.4 Concluding remarks

Overall our studies have shown a better understanding of the effect of B[a]P and PhIP on cell lines with different metabolic potential. We have shown how cells with differential metabolic potential respond to different doses, particularly a dose related response at low doses only in highly metabolically competent cells. Similarly we compared the effect of different doses with two different exposure times of 4h and 24h and the results of this comparison have shown that either an increase in dose or exposure increases the risk of genotoxicity. Our studies have shown an increase in CYP1A1 and CYP1A12 expression in B[a]P and PhIP treated cell lines thus confirming a link between metabolic potential and B[a]P or PhIP induced genotoxicity. Similarly, we have shown that both B[a]P and PhIP increase mutation frequency and cause specific mutations.

7.5 Future work

To further understand the carcinogenicity of B[a]P and PhIP ,, future studies are required to

- determine the effect of very low doses such as 0.1-1μM on genotxicity of cell with different metabolic activity.

- determine the DNA repair mechanisms in response to DNA damage caused by pro-carcinogens and to understand their role in reducing risks of cancer caused by pro-carcinogens.
- determine the effect of low doses of B[a]P and PhIP on the cell cycle mechanism and expression of cell cycle regulatory genes.
- compare the effect of different dose of B[a]P and PhIP on CYP1A1 and CYP1A2 expression.

References

Aden, D. P., Fogel, A., Plotkin, S., Damjanov, I., & Knowles, B. B. (1979). Controlled synthesis of HBsAg in a differentiated human liver carcinoma-derived cell line. *Nature, 282*(5739), 615-616.

Agency for Toxic Substances and Disease Registry (ATSDR). Toxicological Profile for Polycyclic Aromatic Hydrocarbons (PAHs) August 1995. Accessed 12.09.2010

Alaejos, M. S., Gonzalez, V., & Afonso, A. M. (2008). Exposure to heterocyclic aromatic amines from the consumption of cooked red meat and its effect on human cancer risk: a review. [Review]. *Food Addit Contam Part A Chem Anal Control Expo Risk Assess, 25*(1), 2-24.

Albertini, R. J. HPRT mutations in humans: biomarkers for mechanistic studies. *Mutat Res, 489*, 1 –16.

Ames, B. N., Durston, W. E., Yamasaki, E., & Lee, F. D. (1973). Carcinogens are mutagens: a simple test system combining liver homogenates for activation and bacteria for detection. *Proc Natl Acad Sci U S A, 70*(8), 2281-2285.

Ames, B. N., & Gold, L. S. (1991). Endogenous mutagens and the causes of aging and cancer. *Mutat Res, 250*(1-2), 3-16.

Ames, B. N., Gold, L. S., & Willett, W. C. (1995). The causes and prevention of cancer. *Proc Natl Acad Sci, U S A, 92*(12), 5258-5265.

An, J., Yin, L., Shang, Y., Zhong, Y., Zhang, X., Wu, M., . . . Huang, Y. (2011). The combined effects of BDE47 and BaP on oxidatively generated DNA damage in L02 cells and the possible molecular mechanism. *Mutat Res, 721*(2), 192-198.

Anderson, K. E., Sinha, R., Kulldorff, M., Gross, M., Lang, N. P., Barber, C., . . . Kadlubar, F. F. (2002). Meat intake and cooking techniques: associations with pancreatic cancer. *Mutat Res, 506-507*, 225-231.

Anand, A., Prabhakar, S., & Kaul, D. (1999). Genetic polymorphism in muscle biopsies of Duchenne and Becker muscular dystrophy patients. *Neurol India, 47(3),* 218-23.

Arlett, C. F., Turnbull, D., Harcourt, S.A., Lehmann, A. R., & Colella, C. M. (1975). A comparision of the 8-azaguanine and ouabian-resistance systems for the selection of induced mutant Chinese Hamster cells. *Mutat Res, 33*, 261-78.

ATSDR (1995) Agency for Toxic Substances and Disease Registry. Toxicological Profile for Polycyclic Aromatic Hydrocarbons, US Department of Health and Human Services, Atlanta, Georgia.

Au, W. W. (2007). Usefullness of biomarkers in population studies: from exposure to susceptibility and to prediction of cancer. *Int J Hyg Environ Health, 210*(3-4), 239-46.

Aubrecht, J., Goad, M. E., & Schiestl, R. H. (1997). Tissue specific toxicities of the antocancer grug 6-thioguanine is dependent on the Hprty status in transgenic mice. *J Pharmacol Exp Ther, 282*, 1102-8.

Baird, W. M., Hooven, L. A., & Mahadevan, B. (2005). Carcinogenic polycyclic aromatic hydrocarbon-DNA adducts and mechanism of action. *Environ Mol Mutagen, 45*(2-3), 106-114.

Balajee, A. S., & Geard, C. R. (2004). Replication protein A and gamma-H2AX foci assembly is triggered by cellular response to DNA double-strand breaks. *Exp Cell Res, 300*(2), 320-334.

Bansal, S. K., Zaleski, J.& Gessner, T. (1981). Glucuronidation of oxygenated benzo(a)pyrene derivatives by UDP-glucuronyltransferase of nuclear envelope. *Biochemical and Biophysical Research Communications, 98*(1), 131-139.

Bartsch, H., Ohshima, H., & Pignatelli, B. (1988). Inhibitors of endogenous nitrosation mechanisms and implications in human cancer prevention. *Mutation Research/Fundamental and Molecular Mechanisms of Mutagenesis, 202*(2), 307-324.

Belpomme, D., Irigaray, P., Hardell, L., Clapp, R., Montagnier, L., Epstein, S. et al. (2007). The multitude and diversity of environmental carcinogens. *Environ Res, 105*, 414–429.

Benford, D., Bolger, P. M., Carthew, P., Coulet, M., DiNovi, M., Leblanc, J. C., . . . Wildemann, T. (2010). Application of the Margin of Exposure (MOE) approach to substances in food that are genotoxic and carcinogenic. *Food and Chemical Toxicology, 48*, S2-S24.

Bendaly, J., Metry, K. J., Doll, M. A., Giang, G., States, J. C., Smith, N. B.,..... & Hein, D. W. (2009). Role of human CYP1A1 and NAT2 in 2-amino-1-methyl-6-phenylimidazo[4,5-b]pyridine-induced mutagenicity and DNA adducts. *Xenobiotica, 39*(5), 399-406.

Binkova, B., Chvatalova, I., Lnenickova, Z., Milcova, A., Tulupova, E., Farmer, P. B., & Sram, R. J. (2007). PAH-DNA adducts in environmentally exposed population in relation to metabolic and DNA repair gene polymorphisms. *Mutat Res, 620*(1-2), 49-61.

Blount, B. C., Mack, M. M., Wehr, C. M., MacGregor, J. T., Hiatt, R. A., Wang, G., . . . Ames, B. N. (1997). Folate deficiency causes uracil misincorporation into human DNA and chromosome breakage: implications for cancer and neuronal damage. *Proc Natl Acad Sci U S A, 94*(7), 3290-3295.

Boddy, A. V., & Ratain, M. J. (1997). Pharmacogenetics in cancer etiology and chemotherapy. *Clinical cancer research, 3*(7), 1025-1030.

Bolt, H. M., Foth, H., Hengstler, J. G and Degen, G. H. (2004). Carcinogenicity categorization of chemicals – new aspects to be considered in a European perspective. Toxicology Letters, *151*, 29-41.

Bonner, M. R., Rothman, N., Mumford, J. L., He, X., Shen, M., Welch, R., Yeager, M., Chanock, S., Caporaso, N.& Lan, Q. (2005). Green tea consumption, genetic susceptibility, PAH-rich smoky coal, and the risk of lung cancer. *Mutat Res, 582*(1-2), 53-60.,

Boobis, A. R., Lynch, A. M., Murray, S., Delatorre, R., Solans, A., Farre, M., . . . Davies, D. S. (1994). Cyp1a2-Catalyzed Conversion of Dietary Heterocyclic Amines to Their Proximate Carcinogens Is Their Major Route of Metabolism in Humans. *Cancer Res, 54*(1), 89-94.

Botteri, E., Iodice, S., Bagnardi, V., Raimondi, S., Lowenfels, A. B., & Maisonneuve, P. (2008). Smoking and colorectal cancer: a meta-analysis. [Meta-Analysis]. *JAMA, 300*(23), 2765-2778.

Boue, J., Bou, A., & Lazar, P. (1975). Retrospective and prospective epidemiological studies of 1500 karyotyped spontaneous human abortions. *Teratology, 12*(1), 11-26.

Boveri, T. (1914). Zur Frage der Entsehung Maligner Tumouren. Fisher, Jena, Germany.

Boyland, E., & Wolf, G. (1950). Metabolism of polycyclic compounds. 6. Conversion of phenanthrene into dihydroxydihydrophenanthrenes. *Biochem J, 47*(1), 64-69.

Boysen, G., & Hecht, S. S. (2003). Analysis of DNA and protein adducts of benzo[alpha]pyrene in human tissues using structure-specific methods. *Mutation Research-Reviews in Mutation Research, 543*(1), 17-30.

Boyiri, T., Guttenplan, J., Khmelnitsky , M., Kosinska, W., Lin, J-M., Desai, D.,.....EEl-Bayoumy, K. (2004). Mammary carcinogenesis and molecular analysis of *in vivo cII* gene mutations in the mammary tissue of female transgenic rats treated with the environmental pollutant 6-nitrochrysene. *Carcinogenesis, 25*(4), 637-643.

Braithwaite, E., Wu, X., & Wang, Z. (1998). Repair of DNA lesions induced by polycyclic aromatic hydrocarbons in human cell-free extracts: involvement of two excision repair mechanisms in vitro. *Carcinogenesis, 19*(7), 1239-1246.

Bratt,C., Boobis, A. R., Gooderham, N. J., & Davies, D. S. (1994). Detection of DNA adducts of the food carcinogen 2-amino-l-methyl-6-phenylimidazo[4.5-fc]pyridine by 32P-postlabelhng. *Hum. Exp. Toxicol,* 13, 641.

Brooks, R. A., Gooderham, N. J., Zhao, K. C., Edwards, R. J., Howard, L. A., Boobis, A. R., & Winton, D. J. (1994). 2-Amino-1-Methyl-6-Phenylimidazo[4,5-B]Pyridine Is a Potent Mutagen in the Mouse Small-Intestine. *Cancer Res, 54*(7), 1665-1671.

Buening, M. K., Wislocki, P. G., Levin, W., Yagi, H., Thakker, D. R., Akagi, H., Koreeda, M., Jerina, D. M., & Conney, A. H. (1978). Tumorigenicity of the optical enantiomers of the diastereomeric benzo[a]pyrene 7,8-diol-9,10-epoxides in newborn mice: exceptional activity of (+)-7beta,8alpha-dihydroxy-9alpha,10alpha-epoxy-7,8,9,10-tetrahydrobenzo[a]pyrene. *Proc of Nat Acad of Sci, 75*(11), 5358-5361.

Buetow, K. H., Edmonson, M. N., & Cassidy, A. B. (1999). Reliable identification of large numbers of candidate SNPs from public EST data. *Nat Genet, 21*(3), 323-325.

Burczynski, M. E., & Penning, T. M. (2000). Genotoxic polycyclic aromatic hydrocarbon ortho-quinones generated by aldo-keto reductases induce CYP1A1 via nuclear translocation of the aryl hydrocarbon receptor. *Cancer Res, 60*(4), 908-915.

Burkhart-Schultz, K.,Thomas, C. B., Thompson, C. L., Strout, C .L., Brinso, .E. & Jones, I. (1993). Characterization of invivo somatic mutations at the hypoxanthine phosphoribosyltransferase gene of a human control population. *Environ Health Perspect, 101*,68-74.

Bustin, S. A. (2000). Absolute quantification of mRNA using real-time reverse transcription polymerase chain reaction assays. *Journal of Molecular Endocrinology, 25,* 169–193.

Calabrese, E. J. (2009). The road to linearity: why linearity at low doses became the basis for carcinogen risk assessment. *Arch Toxicol, 83*, 203-225.

Calabrese, E. J., and Baldwin, L. A. (2001). Hormesis: A generalizable and unifying hypothesis. *Crit Rev Toxicol. 31*, 353–424.

Camici, M., Micheli, V., Ipata, P. L., & Tozzi, M. G. (2010). Pediatric neurological syndromes and inborn errors of purine metabolism. *Neurochemistry International, 5* (3), 367-378.

Capen, C. C. (1998). Correlation of mechanistic data and histopathology in the evaluation of selected toxic endpoints of the endocrine system. *Toxicol Lett*, 405-409.

Cariello, N. F., Craft, T. R., Vrieling, H., Vanzeeland, A. A., Adams, T., & Skopek, T. R. (1992). Human Hprt Mutant Database - Software for Data-Entry and Retrieval. *Environ Mol Mutagen, 20*(2), 81-83.

Cariello, N. F., & Skopek, T. R. (1993). Analysis of Mutations Occurring at the Human Hprt Locus. *J Mol Biol, 231*(1), 41-57.

Carothrs, A. M., Yuan, W., Hingerty, B. E., Broyde, S., Grunberger, D., & Snyderwine, E. G. (1994). Mutation and Repair Induced by the Carcinogen 2-(Hydroxyamino)-1-Methyl-6-Phenylimidazo[4,5-B]Pyridine (N-Oh-Phip) in the Dihydrofolate-Reductase Gene of Chinese-Hamster Ovary Cells and Conformational Modeling of the Dg-C8-Phip Adduct in DNA. *Chem Res Toxicol, 7*(2), 209-218.

Carter, S. B. (1967). Effects of cytochalasins on mammalian cells. [In Vitro]. *Nature, 213*(5073), 261-264.

Carthew, P., DiNovi, M., & Woodrow Setzer, R. (2010). Application of the Margin of Exposure (MOE) approach to substances in food that are genotoxic and carcinogenic: example: CAS No: 105650-23-5 PhIP (2-amino-1-methyl-6-phenylimidazo[4,5-b]pyridine). *Food Chem Toxicol, 48 Suppl 1*, S98-105.

Casciano, D. A., Aidoo, A., Chen, T., Mittelstaedt, R. A., Manjanatha, M. G., & Heflich, R. H. (1999). Hprt mutant frequency and molecular analysis of Hprt mutations in rats

treated with mutagenic carcinogens. *Mutation Research-Fundamental and Molecular Mechanisms of Mutagenesis, 431*(2), 389-395.

Caskey, C. T., & Kruh, G. D. (1979). Hprt Locus. *Cell, 16*(1), 1-9.

Chen, J., & Thilly, W. G. (1996). Mutational spectra vary with exposure conditions: benzo[*a*]pyrene in human cells. *Mutat Res, 357*(1-20, 209-217.

Chen, R., Maher, V. M., Brouwer, J., van de Putte, P., & McCormiek, J. J. (1992). Preferential repair and strand-specific repair of Benzoa-a-pyrene diol epoxide adducts in the HPRT gene of diploid human fibroblasts. *Proc Nat Acad Sci, USA, 89*, 5413-5417.

Chen, T., Harrington,Brock, K., & Moore, M. M. (2002). Muation frequency and mutational spectra in the tk and hprt genes on N-ethyl-N-nitrosourea-treated mouse lymphoma cellsdagger. *Environ Mol Mutagen, 39*, 269-305.

Cheung, C., Ma, X. C., Krausz, K. W., Kimura, S., Feigenbaum, L., Dalton, T. P., . . . Gonzalez, F. J. (2005). Differential metabolism of 2-amino-1-methyl-6-phenylimidazo[4,5-b]pyridine (PhIP) in mice humanized for CYP1A1 and CYP1A2. *Chem Res Toxicol, 18*(9), 1471-1478.

Chou, H. C., Lang, N. P., & Kadlubar, F. F. (1995). Metabolic-Activation of N-Hydroxy Arylamines and N-Hydroxy Heterocyclic Amines by Human Sulfotransferase(S). *Cancer Res, 55*(3), 525-529.

Choudhary, S., Sood, S., Donnell, R. L., & Wang, H. C. R. (2012). Intervention of human breast cell carcinogenesis chronically induced by 2-amino-1-methyl-6-phenylimidazo[4,5-b]pyridine. *Carcinogenesis, 33*(4), 876-885.

Chung, Y. H., Youn, J., Choi, Y., Paik, D. J., & Cho, Y. J. (2001). Requirement of de novo protein synthesis for aminopterin-induced apoptosis in a mouse myeloma cell line. *Immunol Lett, 77*, 127-31.

Cimino. M. C.(2006). Comparative overview of Current International Strategies and Guidelines for Genetic Toxicology Testing for Regulatory purposes. *Environmental and Molecular Mutagenesis. 47*: 362-390.

Clive, D. & Spector, J. (1975). Laboratory procedure for assessing specific locus mutations at the TK locus in cultured L5178Clive D and Spector J: Laboratory procedure for assessing specific locus mutations at the TK locus in cultured L5178Y mouse lymphoma cells. *Mutation Research, 31*, 17-29.

Cohen, S. M. (2004). Human carcinogenic risk evaluation: an alternative approach to the two-year rodent bioassay. Toxicol. Sci. 80, 225–229.

Cohen, S. M., & Arnold, L. L. (2011). Chemical carcinogenesis. *Toxicol Sci, 120 Suppl 1*, S76-92.

Coles, B., Nowell, S. A., MacLeod, S. L., Sweeney, C., Lang, N. P., & Kadlubar, F. F. (2001). The role of human glutathione S-transferases (hGSTs) in the detoxification of the food-derived carcinogen metabolite N-acetoxy-PhIP, and the effect of a polymorphism in hGSTA1 on colorectal cancer risk. *Mutation Research-Fundamental and Molecular Mechanisms of Mutagenesis, 482*(1-2), 3-10.

COM (2000). Committee on Mutagenicity of Chemicals in Food, Consumer Products and the Environment (Advisory Body for the Department of Health, UK): Guidance on a Strategy for Testing of Chemicals for Mutagenicity

COM, 2011. Committee on Mutagenicity of Chemicals in Food, Consumers Products, and the Environment (COM). Guidance on a strategy for genotoxicity testing of chemical substances.

Committee on Toxicity (2002) Committee on toxicity of chemicals in food, consumer products and the environment: Risk assessment of mixtures of pesticides and similar substances. *FSA*. 1-302.

Conney, A. H. (1992). Induction of microsomal enzymes by foreign chemicals and carcinogenesis by polycyclic aromatic hydrocarbons: G. H. A. Clowes Memorial Lecture. *Cancer Res, 42,* 4875–4917.

Cosman, M., de los Santos, C., Fiala, R., Hingerty, B. E., Singh, S. B., Ibanez, V., . . . et al. (1992). Solution conformation of the major adduct between the carcinogen (+)-anti-benzo[a]pyrene diol epoxide and DNA. *Proc Natl Acad Sci U S A, 89*(5), 1914-1918.

Crebelli, R. (2000). Threshold-mediated mechanisms in mutagenesis: implications in The classification and regulation of chemical mutagens. *Mutat Res, 464*, 129-135.

Crespi, C. L., Gonzalez, F. J., Steimel, D. T., Turner, T. R., Gelboin, H. V., Penman, B. W., & Langenbach, R. (1991). A metabolically competent human cell line expressing five cDNAs encoding procarcinogen-activating enzymes: application to mutagenicity testing. *Chem Res Toxicol, 4*(5), 566-572.

Crespi, C. L., Langenbach, R., & Penman, B. W. (1990). The development of a panel of human cell lines expressing specific human cytochrome P450 cDNAs. *Prog Clin Biol Res, 340B*, 97-106.

Crespi, C. L., Penman, B. W., Leakey, J. A. E., Arlotto, M. P., Stark, A., Parkinson, A., . . . Langenbach, R. (1990). Human Cytochrome P450iia3 - Cdna Sequence, Role of the Enzyme in the Metabolic-Activation of Promutagens, Comparison to Nitrosamine Activation by Human Cytochrome P450iie1. *Carcinogenesis, 11*(8), 1293-1300.

Crespi, C. L., & Thilly, W. G. (1984) Assay for gene mutation in a human lymphoblast line, AHH-1, competent for xenobiotic metabolism. *Mutation Res, 128*, 221-230.

Crofts, F. G., Sutter, T. R., & Strickland, P. T. (1998). Metabolism of 2-amino-1-methyl-6-phenylimidazo[4,5-b]pyridine by human cytochrome P4501A1, P4501A2 and P4501B1. *Carcinogenesis, 19*(11), 1969-1973.

Cross, A. J., Peters, U., Kirsh, V. A., Andriole, G. L., Reding, D., Hayes, R. B., & Sinha, R. (2005). A prospective study of meat and meat mutagens and prostate cancer risk. *Cancer Res, 65*(24), 11779-11784.

Cross, A. J., & Sinha, R. (2004). Meat-related mutagens/carcinogens in the etiology of colorectal cancer. *Environ Mol Mutagen, 44*(1), 44-55.

Dashwood, R. H. (2002). Modulation of heterocyclic amine-induced mutagenicity and carcinogenicity: an 'A-to-Z' guide to chemopreventive agents, promoters, and transgenic models. *Mutat Res, 511*(2), 89-112.

Davies, R. L., Crespi, C. L., Rudo, K., Turner, T. R., &, Langenbach, R. (1989). Development of a human cell line by selection and drug-metabolizing gene transfection with increased capacity to activate promutagens. *Carcinogenesis, 10*(5), 885-91.

Davis, B. B., Thompson, D. A., Howard, L. L., Morisseau, C., Hammock, B. D., & Weiss, R. H. (2002). Inhibitors of soluble epoxide hydrolase attenuate vascular smooth muscle cell proliferation. *Proc Natl Acad Sci U S A, 99*(4), 2222-2227.

Davis, J. M., & Svendsgaard, D. J. (1990). U-Shaped Dose-Response Curves - Their Occurrence and Implications for Risk Assessment. *J Toxicol Environ Health, 30*(2), 71-83.

Daya-Grosjean, L., Dumaz, N. & Sarasin, A. (1995). The specificity of p53 mutation spectra in sunlight induced human cancers. *J. Photochem. Photobiol*, B28 , 115 -124.

De Stefani, E., Boffetta, P., Mendilaharsu, M., Carzoglio, J., & Deneo-Pellegrini, H. (1998). Dietary nitrosamines, heterocyclic amines, and risk of gastric cancer: A case-control study in Uruguay. *Nutrition and Cancer-an International Journal, 30*(2), 158-162.

Dearfield, K. L., Cimino, M. C., McCarroll, N. E., Mauer, I., & Valcovic, L. R. (2002). Genotoxicity risk assessment: a proposed classification strategy. [Guideline]. *Mutat Res, 521*(1-2), 121-135.

DeBaun, J. R., Rowley, J. Y., MUler, E. C., & Miller, J. A.(1968). Sulfotransferase activation of N-hydroxy-2-acetylarrunofluorenc in rodent livers susceptible and resistant to this carcinogen. *Proc Soc Exp Biol Med, 129*, 268-273.

Denissenko, M. F., Pao, A., Tang, M., & Pfeifer, G. P. (1996). Preferential formation of benzo[a]pyrene adducts at lung cancer mutational hotspots in P53. *Science, 274*(5286), 430-432.

Denissenko, M. F., Pao, A., Pfeifer, G. P., & Moon-shong, T. (1998). Slow repair of bulky DNA adducts along the nontranscribed strand of the human p53 gene may explain the strand bias of transversion mutations in cancers. *Oncogene, 16*(10), 1241- 7.

Deutsch-Wenzel R, Brune H, Grimmer G, Dettbarn G and Mis®eld J. (1983). *J. Natl. Cancer Inst, 71*, 539- 543.

Diamond, L., Kruszewski, F., & Baird, W. M. (1982). Expression time for Benzo-a-pyrene-induced 6-thioguanine-resistant mutations in V79 Chinese hamster cells. *Mutat Res, 95*, 353-62.

Diamond, L., Kruszewski, F., Aden, D. P., Knowles, B. B., & Baird, W. M. (1980). Metabolic activation of benzo[a]pyrene by a human hepatoma cell line. *Carcinogenesis, 1*(10), 871-875.

Dipple, A. 1985. Polycyclic Aromatic Hydrocarbon Carcinogenesis.

Dingley, K. H., Curtis, K. D., Nowell, S., Felton, J. S., Lang, N. P., & Turteltaub, K. W. (1999). DNA and protein adduct formation in the colon and blood of humans after exposure to a dietary-relevant dose of 2-amino-1-methyl-6-phenylimidazo[4,5-b]pyridine. *Cancer Epidemiology Biomarkers & Prevention, 8*(6), 507-512.

Doak, S. H., Jenkins, G. J., Johnson, G. E., Quick, E., Parry, E. M., & Parry, J. M. (2007). Mechanistic influences for mutation induction curves after exposure to DNA-reactive carcinogens. *Cancer Res, 67*(8), 3904-3911

Doak, S. H., Bruschafer, K., Dudley, E., Quick, E., Johnson, G., Newton, P. R., & Jenkins, G. J. (2008). No-observed effect lev ls are associated with up-regulation of MGMT following MMS exposure. *Muta Res, 648*, 9-14.

Dogliotti, E., Hainaut, P., Hernandez, T., D'Errico, E., & Demarini, D. M. (1998). Mutation Spectra Resulting from Carcinogenic Exposure: From Model Systems to Cancer-Related Genes. *Genes and Environment in Cancer. 154*, 97-124.

Doherty, A., Ellard, S., Parry, E. and Parry, J (1996) An investigation into the activation of chlorinated hydrocarbons to genotoxins in metabolically competent human cells. *Mutagenesis*. **11**: 247-274.

Duffaud, F., Orsiere, T., Villani, P., Pelissier, A. L., Volot, F., Favre, R., & Botta, A. (1997). Comparison between micronucleated lymphocyte rates observed in healthy subjects and cancer patients. *Mutagenesis, 12*(4), 227-231.

Durling, L. J. K., & Abramsson-Zetterberg, L. (2005). A comparison of genotoxicity between three common heterocyclic amines and acrylamide. *Mutation Research-Genetic Toxicology and Environmental Mutagenesis, 580*(1-2), 103-110.

Edwards, A., Voss, H., Rice, P., Civitello, A., Stegemann, J., Schwager, C., . . . Ansorge, W. (1990). Automated DNA sequencing of the human HPRT locus. *Genomics, 6*(4), 593-608.

Ehrlich, V., Darroudi, F., Uhl, M., Steinkellner, H., Gann, M., Majer, B. J., . . . Knasmuller, S. (2002). Genotoxic effects of ochratoxin A in human-derived hepatoma (HepG2) cells. *Food Chem Toxicol, 40*(8), 1085-1090.

Ehrlich, V., Darroudi, F., Uhl, M., Steinkellner, H., Zsivkovits, M., & Knasmueller, S. (2002). Fumonisin B(1) is genotoxic in human derived hepatoma (HepG2) cells. *Mutagenesis, 17*(3), 257-260.

Elhajouji, A., Tibaldi, F., & Kirsch-Volders, M. (1997). Indication for thresholds of chromosome non-disjunction versus chromosome lagging induced by spindle inhibitors in vitro in human lymphocytes. [In Vitro]. *Mutagenesis, 12*(3), 133-140.

Elhajouji, A., Van Hummelen, P., & Kirsch-Volders, M. (1995). Indications for a threshold of chemically-induced aneuploidy in vitro in human lymphocytes. [Comparative Study]. *Environ Mol Mutagen, 26*(4), 292-304.

Elhajouji, A., Lukamowicz, M., Cammerer, Z., & Kirsch-Volders, M. .(2011). Potential thresholds for genotoxic effects by micronucleus scoring. *Mutagenesis, 26(1),* 199-204.

Esumi, H., Ohgaki, H., Kohzen, E., Takayama, S., & Sugimura, T. (1989). Induction of Lymphoma in Cdf1 Mice by the Food Mutagen, 2-Amino-1-Methyl-6-Phenylimidazo[4,5-B]Pyridine. *Japanese Journal of Cancer Research, 80*(12), 1176-1178.

European Commision (2006) Commission decision: on special conditions governing certain foodstuffs imported from certain third countries due to contamination risks of these products by aflatoxins. *Official Journal of European Union*. **199**: 21-32.

Fatur, T., Tusek, M., Falnoga, I., Scancar, J., Lah, T. T., & Filipic, M. (2002). DNA damage and metallothionein synthesis in human hepatoma cells (HepG2) exposed to cadmium. *Food Chem Toxicol, 40*(8), 1069-1076.

Fede, J. M., Thakur, A. P., Gooderham, N. J., & Turesky, R. J. (2009). Biomonitoring of 2-Amino-1-methyl-6-phenylimidazo[4,5-b]pyridine (PhIP) and Its Carcinogenic Metabolites in Urine. *Chem Res Toxicol, 22*(6), 1096-1105.

Fellows, M. D., & O'Donovan, M. R. (2007). Cytotoxicity in cultured mammalian cells is a function of the method used to estimate it. [Comparative Study]. *Mutagenesis, 22*(4), 275-280.

Felton, J. S., Fultz, E., Dolbeare, F. A., & Knize, M. G. (1994). Effect of Microwave Pretreatment on Heterocyclic Aromatic Amine Mutagens/Carcinogens in Fried Beef Patties. *Food and Chemical Toxicology, 32*(10), 897-903.

Felton, J. S., & Knize, M. G. (1991). Occurrence, Identification, and Bacterial Mutagenicity of Heterocyclic Amines in Cooked Food. *Mutat Res, 259*(3-4), 205-217.

Felton, J. S., Knize, M. G., Wu, R. W., Colvin, M. E., Hatch, F. T., & Malfatti, M. A. (2007). Mutagenic potency of food-derived heterocyclic amines. *Mutation Research-Fundamental and Molecular Mechanisms of Mutagenesis, 616*(1-2), 90-94.

Felton, J. S., Malfatti, M. A., Knize, M. G., Salmon, C. P., Hopmans, E. C., & Wu, R. W. (1997). Health risks of heterocyclic amines. *Mutation Research-Fundamental and Molecular Mechanisms of Mutagenesis, 376*(1-2), 37-41.

Fenech, M. (1997). The advantages and disadvantages of the cytokinesis-block micronucleus method. [Review]. *Mutat Res, 392*(1-2), 11-18.

Fenech, M. (2000). The in vitro micronucleus technique. [Review]. *Mutat Res, 455*(1-2), 81-95.

Fenech, M. (2000b). A mathematical model of the in vitro micronucleus assay predicts false negative results if micronuclei are not specifically scored in binucleated cells or in cells that have completed one nuclear division. *Mutagenesis, 15*(4), 329-336.

Fenech, M., Aitken, C., & Rinaldi, J. (1998). Folate, vitamin B12, homocysteine status and DNA damage in young Australian adults. *Carcinogenesis, 19*(7), 1163-1171.

Fenech, M., Chang, W. P., Kirsch-Volders, M., Holland, N., Bonassi, S., & Zeiger, E. (2003). HUMN project: detailed description of the scoring criteria for the cytokinesis-block micronucleus assay using isolated human lymphocyte cultures. *Mutat Res, 534*(1-2), 65-75.

Fenech, M., & Morley, A. A. (1985). Measurement of micronuclei in lymphocytes. *Mutat Res, 147*(1-2), 29-36.

Fenech, M., Neville, S., & Rinaldi, J. (1994). Sex is an important variable affecting spontaneous micronucleus frequency in cytokinesis-blocked lymphocytes. *Mutat Res, 313*(2-3), 203-207.

Fontele, L. J., & Henderson, J. F. (1969). An enzymatic basis for the inability of erythrocytes to synthsize purine ribonucleotides de novo. *Biochem Biophys Acta, 117*, 175-6.

Fowles J, Bates M. The toxic constituents of tobacco and tobacco smoke: priorities for harm reduction. A report to the New Zealand Ministry of Health. March 2000, www.ndp.govt.nz

Frandsen, H., Grivas, S., Andersson, R., Dragsted, L., & Larsen, J. C. (1992). Reaction of the N-2-Acetoxy Derivative of 2-Amino-1-Methyl-6-Phenylimidazo[4,5-B]Pyridine (Phip) with 2'-Deoxyguanosine and DNA - Synthesis and Identification of N-2-(2'-Deoxyguanosin-8-Yl)-Phip. *Carcinogenesis, 13*(4), 629-635.

Freedman, H. J., Parker, N. B., Marinello, A. J., Gurtoo, H. L., & Minowada, J. (1979). Induction, inhibition and biological properties of aryl hydrocarbonhydrolase in a stable human B-lymphocyte cell line. RPMI-1788. *Cancer Res, 39*, 4612-9.

Friesen, M. D., Kaderlik, K., Lin, D. X., Garren, L., Bartsch, H., Lang, N. P., & Kadlubar, F. F. (1994). Analysis of DNA-Adducts of 2-Amino-1-Methyl-6-Phenylimidazo[4,5-B]Pyridine in Rat and Human Tissues by Alkaline-Hydrolysis and Gas-

Chromatography Electron-Capture Mass-Spectrometry - Validation by Comparison with P-32 Postlabeling. *Chem Res Toxicol, 7*(6), 733-739.

Fukushima, S., Wanibuchi, H., Morimura, K., Iwai, S., Nakae, D., Kishida, H., . . . Furukawa, F. (2004). Existence of a threshold for induction of aberrant crypt foci in the rat colon with low doses of 2-amino-1-methyl-6-phenolimidazo[4,5-b]pyridine. *Toxicological Sciences, 80*(1), 109-114.

Fukutome, K., Ochiai, M., Wakabayashi, K., Watanabe, S., Sugimura, T., & Nagao, M. (1994). Detection of Guanine-C8-2-Amino-1-Methyl-6-Phenylimidazo[4,5-B]Pyridine Adduct as a Single Spot on Thin-Layer Chromatography by Modification of the P-32 Postlabeling Method. *Japanese Journal of Cancer Research, 85*(2), 113-117.

Fuscoe, J. C., Fenwick, R. G., Jr., Ledbetter, D. H., & Caskey, C. T. (1983). Deletion and amplification of the HGPRT locus in Chinese hamster cells. *Mol Cell Biol, 3*(6), 1086-1096.

Garner, R. C., Lightfoot, T. J., Cupid, B. C., Russell, D. Coxhead, J. M., Kutschera, W., ...& Turteltaub, K. W. (1999). Comparative biotransformation studies of MeIQx and PhIP in animal models and humans. *Cancer letters, 143*(2), 161-165.

Gasiewicz, T. A., Henry, E. C., & Collins, L. L. (2008). Expression and activity of aryl hydrocarbon receptors in development and cancer. *Crit Rev Eukaryot Gene Expr, 18*(4), 279-321.

Geacintov, N. E., Cosman, M., Hingerty, B. E., Amin, S., Broyde, S., & Patel, D. J. (1997). NMR solution structures of stereoisomeric covalent polycyclic aromatic carcinogen-DNA adducts: Principles, patterns, and diversity. *Chem Res Toxicol, 10*(2), 111-146.

Ghoshal, A., Davis, C. D., Schut, H. A. J., & Snyderwine, E. G. (1995). Possible Mechanisms for Phip-DNA Adduct Formation in the Mammary-Gland of Female Sprague-Dawley Rats. *Carcinogenesis, 16*(11), 2725-2731.

Ginzinger, D.G. (2002). Gene quantification using real-time quantitative PCR: an emerging technology hits the mainstream. *Exp Hematol, 30*(6), 503-512.

Glaab, W. E., Kort, K. L., & Skopek, T. R. (2000). Specificity of mutations induced by the food-associated heterocyclic amine 2-amino-1-methyl-6-phenylimidazo-[4,5-b]-pyridine in colon cancer cell lines defective in mismatch repair. *Cancer Res, 60*(17), 4921-4925.

Glatt, H., Gemperlein, I., Setiabudi, F., Platt, K. L., & Oesch, F. (*1990*). Expression of xenobiotic-metabolizing enzymes in propagatable cell cultures and induction of micronuclei by 13 compounds. *Mutagenesis, 5, 241–*249.

Glatt, H., Pabel, U., Meinl, W., Frederiksen, H., Frandsen, H., & Muckel, E. (2004). Bioactivation of the heterocyclic aromatic amine 2-amino-3-methyl-9H-pyrido [2,3-b]indole (MeA alpha C) in recombinant test systems expressing human xenobiotic-metabolizing enzymes. *Carcinogenesis, 25*(5), 801-807.

Goldman, R., Enewold, L., Pellizzari, E., Beach, J. B., Bowman, E. D., Krishnan, S. S., & Shields, P. G. (2001). Smoking increases carcinogenic polycyclic aromatic hydrocarbons in human lung tissue. *Cancer Res, 61*(17), 6367-6371.

Gonzalez and Gelboin, (1994). Cytochromes, Pages 450.

Gooderham, N. J., Murray, S., Lynch, A. M., Yadollahi-Farsani, M., Zhao, K., Boobis, A. R., & Davies, D. S. (2001). Food-derived heterocyclic amine mutagens: variable metabolism and significance to humans. *Drug metabolism and disposition: the biological fate of chemicals, 29*(4 Pt 2), 529-534.

Gooderham, N. J., Creton, S., Lauber, S. N., & Zhu, H. (2007). Mechanisms of action of the carcinogenic heterocyclic amine PhIP. *Toxicology letters, 168*, 269-277.

Gooderham, N. J., Murray, S., Lynch, A. M., YadollahiFarsani, M., Zhao, K., Rich, K., . . . Davies, D. S. (1997). Assessing human risk to heterocyclic amines. *Mutation Research-Fundamental and Molecular Mechanisms of Mutagenesis, 376*(1-2), 53-60.

Gorlewska-Roberts, K., Green, B., Fares, M., Ambrosone, C. B., & Kadlubar, F. F. (2002). Carcinogen-DNA adducts in human breast epithelial cells. *Environ Mol Mutagen, 39*(2-3), 184-192.

Greenblatt, M. S., Bennett, W. P., Hollstein, M., & Harris, C. C. (1994). Mutations in the P53 Tumor-Suppressor Gene - Clues to Cancer Etiology and Molecular Pathogenesis. *Cancer Res, 54*(18), 4855-4878.

Griffith, A. F., Miller, J. H., Suzuki, D. T., Lewontin, R. C. & Gilbart, W. M. An introduction to genetic analysis. 7th edition. Newyork: W. H. Freeman; 2000.

Grosovsky, A. J., & Little, J. B. (1983). Effect of growth rate on phenotypic expression of 6-thioguanine resistance in human deploid fibroblasts. *Mutat Res, 110*, 163-70.

Gross, G. A., Turesky, R. J., Fay, L. B., Stillwell, W. G., Skipper, P. L., & Tannenbaum, S. R. (1993). Heterocyclic Aromatic Amine Formation in Grilled Bacon, Beef and Fish and in Grill Scrapings. *Carcinogenesis, 14*(11), 2313-2318.

Guengerich, F. P. (1988). Roles of cytochrome P-450 enzymes in chemical carcinogenesis and cancer chemotherapy. *Cancer Res, 48*(11), 2946-2954.

Guengerich, F. P. (1997). Comparisons of catalytic selectivity of cytochrome P450 subfamily enzymes from different species. *Chem Biol Interact, 106*(3), 161-182.

Guengerich, F. P. (2000). Metabolism of chemical carcinogens. *Carcinogenesis, 21*(3), 345-351.

Guengerich, F. P., Dannan, G. A., Wright, S. T., Martin, M. V., & Kaminsky, L. S. (1982). Purification and characterization of liver microsomal cytochromes p-450: electrophoretic, spectral, catalytic, and immunochemical properties and inducibility of

eight isozymes isolated from rats treated with phenobarbital or beta-naphthoflavone. *Biochemistry, 21*(23), 6019-6030.

Gunter, M. J., Probst-Hensch, N. M., Cortessis, V. K., Kulldorff, M., Haile, R. W., & Sinha, R. (2005). Meat intake, cooking-related mutagens and risk of colorectal adenoma in a sigmoidoscopy-based case-control study. *Carcinogenesis, 26*(3), 637-642.

Guo, N., Faller, D. V. & Vaziri, C. (2002). Carcinogen induced S-Phase arrest is Chk1 mediated and caffeine sensitive. *Cell growth and diffrentiation. 13*, 77-96.

Guest, R. D., & Parry, J. M. (1999). P53 integrity in the genetically engineered cell lines AHH-1 and MCL-5. *Mutat Res, 423*, 39-46.

Hagmar, L., Brogger, A., Hansteen, I. L., Heim, S., Hogstedt, B., Knudsen, L., . . . et al. (1994). Cancer risk in humans predicted by increased levels of chromosomal aberrations in lymphocytes: Nordic study group on the health risk of chromosome damage. *Cancer Res, 54*(11), 2919-2922.

Hainaut, P., & Pfeifer, G. P. (2001). Patterns of p53 G-->T transversions in lung cancers reflect the primary mutagenic signature of DNA-damage by tobacco smoke. *Carcinogenesis, 22*(3), 367-374.

Hammons, G. J., Milton, J. D., Stepps, K., Tukey, R. H & Kadlubar, F. F. (1997) Metabolism of carcinogenic heterocyclic and aromatic amines by recombinant human cytochrome P450 enzymes. *Carcinogenesis,* 18, 851–854.

Hankinson, O. (1995). The aryl hydrocarbon receptor complex. *Annu Rev Pharmacol Toxicol, 35*, 307-340.

Hashizume, T., & Oda, H. Application of a New Genotoxicity Test System with Human Hepatocyte Cell Lines to Improve the Risk Assessment in the Drug Development.

Hasnol, N. et al. (2014). Effect of different types of sugars in a marinating formulation on the formation of heterocyclic amines in grilled chicken. *Food Chemistry, 145*, 514-521.

Hanson-Painton, O., Griffin, M.J. & Tang, J. (1981). Involvement of a cytosolic carrier protein fraction in the microsomal metabolism of benzo[a]pyrene in rat liver. *Cancer Res, 43*:4198-4206.

Hashizume, T. & Oda, H. 2012. Application of a New Genotoxicity Test System with Human Hepatocyte Cell Lines to Improve the Risk Assessment in the Drug Development, Toxicity and Drug Testing, Prof. Bill Acree (Ed.), ISBN: 978-953-51-0004-1.

Hattemer-Frey, H. A., and Travis, C. C. 1991. Benzo-*a*-pyrene. Environmental partitioning and human exposure. Toxicol. Ind. Health, *7:* 141–157

He, S. I., & Baker, R. S. (1989). Initiating carcinogen, triethylenemelamine, induces micronuclei in skin target cells. [Research Support, Non-U.S. Gov't]. *Environ Mol Mutagen, 14*(1), 1-5.

Hecht, S. S. (1999). Tobacco smoke carcinogens and lung cancer. *J Natl Cancer Inst, 91*(14), 1194-1210.

Hecht, S. S. (2002). Tobacco smoke carcinogens and breast cancer. Environ and Mol Muta, 39, 119-126.

Hecht, S. S. (2006). Smoking and lung cancer- a new role for an old toxicant. PNAS, 103(43), 15725-6.

Heddle, J. A. (1990). Micronuclei in vivo. *Prog Clin Biol Res, 340B*, 185-194.

Henderson, L., Alkberini, S., & Aardema, M. (2000). Threshold in genotoxicity responses. *Mutat Res, 464*, 123-128.

Hengstler, J. G., Bogdanffy, M. S., Bolt, H. M and Oesch, F. (2003). Challenging dogma – thresholds for genotoxic carcinogens? The case of vinyl acetate. *Annu Rev Pharmacol Toxicol, 43*, 485-520.

Hess, M. T., Gunz, D., Luneva, N., Geacintov, N. E., & Naegeli, H. (1997). Base pair conformation-dependent excision of Benzo[a]pyrene diol epoxide-guanine adducts by human nucleotide excision repair enzymes. *Molecular and Cellular Biology, 17*(12), 7069-7076.

Hewitt, N. J., & Hewitt, P. (2004). Phase I and Phase II enzyme characterization of two sources of HepG2 cell lines. *In Vitro Toxicol, 34*(3), 243-256.

Hewitt, R., Forero, A., Luncsford, P. J., & Martin, F. L. (2007). Enhanced Micronucleus Formation and Modulation of Bcl-2:Bax in MCF-7 Cells after Exposure to Binary Mixtures. *Environmental Health Perspectives, 115*, 129-136.

Hoffmann, D. & Hoffmann, I. (1997). The changing cigarette, 1950–1995. *Journal of Toxicology and Environmental Health, 50*, 307–364.

Hoeijmakers, J. H. (2001). Genome maintenance mechanisms for preventing cancer. *Nature 411*, 366–374.

Hsu, G. W., Huang, X., Luneva, N. P., Geacintov, N. E., & Beese, L. S. (2005). Structure of a high fidelity DNA polymerase bound to a benzo[a]pyrene adduct that blocks replication. *J Biol Chem, 280*(5), 3764-3770.

Hudson, R. E., Bergthorsson, U., & Ochman, H. (2003). Transcription increases multiple spontaneous point mutations in Salmonella enterica. *Nucleic Acids Res, 31*(15), 4517-4522.

International Agency for Research on Cancer (IARC) (2010). Some Non-Heterocyclic Polycyclic Aromatic Hydrocarbons and Some Related Exposures. In IARC Monographs on the Evaluation of Carcinogenic Risks to Humans 92, pp 35-818, IARC, Lyon, France.

IARC (1993). Some naturally occuring substances: food items and constituents, heterocyclic aromatic amines and mycotoxins. IARC Monographs on the Evaluation of Carcinogenic Risks of Chemicals to Humans, World Health Organization, International Agency for Research on Cancer, Lyon, p.56.

IARC (1987). International Agency for Research on Cancer. Overall Evaluations of Carcinogenicity; an Updating of IARC Monographs Volumes 1 to 42, IARC Monographs on the Evaluation of the Carcinogenic Risk of Chemicals to Humans, Supplement 7, IARC, Lyon.

IARC (2010). Some non-heterocyclic polycyclic aromatic hydrocarbons and some related exposures. IARC Monogr Eval Carcinog Risks Hum, 92: 1–853.

Ingelman-Sundberg, M. (2001). Genetic susceptibility to adverse effects of drugs and environmental toxicants. The role of the CYP family of enzymes. *Mutat Res, 482*(1-2), 11-19.

Irigaray, P., & Belpomme, D. (2010). Basic properties and molecular mechanisms of exogenous chemical carcinogens. *Carcinogenesis, 31*(2), 135-148.

Ito, N., Hasegawa, R., Sano, M., Tamano, S., Esumi, H., Takayama, S., & Sugimura, T. (1991). A New Colon and Mammary Carcinogen in Cooked Food, 2-Amino-1-Methyl-6-Phenylimidazo[4,5-B]Pyridine (Phip). *Carcinogenesis, 12*(8), 1503-1506.

Jackson, A. L., & Loeb, L. A. (2001). The contribution of endogenous sources of DNA damage to the multiple mutations in cancer. *Muta Res, 477*, 7-21.

Jancso, M. A., Sculaccio, S. A., & Thiemann, O. H. (2001). Identification of sugarcane genes involved in the purine synthesis pathway. *Genetics and Molecular Biology, 24*(1-4), 251-255.

Jeffrey, A. M., Grzeskowiak, K., Weinstein, I. B., Nakanishi, K., Roller, P., & Harvey, R. G. (1979). Benzo(a)Pyrene-7,8-Dihydrodiol 9,10-Oxide Adenosine and Deoxyadenosine Adducts - Structure and Stereochemistry. *Science, 206*(4424), 1309-1311.

Jenkins, G. J. S., Doak, S. H., Johnson, G. E., Quick, E., Waters, E. M., & Parry, J. M. (2005). Do dose response thresholds exist for genotoxic alkylating agents? *Mutagenesis, 20*(6), 389-398.

Jenkins, G. J., Zair, Z., Johnson, G. E., & Doak, S. H. (2010). Genotoxic thresholds, DNA repair, and susceptibility in human populations. *Toxicology, 278*(3), 305-310.

Jerina, D. M., & Daly, J. W. In "Drug Metabolism: Parke, D.V., Smith, R.L., Eds., Taylor and Francis, London, 1976, pp. 13-32.

Jinnah, H. A., De Gregorio, L., Harris, J. C., Nyhanb, W. L., & O'Neill, J. P. (2000). The spectrum of inherited mutations causing HPRT deficiency: 75 new cases and a review of 196 previously reported cases. *Mutat Res, 463*, 309-329.

Johnson, G. E. (2012). Mammalian cell HPRT gene mutation assay: Test methods. *Genetic Toxicology*. Springer New York,. 55-67.

Johnson, G. E., Doak, S. H., Griffiths, S. M., Quick, E. L., Skibinski, D. O. F., Zair, Z. M., & Jenkins, G. J. (2009). Non-linear dose response of DNA-reactive genotoxins: Recommendations for data analysis. *Muta Res, 678*, 95-100.

Johnson, G. E., Quick, E. L., Parry, E. M., & Parry, J. M. (2010). Metabolic influences for mutation induction curves after exposure to Sudan-1 and para red. *Mutagenesis, 25*(4), 327-333.

Jolly, D. J., Okayama, H., Berg, P., Esty, A. C., Filpula, D., Bohlen, P.,.....Friedman, T. (1983). Isolation and characterization of a full-length expressible cDNA for human hprt. *Proc Nat Acad Sci, USA, 80*, 477-481.

Kadlubar, F. F., & Badawi, A. F. (1995). Genetic susceptibility and carcinogen-DNA adduct formation in human urinary bladder carcinogenesis. *Toxicol Lett, 82-3*, 627-632.

Kapitulnik, J., Levin, W., Conney, A. H., Yagi, H., & Jerina, D. M. (1977). Benzo[a]Pyrene 7,8-Dihydrodiol Is More Carcinogenic Than Benzo[a]Pyrene in Newborn Mice. *Nature, 266*(5600), 378-380.

Kato, R., & Yamazoe, Y. (1987). Metabolic-Activation and Covalent Binding to Nucleic-Acids of Carcinogenic Heterocyclic Amines from Cooked Foods and Amino-Acid Pyrolysates. *Japanese Journal of Cancer Research, 78*(4), 297-311.

Keating, G. A., Bogen, K. T., & Chan, J. M. (2007). Development of a meat frequency questionnaire for use in diet and cancer studies. *J Am Diet Assoc, 107*(8), 1356-1362.

Kinoshita, A., Wanibuchi, H., Wei, M., & Fukushima, S. (2006). Hormesis in carcinogenecity of Non-genotoxic Carcinogens. *J Toxicol Pathol, 19*, 111-122.

Kirkland, D., Aardema, M., Henderson, L., & Muller, L. (2005). Evaluation of the ability of a battery of three in vitro genotoxicity tests to discriminate rodent carcinogens and non-carcinogens I. Sensitivity, specificity and relative predictivity. *Mutat Res, 584*(1-2), 1-256.

Kirsch-Volders, M., Aardema, M and Elhajouji, A. (2000). Concepts of threshold in mutagenesis and carcinogenesis. *Mutat. Res*. 464, 3-11.

Kirsch-Volders, M., Vanhauwaert, A., Eichenlaub-Ritter, U and Decordier, I. (2003). Indirect mechanisms of genotoxicity. *Toxicology Letters. 140-141*, 63-74.

Kirsch-Volders, M., Decordier, I., Elhajouji, A., Plas, G., Aardema, M. J. & Fenech, M. (2011). *In vitro* genotoxicity testing using the micronucleus assay in cell lines, human lymphocytes and 3D human skin models. *Mutagenesis, 26*(1), 177-184.

Kirsch-Volders, M., Gonzalez, L., Carmichael, P., & Kirkland, D. (2009). Risk assessment of genotoxic mutagens with thresholds: A brief introduction. *Mutat. Res, 687*, 72-75.

Kirsch-Volders, M., Mateuca, R. A., Roelants, M., Tremp, A., Zeiger, E., Bonassi, S., . . . Fenech, M. (2006). The effects of GSTM1 and GSTT1 polymorphisms on micronucleus frequencies in human lymphocytes in vivo. *Cancer Epidemiol Biomarkers Prev, 15*(5), 1038-1042.

Kim D, Guengerich FP. Cytochrome P450 activation of arylamines and heterocyclic amines. Annual Review of Pharmacology and Toxicology 2005;45:27–49

Kim, J. H., Stansbury, K. H., Walker, N. J., Trush, M. A., Strickland, P. T.& Sutter, T. R. (1998). Metabolism of benzo[a]pyrene and benzo[a]pyrene-7,8-diol by human cytochrome P450 1B1. Carcinogenesis, 19(10), (Oct), 1847-1853.

King, R. S., Kadlubar, F. F., Turesky, R. J., 2000. *In vivo* metabolism of heterocyclic amines. In: Nagao, M., Sugimura, T. (Eds.), Food Borne Carcinogens: Heterocyclic Amines. John Wiley & Sons, Ltd., Chichester, England, pp. 90–111.

Klareskog, L., Padyukov, L., & Alfredsson, L. (2007). Smoking as a trigger for inflammatory rheumatic diseases. *Current Opinion in Rheumatology, 19*(1), 49-54.

Klaunig, J. E., Kamendulis, L. M., & Xu, Y. (2000). Epigenetic mechanisms of chemical carcinogenesis. *Human & Experimental Toxicology, 19*(10), 543-555.

Knasmuller, S., Mersch-Sundermann, V., Kevekordes, S., Darroudi, F., Huber, W. W., Hoelzl, C., . . . Majer, B. J. (2004a). Use of human-derived liver cell lines for the detection of environmental and dietary genotoxicants; current state of knowledge. [Review]. *Toxicology, 198*(1-3), 315-328.

Knasmuller, S., Parzefall, W., Sanyal, R., Ecker, S., Schwab, C., Uhl, M., . . . Natarajan, A. T. (1998a). Use of metabolically competent human hepatoma cells for the detection of mutagens and antimutagens. *Mutation Research-Fundamental and Molecular Mechanisms of Mutagenesis, 402*(1-2), 185-202.

Knasmuller, S., Schwab, C. E., Land, S. J., Wang, C. Y., Sanyal, R., Kundi, M., . . . Darroudi, F. (1999). Genotoxic effects of heterocyclic aromatic amines in human derived hepatoma (HepG2) cells. *Mutagenesis, 14*(6), 533-539.

Knasmüller, S., Uhl, M., Fahrig, R., Darroudi, F., Mersch-Sundermann, V., Bader, A., Sanyal, R., Schwab, C., Hietsch, G., Parzefall, W. & Natarajan, A. T. (1999). Development and application of tests with human derived cells for the detection of environmental genotoxins. *J. Indian Genet. Soc.*, in press

Knize, M. G., Dolbeare, F. A., Carroll, K. L., Moore, D. H., 2nd, & Felton, J. S. (1994). Effect of cooking time and temperature on the heterocyclic amine content of fried beef patties. *Food Chem Toxicol, 32*(7), 595-603.

Knize, M. G., Salmon, C. P., Pais, P., & Felton, J. S. (1999). Food heating and the formation of heterocyclic aromatic amine and polycyclic aromatic hydrocarbon mutagens/carcinogens. *Adv Exp Med Biol, 459*, 179-193.

Knowles, B. B., Howe, C. C., & Aden, D. P. (1980). Human hepatocellular carcinoma cell lines secrete the major plasma proteins and hepatitis B surface antigen. S*cience, 209*(4455), 497-499.

Knudson, A.G., Jr. (1971). Mutation and cancer: statistical study of retinoblastoma. *Proc Natl Acad Sci U S A*, 68 , 820-823.

Koch, K. S., Fletcher, R. G., Grond, M. P., Inyang, A. I., Lu, X. P., Brenner, D. A., & Leffert, H. L. (1993). Inactivation of plasmid reporter gene expression by one benzo(a)pyrene diol-epoxide DNA adduct in adult rat hepatocytes. *Cancer Res, 53*(10 Suppl), 2279-2286.

Kohler, S. W., Provost, G. S., Feick, A., Kretz, P. L., Bullock, W. O., Putman, D. L., Sorge, J. A., & Short, J. M. (1991). Analysis of spontaneous and induced mutations in transgenic mice using a lambda ZAP/lacI shuttle vector. *Environ Mol Mutagen, 18*, 316-21.

Korenberg, J. R., Chen, X. N., Schipper, R., Sun, Z., Gonsky, R., Gerwehr, S., . . . et al. (1994). Down syndrome phenotypes: the consequences of chromosomal imbalance. *Proc Natl Acad Sci U S A, 91*(11), 4997-5001.

Ku, W. W., Bigger, A., Brambilla, G., Glatt, H., Gocke, E., Guzzie, P. J., . . . Roberts, S. (2007). Strategy for genotoxicity testing--metabolic considerations. *Mutat Res, 627*(1), 59-77.

Kulling, S. E., & Metzler, M. (1997). Induction of micronuclei, DNA strand breaks and HPRT mutations in cultured Chinese hamster V79 cells by the phytoestrogen coumoestrol. *Food and Chemical Toxicology, 35*(6), 605-613.

Lah, K. (2011). Polycyclic Aromatic Hydrocarbons (PAHs).

Laser Reutersward, A., Skog, K., & Jagerstad, M. (1987). Effects of creatine and creatinine content on the mutagenic activity of meat extracts, bouillons and gravies from different sources. *Food Chem Toxicol, 25*(10), 747-754.

Lauber, S. N., Ali, S., & Gooderham, N. J. (2004). The cooked food derived carcinogen 2-amino-1-methyl-6-phenylimidazo[4,5-b] pyridine is a potent oestrogen: a mechanistic basis for its tissue-specific carcinogenicity. *Carcinogenesis, 25*(12), 2509-2517.

Lehninger, A. L., Vercesi, A., & Bababunmi, E. A. (1978). Regulation of Ca2+ release from mitochondria by the oxidation-reduction state of pyridine nucleotides. *Proc Natl Acad Sci U S A.*

Le Marchand, L., Kolonel, L. N., Wilkens, L. R., Myers, B. C., & Hirohata, T. (1994). Animal fat consumption and prostate cancer: a prospective study in Hawaii. *Epidemiology, 5*(3), 276-282.

Levin, W., Wood, A. W., Wislocki, P. G., Chang, R. L., Kapitulnik, J., Mah, H. D., Yagi, H., Jerina, D. M., & Conney, A. H. (1978) Mutagenicity and carcinogenicity of

benzo[a]pyrene derivatives. In *Polycyclic Hydrocarbons and Cancer* (HV Gelboin and POP Ts'o eds) pp. 189–202. Academic Press, New York.

Levin, W., Wood, A. W., Yagi, H., Jerina, D. M., & Conney, A. H. (1976). (+/-)-trans-7,8-dihydroxy-7,8-dihydrobenzo (a)pyrene: a potent skin carcinogen when applied topically to mice. *Proc Natl Acad Sci U S A, 73*(11), 3867-3871.

Levy, J. A., Virolainen, M., & Defendi, V. (1968). Human lymphoblastoid lines from lymph node and spleen. *Cancer, 22*(3), 517-524.

Lewis, P. D., et al. (2001) Spontaneous mutation spectra in supF: comparative analysis of mammalian cell line base substitution spectra. *Mutagenesis, 16*, 503–515.

Lewis, P., & Parry, J. M. (2002). An exploratory analysis of multiple mutation spectra. *Mutat Res, 518*(2), 163-180.

Li, R., Tian, J., Li, W., & Xie, J. (2013). Effects of 2-amino-1-methyl-6-phenylimidazo [4, 5-b] pyridine (PhIP) on histopathology, oxidative stress, and expression of c-fos, c-jun and p16 in rat stomachs. Food and Chemical Toxicol, 55, 182-191.

Lightfoot, T. J., Skibola, C. F., Willett, E. V., Skibola, D. R., Allan, J. M., Coppede, F., . . . Smith, M. T. (2005). Risk of non-Hodgkin lymphoma associated with polymorphisms in folate-metabolizing genes. *Cancer Epidemiology Biomarkers & Prevention, 14*(12), 2999-3003.

Lin, C. H., Huang, X., Kolbanovskii, A., Hingerty, B. E., Amin, S., Broyde, S., . . . Patel, D. J. (2001). Molecular topology of polycyclic aromatic carcinogens determines DNA adduct conformation: a link to tumorigenic activity. *J Mol Biol, 306*(5), 1059-1080.

Lin, D., Kaderlik, K. R., Turesky, R. J., Miller, D. W., Lay, J. O., Jr., & Kadlubar, F. F. (1992). Identification of N-(Deoxyguanosin-8-yl)-2-amino-1-methyl-6-phenylimidazo [4,5-b]pyridine as the major adduct formed by the food-borne carcinogen, 2-amino-1-methyl-6-phenylimidazo[4,5-b]pyridine, with DNA. [In Vitro]. *Chem Res Toxicol, 5*(5), 691-697.

Lin, D., Meyer, D. J., Ketterer, B., Lang, N. P., & Kadlubar, F. F. (1994). Effects of human and rat glutathione S-transferases on the covalent DNA binding of the N-acetoxy derivatives of heterocyclic amine carcinogens in vitro: a possible mechanism of organ specificity in their carcinogenesis. *Cancer Res, 54*(18), 4920-4926.

Lin, D. X., Kaderlik, K. R., Turesky, R. J., Miller, D. W., Lay, J. O., & Kadlubar, F. F. (1992). Identification of N-(Deoxyguanosin-8-Yl)-2-Amino-1-Methyl-6-Phenylimidazo[4,5-B]Pyridine as the Major Adduct Formed by the Food-Borne Carcinogen, 2-Amino-1-Methyl-6-Phenylimidazo[4,5-B]Pyridine, with DNA. *Chem Res Toxicol, 5*(5), 691-697.

Lindahl, T., & Nyberg, B. (1972). Rate of depurination of native deoxyribonucleic acid. *Biochemistry, 11*(19), 3610-3618.

Ling, Y. H., Chan, J. Y., Beattie, K. L., & Nelson, J. A. (1992). Consequences of 6-Thioguanine Incorporation into DNA on Polymerase, Ligase, and Endonuclease Reactions. *Mol Pharmacol, 42*(5), 802-807.

Liu, S, X., Cao, J., An, H., Shun, H. M., Yang, L. J., & Liu, Y. (2003). Analysis of spontaneous gamma ray and ethylnitrosourea-induced Hprt mutants in HL-60 cells with multiplex PCR. *World J Garteroenterol, 9,* 578-83.

Livak, K. J., Prism, A. B. I. 7700 Sequence detection System User Bulletin #2 Relative quantification of gene expression; 1997 &2001.http://docs.appliSchmittgen,

Loeb, L. A., & Cheng, K. C. (1990). Errors in DNA synthesis: a source of spontaneous mutations. *Mutat Res, 238*(3), 297-304.

Loeb, K. R., & Loeb, L. A. (2000). Significance of multiple mutations in cancer. Carcinogenesis, 21(3), 379-385.

Loeb, L. A., Loeb, K. R., & Anderson, J. P. (2003). Multiple mutations and cancer. *PNAS, 100*(3), 776-781.

Lorge, E., Hayashi, M., Albertini, S., & Kirkland, D. (2008). Comparison of different methods for an accurate assessment of cytotoxicity in the in vitro micronucleus test. I. Theoretical aspects. *Mutat Res, 655*(1-2), 1-3.

Lovell, D. P. (2000). Dose-response and threshold –mediated mechanisms in mutagenesis: statistical models and study design. *Mutat Res, 464*, 87-95.

Luch, A. (2005). Nature and nurture - Lessons from chemical carcinogenesis. *Nature Reviews Cancer, 5*(2), 113-125.

Lutz, W. K. (1982). Inducible repair of DNA methylated by carcinogens. *Trends Pharmacol. Sci. 3*, 398–399.

Lutz, W. K. (1998). Dose-response relationships in chemical carcinogenesis: superposition of different mechanisms of action, resulting in linear-non-linear curves, practical thresholds, J-shapes. *Mutat Res, 405*, 117-124.

Lutz, W. K. (1990). Dose-esponse relaMomsMp and low dose extrapolation in chemical Carcinogenesis. *Carcinogenesis, 11*(8), 1243-1247.

Lutz, U., Lugli, S., Bitsch, A., Schlatter, J., and Lutz, W. K. (1997). Dose response for the stimulation of cell division by caffeic acid in forestomach and kidney of the male F344 rat. *Fundam. Appl. Toxicol. 39*, 131–137.

Lutz, W. K., & Lutz, R. W. (2009). Statistical model to estimate a threshold dose and its confidence limits for the analysis of sub-linear dose-response relationships, examplified for mutagencity data. *Mutat Res, 678*, 118-122.

Lynch, A. M., Gooderham, N. J., Davies, D. S., & Boobis, A. R. (1998). Genetic analysis of PHIP intestinal mutations in Muta (TM) Mouse. *Mutagenesis, 13*(6), 601-605.

Lynch, A., Harvey, J., Aylott, M., Nicholas, E., Burmann, M., Siddiqui, A., Walker, S., & Rees, R. (2003). Investigation into the concept of a threshold for topoisomerase inhibitor- induced clastogenecity. *Mutatgensis, 18*, 345-353.

MacGregor, J. T., Casciano, D., & Muller, L. (2000). Strategies and testing methods for identifying mutagenic risks. [Review]. *Mutat Res, 455*(1-2), 3-20.

Madle,S., van der Hude, W., Broschinski, L and Janig, G (2002) Threshold effects in genetic toxicity:perspective of chemical regulation in Germany. *Mutat. Res.* 464, 149-153.

Magagnotti, C., Pastorelli, R., Pozzi, S., Andreoni, B., Fanelli, R., & Airoldi, L. (2003). Genetic polymorphisms and modulation of 2-amino-1-methyl-6-phenylimidazo[4,5-b]pyridine (PhIP)-DNA adducts in human lymphocytes. *International Journal of Cancer, 107*(6), 878-884.

Majer, B. J., Mersch-Sundermann, V., Darroudi, F., Laky, B., de Wit, K., & Knasmuller, S. (2004). Genotoxic effects of dietary and lifestyle related carcinogens in human derived hepatoma (HepG2, Hep3B) cells. *Mutat Res, 551*(1-2), 153-166.

Malfatti, M. A., Dingley, K. H., Nowell-Kadlubar, S., Ubick, E. A., Mulakken, N., Nelson, D., . . . Turteltaub, K. W. (2006). The urinary metabolite profile of the dietary carcinogen 2-amino-1-methyl-6-phenylimidazo[4,5-b]pyridine is predictive of colon DNA adducts after a low-dose exposure in humans. *Cancer Res, 66*(21), 10541-10547.

Malfatti, M. A., & Felton, J. S. (2004). Human UDP-glucuronosyltransferase 1A1 is the primary enzyme responsible for the N-glucuronidation of N-hydroxy-PhIP in vitro. *Chem Res Toxicol, 17*(8), 1137-1144.

Manabe, S., Kurihara, N., Wada, O., Izumikawa, S., Asakuno, K., & Morita, M. (1993). Detection of a carcinogen, 2-amino-1-methyl-6-phenylimidazo [4,5-b]pyridine, in airborne particles and diesel-exhaust particles. *Environmental Pollution, 80*(3), 281-286.

Manabe, S., Suzuki, H., Wada, O., & Ueki, A. (1993). Detection of the carcinogen 2-amino-1-methyl-6-phenylimidazo[4,5-b]pyridine (PhIP) in beer and wine. *Carcinogenesis, 14*(5), 899-901.

Mapoles, J., Berthou, F., Alexander, A., Simon, F. and Menez, J.-F. (1993). Mammalian PC-12 cell genetically engineered for human cytochrome P450 2E1 expression. *Eur. J. Biochem.* 214, 735–745.

Marnett, L. J., & Plastaras, J. P. (2001). Endogenous DNA damage and mutation. [Review]. *Trends in Genetics, 17*(4), 214-221.

Masunaga, S., Ono, K., & Abe, M. (1991). A method for the selective measurement of the radiosensitivity of quiescent cells in solid tumors--combination of immunofluorescence staining to BrdU and micronucleus assay. *Radiat Res, 125*(3), 243-247.

Mateuca, R., Lombaert, N., Aka, P. V., Decordier, I., & Kirsch-Volders, M. (2006). Chromosomal changes: induction, detection methods and applicability in human biomonitoring. *Biochimie, 88*(11), 1515-1531.

Matsumoto, T., Yoshida, D., & Tomita, H. (1981). Determination of mutagens, amino-alpha-carbolines in grilled foods and cigarette smoke condensate. *Cancer Lett, 12*(1-2), 105-110.

Mersch-Sundermann, V., Knasmuller, S., Wu, X. J., Darroudi, F., & Kassie, F. (2004). Use of a human-derived liver cell line for the detection of cytoprotective, antigenotoxic and cogenotoxic agents. *Toxicology, 198*(1-3), 329-340.

Meschini, R., Berni, A., Marotta, E., Filippi, S., Fiore, M., Mancinelli, P., . . . Palitti, F. (2010). DNA repair mechanisms involved in the removal of DBPDE-induced lesions leading to chromosomal alterations in CHO cells. *Cytogenet Genome Res, 128*(1-3), 124-130.

Meschini, R., Marotta, E., Berni, A., Filippi, S., Fiore, M., Mancinelli, P., . . . Palitti, F. (2008). DNA repair deficiency and BPDE-induced chromosomal alterations in CHO cells. *Mutation Research-Fundamental and Molecular Mechanisms of Mutagenesis, 637*(1-2), 93-100.

Miller.E. and Miller *J.* (1966) Mechanisms of chemical carcinogenesis: nature of proximate carcinogens and interactions with macromolecules. *Pharmacol Rev,* 18, 805-835.

Miller, K. P., & Ramos, K. S. (2008). Molecular mechanisms of environmental atherogenesis. *Atherosclerosis and Oxidant Stress, 8,* 161-211.

Miller, K. P., & Ramos, K. S. (2001). Impact of cellular metabolism on the biological effects of benzo[a]pyrene and related hydrocarbons. *Drug Metab Rev, 33*(1), 1-35.

Mimura, J., Ema, M., Sogawa, K., & Fujii-Kuriyama, Y. (1999). Identification of a novel mechanism of regulation of Ah (dioxin) receptor function. [Research Support, Non-U.S. Gov't]. *Genes Dev, 13*(1), 20-25.

Minchin, R. F., Reeves, P. T., Teitel, C. H., McManus, M. E., Mojarrabi, B., Ilett, K. F., & Kadlubar, F. F. (1992). N-and O-acetylation of aromatic and heterocyclic amine carcinogens by human monomorphic and polymorphic acetyltransferases expressed in COS-1 cells. *Biochem Biophys Res Commun, 185*(3), 839-844.

Mocquet, V., Kropachev, K., Kolbanovskiy, M., Kolbanovskiy, A., Tapias, A., Cai, Y., . . . Egly, J. M. (2007). The human DNA repair factor XPC-HR23B distinguishes stereoisomeric benzo[a]pyrenyl-DNA lesions. *Embo Journal, 26*(12), 2923-2932.

Morgan, C., & Lewis, P. D. (2006). iMARS - Mutation analysis reporting software: An analysis of spontaneous cII mutation spectra. *Mutation Research-Genetic Toxicology and Environmental Mutagenesis, 603*(1), 15-26.

Morgenthaler, P. M. L., & Holzhauser, D. (1995). Analysis of Mutations Induced by 2-Amino-1-Methyl-6-Phenylimidazo[4,5-B]Pyridine (Phip) in Human Lymphoblastoid-Cells. *Carcinogenesis, 16*(4), 713-718.

Morrison, T. B., Weis, J. J., & Wittwer, C. T., (1998). Quantification of low-copy transcripts by continuous SYBR Green I monitoring during amplification. *Biotechniques, 24*(6), 954-962.

Muller, L., Mauthe, R. J., Riley, C. M., Andino, M. M., Antonis, D. D., Beels, C., . . . Yotti, L. (2006). A rationale for determining, testing, and controlling specific impurities in pharmaceuticals that possess potential for genotoxicity. *Regul Toxicol Pharmacol, 44*(3), 198-211. doi: 10.1016/j.yrtph.2005.12.001

Muñoz, B., & Albores, A. (2011). "DNA Damage Caused by Polycyclic Aromatic Hydrocarbons: Mechanisms and Markers."

Murli, S., & Walker, G. C. (1993). SOS mutagenesis. *Curr Opin Genet Dev, 3*(5), 719-725.

Nagaoka, H., Wakabayashi, K., Kim, S. B., Kim, I. S., Tanaka, Y., Ochiai, M., . . . Nagao, M. (1992). Adduct Formation at C-8 of Guanine on Invitro Reaction of the Ultimate Form of 2-Amino-1-Methyl-6-Phenylimidazo[4,5-B]Pyridine with 2'-Deoxyguanosine and Its Phosphate-Esters. *Japanese Journal of Cancer Research, 83*(10), 1025-1029.

Nagata, K., & Yamazoe, Y. (2002). Genetic polymorphism of human cytochrome p450 involved in drug metabolism. *Drug Metab Pharmacokinet, 17*(3), 167-189.

Natarajan, A. T., & Darroudi, F. (1991). Use of human hepatoma cells for in vitro metabolic activation of chemical mutagens/carcinogens. *Mutagenesis, 6*(5), 399-403.

National Toxicology Program, 2011. US Department of Health and Human Services Public Health Service, National Toxicology Program. Report on Carcinogens, 12th ed., pp. 220–222

National Toxicology Program. Report on Carcinogenesis. Eleventh Edition. U.S. Department of Health and Human Services, Public Health Service, Research Triangle Park; N.C.: 2005. National Toxicology Program.

Natsumeda, Y., Prajda, N., Donohue, J. P. Glover, J. L. & Weber, G. (1984). Enzymic Capacities of Purine *de Novo* and Salvage Pathways for Nucleotide Synthesis in Normal and Neoplastic Tissues. *Cancer Res, 44*, 2475.

Neal, M. S., Zhu, E., & Foster, W. G. (2008). Quantification of benzo[a]pyrene and other PAHs in the serum and follicular fluid of smokers versus non-smokers. *Reproductive Toxicology, 25*(1), 100-106.

Nebert, D. W., Roe, A. L., Dieter, M. Z., Solis, W. A., Yang, Y., & Dalton, T. P. (2000). Role of the aromatic hydrocarbon receptor and [Ah] gene battery in the oxidative stress response, cell cycle control, and apoptosis. *Biochem Pharmacol, 59*(1), 65-85.

Nelson, J. A., Carpenter, J. W., Rose, L. M., & Adamson, D. J. (1975). Mechanisms of action of 6-thioguanine, 6-mercaptopurine, and 8-azaguanine. *Cancer Res, 35*, 2872-8.

Nesnow, S., Ross, J., Stoner, G., & Mass, M. (1995*). Toxicology, 103*, 403 - 413.

Nguyen, L. P., & Bradfield, C. A. (2008). The search for endogenous activators of the aryl hydrocarbon receptor. *Chem Res Toxicol, 21*(1), 102-116.

Ni, W., McNaughton, L., LeMaster, D. M., Sinha, R., & Turesky, R. J. (2008). Quantitation of 13 heterocyclic aromatic amines in cooked beef, pork, and chicken by liquid chromatography-electrospray ionization/tandem mass spectrometry. [Research Support, Non-U.S. Gov't]. *Journal of agricultural and food chemistry, 56*(1), 68-78.

Norman, D., Abuaf, P., Hingerty, B. E., Live, D., Grunberger, D., Broyde, S., & Patel, D. J. (1989). Nmr and Computational Characterization of the N-(Deoxyguanosin-8-Yl)Aminofluorene Adduct [(Af)G] Opposite Adenosine in DNA - (Af)G[Syn].A[Anti] Pair Formation and Its Ph-Dependence. *Biochemistry, 28*(18), 7462-7476.

Norrish, A. E., Ferguson, L. R., Knize, M. G., Felton, J. S., Sharpe, S. J., & Jackson, R. T. (1999). Heterocyclic amine content of cooked meat and risk of prostate cancer. *J Natl Cancer Inst, 91*(23), 2038-2044.

Odagiri, Y., Takemoto, K., & Fenech, M. (1994). Micronucleus induction in cytokinesis-blocked mouse bone marrow cells in vitro following in vivo exposure to X-irradiation and cyclophosphamide. *Environ Mol Mutagen, 24*(1), 61-67.

OECD, 2007. Organization of economic cooperation and development. OECD guideline for the testing of chemicals, draft proposal for a new guideline 487: *In vitro* Mammalian Cell Micronucleus Test (MNvit).

OECD (1997) Organisation for Economic Co-operation and Development. Ninth adden- dum to the OECD Guidelines for the Testing of Chemicals. In Vitro Mammalian Cell Gene Mutation Test: 476.

Olaharski, A. J., Sotelo, R., Solorza-Luna, G., Gonsebatt, M. E., Guzman, P., Mohar, A., & Eastmond, D. A. (2006). Tetraploidy and chromosomal instability are early events during cervical carcinogenesis. *Carcinogenesis, 27*(2), 337-343.

O'Neil, J. P., Rogan, P. K., Cariello, N., & Nicklas, J. A. (1998). Mutations that alter RNA splicing of the human HPRT gene: a review of the spectrum. *Mutation Research-Reviews in Mutation Research, 411*(3), 179-214.

Obach, R. S., & Dobo, K. L. (2008). Comparison of metabolite profiles generated in Aroclor-induced rat liver and human liver subcellular fractions: considerations for in vitro genotoxicity hazard assessment. [Comparative Study]. *Environ Mol Mutagen, 49*(8), 631-641.

Okonogi, H., Ushijima, T., Zhang, X. B., Heddle, J. A., Suzuki, T., Sofuni, T., . . . Nagao, M. (1997). Agreement of mutational characteristics of heterocyclic amines in lacI of the

Big Blue(R) mouse with those in tumor related genes in rodents. *Carcinogenesis, 18*(4), 745-748.

Otsuka, C., Miura, K. F., Satoh, T., Hatanaka, M., Wakabayashi, K., & Ishidate, M., Jr. (1996). Cytogenetic effects of a food mutagen, 2-amino-1-methyl-6-phenylimidazo[4,5-beta]pyridine (PhIP), and its metabolite, 2-hydroxyamino-1-methy-6-phenylimidazo[4,5-beta]pyridine (N-OH-PhIP), on human and Chinese hamster cells in vitro. *Mutat Res, 367*(3), 115-121.

Oyama, T., Kagawa, N., Kunugita, N., Kitagawa, K., Ogawa, M., Yamaguchi, T. *et al.* (2004). *Front Biosci, 9*, 1967–1976.

Pai, G. S., Sprenkle, J. A., Do, T. T., Mareni, C. E., & Migeon, B. R. (1980). Localization of loci for hypoxanthine phosphoribosyltransferase and glucose-6-phosphate dehydrogenase and biochemical evidence of nonrandom X chromosome expression from studies of a human X-autosome translocation. *Proc Natl Acad Sci U S A, 77*(5), 2810-2813.

Paolini, M., & Cantelli-Forti, G. (1997). On the metabolizing systems for short-term genotoxicity assays: a review. *Mutat Res, 387*(1), 17-34.

Parry J M, Parry E M, Johnson G, Quick E and Waters E M (2005) The detection of genotoxic activity and the quantitative and qualitative assessment of the consequences of exposures, Exp Toxicol Pathol57: Suppl 1 205–212.

Patel, P. I., Nussbaum, R. L., Gramson, P. E., Ledbetter, D. H., Caskey, C. T., & Chinault, A. C. (1984). Organization of the HPRT gene and related sequences in the human genome. *Somat Cell Mol Genet, 10*(5), 483-93.

Patterson, A. D., Gonzalez, F. J., & Idle, J. R. (2010). Xenobiotic metabolism: A review through the metabolometer. Chem Res Toxicol, 23, 851-860.

Pecorino, L. (2006). *Molecular Biology Of Cancer*, Oxford University Press.

Pelkonen, O., & Nebert, D. W. (1982). Metabolism of polycyclic aromatic hydrocarbons: etiologic role in carcinogenesis. *Pharmacol Rev, 34*(2), 189-222.

Penman, B. W., Chen, L., Gelboin, H. V., Gonzalez, F. J., & Crespi, C. L. (1994). Development of a human lymphoblastoid cell line constitutively expressing human CYP1A1 cDNA: substrate specificity with model substrates and promutagens. [Comparative Study]. *Carcinogenesis, 15*(9), 1931-1937.

Perez, C., Lopez de Cerain, A., & Bello, J. (2002). Induction of micronuclei in V79 cells after combined treatments with heterocyclic aromatic amines. *Food Chem Toxicol, 40*(10), 1463-1467.

Peyton, R. (1911). A Sarcoma of the Fowl Transmissible by an Agent Separable from the Tumor Cells. *Journal of Experimental Medicine 13*(4), 397–411.

Pfau, W., Martin, F. L., Cole, K. J., Venitt, S., Phillips, D. H., Grover, P. L., & Marquardt, H. (1999). Heterocyclic aromatic amines induce DNA strand breaks and cell transformation. *Carcinogenesis, 20*(4), 545-551.

Pfau, W., Schulze, C., Shirai, T., Hasegawa, R., & Brockstedt, U. (1997). Identification of the major hepatic DNA adduct formed by the food mutagen 2-amino-9H-pyrido[2,3-b]indole (A alpha C). *Chem Res Toxicol, 10*(10), 1192-1197.

Pfeifer, G. P., Denissenko, M. F., Olivier, M., Tretyakova, N., Hecht, S. S., & Hainaut, P. (2002). Tobacco smoke carcinogens, DNA damage and p53 mutations in smoking-associated cancers. *Oncogene, 21*(48), 7435-7451.

Phillips, D. H. (1999). Polycyclic aromatic hydrocarbons in the diet. [Review]. *Mutat Res, 443*(1-2), 139-147.

Poirier, M. C., Santella, R. M. & Weston, A. (2000). Carcinogen macromolecular adducts and their measurement. *Carcinogenesis, 21*, 353-359

Pullman, A., & Pullman, B. (1955). *Adv. Cancer. Res. 3*, 117-69.

Quinn, A. M., Harvey, R. G., & Penning, T. M. (2008). Oxidation of PAH trans-Dihydrodiols by Human Aldo-Keto Reductase AKR1B10. *Chemical Research in Toxicology, 21*(11), 2207-2215.

Richard, L., James, W. D., Tania, B. A., Stephen, B., Alexander, G., & Michael, L. W. (2008). *Molecular biology of the gene* (6th ed.). San Francisco: Pearson/Benjamin Cummings. ISBN 0-8053-9592-X.

Rodriguez, H., & Loechler, E. L. (1993b). Mutational Specificity of the (+)-Anti-Diol Epoxide of Benzo[a]Pyrene in a Supf Gene of an Escherichia-Coli Plasmid - DNA-Sequence Context Influences Hotspots, Mutagenic Specificity and the Extent of Sos Enhancement of Mutagenesis. *Carcinogenesis, 14*(3), 373-383.

Roemer, E., Stabbert, R., Rustemeier, K., Veltel, D. J., Meisgen, T. J., Reininghaus, W., ... & Podraza, K. F. (2004). Chemical composition, cytotoxicity and mutagenicity of smoke from US commercial and reference cigarettes smoked under two sets of machine smoking conditions. *Toxicology, 195*(1), 31-52.

Rogozin, I. B. et al. (2003) Theoretical analysis of mutation hotspots and their DNA sequence context specificity. *Mutat. Res, 544*, 65–85.

Rudd, N. L., Hoar, D. I., Greentree, C. L., Dimnik, L. S., & Hennig, U. G. (1988). Micronucleus assay in human fibroblasts: a measure of spontaneous chromosomal instability and mutagen hypersensitivity. *Environ Mol Mutagen, 12*(1), 3-13.

Sachse, C., Bhambra, U., Smith, G., Lightfoot, T. J., Barrett, J. H., Scollay, J., . . . Gooderham, N. J. (2003). Polymorphisms in the cytochrome P450 CYP1A2 gene (CYP1A2) in colorectal cancer patients and controls: allele frequencies, linkage disequilibrium and influence on caffeine metabolism. *Br J Clin Pharmacol, 55*(1), 68-76.

Salmon, C. P., Knize, M. G., & Felton, J. S. (1997). Effects of marinating on heterocyclic amine carcinogen formation in grilled chicken. *Food Chem Toxicol, 35*(5), 433-441.

Sanger, F., Nicklen, S., & Coulson, A. R. (1977). DNA sequencing with chain-terminating inhibitors. *Proc Natl Acad Sci U S A, 74*(12), 5463-5467.

Sawada, M., & Kamataki, T. (1998). Genetically engineered cells stably expressing cytochrome P450 and their application to mutagen assays. [Review]. *Mutat Res, 411*(1), 19-43.

Scherer, G., Frank, S., Riedel, K., Meger-Kossien, I and Renner, T. 2000. Biomonitoring of exposure to Polycyclic Aromatic Hydrocarbons of Nonoccupationally Exposed Persons. *Cancer Epidemiol Biomarkers Prev.* 9:373-380.

Schmittgen, T. D., Zakrajsek, B. A., Mills, A. G., Gorn, V., Singer, M. J., & Reed, M. W. (2000) Quantitative reverse transcription-polymerase chain reaction to study mRNA decay: comparison of endpoint and real-time methods. *Anal Biochem, 285*, 194.

Schut, H. A., & Snyderwine, E. G. (1999). DNA adducts of heterocyclic amine food mutagens: implications for mutagenesis and carcinogenesis. *Carcinogenesis, 20*(3), 353-368.

Schweikl, H., Taylor, J. A., Kitareewan, S., Linko, P., Nagorney, D., & Goldstein, J. A. (1993). Expression of CYP1A1 and CYP1A2 genes in human liver. *Pharmacogenetics, 3*(5), 239-249.

Seager, A. L., Shah, U-K., Mikhail, J. M., Nelson, B. C., Marquis, B. J., Doak, S. H., Johnson, G. E., Griffiths, S. M., Carmichael, P. L., Scott, S. J., Scott, A. D., & Jenkins. G. J. S. (2012). Pro-oxidant Induced DNA Damage in Human Lymphoblastoid Cells: Homeostatic Mechanisms of Genotoxic Tolerance. *Toxicol Sci, 128*(2), 387-397.

Sellakumar, A., & Shubik, P. (1974). *J. Natl. Cancer Inst, 53*, 1713- 1719.

Seaton, M. J., Follansbee, M. H., & Bond, J. A. (1995). Oxidation of 1, 2-epoxy-3-butene to 1, 2: 3, 4-diepoxybutane by cDNA-expressed human cytochromes P450 2E1 and 3A4 and human, mouse and rat liver microsomes. *Carcinogenesis, 16*(10), 2287-2293.

Shibutani, S., Fernandes, A., Suzuki, N., Zhou, L., Johnson, F., & Grollman, A. P. (1999). Mutagenesis of the N-(deoxyguanosin-8-yl)-2-amino-1-methyl-6-phenylimidazo[4, 5-b]pyridine DNA adduct in mammalian cells. Sequence context effects. *J Biol Chem, 274*(39), 27433-27438.

Shibutani, S., Takeshita, M., & Grollman, A. P. (1991). Insertion of specific bases during DNA synthesis past the oxidation-damaged base 8-oxodG. *Nature, 349*(6308), 431-434.

Shimada, T. (2006). Xenobiotic-metabolizing enzymes involved in activation and detoxification of carcinogenic polycyclic aromatic hydrocarbons. [Review]. *Drug Metab Pharmacokinet, 21*(4), 257-276.

Shimada, T., & Fujii-Kuriyama, Y. (2004). Metabolic activation of polycyclic aromatic hydrocarbons to carcinogens by cytochromes P450 1A1 and 1B1. *Cancer Sci, 95*(1), 1-6.

Shimada, T., Inoue, K., Suzuki, Y., Kawai, T., Azuma, E., Nakajima, T., Shindo, M., Kurose, K., Sugie, A., Yamagish,i Y., Fujii-Kuriyama, Y., & Hashimoto, M. (2002). Arylhydrocarbon receptor-dependent induction of liver and lung cytochromes P450 1A1, 1A2, and 1B1 by polycyclic aromatic hydrocarbons and polychlorinated biphenyls in genetically engineered C57Bl/6J mice. *Carcinogenesis, 23*, 1199-1207.

Shimada, T., Martin, M. V., Pruessschwartz, D., Marnett, L. J., & Guengerich, F. P. (1989). Roles of Individual Human Cytochrome-P-450 Enzymes in the Bioactivation of Benzo(a)Pyrene, 7,8-Dihydroxy-7,8-Dihydrobenzo(a)Pyrene, and Other Dihydrodiol Derivatives of Polycyclic Aromatic-Hydrocarbons. *Cancer Res, 49*(22), 6304-6312.

Simpson, D., Crosby, R. M., & Skopek, T. R. (1988). A method for specific cloning and sequencing of human hprt cDNA for mutation analysis. *Biochem Biophys Res Commun, 151*, 487-92.

Singer, B., & Grunberger, D. (1983). Molecular biology of mutagens and carcinogens. Plenum Press, New York, pp.68-78.

Sinha, R., Chow, W. H., Kulldorff, M., Denobile, J., Butler, J., Garcia-Closas, M., . . . Rothman, N. (1999). Well-done, grilled red meat increases the risk of colorectal adenomas. *Cancer Res, 59*(17), 4320-4324.

Sinha, R., Cross, A., Curtin, J., Zimmerman, T., McNutt, S., Risch, A., & Holden, J. (2005). Development of a food frequency questionnaire module and databases for compounds in cooked and processed meats. *Mol Nutr Food Res, 49*(7), 648-655.

Sinha, R. (2002). An epidemiologic approach to studying heterocyclic amines. [Review]. *Mutat Res, 506-507*, 197-204.

Sinha, R., Gustafson, D. R., Kulldorff, M., Wen, W. Q., Cerhan, J. R., & Zheng, W. (2000). 2-amino-1-methyl-6-phenylimidazo[4,5-b]pyridine, a carcinogen in high-temperature-cooked meat, and breast cancer risk. *J Natl Cancer Inst, 92*(16), 1352-1354.

Sinha, R. (2002). An epidemiologic approach to studying heterocyclic amines. [Review]. *Mutat Res, 506-507*, 197-204.

Sinha, R., Kulldorff, M., Chow, W. H., Denobile, J., & Rothman, N. (2001). Dietary intake of heterocyclic amines, meat-derived mutagenic activity, and risk of colorectal adenomas. *Cancer Epidemiol Biomarkers Prev, 10*(5), 559-562.

Sinha, R., Kulldorff, M., Curtin, J., Brown, C. C., Alavanja, M. C., & Swanson, C. A. (1998). Fried, well-done red meat and risk of lung cancer in women (United States). *Cancer Causes Control, 9*(6), 621-630.

Sinha, R., Rothman, N., Brown, E. D., Salmon, C. P., Knize, M. G., Swanson, C. A., . . . Felton, J. S. (1995). High concentrations of the carcinogen 2-amino-1-methyl-6-phenylimidazo- [4,5-b]pyridine (PhIP) occur in chicken but are dependent on the cooking method. *Cancer Res, 55*(20), 4516-4519.

Skog, K. I., Johansson, M. A., & Jagerstad, M. I. (1998). Carcinogenic heterocyclic amines in model systems and cooked foods: a review on formation, occurrence and intake. *Food Chem Toxicol, 36*(9-10), 879-896.

Slaga, T. J., Bracken, W. M., Dresner, S., Levin, W., Yagi, H., Jerina, D. M., & Conney, A. H. (1978). Skin tumor-initiating activities of the twelve isomeric phenols of benzo(a)pyrene. *Cancer Res, 38*(3), 678-681.

Smith, L. E., Denissenko, M. F., Bennett, W. P., Li, H., Amin, S., Tang, M. S., Pfeifer, G. P. (2000). Targeting of lung cancer mutational hotspots by polycyclic aromatic hydrocarbons. *J Natl Cancer Instit, 92*, 803-811.

Snyderwine, E. G., Schut, H. A. J., Adamson, R. H., Thorgeirsson, U. P., & Thorgeirsson, S. S. (1992). Metabolic-Activation and Genotoxicity of Heterocyclic Arylamines. *Cancer Res, 52*(7), S2099-S2102.

Snyderwine, E. G., Yoon, H. S., Knight-Jones, L. P., Tran, M., Schut, H. A., & Yu, M. (2003). Mutagenesis and DNA adduct formation in the mouse mammary gland exposed to 2-hydroxyamino-1-methyl-6-phenylimidazo-[4,5-b]pyridine in whole organ culture. [Comparative Study]. *Mutagenesis, 18*(1), 7-12.

Stadler, R. H. and Lineback, D. R. (2008). FOOD TOXICANTS: Occurrence, Formation, Mitigation and Health Risks. John Wiley and Sons- Technology and Engineering. pp89 *books.google.co.uk/books?isbn=0470430095*

Stout, J. T. & Caskey, C. T. (1985). HPRT: gene structure, expression and Mutation. Annu *Rev Genet, 19*, 127-48.

Streffer, C., Bolt, H. M., Føllesdal, D., Hall, P., Hengstler, J. G., Jacob, P., Oughton, D., Priess, K., Rehbinder, E., & Swaton, E. (2004). Environmental standards - dose effect relations in the low dose range and risk evaluation. *Springer-Verlag,* Berlin.

Stuart, G. R., Thorleifson, E., Okochi, E., de Boer, J. G., Ushijima, T., Nagao, M., & Glickman, B. W. (2000). Interpretation of mutational spectra from different genes: analyses of PhIP-induced mutational specificity in the lacI and cII transgenes from colon of Big Blue (R) rats. *Mutation Research-Fundamental and Molecular Mechanisms of Mutagenesis, 452*(1), 101-121.

Sugimura, T. (1997). Overview of carcinogenic heterocyclic amines. *Mutation Research-Fundamental and Molecular Mechanisms of Mutagenesis, 376*(1-2), 211-219.

Sugimura, T., & Sato, S. (1983). Mutagens-carcinogens in foods. [Research Support, Non-U.S. Gov't]. *Cancer Res, 43*(5 Suppl), 2415s-2421s.

Sugimura, T., Wakabayashi, K., Nakagama, H., & Nagao, M. (2004). Heterocyclic amines: Mutagens/carcinogens produced during cooking of meat and fish. [Review]. *Cancer Sci, 95*(4), 290-299.

Swenberg, J. A., La, D. K., & Scheller, N. A., Wu, K. Y. (1995). Dose-response relationships for carcinogens. *Toxicol let, 82*(83), 751-6.

Swenberg, J. A., Fryar-Tita, E., Jeong, Y., Boysen, G., Starr, T., Walker, V. E., & Albertini, R. J. (2008). Biomarkers in toxicology and risk assessment: informing critical dose–response relationships. *Chem. Res Toxicol. 21*, 253–265.

Tabish, A. M., Poels, K., Hoet, P., & Godderis, L. (2012). Epigenetic factors in cancer risk: effect of chemical carcinogens on global DNA methylation pattern in human TK6 cells. *PLoS One, 7*(4), e34674.

Tang, D., Liu, J. J., Rundle, A., Neslund-Dudas, C., Savera, A. T., Bock, C. H., . . . Rybicki, B. A. (2007). Grilled meat consumption and PhIP-DNA adducts in prostate carcinogenesis. [Research Support, N.I.H., Extramural]. *Cancer Epidemiol Biomarkers Prev, 16*(4), 803-808.

Tates, A. D., van Dam, F. J., de Zwart, F. A., van Teylingen, C. M, & Natarajan, A. T. (1994). Development of a cloning assay with high clon- ing efficiency to detect induction of 6-thiogua-nine-resistant lymphocytes in spleen of adult mice following in vivo inhalation exposure to 1,3-butadiene. *Mutat Res, 309*, 299–306.

Thiebaud, H. P., Knize, M. G., Kuzmicky, P. A., Hsieh, D. P., & Felton, J. S. (1995). Airborne mutagens produced by frying beef, pork and a soy-based food. *Food Chem Toxicol, 33*(10), 821-828.

Thomas, R. D., Green, M. R., Wilson, C., Weckle, A. L., Duanmu, Z., Kocarek, T. A., & Runge-Morris, M. (2006). Cytochrome P450 expression and metabolic activation of cooked food mutagen 2-amino-1-methyl-6-phenylimidazo[4,5-b]pyridine (PhIP) in MCF10A breast epithelial cells. *Chem Biol Interact, 160*(3), 204-216.

Thompson, L. H., Tucker, J. D., Stewart, S. A., Christensen, M. L., Salazar, E. P., Carrano, A. V., & Felton, J. S. (1987). Genotoxicity of Compounds from Cooked Beef in Repair-Deficient Cho Cells Versus Salmonella Mutagenicity. *Mutagenesis, 2*(6), 483-487.

Tindall, K. R., & Stankowski J, L F. (1989). Molecular analysis of spontaneous mutations at the gpt locus in Chinese hamster ovary (AS52) cells. *Mutation Research/Reviews in Genetic Toxicology, 220*, 241–253.

Tippin, B., Pham, P., & Goodman, M. F. (2004). Error-prone replication for better or worse. *Trends in microbiology, 12*(6), 288-295.

Tomita-Mitchell, A., Ling, L. L., Glover, C. L., Goodluck-Griffith, J., & Thilly, W. G. (2003). The mutational spectrum of the HPRT gene from human T cells in vivo shares a significant concordant set of hot spots with MNNG-treated human cells. *Cancer Res, 63*(18), 5793-5798.

Torres, R. J., & Puig, J. G. (2007). Hypoxanthine-guanine phosphoribosyltransferase (HPRT) deficiency: Lesch-Nyhan Syndrome. *Orphanet J Rare Dis. 2*, 1.

Touil, N., Aka, P. V., Buchet, J. P., Thierens, H., & Kirsch-Volders, M. (2002). Assessment of genotoxic effects related to chronic low level exposure to ionizing radiation using biomarkers for DNA damage and repair. *Mutagenesis, 17*(3), 223-232.

Tsurusawa, M., Niwa, M., Katano, N., & Fujimoto, T. (1990). Methotrexate cytotoxicity as related to irreversible S phase arrest in mouse L1210 leukemia cells. *Jpn J Cancer Res, 81*, 85-90.

Turesky, R. J. (2002). Heterocyclic aromatic amine metabolism, DNA adduct formation, mutagenesis, and carcinogenesis. *Drug metabolism reviews, 34*(3), 625-650.

Turesky, R. J. (2004). The role of genetic polymorphisms in metabolism of carcinogenic heterocyclic aromatic amines. *Curr Drug Metab, 5*, 169 – 80.

Turesky, R. J. (2007). Formation and biochemistry of carcinogenic heterocyclic aromatic amines in cooked meats. *Toxicol Lett, 168*(3), 219-227.

Turesky, R. J., Constable, A., Richoz, J., Varga, N., Markovic, J., Martin, M. V., & Guengerich, F. P. (1998). Activation of heterocyclic aromatic amines by rat and human liver microsomes and by purified rat and human cytochrome P450 1A2. *Chem Res Toxicol, 11*(8), 925-936.

Turesky, R. J., Guengerich, F. P., Guillouzo, A., & Langouet, S. (2002). Metabolism of heterocyclic aromatic amines by human hepatocytes and cytochrome P4501A2. *Mutat Res, 506-507*, 187-195.

Turesky, R. J., & Vouros, P. (2004). Formation and analysis of heterocyclic aromatic amine-DNA adducts in vitro and in vivo. *Journal of chromatography B, Analytical technologies in the biomedical and life sciences, 802*(1), 155-166.

Turesky, R. J., Goodenough, A. K., Ni, W., McNaughton, L., LeMaster, D. M., Holland, R. D., . . . Felton, J. S. (2007). Identification of 2-amino-1,7-dimethylimidazo[4,5-g]quinoxaline: an abundant mutagenic heterocyclic aromatic amine formed in cooked beef. *Chem Res Toxicol, 20*(3), 520-530.

Turesky, R. J., & Le Marchand, L. (2011). Metabolism and biomarkers of heterocyclic aromatic amines in molecular epidemiology studies: lessons learned from aromatic amines. *Chem Res Toxicol, 24*(8), 1169-1214.

Turesky, R. J., & Markovic, J. (1994). DNA Adduct Formation of the Food Carcinogen 2-Amino-3-Methylimidazo[4,5-F]Quinoline at the C-8 and N-2 Atoms of Guanine. *Chem Res Toxicol, 7*(6), 752-761.

Uno, S., & Makishima. M. (2009). Benzo[a]pyrene toxicity and inflammatory disease. *Current Rheumatology Reviews, (5)*, 266-271.

U.S. Centers for Disease Control Agency for Toxic Substances and Disease Registry (ATSDR). 1995. "Toxicological Profile for Agency for Toxic Substances and Disease Registry. (1990) Toxicological Profile for TEACH, 2007 *http://www.epa.gov/teach/*

USEPA (2001) United States Environmental Protection Agency. Benzo[a]pyrene , Integrated Risk Information System (IRIS, the USEPA 's online chemical toxicity service), Washington, DC

Vähäkangas, K. (2003) Molecular epidemiology of human cancer risk. Gene-environment interactions and p53 mutation spectrum in hum an lung cancer. *Methods Mol Med 74*, 43-59.

Van Dam, F. J., Natarajan, A. T., & Tates, A. D. (1992). Use of a T-lymphocyte clonal assay for determining HPRT mutant frequencies in individual rats. *Mutat Res, 271*, 231–242.

Van Diggelen, O. P., Donahue, T. F., & Shin, S. I. (1979). Basis for Differential Cellular Sensitivity to 8-Azaguanine and 6-Thioguanine. *J Cell Physiol, 98*(1), 59-71.

Van Zeeland, A. A., Mohn, G. R., Mullenders, L. H., Natarajann, A. T.,.....Et Al. (1989). Relationship between DNA-adduct formation, DNA repair, mutation frequency and mutation spectra. *Ann Ist Super Sanita, 25*, 223-8.

Varga, D., Johannes, T., Jainta, S., Schuster, S., Schwarz-Boeger, U., Kiechle, M., . . . Vogel, W. (2004). An automated scoring procedure for the micronucleus test by image analysis. *Mutagenesis, 19*(5), 391-397.

Vineis, P., & Porta, M. (1996). Causal thinking, biomarkers, and mechanisms of carcinogenesis. [Review]. *Journal of Clinical Epidemiology, 49*(9), 951-956.

Vral, A., Thierens, H., & De Ridder, L. (1997). In vitro micronucleus-centromere assay to detect radiation-damage induced by low doses in human lymphocytes. *Int J Radiat Biol, 71*(1), 61-68.

Walters, D. G., Young, P. J., Agus, C., Knize, M. G., Boobis, A. R., Gooderham, N. J., & Lake, B. G. (2004). Cruciferous vegetable consumption alters the metabolism of the dietary carcinogen 2-amino-1-methyl-6-phenylimidazo[4,5-b]pyridine (PhIP) in humans. *Carcinogenesis, 25*, 1659–1669.

Wakabayashi, K., Nagao, M., Esumi, H., & Sugimura, T. (1992). Food-derived mutagens and carcinogens. *Cancer Res, 52*(7 Suppl), 2092s-2098s.

Ward, M. H., Sinha, R., Heineman, E. F., Rothman, N., Markin, R., Weisenburger, D. D., . . . Zahm, S. H. (1997). Risk of adenocarcinoma of the stomach and esophagus with meat cooking method and doneness preference. *Int J Cancer, 71*(1), 14-19.

Wei, S. J., Chang, R. L., Bhachech, N., Cui, X. X., Merkler, K. A., Wong, C. Q., . . . Conney, A. H. (1993). Dose-dependent differences in the profile of mutations induced by (+)-7R,8S-dihydroxy-9S,10R-epoxy-7,8,9,10-tetrahydrobenzo(a)pyrene in the coding

region of the hypoxanthine (guanine) phosphoribosyltransferase gene in Chinese hamster V-79 cells. *Cancer Res, 53*(14), 3294-3301.

Wei, S. J., Chang, R. L., Wong, C. Q., Bhachech, N., Cui, X. X., Hennig, E., . . . et al. (1991). Dose-dependent differences in the profile of mutations induced by an ultimate carcinogen from benzo[a]pyrene. *Proc Natl Acad Sci U S A, 88*(24), 11227-11230.

Weinstein, I. B., Jeffrey, A. M., Jennette, K. W., Blobstein, S. H., Harvey, R. G., Harris, C., . . . Nakanishi, K. (1976). Benzo(a)pyrene diol epoxides as intermediates in nucleic acid binding in vitro and in vivo. *Science, 193*(4253), 592-595.

Westerink, W. M., & Schoonen, W. G. (2007). bCytochrome P450 enzyme levels in HepG2 cells and cryopreserved primary human hepatocytes and their induction in HepG2 cells. *Toxicol In Vitro, 21*(8), 1581-91.

WHO (World Health Organization). 1997. Tobacco or health: a global status report. Geneva: WHO. p 1–48.

WHO (1987) World Health Organization. Air Quality Guidelines for Europe, WHO Regional Publications, European Series No 23, WHO Regional Office for Europe, Copenhagen.

Williams, J. A. (2001). Single nucleotide polymorphisms, metabolic activation and environmental carcinogenesis: why molecular epidemiologists should think about enzyme expression. [Review]. *Carcinogenesis, 22*(2), 209-214.

William, M., Rainville, I. R., & Nickl;as, J. A. (2002). Use of inverse PCR to amplify and sequence break points of HPRT deletion and translocation mutations. *Environ Mol Mutagen, 39*, 22-32.

Wilson, J. M., Tarr, G. E., & Kelley, W. N. (1983). Human hypoxanthine (guanine) phosphoribosyltransferase: an amino acid substitution in a mutant form of the enzyme isolated from a patient with gout. *Proc Natl Acad Sci U S A, 80*(3), 870-873.

Wincent, E., Amini, N., Luecke, S., Glatt, H., Bergman, J., Crescenzi, C., . . . Rannug, U. (2009). The suggested physiologic aryl hydrocarbon receptor activator and cytochrome P4501 substrate 6-formylindolo[3,2-b]carbazole is present in humans. *J Biol Chem, 284*(5), 2690-2696.

Wiswman, H., & Halliwell, B. (1996). Review, Damage to DNA by reactive oxygen and nitrogen species: role in inflammatory disease and progression to cancer. *Biochem J, 313*, 17-29.

Wolfel, C., Heinrichhirsch, B., Schulzschalge, T., Seidel, A., Frank, H., Ramp, U., . . . Doehmer, J. (1992). Genetically Engineered V79 Chinese-Hamster Cells for Stable Expression of Human Cytochrome-P450ia2. *European Journal of Pharmacology-Environmental Toxicology and Pharmacology Section, 228*(2-3), 95-102.

Wu, R. W., Panteleakos, F. N., Kadkhodayan, S., Bolton-Grob, R., McManus, M. E., & Felton, J. S. (2000). Genetically modified Chinese hamster ovary cells for investigating sulfotransferase-mediated cytotoxicity and mutation by 2-amino-1-methyl-6- phenylimidazo[4,5-b]pyridine. *Environ Mol Mutagen, 35*(1), 57-65.

Wu, R. W., Wu, E. M., Thompson, L. H., & Felton, J. S. (1995). Identification of aprt gene mutations induced in repair-deficient and P450-expressing CHO cells by the food-related mutagen/carcinogen, PhIP. *Carcinogenesis, 16*(5), 1207-1213.

www.emea.eu (Access data march 03, 2007)

Xue, W., & Warshawsky, D. (2005). Metabolic activation of polycyclic and heterocyclic aromatic hydrocarbons and DNA damage: a review. *Toxicol Appl Pharmacol, 206*(1), 73-93.

Yadollahi-Farsani, M., Davies, D. S., & Boobis, A. R. (2002). The mutational signature of alpha-hydroxytamoxifen at Hprt locus in Chinese hamster cells. *Carcinogenesis, 23*(11), 1947-1952.

Yadollahi-Farsani, M., Gooderham, N. J., Davies, D. S., & Boobis, A. R. (1996). Mutational spectra of the dietary carcinogen 2-amino-1-methyl-6-phenylimidazo[4,5-b]pyridine (PhIP) at the Chinese hamster hprt locus. *Carcinogenesis, 17*(4), 617-624.

Yamakage, K., Omori, Y., Piccoli, C., & Yamasaki, H. (1998). *Mol. Carcinogen., 23*, 121–128.

Yan, T., Berry, S. E., Desai, A. B., & Kinsella, T. J. (2003). DNA mismatch repair (MMR) mediates 6-thioguanine genotoxicity by introducing single-strand breaks to signal a G2-M arrest in MMR-proficient RKO cells. *Clin Cancer Res, 9*(6), 2327-2334.

Yang, C. C., Jenq, S. N., & Lee, H. (1998). Characterization of the carcinogen 2-amino-3,8-dimethylimidazo[4,5-f]quinoxaline in cooking aerosols under domestic conditions. *Carcinogenesis, 19*(2), 359-363.

Yoon, J.-H., Lee, C.-S., & Pfeifer, G. P. (2003). Simulated sunlight and benzo[a]pyrene diol epoxide induced mutagenesis in the human p53 gene evaluated by the yeast functional assay: lack of correspondence to tumor mutation spectra. *Carcinogenesis, 24*(1), 113-119.

Yoon, J. H., Smith, L. E., Feng, Z., Tang, M., Lee, C. S., & Pfeifer, G. P. (2001). Methylated CpG dinucleotides are the preferential targets for G-to-T transversion mutations induced by benzo[a]pyrene diol epoxide in mammalian cells: similarities with the p53 mutation spectrum in smoking-associated lung cancers. *Cancer Res, 61*(19), 7110-7117.

Yu, M.-H. (2005). Environmental toxicology: biological and health effects of pollutants (2nd), CRC Press, 156670670X (alk. paper), Boca Raton.

Yu, Z., & and Quinn, P. (1994). Dimethyl sulphoxide: A review of its applications in cell biology. *Bioscience reports, 14*, 259-281.

Zair, Z. M., Jenkins, G. J., Doak, S. H., Singh, R., Brown, K., & Johnson, G. E. (2011). N-methylpurine DNA glycosylase plays a pivotal role in the threshold response of ethyl methanesulfonate-induced chromosome damage. *Toxicol Sci, 119*(2), 346-358.

Zhang, L. H., Vrieling, H., van Zeeland, A. A., & Jenssen, D. (1992). Spectrum of spontaneously occurring mutations in the hprt gene of V79 Chinese hamster cells. *J Mol Biol, 223*(3), 627-635.

Zhang, X. B., Felton, J. S., Tucker, J. D., Urlando, C., & Heddle, J. A. (1996). Intestinal mutagenicity of two carcinogenic food mutagens in transgenic mice: 2-amino-1-methyl-6-phenylimidazo[4,5-b]pyridine and amino(alpha)carboline. *Carcinogenesis, 17*(10), 2259-2265.

Zhang, Y., Yu, C., Mei. J., & Wang, S. (2013). Formation and mitidation of heterocyclic aromatic amines in fried pork. *Food Additives and Contaminants: Part A, 30* (9).

Zhao, K., Murray, S., Davies, D. S., Boobis, A. R., & Gooderham, N. J. (1994). Metabolism of the food derived mutagen and carcinogen 2-amino-1-methyl-6-phenylimidazo(4,5-b)pyridine (PhIP) by human liver microsomes. *Carcinogenesis, 15*(6), 1285-1288.

Zheng, W., & Lee, S.-A. (2009). Well-done meat intake, heterocyclic amine exposure, and cancer risk. *Nutrition and cancer, 61*(4), 437-446.

Zhong, Y., Carmella, S. G., Upadhyaya, P., Hochalter, J. B., Rauch, D., Oliver, A., . . . Hecht, S. S. (2011). Immediate consequences of cigarette smoking: rapid formation of polycyclic aromatic hydrocarbon diol epoxides. *Chem Res Toxicol, 24*(2), 246-252.

Zhu, H. J., Boobis, A. R., & Gooderham, N. J. (2000). The food-derived carcinogen 2-amino-1-methyl-6-phenylimidazo[4,5-b]pyridine activates S-Phase checkpoint and apoptosis, and induces gene mutation in human lymphoblastoid TK6 cells. *Cancer Res, 60*(5), 1283-1289.

Zhu, J., Rashid, A., Cleary, K., Abbruzzese, J. L., Friess, H., Takahashi, S., . . . Li, D. (2006). Detection of 2-amino-1-methyl-6-phenylimidazo [4,5-b]-pyridine (PhIP)-DNA adducts in human pancreatic tissues. *Biomarkers, 11*(4), 319-328.

Zhu, J. J., Chang, P., Bondy, M. L., Sahin, A. A., Singletary, S. E., Takahashi, S., . . . Li, D. H. (2003). Detection of 2-amino-1-methyl-6-phenylimidazo[4,5-b]-pyridine-DNA adducts in normal breast tissues and risk of breast cancer. *Cancer Epidemiology Biomarkers & Prevention, 12*(9), 830-837.

Appendix I (Chapter 2)

A. Preparation of Hygromycin B (Invitrogen)

All the preparation was done under aseptic conditions in sterile Biological safety Cabinets (Scanlaf Mars Pro class2, VWR International Ltd, Leicestershire, UK) UV sterilized and pre-cleaned with 70% ethanol.

1. A mixture of 25ml PBS (Gibco) + 50µl Acetic acid (Fisher scientific) was prepared
2. 3.85ml Hygromycin B (50mg/ml) was added to 6.12ml of PBS mixture
3. The diluted Hygromycin B was filter sterilized
4. 200µl aliquots (at a concentration of 200µg/ml) were prepared and stored at -20°C

B. Preparation of 0.1M NaOH

1g of Sodium hydroxide (NaOH; Sigma, Gillingham, UK) was dissolved in 250ml distilled water and autoclaved.

C. Preparation of 0.5M EDTA

EDTA (Ethyldiamine tetraacetic acid) was prepared by dissolving 93.05g of EDTA (Sigma) in 400ml distilled water. The pH was adjusted with 2M sodium hydroxide (pH 8) and the final volume increased to 500ml with distilled water.

D. Preparation of 1x TBE (Tris-Borate-EDTA)

1x TBE buffer was prepared by adding 100ml of 10x TBE into 900ml distilled water.

Chemicals	Supplier	Amount	Final Volume
10X TBE Tris Boric acid 0.5M EDTA Distilled H_2O	 Sigma, Gillingham, UK Sigma, Gillingham, UK Sigma, Gillingham, UK	 108g 55g 40ml	1L (Autoclaved for 20 min)
10% APS Ammonium per sulphate (APS) Distilled H_2O	Sigma, Gillingham, UK	1g	10ml
Silver stain 0.1% Silver nitrate ($AgNO_3$) Distilled H_2O	Sigma, Gillingham, UK	1g	1L
Developer Sodium hydroxide (NaOH) 37% formaldehyde (CH_2O) Distilled H_2O	 Sigma, Gillingham, UK Sigma, Gillingham, UK	 13.5g 3.6µl	1L

Appendix II (Chapter 3)

Micronucleus assay raw data tables for B[a]P

Terminology used in data tables

PD	Population doubling
%RPD	Percentage relative population doubling
Bn	Number of binucleated cells
Mn	Number of mononucleated cells
%Mn/Bn	Frequency of micronucleate in binucleated cells
Av.	Average

Table A. 1 CBMN raw data for TK6 cell line treated with BaP for 24h (24h+24h).

DOSE (μM)	DAY 1	DAY 2	PD	%RPD	Av. %RPD	Bn	Mn	%Mn/Bn	Total Mn	Total Bn	Av. %Mn/Bn
0	121800	360600	1.57	100.00	100.00	3335	29	0.87	10000	91	0.91
0	190600	1757000	3.20	100.00		3335	32	0.96			
0	198000	1160000	2.55	100.00		3330	30	0.90			
1	110600	297000	1.43	91.01	101.55	3335	28	0.84	10000	82	0.82
1	192000	1561000	3.02	94.35		3335	25	0.75			
1	146200	1205000	3.04	119.31		3330	29	0.87			
2	124600	599800	2.27	144.79	104.63	3335	29	0.87	10000	87	0.87
2	177400	815200	2.20	68.66		3335	30	0.90			
2	101800	601200	2.56	100.45		3330	28	0.84			
3	135900	581400	2.10	133.92	102.73	3335	28	0.84	10000	84	0.84
3	175000	2236000	3.68	114.70		3335	26	0.78			
3	116000	332600	1.52	59.58		3330	30	0.90			
4	122400	453800	1.89	120.73	106.68	3335	26	0.78	10000	80	0.80
4	158800	2311000	3.86	120.56		3335	25	0.75			
4	109000	438600	2.01	78.75		3330	29	0.87			
5	124200	281400	1.18	75.35	109.02	3335	28	0.84	10000	82	0.82
5	113800	1842000	4.02	125.35		3335	29	0.87			
5	143200	1337000	3.22	126.36		3330	25	0.75			
10	115000	262200	1.19	75.93	101.62	3335	25	0.75	10000	78	0.78
10	145000	1710000	3.56	111.09		3335	27	0.81			
10	188000	1510000	3.01	117.85		3330	26	0.78			
25	118000	235000	0.99	63.47	107.63	3335	25	0.75	10000	77	0.77
25	125200	1707000	3.77	117.62		3335	28	0.84			
25	120600	1479000	3.62	141.79		3330	24	0.72			
30	113800	211400	0.89	57.06	112.82	3335	24	0.72	10000	78	0.78
30	104200	2119000	4.35	135.62		3335	26	0.78			
30	120800	1590000	3.72	145.79		3330	28	0.84			
50	102200	199000	0.96	61.39	101.76	3335	27	0.81	10000	79	0.79
50	149800	2089000	3.80	118.64		3335	23	0.69			
50	149000	1364000	3.19	125.25		3330	29	0.87			
70	101600	194000	0.93	59.59	85.70	3335	27	0.81	10000	81	0.81
70	161000	2019000	3.65	113.86		3335	25	0.75			
70	209000	917200	2.13	83.66		3330	29	0.87			

Table A. 2 CBMN raw data for AHH-1 cell line treated with BaP for 24h (24h+24h).

DOSE (μM)	DAY 1	DAY 2	PD	%RPD	Av.%RPD	Bn	Mn	%Mn/Bn	Total Mn	Total Bn	Av. % Mn/Bn
0	111400	492000	2.14	100.00	100.00	3335	46	1.38	135	10000	1.35
0	102600	657400	2.68	100.00		3335	44	1.32			
0	199800	1341000	2.75	100.00		3330	45	1.35			
1	115200	537100	2.22	103.65	104.95	3335	45	1.35	133	10000	1.33
1	108600	743600	2.78	103.57		3335	44	1.32			
1	182600	1416900	2.96	107.62		3330	44	1.32			
2	154700	896000	2.53	118.25	104.36	3335	46	1.38	136	10000	1.36
2	179400	1015200	2.50	93.31		3335	45	1.35			
2	140200	968800	2.79	101.53		3330	45	1.35			
3	160000	780000	2.29	106.65	102.42	3335	47	1.41	142	10000	1.42
3	148600	842500	2.50	93.41		3335	47	1.41			
3	113000	870000	2.94	107.21		3330	48	1.44			
4	148900	613000	2.04	95.27	96.13	3335	49	1.47	150	10000	1.50
4	136200	798400	2.55	95.21		3335	50	1.50			
4	104400	673200	2.69	97.90		3330	51	1.53			
5	106200	689000	2.70	125.89	95.46	3335	52	1.56	157	10000	1.57
5	114600	584400	2.35	87.71		3335	53	1.59			
5	198600	794000	2.00	72.79		3330	52	1.56			
10	103400	451800	2.13	99.28	91.57	3335	56	1.68	172	10000	1.72
10	104200	462200	2.15	80.20		3335	57	1.71			
10	145400	891000	2.62	95.22		3330	59	1.77			
25	109000	355000	1.70	79.49	83.20	3335	63	1.89	182	10000	1.82
25	123400	545600	2.14	80.03		3335	60	1.80			
25	198700	1104000	2.47	90.08		3330	59	1.77			
30	114600	422600	1.88	87.86	81.78	3335	69	2.07	205	10000	2.05
30	113400	481000	2.08	77.79		3335	70	2.10			
30	140800	642000	2.19	79.69		3330	66	1.98			
50	104600	358000	1.78	82.83	81.06	3335	76	2.28	210	10000	2.10
50	101400	437600	2.11	78.72		3335	71	2.13			
50	129200	611000	2.24	81.61		3330	73	2.19			
70	113200	396800	1.81	84.44	61.49	3335	77	2.31	223	10000	2.23
70	193400	399400	1.05	39.04		3335	75	2.25			
70	130800	417600	1.67	60.97		3330	71	2.13			

Table A. 3 CBMN raw data for MCL-5 cell line treated with BaP for 24h (24h+24h).

DOSE (μM)	DAY 1	DAY 2	PD	%RPD	Av.%RPD	Bn	Mn	%Mn/Bn	Total Mn	Total Bn	Av. % Mn/Bn
0	163200	404400	1.31	100.00	100.00	3335	52	1.56	151	10000	1.51
0	208600	472800	1.18	100.00		3335	49	1.47			
0	163600	358200	1.13	100.00		3330	50	1.50			
1	154900	298000	0.94	72.11	72.80	3335	58	1.74	167	10000	1.67
1	216200	371800	0.78	66.26		3335	54	1.62			
1	152200	285000	0.90	80.05		3330	55	1.65			
2	158000	321200	1.02	78.18	70.98	3335	61	1.83	181	10000	1.81
2	225400	393800	0.80	68.19		3335	59	1.77			
2	151000	254400	0.75	66.56		3330	61	1.83			
3	168900	317500	0.91	69.56	65.85	3335	71	2.13	205	10000	2.05
3	233400	389400	0.74	62.55		3335	67	2.01			
3	119400	199400	0.74	65.44		3330	67	2.01			
4	163600	325000	0.99	75.64	63.98	3335	79	2.37	218	10000	2.18
4	211600	335000	0.66	56.15		3335	69	2.07			
4	157400	252200	0.68	60.16		3330	70	2.10			
5	193400	355800	0.88	67.18	60.41	3335	84	2.52	220	10000	2.20
5	200000	311000	0.64	53.95		3335	71	2.13			
5	145000	232200	0.68	60.08		3330	65	1.95			
10	138600	229900	0.73	55.77	55.78	3335	81	2.43	232	10000	2.32
10	212800	329400	0.63	53.40		3335	76	2.28			
10	183200	289000	0.66	58.17		3330	75	2.25			
25	154800	257200	0.73	55.95	52.72	3335	83	2.49	242	10000	2.42
25	215200	346600	0.69	58.25		3335	80	2.40			
25	192000	271000	0.50	43.98		3330	79	2.37			
30	138600	229900	0.73	55.77	41.04	3335	91	2.73	276	10000	2.76
30	212800	229400	0.11	9.18		3335	95	2.85			
30	183200	289000	0.66	58.17		3330	90	2.70			
50	182600	299000	0.71	54.35	38.25	3335	95	2.85	296	10000	2.96
50	218600	286800	0.39	33.19		3335	98	2.94			
50	176600	218600	0.31	27.23		3330	103	3.09			
70	187200	222800	0.25	19.19	16.04	3335	121	3.63	338	10000	3.38
70	214000	241000	0.17	14.52		3335	116	3.48			
70	180800	202400	0.16	14.40		3330	101	3.03			

Table A. 4 CBMN raw data for HepG2 cell line treated with BaP for 24h (24h+24h).

DOSE (μM)	DAY 1	DAY 2	PD	%RPD	Av.%RPD	Bn	Mn	%Mn/Bn	Total Mn	Total Bn	Av. %Mn/Bn
0	109000	614600	2.50	100.00	100.00	3200	19	0.59	62	9535	0.65
0	111980	732000	2.71	100.00		3000	21	0.70			
0	114000	662800	2.54	100.00		3335	22	0.66			
1	127200	498000	1.97	78.91	84.42	3200	21	0.66	73	9535	0.77
1	111600	521800	2.23	82.15		3000	24	0.80			
1	102800	521000	2.34	92.20		3335	28	0.84			
2	125000	503800	2.01	80.59	77.99	3200	28	0.88	85	9535	0.89
2	111360	438800	1.98	73.04		3000	26	0.87			
2	106700	439000	2.04	80.36		3335	31	0.93			
3	117600	451900	1.94	77.83	77.73	3200	32	1.00	99	9535	1.04
3	106000	474000	2.16	79.78		3000	29	0.97			
3	112600	426000	1.92	75.59		3335	38	1.14			
4	142400	416400	1.55	62.04	61.45	3100	32	1.03	107	9430	1.13
4	127200	350400	1.46	53.97		3000	35	1.17			
4	116200	387000	1.74	68.35		3330	40	1.20			
5	69800	160850	1.20	48.27	53.61	1683	20	1.19	53	3862	1.39
5	108400	332600	1.62	59.71		923	12	1.30			
5	129000	327000	1.34	52.84		1256	21	1.67			
10	79800	126000	0.66	26.41	38.04	1167	15	1.29	52	3484	1.50
10	135400	272000	1.01	37.15		992	17	1.71			
10	104300	254000	1.28	50.56		1325	20	1.51			
25	89600	98700	0.14	5.59	17.48						
25	79800	170000	1.09	40.28							
25	121000	135800	0.17	6.56							

Table A. 5 CBMN assay raw data for AHH-1 cell line treated with BaP for 4h (4h+24).

DOSE (μM)	DAY 1	DAY 2	PD	% RPD	Av. %RPD	Bn	Mn	%Mn/Bn	Total Mn	Total Bn	Av. %Mn/Bn
0	239000	830400	1.80	100	100.00	3335	45	1.35	132	10000	1.32
0	237200	861000	1.86	100		3335	42	1.26			
0	192400	1185000	2.62	100		3330	45	1.35			
10	189300	1194000	2.66	147.88	122.31	3335	43	1.29	137	10000	1.37
10	279000	1242000	2.15	115.83		3335	49	1.47			
10	199800	1305000	2.71	103.23		3330	45	1.35			
20	211800	1004000	2.24	124.94	107.43	3335	45	1.35	136	10000	1.36
20	241000	916000	1.93	103.57		3335	50	1.50			
20	180800	994600	2.46	93.79		3330	41	1.23			
30	222200	989400	2.15	119.92	108.23	3335	39	1.17	132	10000	1.32
30	221800	884400	2.00	107.29		3335	51	1.53			
30	210800	1240000	2.56	97.47		3330	42	1.26			
40	233400	877400	1.91	106.32	98.04	3335	33	0.99	130	10000	1.30
40	245000	908200	1.89	101.63		3335	51	1.53			
40	173200	829600	2.26	86.17		3330	46	1.38			
50	205000	887300	2.11	117.64	96.55	3335	43	1.29	141	10000	1.41
50	233600	751500	1.69	90.64		3335	52	1.56			
50	182800	802400	2.13	81.37		3330	46	1.38			
60	210200	1029500	2.29	127.57	107.16	3335	39	1.17	143	10000	1.43
60	220200	890400	2.02	108.37		3335	53	1.59			
60	170600	807800	2.24	85.54		3330	51	1.53			
70	244600	893000	1.87	103.98	92.02	3335	49	1.47	154	10000	1.54
70	243400	830200	1.77	95.17		3335	52	1.56			
70	223600	905200	2.02	76.92		3330	53	1.59			

Table A. 6 CBMN assay raw data set for MCL-5 cell line treated with BaP for 4h (4h+24h).

DOSE (μM)	DAY 1	DAY 2	PD	% RPD	Av. %RPD	Bn	Mn	%Mn/Bn	Total Mn	Total Bn	Av.%Mn/Bn
0	115200	892000	2.95	100	100.00	3335	47	1.41	144	10000	1.44
0	177800	574200	1.69	100		3335	48	1.44			
0	186400	355000	0.93	100		3330	49	1.47			
10	147400	700400	2.25	76.14	86.01	3335	48	1.44	146	10000	1.46
10	178400	502200	1.49	88.28		3335	46	1.38			
10	181000	330800	0.87	93.60		3330	52	1.56			
20	152600	639400	2.07	70.00	80.66	3335	48	1.44	153	10000	1.53
20	192000	489200	1.35	79.78		3335	48	1.44			
20	176000	318800	0.86	92.22		3330	57	1.71			
30	194400	728400	1.91	64.54	67.57	3335	50	1.50	156	10000	1.56
30	176600	428600	1.28	75.63		3335	48	1.44			
30	203200	304000	0.58	62.53		3330	58	1.74			
40	182600	761600	2.06	69.77	67.34	3335	58	1.74	175	10000	1.75
40	165800	389000	1.23	72.74		3335	58	1.74			
40	191800	281400	0.55	59.50		3330	59	1.77			
50	197400	708200	1.84	62.41	60.42	3335	65	1.95	184	10000	1.84
50	168400	349400	1.05	62.26		3335	59	1.77			
50	198200	285400	0.53	56.60		3330	60	1.80			
60	181000	680200	1.91	64.68	56.90	3335	69	2.07	201	10000	2.01
60	182800	303800	0.73	43.33		3335	65	1.95			
60	171200	256400	0.58	62.70		3330	67	2.01			
70	247600	761400	1.62	54.88	45.18	3335	72	2.16	226	10000	2.26
70	144400	227200	0.65	38.66		3335	79	2.37			
70	180200	236200	0.39	42.01		3330	75	2.25			

able A. 7: CBMN assay raw data set for HepG2 cell line treated with BaP for 4h (4h+24h).

DOSE (µM)	DAY 1	DAY 2	PD	%RPD	Av. %RPD	Bn	Mn	%Mn/Bn	Total Mn	Total Bn	Av.%Mn/Bn
0	104000	209400	0.78	100	100.00	3335	37	1.11	110	10000	1.10
0	118400	192800	0.70	100		3335	37	1.11			
0	113600	198300	0.80	100		3330	36	1.08			
10	122200	134200	0.34	43.80	52.25	3335	45	1.35	127	10000	1.27
10	101200	126200	0.32	45.28		3335	40	1.20			
10	102200	149000	0.54	67.67		3330	42	1.26			
20	106000	129000	0.28	35.76	41.00	3335	50	1.50	151	10000	1.51
20	123200	151600	0.30	42.54		3335	49	1.47			
20	102900	132000	0.36	44.70		3330	52	1.56			
30	106400	116400	0.19	24.52	32.75	3335	54	1.62	155	10000	1.55
30	103600	125400	0.28	39.17		3335	53	1.59			
30	116300	141000	0.28	34.57		3330	48	1.44			
40	102000	126600	0.16	20.12	35.05	3335	50	1.50	157	10000	1.57
40	106400	122800	0.21	29.40		3335	58	1.74			
40	109300	149000	0.45	55.62		3330	49	1.47			
50	113600	116400	0.14	18.43	29.59	3335	54	1.62	185	10000	1.85
50	131600	144200	0.13	18.75		3335	62	1.86			
50	104500	139300	0.41	51.60		3330	69	2.07			
60	105400	105200	0.06	7.20	9.46	3335	60	1.80	132	10000	2.11
60	104200	109000	0.06	9.24		3335	72	2.16			
60	113200	121000	0.10	11.96		3330	79	2.37			
70	101200	105200	0.06	7.20	7.20	3335	75	2.25	160	10000	2.49
70	116600	119400	0.03	4.87		3335	85	2.55			
70	106200	112000	0.08	9.54		3330	89	2.67			

Table A. 8: Raw data set for the NCND effect on the MN frequency in MCL-5 cell line.

Treatments	DAY 1	DAY 2	PD	%RPD	Av. %RPD	Bn	Mn	%Mn/Bn	Total Mn	Total Bn	Av. %Mn/Bn
Control	115300	676000	2.55	100.00	100.00	3200	31	0.97	133	10000	1.33
Control	194700	806000	2.05	100.00		3200	50	1.56			
Control	142000	708200	2.32	100.00		3600	52	1.44			
NCND	134500	845000	2.65	103.91	118.40	3200	45	1.41	182	10000	1.82
NCND	153000	943400	2.62	128.05		3200	62	1.94			
NCND	124000	898700	2.86	123.26		3600	75	2.08			
NCND+BaP	156700	594000	1.92	75.34	74.13	3200	58	1.81	193	10000	1.93
NCND+BaP	143000	451200	1.66	80.88		3200	64	2.00			
NCND+BaP	167000	483600	1.53	66.17		3600	71	1.97			
BaP	123000	162400	0.40	15.71	19.71	3200	105	3.28	315	10000	3.15
BaP	152000	209600	0.46	22.62		3200	100	3.13			
BaP	121000	169000	0.48	20.79		3600	110	3.06			

Appendix III (Chapter 3)

Fold change in CYPs expressions (B[a]P)

Figure A. 1. Comparisons of Basal and Induced expression of CYP 1A1 and 1A2 enzymes in MCL-5, AHH-1, TK6 and HepG2 cell lines treated with selected B[a]P doses for 24h. Lane1: Untreated control, Lane2: Treated with LOEL dose, Lane3: Dose above LOEL.

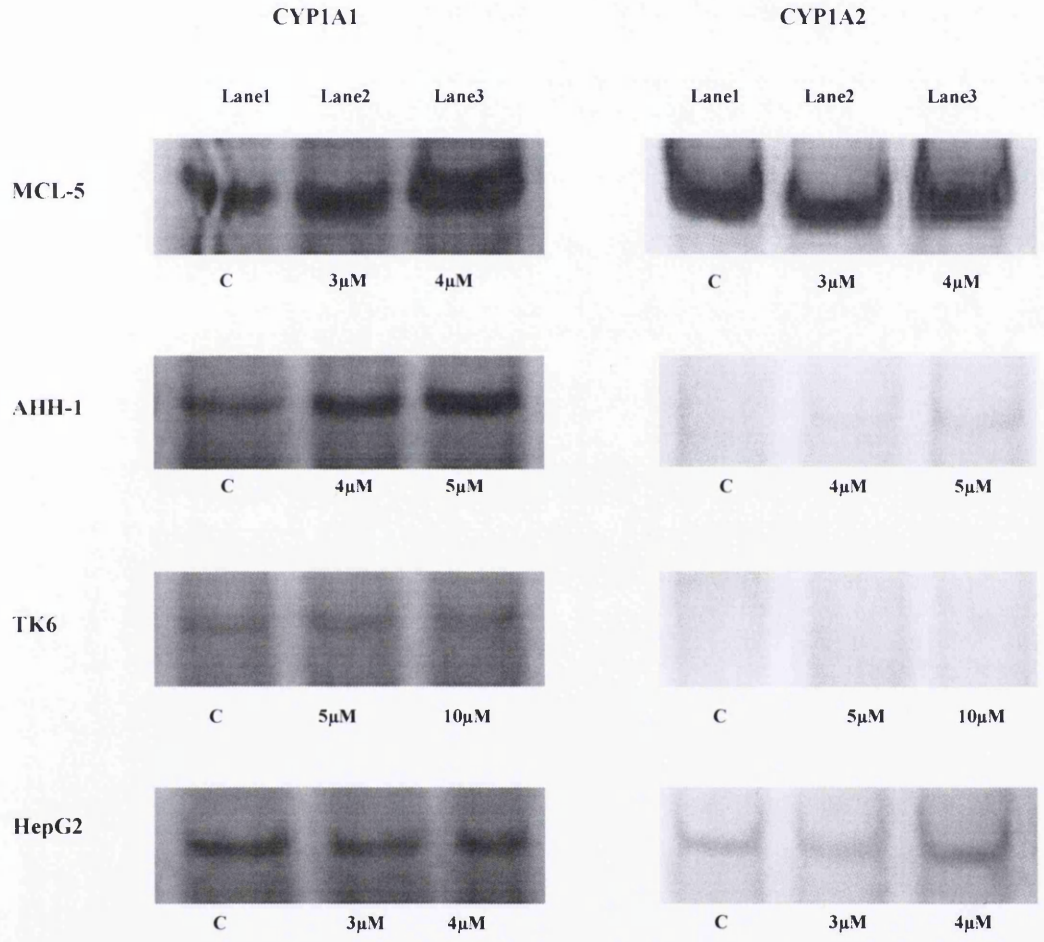

Appendix IV (Chapter 4)

HPRT assay raw data tables for B[a]P

Terminology used in data tables

Xo Number of wells with out colonies

No Total number of wells scored

Xs Number of wells without colonies

Ns Total number of wells scored

Table A. 9 HPRT raw data set for AHH-1 cell line Untreated (0) and solvent control

Replicate 1

BaP (μM)	Plating Efficiency		Mutation Frequency					
	Xo	No	Xs	Ns	Plating Efficiency %	Cell Viability %	Mutation Frequency	Dilution factor
0	25	300	297	300	248.49	98.4	2.02E-06	0.0005
Solvent control	26	300	298	300	244.57	100.0	1.37E-06	0.0005

Replicate 2

BaP (μM)	Plating Efficiency		Mutation Frequency					
	Xo	No	Xs	Ns	Plating Efficiency %	Cell Viability %	Mutation Frequency	Dilution factor
0	27	300	296	300	240.79	98.5	2.79E-06	0.0005
Solvent control	28	300	297	300	237.16	98.5	2.12E-06	0.0005

Replicate 3

BaP (μM)	Plating Efficiency		Mutation Frequency					
	Xo	No	Xs	Ns	Plating Efficiency %	Cell Viability %	Mutation Frequency	Dilution factor
0	15	300	295	300	299.57	93.9	2.81E-06	0.0005
Solvent control	18	300	297	300	281.34	100.0	1.79E-06	0.0005

Table A. 10 PRT raw data set for AHH-1 cell line treated with BaP for 24h.

Replicate 1

BaP (µM)	Plating Efficiency		Mutation Frequency					
	Xo	No	Xs	Ns	Plating Efficiency %	Cell Viability %	Mutation Frequency	Dilution factor
Control	26	300	298	300	244.57	100.0	1.37E-06	0.0005
1	27	300	286	300	240.79	98.5	9.92E-06	0.0005
2	20	300	275	300	270.81	110.7	1.61E-05	0.0005
3	28	300	267	300	237.16	97.0	2.46E-05	0.0005
4	26	300	251	300	244.57	100.0	3.65E-05	0.0005
5	35	300	235	300	214.84	87.8	5.68E-05	0.0005
10	37	300	220	300	209.29	85.6	7.41E-05	0.0005

Replicate 2

BaP (µM)	Plating Efficiency		Mutation Frequency					
	Xo	No	Xs	Ns	Plating Efficiency %	Cell Viability %	Mutation Frequency	Dilution factor
Control	28	300	297	300	237.16	100.0	2.12E-06	0.0005
1	28	300	295	300	237.16	100.0	3.54E-06	0.0005
2	27	300	292	300	240.79	101.5	5.61E-06	0.0005
3	29	300	284	300	233.65	98.5	1.17E-05	0.0005
4	29	300	259	300	233.65	98.5	3.14E-05	0.0005
5	30	300	247	300	230.26	97.1	4.22E-05	0.0005
10	31	300	232	300	226.98	95.7	5.66E-05	0.0005

Replicate 3

BaP (µM)	Plating Efficiency		Mutation Frequency					
	Xo	No	Xs	Ns	Plating Efficiency %	Cell Viability %	Mutation Frequency	Dilution factor
Control	18	300	297	300	281.34	100.0	1.79E-06	0.0005
1	18	300	291	300	281.34	100.0	5.41E-06	0.0005
2	19	300	285	300	275.93	98.1	9.29E-06	0.0005
3	19	300	276	300	275.93	98.1	1.51E-05	0.0005
4	20	300	260	300	270.81	96.3	2.64E-05	0.0005
5	20	300	250	300	270.81	96.3	3.37E-05	0.0005
10	21	300	249	300	265.93	94.5	3.50E-05	0.0005

TableA. 11 HPRT raw data set for MCL-5 cell line untreated (0) and solvent control.

Replicate 1

BaP (μM)	Plating Efficiency		Mutation Frequency					
	Xo	No	Xs	Ns	Plating Efficiency %	Cell Viability %	Mutation Frequency	Dilution factor
0	110	300	570	600	100.33	101.8	2.56E-05	0.0005
Solvent control	112	300	572	600	98.53	100.0	2.43E-05	0.0005

Replicate 2

BaP (μM)	Plating Efficiency		Mutation Frequency					
	Xo	No	Xs	Ns	Plating Efficiency %	Cell Viability %	Mutation Frequency	Dilution factor
0	100	300	571	600	109.86	99.1	2.25E-05	0.0005
Solvent control	99	300	574	600	110.87	100.0	2.00E-05	0.0005

Replicate 3

BaP (μM)	Plating Efficiency		Mutation Frequency					
	Xo	No	Xs	Ns	Plating Efficiency %	Cell Viability %	Mutation Frequency	Dilution factor
0	100	300	569	600	109.86	99.1	2.41E-05	0.0005
Solvent control	99	300	572	600	110.87	100.0	2.16E-05	0.0005

TableA. 12 HPRT raw data set for MCL-5 cell line treated with BaP for 24h.

Replicate 1

BaP (μM)	Plating Efficiency		Mutation Frequency					
	Xo	No	Xs	Ns	Plating Efficiency %	Cell Viability %	Mutation Frequency	Dilution factor
Solvent control	112	300	572	600	98.53	100.0	2.43E-05	0.0005
1	110	300	490	600	100.33	101.8	1.01E-04	0.0005
2	112	300	361	600	98.53	100.0	2.58E-04	0.0005
3	118	300	325	600	93.31	94.7	3.29E-04	0.0005
4	121	300	247	600	90.80	92.2	4.89E-04	0.0005
5	131	300	239	600	82.86	84.1	5.55E-04	0.0005
10	141	300	75	600	75.50	76.6	1.38E-03	0.0005

Replicate 2

BaP (μM)	Plating Efficiency		Mutation Frequency					
	Xo	No	Xs	Ns	Plating Efficiency %	Cell Viability %	Mutation Frequency	Dilution factor
Solvent control	99	300	574	600	110.87	100.0	2.00E-05	0.0005
1	100	300	410	600	109.86	99.1	1.73E-04	0.0005
2	100	300	337	600	109.86	99.1	2.63E-04	0.0005
3	104	300	326	600	105.94	95.6	2.88E-04	0.0005
4	103	300	290	600	106.91	96.4	3.40E-04	0.0005
5	115	300	263	600	95.89	86.5	4.30E-04	0.0005
10	137	300	74	600	78.38	70.7	1.34E-03	0.0005

Replicate 3

BaP (μM)	Plating Efficiency		Mutation Frequency					
	Xo	No	Xs	Ns	Plating Efficiency %	Cell Viability %	Mutation Frequency	Dilution factor
Solvent control	99	300	572	600	110.87	100.0	2.16E-05	0.0005
1	100	300	434	600	109.86	99.1	1.47E-04	0.0005
2	104	300	416	600	105.94	95.6	1.73E-04	0.0005
3	107	300	362	600	103.10	93.0	2.45E-04	0.0005
4	103	300	260	600	106.91	96.4	3.91E-04	0.0005
5	119	300	204	600	92.47	83.4	5.83E-04	0.0005
10	138	300	69	600	77.65	70.0	1.39E-03	0.0005

Table A. 13 HPRT raw data for AHH-1 cell line for untreated (0) and solvent control.

Replicate 1

BaP (μM)	Plating Efficiency		Mutation Frequency					
	Xo	No	Xs	Ns	Plating Efficiency %	Cell Viability %	Mutation Frequency	Dilution factor
0	2	300	293	300	501.06	100.0	2.36E-06	0.0005
Solvent control	1	300	291	300	570.38	113.8	2.67E-06	0.0005

Replicate 2

BaP (μM)	Plating Efficiency		Mutation Frequency					
	Xo	No	Xs	Ns	Plating Efficiency %	Cell Viability %	Mutation Frequency	Dilution factor
0	15	300	296	300	299.57	100.0	2.24E-06	0.0005
Solvent control	12	300	298	300	321.89	107.4	1.04E-06	0.0005

Replicate 3

BaP (μM)	Plating Efficiency		Mutation Frequency					
	Xo	No	Xs	Ns	Plating Efficiency %	Cell Viability %	Mutation Frequency	Dilution factor
0	30	300	295	300	230.26	100.0	3.65E-06	0.0005
Solvent control	32	300	290	300	223.80	97.2	7.57E-06	0.0005

Table A. 14 HPRT raw data set for AHH-1 cell line treated with BaP for 4h.

Replicate 1

BaP (µM)	Plating Efficiency		Mutation Frequency					
	Xo	No	Xs	Ns	Plating Efficiency %	Cell Viability %	Mutation Frequency	Dilution factor
Solvent control	1	300	291	300	570.38	100.0	2.67E-06	0.0005
10	2	300	271	300	501.06	87.8	1.01E-05	0.0005
20	3	300	267	300	460.52	80.7	1.27E-05	0.0005
25	3	300	265	300	460.52	80.7	1.35E-05	0.0005
30	3	300	261	300	460.52	80.7	1.51E-05	0.0005
50	2	300	260	300	501.06	87.8	1.43E-05	0.0005

Replicate 2

BaP (µM)	Plating Efficiency		Mutation Frequency					
	Xo	No	Xs	Ns	Plating Efficiency %	Cell Viability %	Mutation Frequency	Dilution factor
Solvent control	12	300	298	300	321.89	100.0	1.04E-06	0.0005
10	10	300	298	300	340.12	105.7	9.83E-07	0.0005
20	12	300	290	300	321.89	100.0	5.27E-06	0.0005
25	14	300	288	300	306.47	95.2	6.66E-06	0.0005
30	13	300	286	300	313.88	97.5	7.61E-06	0.0005
50	15	300	280	300	299.57	93.1	1.15E-05	0.0005

Replicate 3

BaP (µM)	Plating Efficiency		Mutation Frequency					
	Xo	No	Xs	Ns	Plating Efficiency %	Cell Viability %	Mutation Frequency	Dilution factor
Solvent control	32	300	290	300	223.80	100.0	7.57E-06	0.0005
10	13	300	271	300	313.88	140.2	1.62E-05	0.0005
20	20	300	270	300	270.81	121.0	1.95E-05	0.0005
25	18	300	262	300	281.34	125.7	2.41E-05	0.0005
30	29	300	268	300	233.65	104.4	2.41E-05	0.0005
50	28	300	270	300	237.16	106.0	2.22E-05	0.0005

Table A. 15 HPRT raw data set for MCL-5 cell line untreated (0) and solvent control.

Replicate 1

BaP (µM)	Plating Efficiency		Mutation Frequency					
	Xo	No	Xs	Ns	Plating Efficiency %	Cell Viability %	Mutation Frequency	Dilution factor
0	40	300	273	300	201.49	100.0	2.34E-05	0.0005
Solvent control	45	300	275	300	189.71	94.2	2.29E-05	0.0005

Replicate 2

BaP (µM)	Plating Efficiency		Mutation Frequency					
	Xo	No	Xs	Ns	Plating Efficiency %	Cell Viability %	Mutation Frequency	Dilution factor
0	54	300	230	300	171.48	100.0	7.75E-05	0.0005
Solvent control	53	300	234	300	173.35	101.1	7.17E-05	0.0005

Replicate 3

BaP (µM)	Plating Efficiency		Mutation Frequency					
	Xo	No	Xs	Ns	Plating Efficiency %	Cell Viability %	Mutation Frequency	Dilution factor
0	30	300	275	300	230.26	100.0	1.89E-05	0.0005
Solvent control	29	300	270	300	233.65	101.5	2.25E-05	0.0005

Table A. 16 HPRT raw data set for MCL-5 cell line treated with BaP for 4h.

Replicate 1

BaP (µM)	Plating Efficiency		Mutation Frequency					
	Xo	No	Xs	Ns	Plating Efficiency %	Cell Viability %	Mutation Frequency	Dilution factor
Solvent control	45	300	275	300	189.71	100.0	2.29E-05	0.0005
5	57	300	223	300	166.07	87.5	8.93E-05	0.0005
10	58	300	169	300	164.33	86.6	1.75E-04	0.0005
15	62	300	184	300	157.66	83.1	1.55E-04	0.0005
20	68	300	161	300	148.43	78.2	2.10E-04	0.0005
25	73	300	159	300	141.33	74.5	2.25E-04	0.0005
30	79	300	153	300	133.43	70.3	2.52E-04	0.0005
50	82	300	149	300	129.71	68.4	2.70E-04	0.0005

Replicate 2

BaP (µM)	Plating Efficiency		Mutation Frequency					
	Xo	No	Xs	Ns	Plating Efficiency %	Cell Viability %	Mutation Frequency	Dilution factor
Solvent control	53	300	234	300	173.35	100.0	7.17E-05	0.0005
5	48	300	240	300	183.26	105.7	6.09E-05	0.0005
10	52	300	195	300	175.25	101.1	1.23E-04	0.0005
15	57	300	215	300	166.07	95.8	1.00E-04	0.0005
20	58	300	170	300	164.33	94.8	1.73E-04	0.0005
25	58	300	161	300	164.33	94.8	1.89E-04	0.0005
30	63	300	117	300	156.06	90.0	3.02E-04	0.0005
50	67	300	110	300	149.91	86.5	3.35E-04	0.0005

Replicate 3

BaP (µM)	Plating Efficiency		Mutation Frequency					
	Xo	No	Xs	Ns	Plating Efficiency %	Cell Viability %	Mutation Frequency	Dilution factor
Solvent control	29	300	270	300	233.65	100.0	2.25E-05	0.0005
5	27	300	213	300	240.79	103.1	7.11E-05	0.0005
10	29	300	171	300	233.65	100.0	1.20E-04	0.0005
15	30	300	182	300	230.26	98.5	1.09E-04	0.0005
20	35	300	113	300	214.84	92.0	2.27E-04	0.0005
25	35	300	103	300	214.84	92.0	2.49E-04	0.0005
30	36	300	100	300	212.03	90.7	2.59E-04	0.0005
50	38	300	98	300	206.62	88.4	2.71E-04	0.0005

Appendix V (Chapter 4)

Screen shots of HPRT mutations (B|a|P)

A. Screen shots of spontaneous and induced mutation spectra of AHH-1 mutant colonies

Figure A. 2 Spontaneous mutation spectra of AHH-1 solvent mutants.

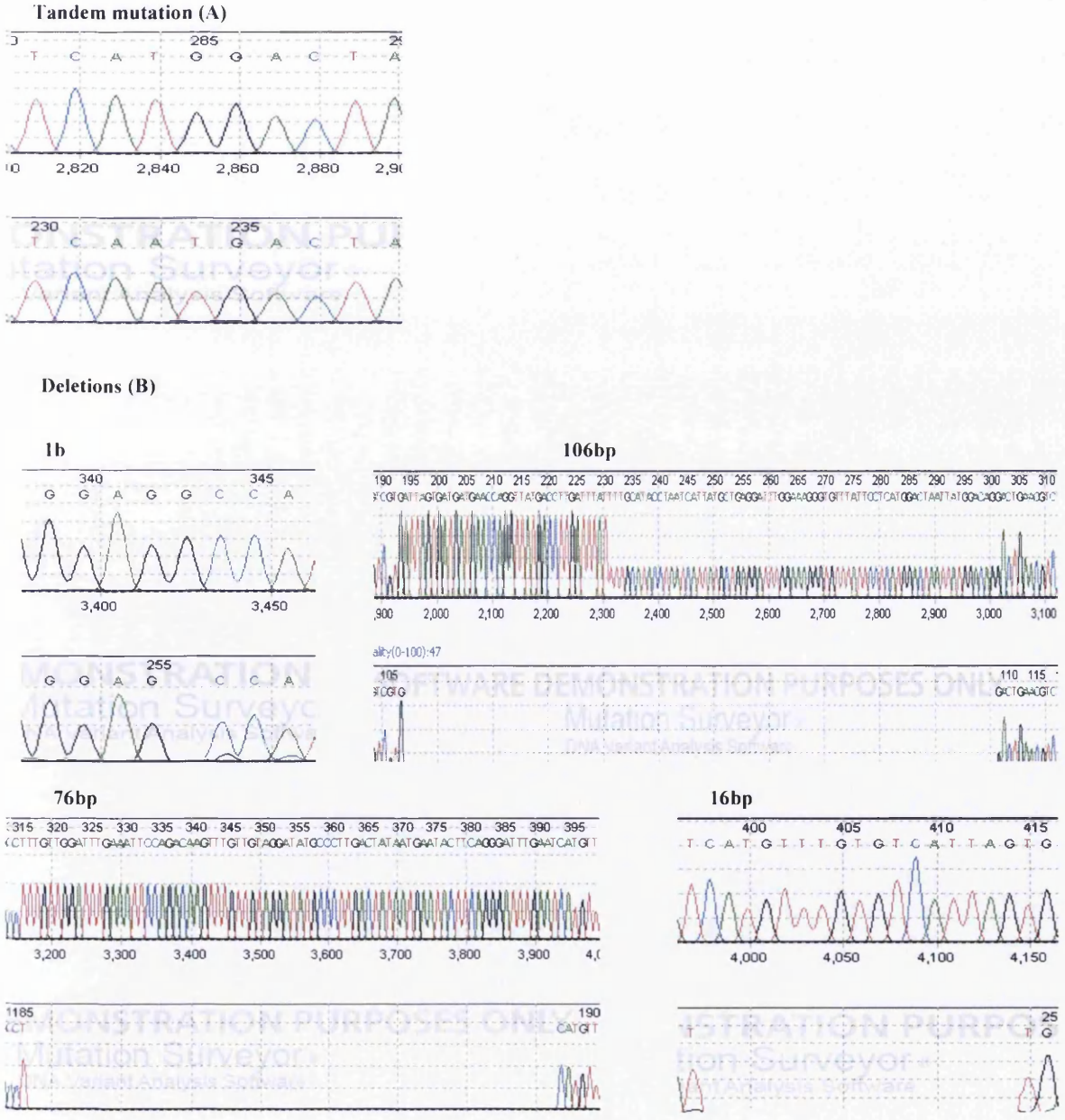

Figure A. 3 BaP-induced mutation spectra of AHH-1 mutants colonies.

Point mutations (A)

255G→T

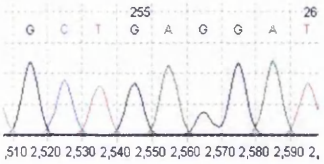

289T→C

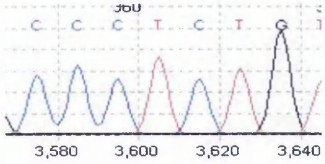

333G→T

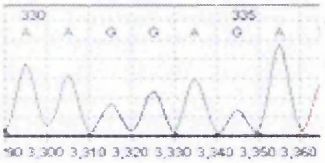

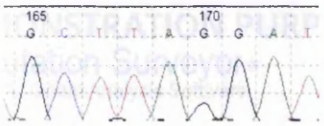

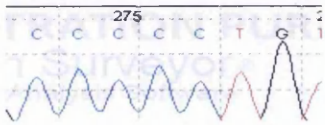

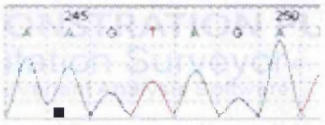

361T→C

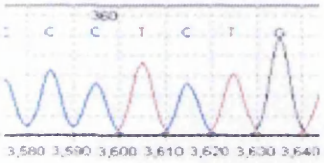

375G→T

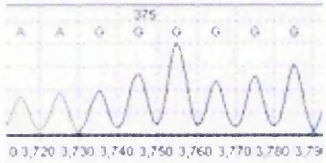

767G→C

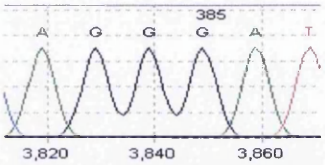

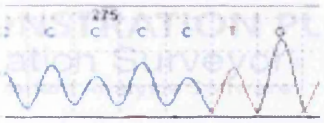

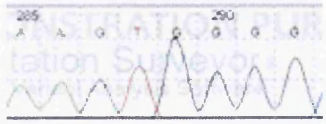

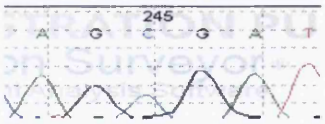

Insertion (B)

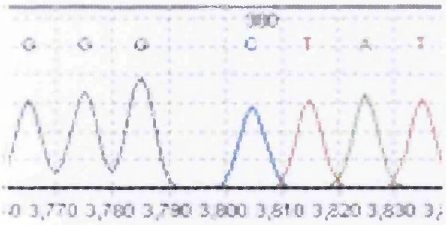

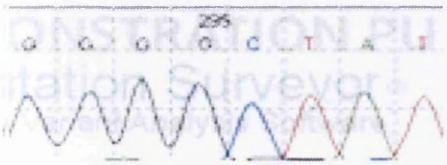

Deletions (C)

2bp

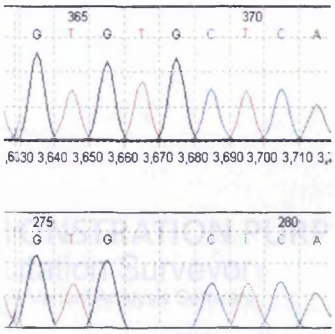

46b

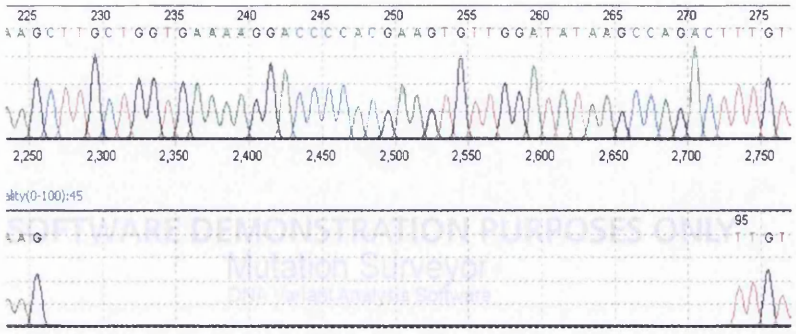

B. Screen shots of spontaneous and induced mutation spectra of MCL-5 mutant colonies

Figure A. 4 Spontaneous mutation spectra of MCL-5 solvent mutants.

Point mutations (A)

375G→T

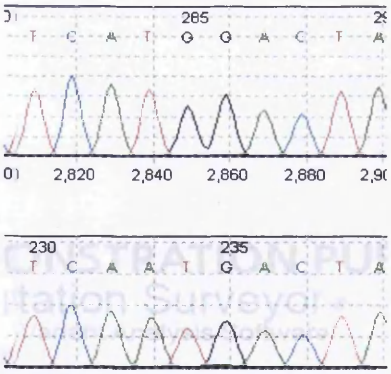

648G→C

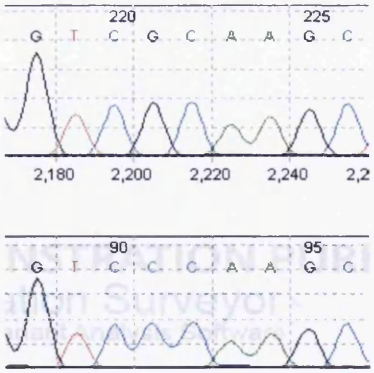

Tandem mutation (B)

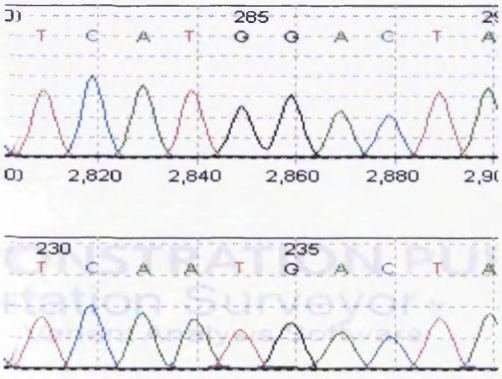

Deletions (C)

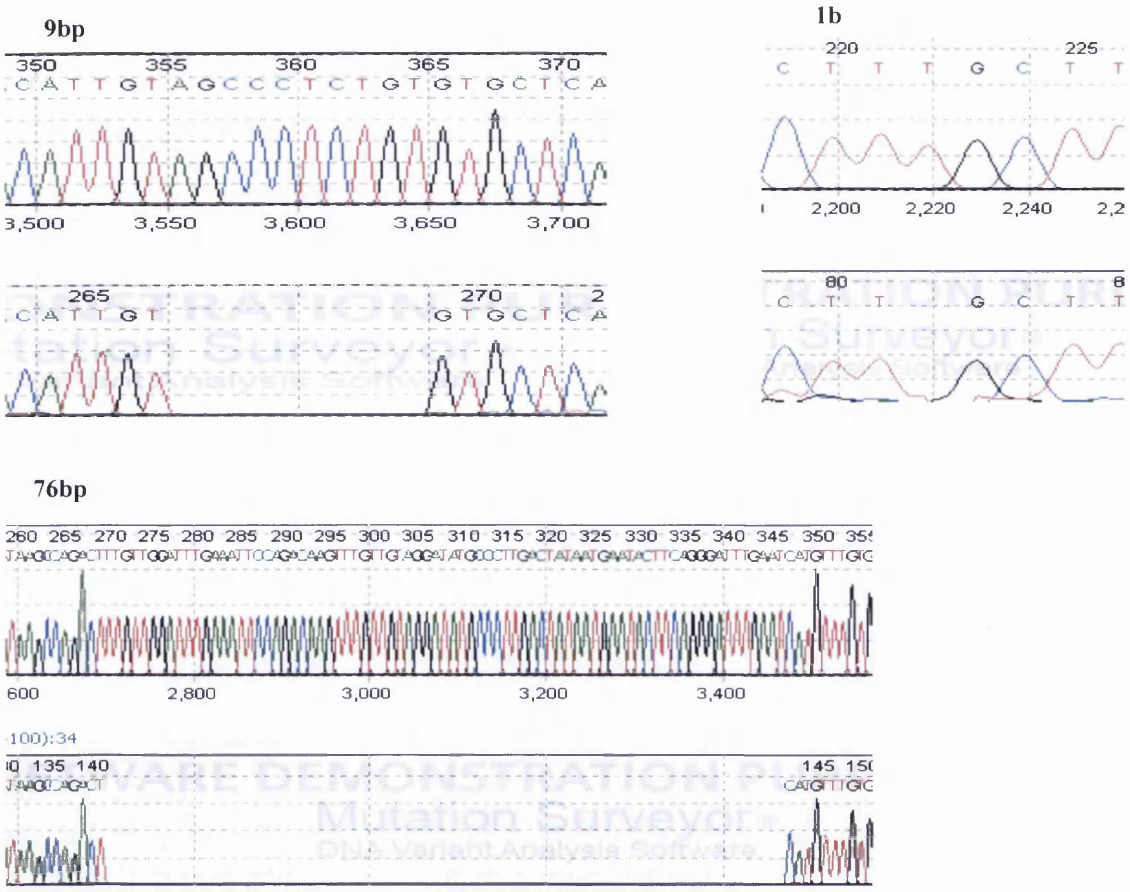

Figure A. 5 BaP-induced mutation spectra of MCL-5 mutants colonies.

Point mutations (A)

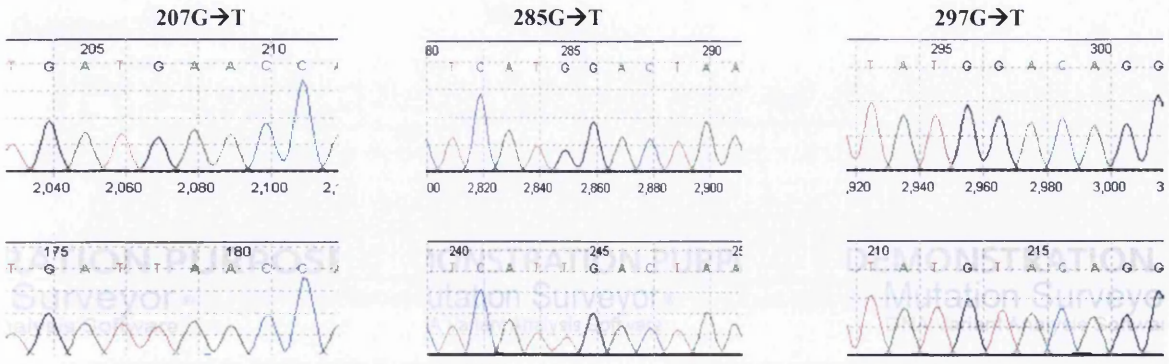

306G→T

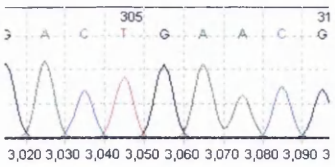

378G→T

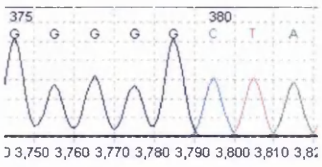

586G→T

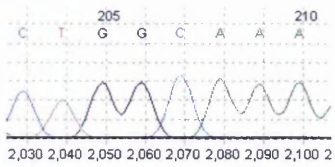

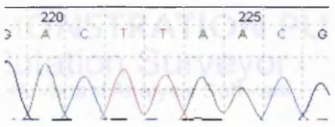

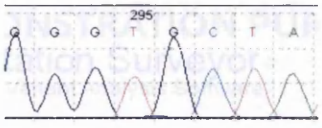

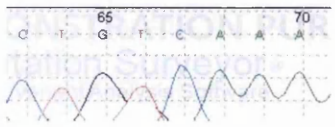

675C→T

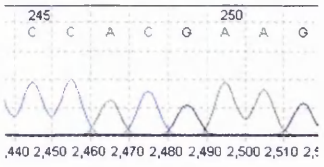

696G→T

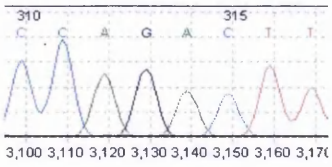

736G→C

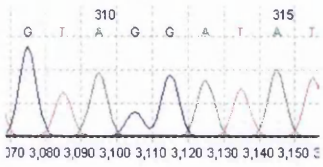

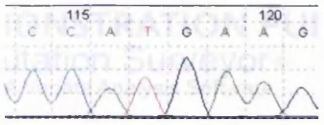

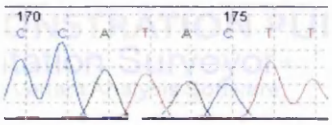

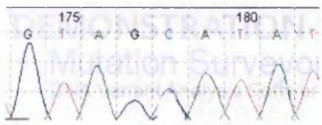

766G→T

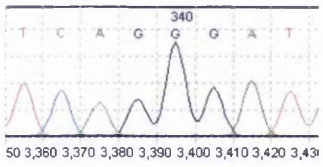

767G→T

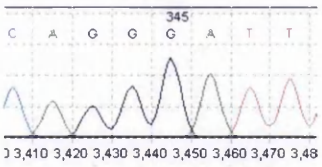

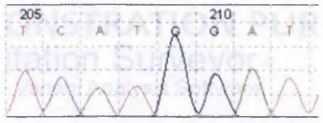

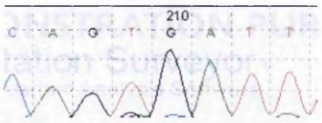

Deletions (B)

5bp

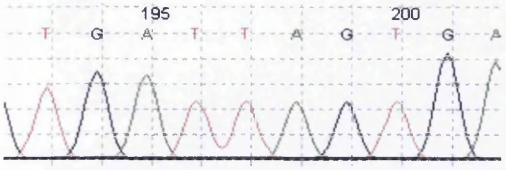

4bp

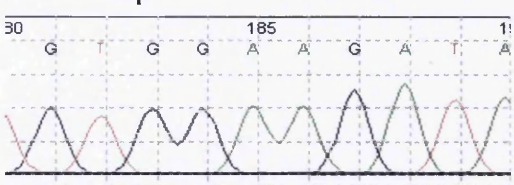

1bpG

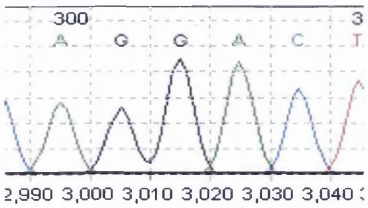
300
A G G A C T
2,990 3,000 3,010 3,020 3,030 3,040

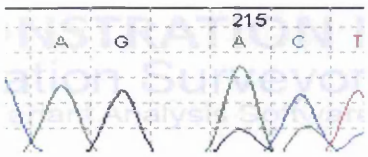
215
A G A C T

20bp

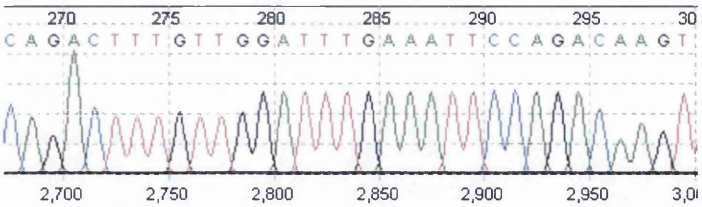
270 275 280 285 290 295
C A G A C T T T G T T G G A T T T G A A A T T C C A G A C A A G T
2,700 2,750 2,800 2,850 2,900 2,950


140 145
C A G A C T
A C A A G T

Appendix VI (Chapter 5)

Micronucleus assay raw data tables for PhIP

Terminology used in data tables

PD	Population doubling
%RPD	Percentage relative population doubling
Bn	Number of binucleated cells
Mn	Number of mononucleated cells
%Mn/Bn	Frequency of micronucleate in binucleated cells
Av.	Average

Table A. 17 CBMN assay raw data set for MCL-5 cell line treated with PhIP for 24h (24h+24h).

DOSE (µM)	DAY 1	DAY 2	PD	%RPD	Av. %RPD	Bn	Mn	%Mn/Bn	Total Mn	Total Bn	Av. % Mn/Bn
0	143200	1720000	3.59	100.00	100.00	2000	30	1.50	87	6000	1.45
0	145400	1782000	3.62	100.00		2000	28	1.40			
0	118000	1731000	3.87	100.00		2000	29	1.45			
2.5	134900	1681000	3.64	101.48	99.96	2000	27	1.35	80	6000	1.33
2.5	146200	1718000	3.55	98.32		2000	26	1.30			
2.5	112200	1650000	3.88	100.09		2000	27	1.35			
5	133600	1250000	3.23	89.95	98.32	2000	27	1.35	78	6000	1.30
5	121400	1606000	3.73	103.04		2000	25	1.25			
5	103800	1605000	3.95	101.96		2000	26	1.30			
7.5	138900	1675000	3.59	100.16	98.55	2000	25	1.25	77	6000	1.28
7.5	133400	1594000	3.58	98.99		2000	26	1.30			
7.5	119400	1594000	3.74	96.49		2000	26	1.30			
10	134200	1630000	3.60	100.45	99.04	2000	24	1.20	74	6000	1.23
10	106800	1296000	3.60	99.60		2000	21	1.05			
10	111400	1510000	3.76	97.06		2000	29	1.45			
15	193400	2158000	3.48	97.04	95.35	2000	29	1.45	87	6000	1.45
15	142000	1610000	3.50	96.89		2000	28	1.40			
15	145000	1722000	3.57	92.13		2000	30	1.50			
20	138600	1599000	3.53	98.38	94.45	2000	26	1.30	91	6000	1.52
20	112800	1394000	3.63	100.33		2000	36	1.80			
20	143200	1390000	3.28	84.62		2000	29	1.45			
25	160800	1082000	2.75	76.69	85.47	2000	33	1.65	96	6000	1.60
25	121200	1391800	3.52	97.40		2000	28	1.40			
25	126000	1150000	3.19	82.33		2000	35	1.75			
35	148600	1030000	2.79	77.88	78.52	2000	36	1.80	111	6000	1.85
35	142800	1010000	2.82	78.06		2000	42	2.10			
35	133200	1130000	3.08	79.61		2000	33	1.65			
50	128800	551200	2.10	58.48	54.13	2000	45	2.25	136	6000	2.27
50	193000	569800	1.56	43.20		2000	48	2.40			
50	125200	639400	2.35	60.71		2000	43	2.15			
100	120600	395800	1.71	47.81	30.40	2000	42	2.10	122	6000	2.03
100	133000	209000	0.65	18.04		2000	41	2.05			
100	221600	438000	0.98	25.37		2000	39	1.95			

Table A. 18 CBMN raw data set for HepG2 cell line treated with PhIP for 24h (24h+24h).

DOSE (µM)	DAY 1	DAY 2	PD	%RPD	Av. %RPD	Bn	Mn	%Mn/Bn	Total Mn	Total Bn	Av. % Mn/Bn
0	135600	841600	2.63	100.00	100.00	2000	18	0.90	54	6000	0.90
0	108200	550200	2.35	100.00		2000	16	0.80			
0	100200	735400	2.88	100.00		2000	20	1.00			
2.5	134900	681000	2.34	88.68	98.11	2000	17	0.85	54	6000	0.90
2.5	106200	718000	2.76	117.51		2000	19	0.95			
2.5	112200	650000	2.53	88.13		2000	18	0.90			
5	129000	835600	2.70	102.34	94.20	2000	17	0.85	55	6000	0.92
5	117400	470400	2.00	85.35		2000	20	1.00			
5	103000	683000	2.73	94.91		2000	18	0.90			
7.5	130900	775000	2.57	97.42	90.15	2000	20	1.00	61	6000	1.02
7.5	133400	692000	2.38	82.59		2000	21	1.05			
7.5	114400	694000	2.60	90.44		2000	20	1.00			
10	132200	775400	2.55	96.90	89.72	2000	24	1.20	72	6000	1.20
10	117800	526400	2.16	92.05		2000	25	1.25			
10	98400	486800	2.31	80.21		2000	23	1.15			
15	133400	558000	2.06	78.39	87.69	2000	24	1.20	76	6000	1.27
15	122000	510000	2.06	87.95		2000	26	1.30			
15	105000	722000	2.78	96.73		2000	26	1.30			
20	138600	599000	2.11	80.17	83.05	2000	26	1.30	80	6000	1.33
20	112800	494000	2.13	90.81		2000	27	1.35			
20	103200	490000	2.25	78.15		2000	27	1.35			
25	115800	774000	2.74	104.06	82.40	2000	27	1.35	85	6000	1.42
25	104200	426000	2.03	86.58		2000	28	1.40			
25	101600	313600	1.63	56.54		2000	30	1.50			
35	108600	303000	1.48	56.20	64.89	2000	32	1.60	95	6000	1.58
35	112800	501000	2.15	91.68		2000	30	1.50			
35	123200	313000	1.35	46.78		2000	33	1.65			
50	123200	137800	0.16	6.13	17.93	2000	32	1.60	100	6000	1.67
50	117200	228600	0.96	41.08		2000	35	1.75			
50	97000	110600	0.19	6.58		2000	33	1.65			

Table A. 19 CBMN assay raw data set for MCL-5 cell line treated with PhIP for 4h (4h+24h).

DOSE (µM)	DAY 1	DAY 2	PD	%RPD	Av. %RPD	Bn	Mn	%Mn/Bn	Total Mn	Total Bn	Av. % Mn/Bn
0	141000	369400	1.39	100.00	100.00	2000	32	1.60	89	6000	1.48
0	122800	395700	1.69	100.00		2000	31	1.55			
0	143500	377000	1.39	100.00		2000	26	1.30			
2.5	134500	345000	1.36	97.81	101.42	2000	30	1.50	87	6000	1.45
2.5	124000	448400	1.85	109.85		2000	29	1.45			
2.5	132000	335600	1.35	96.61		2000	28	1.40			
5	109400	333800	1.61	115.82	109.20	2000	28	1.40	84	6000	1.40
5	111200	320000	1.52	90.33		2000	27	1.35			
5	130400	421400	1.69	121.44		2000	29	1.45			
7.5	132500	398000	1.59	114.20	111.16	2000	29	1.45	86	6000	1.43
7.5	101200	321000	1.67	98.65		2000	27	1.35			
7.5	100400	321900	1.68	120.62		2000	30	1.50			
10	110400	310800	1.49	107.47	108.15	2000	24	1.20	82	6000	1.37
10	98000	219600	1.16	68.95		2000	35	1.75			
10	113400	473800	2.06	148.03		2000	23	1.15			
25	114200	415600	1.86	134.12	122.54	2000	23	1.15	75	6000	1.25
25	108000	363600	1.75	103.75		2000	25	1.25			
25	132600	464400	1.81	129.76		2000	27	1.35			
50	102200	230800	1.18	84.58	95.16	2000	34	1.70	92	6000	1.53
50	102400	306800	1.58	93.78		2000	32	1.60			
50	129400	364200	1.49	107.13		2000	26	1.30			
100	144200	265800	0.88	63.50	67.68	2000	36	1.80	105	6000	1.75
100	135900	302100	1.15	68.27		2000	32	1.60			
100	155600	309700	0.99	71.26		2000	37	1.85			
120	192600	317800	0.72	52.00	43.56	2000	52	2.60	163	6000	2.72
120	152800	280200	0.87	51.82		2000	56	2.80			
120	172200	223200	0.37	26.86		2000	55	2.75			

Table A. 20 CBMN assay raw data set for HepG2 cell line treated with PhIP for 4h (4h+24h).

DOSE (µM)	DAY 1	DAY 2	PD	%RPD	Av. %RPD	Bn	Mn	%Mn/Bn	Total Mn	Total Bn	Av. % Mn/Bn
0	154800	700000	2.177	100.00	100.00	2000	21	1.05	58	6000	0.97
0	128800	925800	2.846	100.00		2000	18	0.90			
0	140600	829600	2.561	100.00		2000	19	0.95			
2.5	124500	655000	2.395	110.03	101.09	2000	15	0.75	39	6000	0.65
2.5	134000	898400	2.745	96.47		2000	12	0.60			
2.5	132000	735600	2.478	96.78		2000	12	0.60			
5	151200	589600	1.963	90.18	90.58	2000	17	0.85	47	6000	0.78
5	147600	876000	2.569	90.29		2000	15	0.75			
5	130800	661000	2.337	91.27		2000	15	0.75			
7.5	132500	628000	2.245	103.12	89.39	2000	19	0.95	56	6000	0.93
7.5	121100	621000	2.358	82.88		2000	17	0.85			
7.5	121400	521900	2.104	82.16		2000	20	1.00			
10	124200	446600	1.846	84.81	79.52	2000	25	1.25	66	6000	1.10
10	134600	640200	2.250	79.06		2000	22	1.10			
10	137800	518800	1.913	74.69		2000	19	0.95			
25	142400	466600	1.712	78.65	83.39	2000	24	1.20	69	6000	1.15
25	149200	582000	1.964	69.01		2000	22	1.10			
25	142800	881000	2.625	102.51		2000	23	1.15			
50	122000	471600	1.951	89.61	80.30	2000	25	1.25	81	6000	1.35
50	133000	666600	2.325	81.72		2000	28	1.40			
50	123600	425000	1.782	69.58		2000	28	1.40			
100	160400	339600	1.082	49.71	50.49	2000	29	1.45	89	6000	1.48
100	121600	328600	1.434	50.40		2000	29	1.45			
100	131600	327400	1.315	51.35		2000	31	1.55			
120	125000	214400	0.778	35.76	34.07	2000	35	1.75	112	6000	1.87
120	102900	214133	1.057	37.15		2000	39	1.95			
120	119700	201400	0.751	29.31		2000	38	1.90			

Appendix VII (Chapter 5)

Fold change in CYPs expressions (PhIP)

Figure A, 8 Comparisons of basal and induced expression of CYP 1A1 and 1A2 enzymes in MCL-5 and HepG2 cell lines treated with selected PhIP doses for 24h. Lane1: Untreated control, Lane2: Treated with LOEL dose, Lane3: Dose above LOEL.

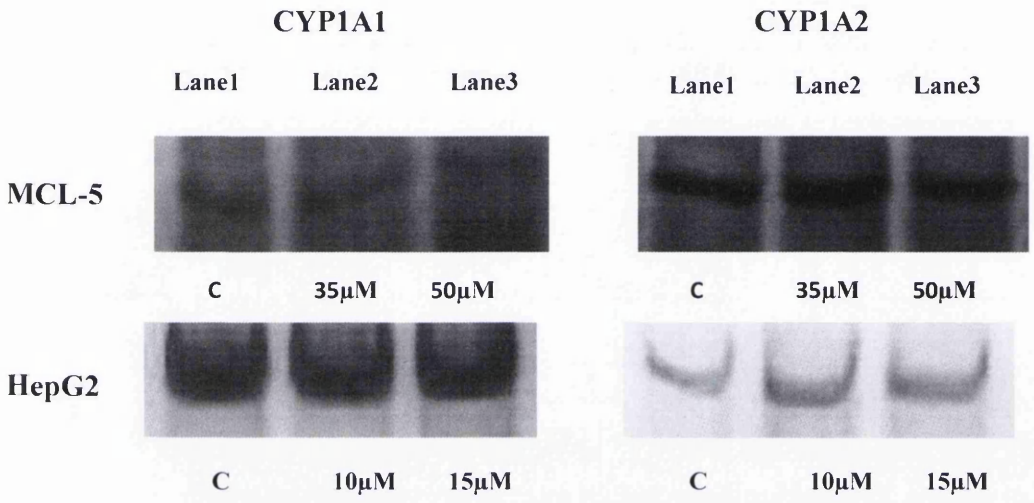

Appendix VIII (Chapter 6)

HPRT assay raw data tables for PhIP

Terminology used in data tables

Xo Number of wells with out colonies

No Total number of wells scored

Xs Number of wells without colonies

Ns Total number of wells scored

Table A 21 HPRT assay data set for MCL-5 cells untreated and solvent treated for 24h.

Replicate 1

PhIP (µM)	Plating Efficiency		Mutation Frequency					
	Xo	No	Xs	Ns	Plating Efficiency %	Cell Viability %	Mutation Frequency	Dilution factor
0	26	300	265	300	244.57	100.0	2.54E-05	0.0005
Solvent control	24	300	268	300	252.57	103.3	2.23E-05	0.0005

Replicate 2

PhIP (µM)	Plating Efficiency		Mutation Frequency					
	Xo	No	Xs	Ns	Plating Efficiency %	Cell Viability %	Mutation Frequency	Dilution factor
0	24	300	285	300.00	2.53E+02	100	1.01542E-05	0.0005
Solvent control	22	300	280	300.00	2.61E+02	103.4	1.29722E-05	0.0005

Replicate 3

PhIP (µM)	Plating Efficiency		Mutation Frequency					
	Xo	No	Xs	Ns	Plating Efficiency %	Cell Viability %	Mutation Frequency	Dilution factor
0	22	300	261	300	261.27	100.0	2.67E-05	0.0005
Solvent control	20	300	263	300	270.81	103.6	2.43E-05	0.0005

Table A 22 HPRT assay data set for MCL-5 cells treated with PhIP for 24h.

Replicate 1

PhIP(μM)	Plating Efficiency		Mutation Frequency					
	Xo	No	Xs	Ns	Plating Efficiency %	Cell Viability %	Mutation Frequency	Dilution factor
Solvent control	24	300	268	300	252.57	103.27	2.23E-05	0.0005
2.5	21	300	270	300	265.93	108.73	1.98E-05	0.0005
5	20	300	270	300	270.81	110.73	1.95E-05	0.0005
7.5	23	300	269	300	256.83	105.01	2.12E-05	0.0005
10	27	300	252	300	240.79	98.46	3.62E-05	0.0005
20	30	300	236	300	230.26	94.15	5.21E-05	0.0005
25	32	300	241	300	223.80	91.51	4.89E-05	0.0005
35	42	300	229	300	196.61	80.39	6.87E-05	0.0005
50	50	300	207	300	179.18	73.26	1.04E-04	0.0005

Replicate 2

PhIP(μM)	Plating Efficiency		Mutation Frequency					
	Xo	No	Xs	Ns	Plating Efficiency %	Cell Viability %	Mutation Frequency	Dilution factor
solvent control	22	300	280	300	261.27	103.4	1.30E-05	0.0005
2.5	23	300	282	300	256.83	101.7	1.22E-05	0.0005
5	21	300	279	300	265.93	105.3	1.76E-05	0.0005
7.5	24	300	270	300	252.57	100.0	2.15E-05	0.0005
10	38	300	245	300	206.62	80.5	4.27E-05	0.0005
20	26	300	239	300	244.57	96.8	4.79E-05	0.0005
25	28	300	231	300	237.16	93.9	5.51E-05	0.0005
35	28	300	223	300	237.16	93.9	7.27E-05	0.0005
50	39	300	205	300	204.02	80.8	9.33E-05	0.0005

Replicate 3

PhIP(μM)	Plating Efficiency		Mutation Frequency					
	Xo	No	Xs	Ns	Plating Efficiency %	Cell Viability %	Mutation Frequency	Dilution factor
solvent control	20	300	263	300	270.81	103.65	2.43032E-05	0.0005
2.5	19	300	262	300	275.93	105.61	2.45417E-05	0.0005
5	18	300	272	300	281.34	107.68	1.74131E-05	0.0005
7.5	21	300	269	300	265.93	101.78	2.05078E-05	0.0005
10	23	300	247	300	256.83	98.30	3.78451E-05	0.0005
20	24	300	239	300	252.57	96.67	4.50007E-05	0.0005
25	30	300	235	300	230.26	88.13	5.30267E-05	0.0005
35	35	300	225	300	214.84	82.23	6.69516E-05	0.0005
50	39	300	198	300	204.02	78.09	0.000101831	0.0005

Appendix IX (Chapter 6)

Screen shots of HPRT mutations (PhIP)

Screen shots of spontaneous and induced mutations in MCL-5 cell line treated with PhIP (25µM for 24h)

Figure A. 9 Spontaneous mutations in MCL-5 solvent controls.

Translocation (A)

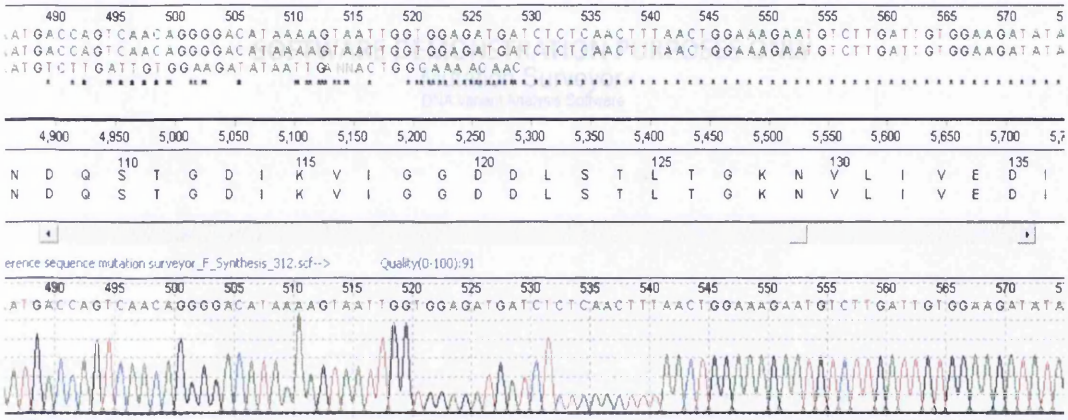

Point and Tandem mutations (B)

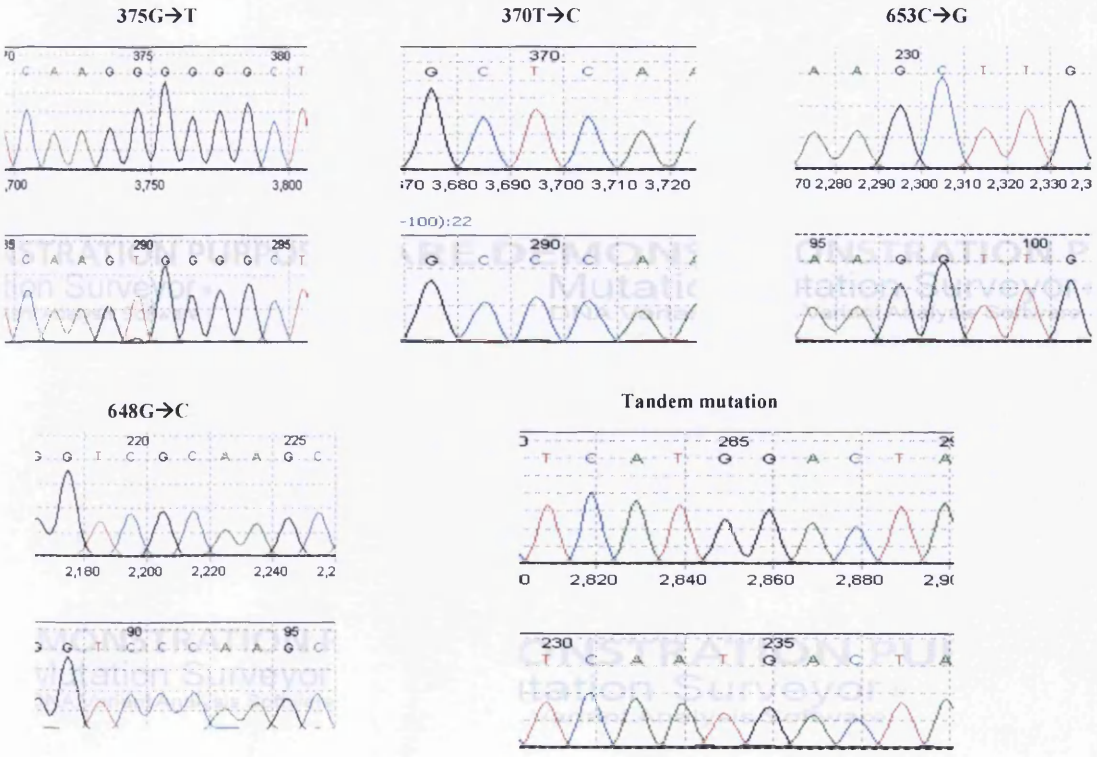

Deletions (C)

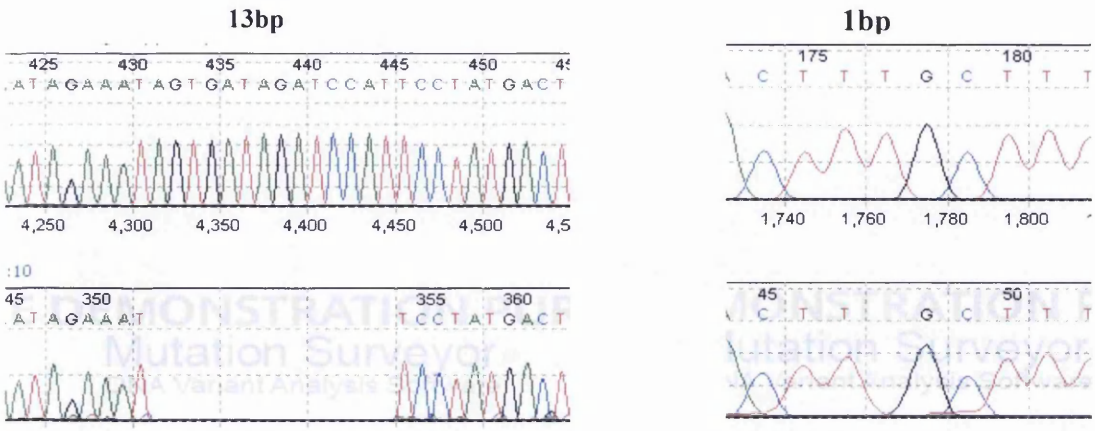

Figure A. 10 PhIP-Induced (25µM for 24h) mutations in MCL-5 cell line.

Point mutations (A)

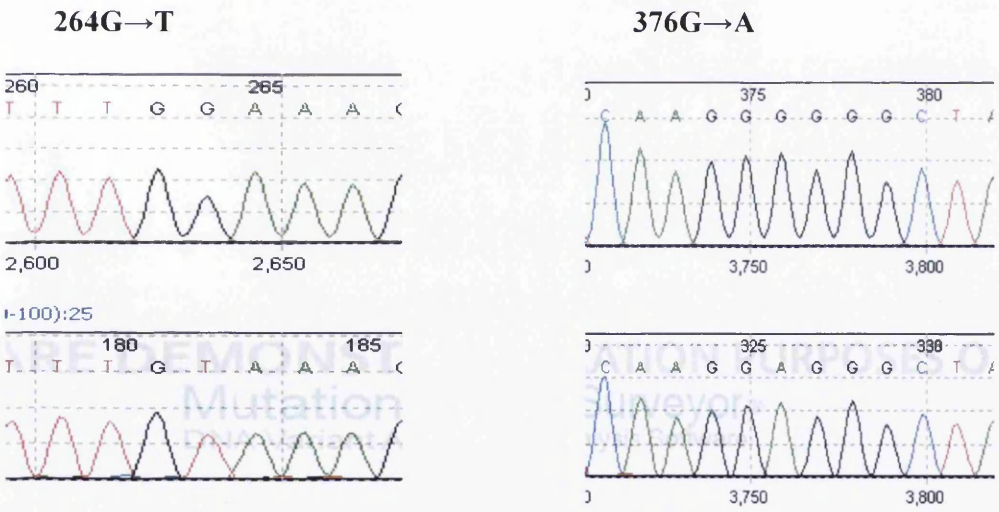

Deletions (B)

17bp

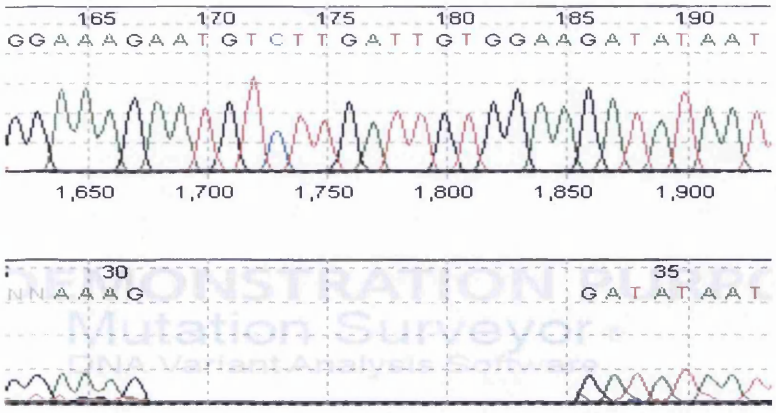

58bp deleted from position 1181-1239 position and translocated at 776 position on mRNA (C)